https://doi.org/10.15388/vu.thesis.1009
https://orcid.org/0000-0002-9718-5157

VILNIAUS UNIVERSITETAS
FIZINIŲ IR TECHNOLOGIJOS MOKSLŲ CENTRAS

Margarita Poderytė

Gyvų ląstelių tyrimas ir jų membranų modifikavimas naudojant elektrocheminius metodus

DAKTARO DISERTACIJA

Gamtos mokslai
Chemija (N 003)

VILNIUS 2026

Disertacija rengta 2021–2026 metais Vilniaus universitete, Chemijos ir Geomokslų fakultete.
Mokslinius tyrimus rėmė Europos regioninės plėtros fondas (projekto Nr. 01.2.2-LMT-K-718-01-0063), administruojamas Lietuvos mokslo tarybos.

Mokslinė vadovė – prof. dr. Aušra Valiūnienė (Vilniaus universitetas, gamtos mokslai, chemija, N 003).

Gynimo taryba:
Pirmininkė – prof. dr. Almira Ramanavičienė (Vilniaus universitetas, gamtos mokslai, chemija, N 003).
Nariai:
prof. dr. Henrikas Cesiulis (Vilniaus universitetas, gamtos mokslai, chemija, N 003),
prof. dr. Rasa Pauliukaitė (Fizinių ir technologijos mokslų centras, gamtos mokslai, chemija, N 003),
prof. dr. Tautgirdas Ruzgas (Malmö universitetas, Švedija, gamtos mokslai, chemija, N 003),
dr. Povilas Virbickas (Vilniaus universitetas, gamtos mokslai, chemija, N 003).

Disertacija ginama viešame Gynimo tarybos posėdyje 2026 m. lapkričio mėn. 30 d. 10 val. Vilniaus universiteto Chemijos ir geomokslų fakulteto Fizinės chemijos katedros Fizikinės chemijos auditorijoje (posėdis vyks mišriu/hibridiniu būdu, taip pat transliuojant Microsoft Teams platformoje). Adresas: Naugarduko g. 24, Vilnius, Lietuva; el. paštas ausra.valiuniene@chf.vu.lt

Disertaciją galima peržiūrėti Vilniaus universiteto bibliotekose ir VU interneto svetainėje adresu:
https://www.vu.lt/naujienos/ivykiu-kalendorius

https://doi.org/10.15388/vu.thesis.1009
https://orcid.org/0000-0002-9718-5157

VILNIUS UNIVERSITY
CENTER FOR PHYSICAL SCIENCES AND TECHNOLOGY

Margarita Poderyte

Investigation of Living Cells and Modification of Their Membranes Using Electrochemical Methods

DOCTORAL DISSERTATION

Natural Sciences
Chemistry (N 003)

VILNIUS 2026

The dissertation was prepared between 2021 and 2026 at Vilnius University, Faculty of Chemistry and Geosciences. The research was supported by the European Regional Development Fund (project No. 01.2.2-LMT-K-718-01-0063), administered by the Research Council of Lithuania.

Academic Supervisor – Prof. Dr. Aušra Valiūnienė (Vilnius University, Natural Sciences, Chemistry, N 003).

This Doctoral Dissertation will be Defended in a Public Meeting of the Dissertation Defence Panel:

Chairman – Prof. Dr. Almira Ramanavičienė (Vilnius University, Natural Sciences, Chemistry, N 003).
Members:
Prof. Dr. Henrikas Cesiulis (Vilnius University, Natural Sciences, Chemistry, N 003),
Prof. Dr. Rasa Pauliukaitė (Center for Physical Sciences and Technology, Natural Sciences, Chemistry, N 003),
Prof. Dr. Tautgirdas Ruzgas (Malmö University, Sweden, Natural Sciences, Chemistry, N 003),
Dr. Povilas Virbickas (Vilnius University, Natural Sciences, Chemistry, N 003).

The dissertation shall be defended at a public meeting of the Dissertation Defence Panel at 10:00 on 30 November 2026 in the Physical Chemistry Auditorium of the Faculty of Chemistry and Geosciences, Vilnius University (the meeting will be held in hybrid format, also broadcast via Microsoft Teams).
Address: Naugarduko g. 24, Vilnius, Lithuania
E-mail: ausra.valiuniene@chf.vu.lt

The text of this dissertation can be accessed at the libraries of Vilnius University, as well as on the website of Vilnius University:
www.vu.lt/lt/naujienos/ivykiu-kalendorius

TURINYS

SUTRUMPINIMŲ SĄRAŠAS 7
ĮVADAS 9
Temos aktualumas 9
Tyrimo objektas ir problema 10
Tyrimo tikslas 11
Uždaviniai 11
Darbo naujumas 11
Praktinė reikšmė 12
Gynimui teikiami teiginiai 12
LITERATŪROS APŽVALGA 13
1. BIOLOGINĖS MEMBRANOS IR JŲ MODELIAI 13
    1.1. Plazminės membranos reikšmė ir savybės 13
    1.2. Modelinių membranų poreikis 16
    1.3. Juodosios lipidinės membranos (BLM) 16
    1.4. Ant kieto paviršiaus palaikomos membranos (sBLM) 18
    1.5. Hibridinės membranos (hBLM) 19
    1.6. Tvirtinamos membranos (tBLM) 20
2. ELEKTROPORACIJA: MECHANIZMAI IR TAIKYMO SRITYS 22
    2.1. Elektroporacijos fenomeno samprata 22
    2.2. Grįžtama ir negrįžtama elektroporacija 23
    2.3. Elektroporacijos parametrus lemiantys veiksniai 25
    2.4. Elektroporacijos taikymo sritys 27
    2.5. Dirbtinių fosfolipidinių membranų vaidmuo elektroporacijos tyrimuose 28
3. SKENUOJANČIOJI ELEKTROCHEMINĖ MIKROSKOPIJA (SECM) IR ELEKTROCHEMINĖ IMPEDANSO SPEKTROSKOPIJA (EIS) 30
    3.1. SECM metodo atsiradimas ir veikimo principai 30
    3.2. SECM veikimo režimai 32
    3.3. SECM privalumai ir ribojimai 33
    3.4. Elektrocheminė impedanso spektroskopija (EIS) 35
    3.5. SECM ir EIS kombinacija 36
4. SECM PRITAIKYMAI GYVŲ LĄSTELIŲ TYRIMUOSE 39

4.1. SECM reikšmė biologijoje 39
4.2. Pagrindinės SECM taikymo sritys gyvų ląstelių tyrimuose 40
4.3. Išvados apie SECM taikymą gyvoms ląstelėms 41
5. LITERATŪROS APIBENDRINIMAS 43
6. TYRIMŲ METODIKA 44
6.1. Mielių ląstelių ir substrato paruošimas 44
6.2. Hibridinės membranos (hBLM) paruošimas 44
6.3. Tvirtinamos membranos (tBLM) paruošimas 45
6.4. Ultramikroelektrodų (UME) paruošimas ir SECM/EIS sąranga 45
6.5. Elektroporacijos protokolai 46
6.6. Elektrocheminės impedanso spektroskopijos (EIS) matavimai ir duomenų analizė 47
6.7. Naudoti reagentai ir įranga 49
7. PAGRINDINIŲ REZULTATŲ APIBENDRINIMAS: DIRBTINIŲ MEMBRANŲ (HBLM, TBLM) IR MIELIŲ LĄSTELIŲ ELEKTROPORACIJA 51
IŠVADOS 59
LITERATŪROS SĄRAŠAS 61
SUMMARY 69
PADĖKA 77
DALYVAVIMAS MOKSLINIUOSE RENGINIUOSE 78
GYVENIMO IR MOKSLINĖS BEI KŪRYBINĖS VEIKLOS APRAŠYMAS 79
PUBLIKACIJŲ SĄRAŠAS 80
PUBLIKACIJŲ KOPIJOS 81

SUTRUMPINIMŲ SĄRAŠAS

Santrumpa	Paaiškinimas
AFM	atominės jėgos mikroskopija (angl. Atomic Force Microscopy)
ALP	šarminė fosfatazė (angl. Alkaline Phosphatase)
ATS	aliltrichlorsilanas (angl. allyltrichlorosilane)
BLM	juodoji lipidinė membrana (angl. Black Lipid Membrane)
CD	dvigubo elektrinio sluoksnio talpa
CPE	pastovios fazės elementas (angl. Constant Phase Element)
CV	ciklinė voltamperometrija (angl. Cyclic Voltammetry)
DOPC	1,2-dioleoil-sn-glicero-3-fosfocholinas
EIS	elektrocheminė impedanso spektroskopija (angl. Electrochemical Impedance Spectroscopy)
FFT-EIS	greitosios Furjė transformacijos elektrocheminė impedanso spektroskopija (angl. Fast Fourier Transform EIS)
FTO	fluoru dopintas alavo oksidas (angl. Fluorine-doped Tin Oxide)
G/C	generavimo/surinkimo režimas (angl. generation/collection mode)
GOx	gliukozės oksidazė (angl. Glucose Oxidase)
hBLM	hibridinė lipidinė membrana (angl. hybrid Bilayer Lipid Membrane)
IRE	negrįžtama elektroporacija (angl. Irreversible Electroporation)
MRP1	daugiavaistio atsparumo baltymas 1 (angl. Multidrug Resistance-associated Protein 1)
OCR	deguonies suvartojimo greitis (angl. Oxygen Consumption Rate)
OTS	oktadeciltrichlorsilanas (angl. octadecyltrichlorosilane)
PBS	fosfatinis buferinis tirpalas (angl. Phosphate-Buffered Saline)
PEF	pulsinis elektrinis laukas (angl. Pulsed Electric Field)
P-SECM	programuojama skenuojančioji elektrocheminė mikroskopija (angl. Programmable SECM)
SAM	savitvarkis monosluoksnis (angl. Self-Assembled Monolayer)
sBLM	ant kieto paviršiaus palaikoma membrana (angl. solid-supported Bilayer Lipid Membrane)

SECM	skenuojančioji elektrocheminė mikroskopija (angl. Scanning Electrochemical Microscopy)
SEIM	skenuojančioji elektrocheminės impedanso mikroskopija (angl. Scanning Electrochemical Impedance Microscopy)
SG/TC	substrato generavimo/zondo surinkimo režimas (angl. Substrate Generation/Tip Collection)
SICM	skenuojančioji jonų laidumo mikroskopija (angl. Scanning Ion Conductance Microscopy)
STM	skenuojančioji tunelinė mikroskopija (angl. Scanning Tunneling Microscopy)
tBLM	tvirtinama lipidinė membrana (angl. tethered Bilayer Lipid Membrane)
TG/SC	zondo generavimo/substrato surinkimo režimas (angl. Tip Generation/Substrate Collection)
TOPS	trichloro(3-(oktadeciltio)propil)silanas
UME	ultramikroelektrodas (angl. Ultramicroelectrode)
$\Delta\Psi m$	transmembraninis potencialas

ĮVADAS

Temos aktualumas

Plazminė membrana yra viena svarbiausių ląstelės struktūrų, užtikrinanti medžiagų transportą, signalų perdavimą ir gyvybinės pusiausvyros palaikymą. Jos selektyvus pralaidumas lemia ląstelės gyvybingumą ir prisitaikymą prie aplinkos sąlygų. Nors natūralios membranos yra itin sudėtingos, jau nuo XX a. antrosios pusės buvo ieškoma supaprastintų modelių, leidžiančių tirti fundamentinius membranos veikimo aspektus.

Vienas reikšmingiausių tyrimo objektų yra elektroporacija – laikinas arba nuolatinis porų susidarymas membranoje, veikiant ją elektriniu lauku. Šis reiškinys yra svarbus tiek fundamentiniu, tiek taikomuoju požiūriu, nes sudaro sąlygas į ląsteles įvesti įvairias molekules arba selektyviai sunaikinti nepageidaujamas ląsteles. Elektroporacija plačiai taikoma biomedicinoje (elektrochemoterapijoje, genų terapijoje, vakcinų kūrime), biotechnologijoje (mikroorganizmų transformacijoje, biosensoriuose) ir maisto pramonėje (sterilizacijoje, mikroorganizmų inaktyvacijoje). Tačiau procesas išlieka nevisiškai kontroliuojamas – porų dydis, skaičius ir išliekamumas priklauso nuo daugelio parametrų, todėl būtina kurti patikimus modelius ir metodikas, leidžiančias tiksliai sekti šio reiškinio eigą.

Teoriniu požiūriu elektroporacija grindžiama transmembraninio potencialo ($\Delta\Psi m$) samprata: kai išorinio elektrinio lauko sukeltas potencialų skirtumas membranoje viršija kritinę ribą (paprastai 0,2–1 V), lipidų dvisluoksnyje spontaniškai susidariusios mikroskopinės ertmės tampa termodinamiškai palankios ir plečiasi į hidrofilines poras. Kadangi $\Delta\Psi m$ yra proporcingas elektrinio lauko stipriui ir ląstelės (arba paviršiaus taško) spinduliui bei priklauso nuo taško kampinės padėties elektrinio lauko atžvilgiu ($\Delta\Psi m = 1{,}5 \cdot E \cdot R \cdot \cos\theta$, (1)), akivaizdu, kad tas pats išorinis laukas skirtingus membranos taškus veikia nevienodai. Tradiciniuose dviejų elektrodų elektroporatoriuose elektrinis laukas yra praktiškai homogeniškas visame tūryje, todėl vienodai veikiamos visos mėginyje esančios ląstelės ir jų membranos. Tokiu atveju nėra galimybės nei erdviškai apriboti poveikio zonos, nei realiuoju laiku stebėti poveikio proceso. Toks „aklas“ metodas yra pakankamas masinei ląstelių transfekcijai ar sterilizacijai, tačiau netinka, kai reikia paveikti tik pavienes ląsteles arba tik apibrėžtą membranos regioną, paliekant aplinkines struktūras nepažeistas. Būtent tokio selektyvumo reikalauja tikslinė vaistų pernaša, genų terapija ir navikinių ląstelių naikinimas, kartu išsaugant sveiką audinį.

Būtent šiems apribojimams įveikti ypač perspektyvi yra skenuojančioji elektrocheminė mikroskopija (SECM). Kadangi SECM naudojamas ultramikroelektrodas (UME) veikia kaip lokalus, erdviškai apibrėžtas elektrinio lauko šaltinis, kurio padėtį galima valdyti mikrometro tikslumu x, y ir z kryptimis, elektrinis laukas gali būti sutelktas tiksliai pasirinktoje vietoje virš ląstelės ar membranos, nepaliečiant aplinkinių sričių. Be to, tas pats UME po impulso gali būti iš karto panaudotas kaip jutiklis – registruojant srovės pokytį arba grįžtamojo ryšio kreivę. Todėl elektroporacijos indukavimas ir jos rezultatų stebėjimas realiuoju laiku atliekami ta pačia priemone, nenaudojant papildomų žymenų ar destruktyvių metodų. Tai iš esmės skiriasi nuo klasikinių metodų, kuriuose poveikis ir jo vertinimas yra atskirti tiek laike, tiek erdvėje.

Elektrocheminė impedanso spektroskopija (EIS) papildomai leidžia kiekybiškai įvertinti membranos krūvio pernašos varžos ir talpos pokyčius, todėl galima ne tik nustatyti, kad poveikis įvyko, bet ir įvertinti jo mastą bei membranos atsistatymo dinamiką. Toks metodologinis derinys – lokalus poveikis ir lokalus, nedestruktyvus stebėjimas – teoriškai leidžia spręsti problemą, kuri dešimtmečius ribojo elektroporacijos taikymą tiksliniam gydymui: kaip vienu metu kontroliuoti porų susidarymo vietą, jų dydį ir grįžtamumą.

Tyrimo objektas ir problema

Pagrindinis tyrimo objektas – fosfolipidinių membranų elektroporacija, tiriama tiek dirbtinėse membranose (hibridinėse (hBLM) ir tvirtinamose (tBLM)), tiek gyvose mielių ląstelėse (*Saccharomyces cerevisiae*). Nepaisant plataus elektroporacijos taikymo, jos tyrimuose vis dar kyla reikšmingų iššūkių: i) klasikinės lipidinės dvisluoksnės membranos (BLM) yra trapios; ii) hibridinės membranos (hBLM) tik iš dalies atspindi biologinių membranų lankstumą; iii) gyvos ląstelės yra heterogeniškos ir sunkiai kontroliuojamos. Todėl svarbu sukurti stabilią ir praktišką metodologiją, kuri leistų lokalizuotai ir kontroliuojamai indukuoti elektroporaciją bei realiuoju laiku registruoti membranos pokyčius.

Platesnė mokslinės literatūros analizė rodo, kad SECM, derinama su EIS (ši kombinacija literatūroje vadinama skenuojančiąja elektrochemine impedanso mikroskopija, SEIM), jau sėkmingai taikyta ir kitiems su membranos pralaidumu susijusiems reiškiniams tirti. Pavyzdžiui, šis metodas buvo taikytas HeLa ląstelių membranos pažeidimui, sukeltam nejoninio paviršinio aktyvumo junginio Triton X-100, tirti. Nustatyta, kad membranos pralaidumas hidrofilinėms molekulėms padidėja jau esant maždaug 0,17 mM

detergento koncentracijai. SEIM taip pat taikyta ankstyvosioms ferroptozės – geležies sukeltos, lipidų peroksidacija grįstos ląstelių žūties formos – stadijoms stebėti pavienėse hepatoceliulinės karcinomos ląstelėse.

Tačiau dauguma šių tyrimų apsiriboja fenomenologiniu stebėjimu ir nepasiūlo sistemingo, kiekybinio modelio, kuris tiesiogiai susietų elektrodo geometriją (skersmenį), atstumą tarp elektrodo ir paviršiaus bei membranos tipą (dirbtinė ar gyva, hibridinė ar tvirtinama) su elektroporacijos baigtimi – jos grįžtamumu, paveiktos srities dydžiu ir membranos atsistatymo trukme. Būtent šių sisteminių sąsajų atskleidimas yra pagrindinis šios disertacijos tiriamasis uždavinys.

Tyrimo tikslas

Sukurti ir eksperimentiškai įvertinti kontroliuojamos lokalizuotos elektroporacijos metodiką, pagrįstą skenuojančiosios elektrocheminės mikroskopijos (SECM) ir elektrocheminės impedanso spektroskopijos (EIS) deriniu, bei ištirti jos taikymą dirbtinėms lipidinėms membranoms ir gyvoms mielių ląstelėms.

Uždaviniai

1. Nustatyti ir palyginti hBLM ir tBLM membranų atsparumą lokalizuotam elektriniam poveikiui, taikant mažos amplitudės potencialo impulsus.
2. Nustatyti grįžtamosios ir negrįžtamosios elektroporacijos sąlygas, atsižvelgiant į taikomo elektrinio poveikio parametrus.
3. Sukurti ir eksperimentiškai išbandyti SECM pagrįstą lokalizuotos membranų elektroporacijos indukavimo metodiką, naudojant mažos amplitudės potencialo impulsus.
4. Pritaikyti SECM ir EIS metodų derinį gyvų Saccharomyces cerevisiae ląstelių lokalizuotai elektroporacijai tirti.
5. Nustatyti ultramikroelektrodo geometrinių parametrų ir elektrodo–paviršiaus atstumo įtaką lokalizuotos elektroporacijos rezultatams.

Darbo naujumas

Šio darbo naujumą sudaro lokalizuotos elektroporacijos indukavimo naudojant SECM metodikos sukūrimas ir eksperimentinis įvertinimas; skirtingos architektūros hBLM ir tBLM membranų atsako į lokalizuotą elektrinį poveikį sisteminis palyginimas; ultramikroelektrodo skersmens ir elektrodo–paviršiaus atstumo įtakos lokalizuotos elektroporacijos rezultatams įvertinimas; SECM ir EIS metodų derinio pritaikymas elektroporacijos

sukeltų membranos elektrinių savybių pokyčių kiekybiniam ir dinaminiam vertinimui; taip pat sukurtos metodinės prieigos pritaikymas gyvų *Saccharomyces cerevisiae* ląstelių lokalizuotos elektroporacijos tyrimams.

Praktinė reikšmė

Darbo metu sukurta metodika gali būti taikoma fundamentiniams biologinių membranų elektrinio atsako ir elektroporacijos tyrimams bei tolesniam lokalizuotų elektrocheminių poveikių biologinėse sistemose vystymui. SECM ir EIS derinys suteikia galimybę kontroliuoti elektrinio poveikio vietą ir kiekybiškai vertinti jo sukeltus membranos elektrinių savybių pokyčius. Sukurta metodinė prieiga gali būti aktuali tobulinant lokalizuoto ląstelių poveikio, biosensorių ir kitų bioelektrocheminių sistemų tyrimo metodus.

Gynimui teikiami teiginiai

1. Hibridinės ir tvirtinamos lipidinės membranos pasižymi skirtingu atsparumu lokalizuotam elektriniam poveikiui ir skirtingomis elektroporacijos sąlygomis.
2. Lokalizuotos grįžtamosios ir negrįžtamosios elektroporacijos baigtį galima kontroliuoti keičiant ultramikroelektrodo geometriją, elektrodo–paviršiaus atstumą ir elektrinio poveikio parametrus.
3. Elektrocheminė impedanso spektroskopija leidžia kiekybiškai įvertinti elektroporacijos sukeltus membranos elektrinių savybių pokyčius ir jų raidą laike.
4. SECM gali būti pritaikyta lokalizuotai gyvų Saccharomyces cerevisiae ląstelių elektroporacijai indukuoti ir jos erdviniam mastui įvertinti.
5. SECM ir EIS derinys leidžia susieti lokalizuoto elektrinio poveikio erdvinę lokalizaciją su elektroporacijos metu ir po jos vykstančiais membranos elektrinių savybių pokyčiais.

LITERATŪROS APŽVALGA

1. BIOLOGINĖS MEMBRANOS IR JŲ MODELIAI

1.1. Plazminės membranos reikšmė ir savybės

Plazminė membrana yra gyvybiškai svarbi kiekvienos ląstelės sudedamoji dalis, atliekanti daugybę funkcijų: ji palaiko vidinės ląstelės aplinkos stabilumą, reguliuoja medžiagų pernašą, dalyvauja signalų perdavime, saugo ląstelę nuo išorinių veiksnių ir koordinuoja tarpląstelinę komunikaciją. Ji sudaryta iš fosfolipidų dvisluoksnio, į kurį įterpti baltymai, steroliai (gyvūnų ląstelėse – cholesterolis) ir kiti komponentai (Pav. 1).[1] Tokia sandara suteikia membranai selektyvų pralaidumą ir dinamiškumą, leidžiantį prisitaikyti prie kintančių aplinkos sąlygų.[1,2]

Fosfolipidai yra amfipatinės molekulės, kurių hidrofobinės uodegėlės vengia kontakto su vandeniu, o hidrofilinės galvutės sąveikauja su vandenine aplinka.[3] Dėl šių savybių jie spontaniškai susitelkia į dvisluoksnę struktūrą, kurios hidrofilinės galvutės nukreiptos į išorę, o hidrofobinės uodegėlės – į vidų. Šią struktūrą stabilizuoja hidrofobinės sąveikos, van der Valso sąveikos ir elektrostatinės jėgos.[3,4]

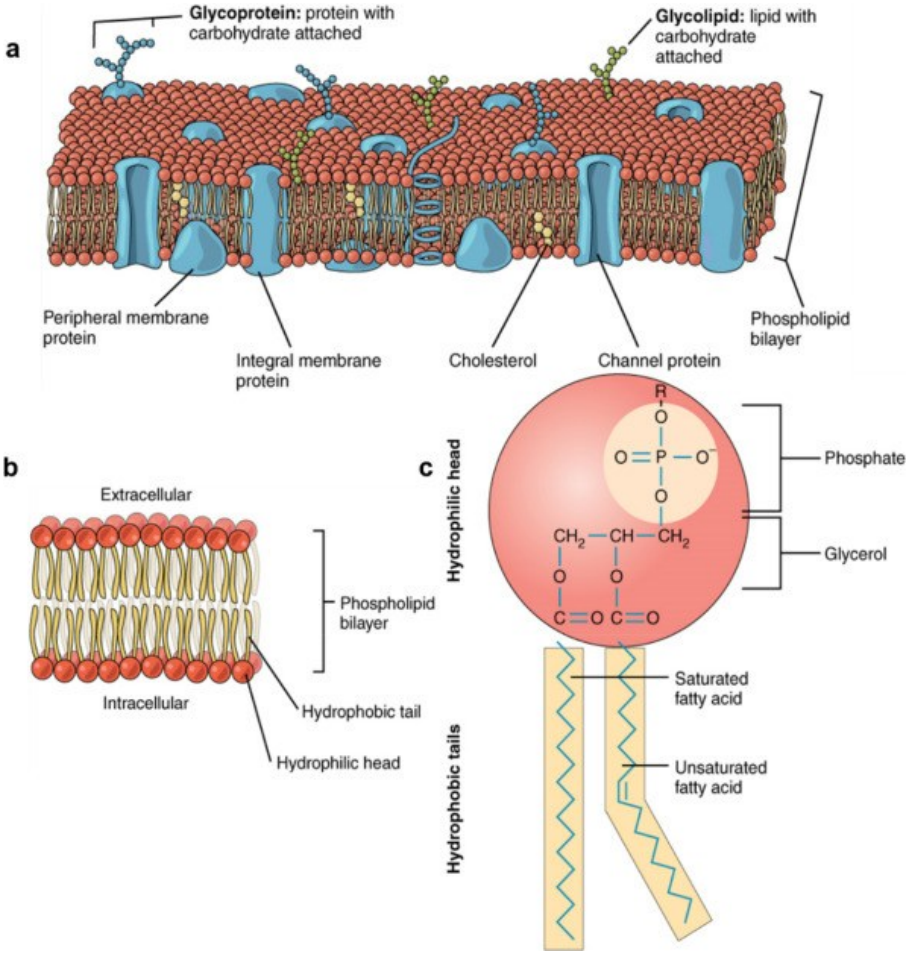
Šiuolaikinis membranos struktūros supratimas grindžiamas S. J. Singerio ir G. L. Nicolsono 1972 m. pasiūlytu skysčio mozaikos modeliu (angl. *fluid mosaic model*), pagal kurį membrana nėra statiška struktūra, o dinamiška dvimatė lipidų „jūra“, kurioje baltymai ir kiti komponentai laisvai difunduoja membranos plokštumoje.[1,2] Šis modelis paaiškina, kodėl membrana geba greitai keisti savo formą, prisitaikyti prie mechaninio poveikio ir išlaikyti savo funkcijas, nepaisant nuolatinio komponentų judėjimo. Membranos takumą (fluidiškumą) lemia lipidų riebalų rūgščių grandinių ilgis ir prisotinimo laipsnis: nesočiosios grandinės, turinčios cis dvigubąsias jungtis, didina tarpmolekulinius atstumus ir membranos takumą, o sočiosios grandinės jį mažina. Cholesterolis veikia kaip membranos takumo moduliatorius – mažina takumą aukštesnėje temperatūroje ir neleidžia membranai pernelyg sukietėti žemoje temperatūroje.[5] Kintant temperatūrai, membrana gali pereiti iš standžios gelio fazės į skystosios kristalinės fazės būseną. Šis virsmas vyksta ties fazinio virsmo temperatūra (Tm) ir tiesiogiai veikia membranos pralaidumą bei jautrumą elektroporacijai.[6]

Svarbu ir tai, kad membrana nėra simetriška: vidinis ir išorinis dvisluoksnio sluoksniai skiriasi lipidų sudėtimi (pvz., fosfatidilserinas paprastai lokalizuotas vidiniame sluoksnyje), todėl susidaro asimetriškas paviršiaus krūvio pasiskirstymas, turintis įtakos baltymų orientacijai ir signalų

perdavimo procesams.[7] Be to, membranoje egzistuoja specializuoti mikrodomenai, vadinami lipidų plaustais (angl. *lipid rafts*), – cholesterolio ir sfingolipidų praturtintos, palyginti standesnės sritys, kuriose koncentruojasi tam tikri signaliniai baltymai.[8] Tokių domenų buvimas rodo, kad membranos heterogeniškumas yra struktūriškai organizuotas ir funkciškai reikšmingas jos savybių aspektas. Į tai svarbu atsižvelgti interpretuojant elektroporacijos eksperimentų rezultatus, nes skirtingos membranos sritys į tą patį elektrinį lauką gali reaguoti nevienodai.[9]

Vienas svarbiausių membranos komponentų yra cholesterolis, kuris įsiterpia tarp fosfolipidų ir reguliuoja membranos mechanines savybes bei pralaidumą. Jis mažina membranos pralaidumą mažoms poliarinėms molekulėms ir jonams, taip prisidėdamas prie membranos vientisumo palaikymo.[10] Be to, membranoje gausu įvairių baltymų – jonų kanalų, pernešiklių ir receptorių, kurie suteikia jai specifinių funkcijų. Vieni baltymai yra įterpti per visą dvisluoksnį (integraliniai), kiti prisijungę prie membranos paviršiaus (periferiniai).[1,2]

Nepaisant santykinai paprastos fosfolipidinės struktūros, plazminė membrana yra itin sudėtinga ir dinamiška sistema, kurioje baltymų, lipidų ir kitų komponentų tarpusavio sąveika lemia įvairius struktūrinius ir funkcinius procesus. Membrana atlieka ne tik fizinio barjero funkciją, bet ir yra svarbi signalų perdavimo bei ląstelės atsako į cheminius ir fizikinius dirgiklius sąsaja.[1,2,11]



Pav. 1. **Ląstelės membranos ir fosfolipido struktūra**: (a) ląstelės membrana, sudaryta iš fosfolipidų dvisluoksnio, kuriame yra įvairių molekulinių komponentų, (b) padidintas fosfolipidų dvisluoksnio vaizdas ir (c) fosfolipido struktūra. Pateikta pagal Chen ir kt., Adv. Membr. 2022, 2, 10003, naudojant CC BY-NC-ND 4.0 licencijos sąlygomis.[12] *Paveiksle vartojami angliški terminai lietuviškai: Glycoprotein – glikoproteinas; Glycolipid – glikolipidas; Peripheral membrane protein – periferinis membranos baltymas; Integral membrane protein – integralinis membranos baltymas; Cholesterol – cholesterolis; Channel protein – kanalo baltymas; Phospholipid bilayer – fosfolipidų dvisluoksnis; Extracellular – ląstelės išorė; Intracellular – ląstelės vidus; Hydrophilic head – hidrofilinė galvutė; Hydrophobic tail – hidrofobinė uodegėlė; Phosphate – fosfatas; Glycerol – glicerolis; Saturated/unsaturated fatty acid – sotoji/nesotoji riebalų rūgštis.*

1.2. Modelinių membranų poreikis

Natūralios biologinės membranos yra itin sudėtingos, dinamiškos ir heterogeniškos sistemos, todėl jų tiesioginis tyrimas kelia reikšmingų metodologinių iššūkių. Pirma, membranos struktūra nėra homogeniška – joje formuojasi skirtingos lipidų ir baltymų sudėties bei savybių mikrodomenai, galintys lemti nevienodą lokalų membranos funkcionalumą.[8] Antra, membranos struktūrinė ir funkcinė būklė yra glaudžiai susijusi su ląstelės fiziologine būsena bei aplinkos sąlygomis, įskaitant osmosinį slėgį, joninę sudėtį, temperatūrą ir kitus fizikinius bei cheminius veiksnius.[13] Trečia, membranoje vykstantys procesai apima platų laiko skalių spektrą – nuo itin greitų molekulinių ir konformacinių pokyčių iki lėtesnių struktūrinių persitvarkymų, todėl jų visapusiškam charakterizavimui būtini didelio jautrumo ir tinkamos laikinės bei erdvinės skiriamosios gebos metodai.[14,15]

Dėl šių priežasčių XX a. pradėtos kurti dirbtinės membranos, leidžiančios imituoti natūralios membranos savybes, tačiau išvengti biologinės sistemos sudėtingumo. Tokios membranos yra supaprastintos, stabilios, lengvai atkuriamos ir tinkamos įvairiems elektrocheminiams metodams taikyti. Jos tapo vienu pagrindinių membranų biofizikos ir bioelektrochemijos tyrimų įrankių.[16] Modelinės membranos leido atsakyti į fundamentinius klausimus: i) koks yra elektroporacijos slenkstis lipidų dvisluoksnyje;[17] ii) kaip lipidų sudėtis (pvz., cholesterolio kiekis) veikia membranos stabilumą;[5] iii) kokį vaidmenį atlieka submembraninė struktūra;[18] iv) kaip elektrinis laukas sukelia porų formavimąsi ir kokia yra jų gyvavimo dinamika.[19]

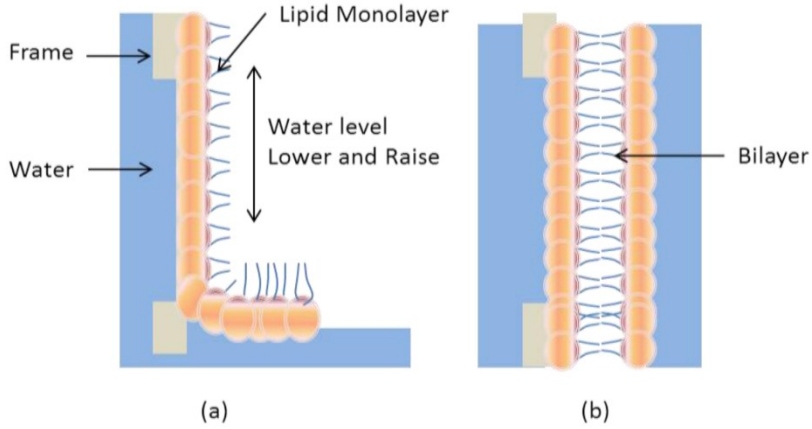
Istoriškai modelinių membranų raida vyko nuosekliai didėjančio stabilumo ir vis geresnio biologinio panašumo kryptimi – nuo laisvai pakabintų juodųjų lipidinių membranų (BLM), per kietu paviršiumi paremtas (sBLM) ir hibridines (hBLM) sistemas, iki tvirtinamų lipidinių dvisluoksnių (tBLM), turinčių submembraninį vandeninį rezervuarą. Kiekvienas naujas modelis buvo kuriamas siekiant pašalinti ankstesnių modelių trūkumus, tokius kaip trapumas, ribotas lipidų judrumas ar submembraninio tarpo nebuvimas, kartu išlaikant pakankamą sistemos paprastumą kiekybinei elektrocheminei analizei.[16,20]

1.3. Juodosios lipidinės membranos (BLM)

Pirmasis plačiai taikytas modelinės membranos tipas buvo juodoji lipidinė membrana (angl. *Black Lipid Membrane*, BLM), kurią 1962 m. aprašė Mueller ir bendraautoriai. Ji formuojama tarp dviejų fazių (dažniausiai vandeninės ir organinės), sudarant ploną lipidų dvisluoksnį. Šis dvisluoksnis atrodo

„juodas“, nes dėl mažo storio beveik nesukelia matomos šviesos interferencijos.[21]

Klasikinis BLM formavimo metodas – vadinamoji „tapymo“ technika (angl. *painting method*): lipidų tirpalas organiniame tirpiklyje (dažniausiai *n*-dekane arba chloroforme) teptuku užtepamas ant nedidelės (kelių šimtų mikrometrų–kelių milimetrų skersmens) angos hidrofobinėje pertvaroje (paprastai teflloninėje), skiriančioje dvi vandenines kameras (Pav. 2).[22] Tirpikliui palaipsniui difunduojant iš centrinės srities į angos kraštus, susiformuoja savaime plonėjantis lipidų dvisluoksnis, kurio storis (~4–5 nm) yra artimas natūralios plazminės membranos storiui. Taip suformuota BLM pasižymi santykinai dideliu specifiniu elektriniu pasipriešinimu (~10^8–10^9 Ω·cm^2) ir maža specifine elektrine talpa (~0,3–1 μF/cm^2), t. y. elektriniu požiūriu elgiasi panašiai kaip lipidų dvisluoksnis be membraninių baltymų.[23]



Pav. 2. Juodosios lipidinės membranos (BLM) formavimas: (**a**) vienkartinis mechaninio laikiklio panardinimas į lipidais padengtą vandenį ir jo ištraukimas lemia monosluoksnio susidarymą; (**b**) du kartus nuleidus substratą, vandens sąsajoje susidaro BLM. Pateikta pagal Khan, Dosoky ir Williams, Int. J. Mol. Sci. 2013, 14(11), 21561–21597, licencijuota pagal CC BY 3.0. 24.[24] *Paveiksle vartojami angliški terminai lietuviškai: Frame – rėmas; Water – vanduo; Lipid monolayer – lipidų monosluoksnis; Water level lower and raise – vandens lygio nuleidimas ir pakėlimas; Bilayer – dvisluoksnis.*

BLM buvo ypač svarbi ankstyviesiems membranos elektrinių savybių tyrimams: ji leido registruoti srovės svyravimus, susijusius su jonų kanalų veikimu, tirti medžiagų pernašą ir pirmą kartą eksperimentiškai patvirtinti elektroporacijos reiškinį. Į BLM inkorporuoti jonų kanalų baltymai (pvz., gramicidinas ir alameticinas) pirmą kartą leido tiesiogiai stebėti pavienių kanalų laidumo šuolius. Šie tyrimai padėjo pagrindus elektrofiziologijos raidai ir vėlesniam pleistrinio įspaudimo (angl. *patch-clamp*) metodo sukūrimui.[25,26]

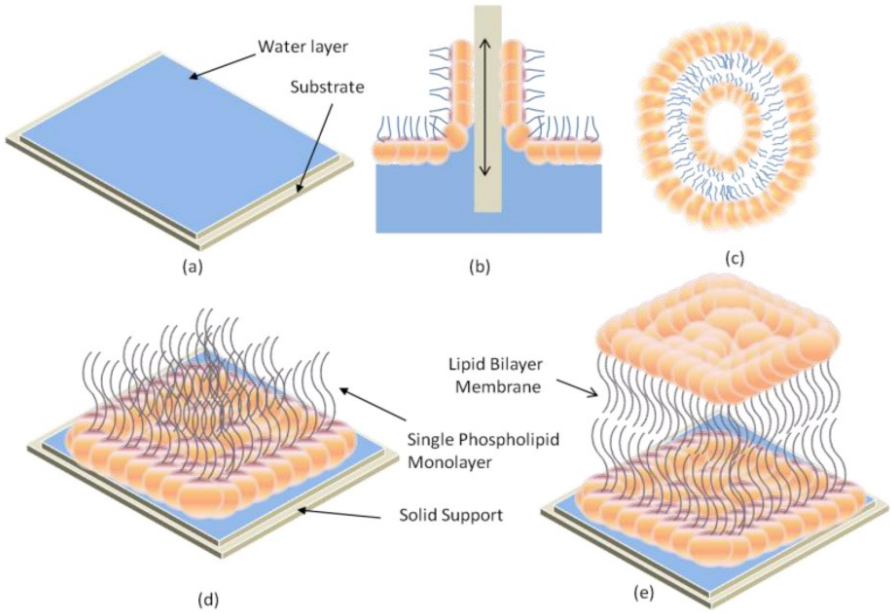
Tačiau BLM turėjo vieną esminį trūkumą – buvo itin trapios. Tokios membranos greitai suyra, yra jautrios mechaniniam ir elektriniam poveikiui, todėl netinka ilgalaikiams tyrimams: tipinė jų gyvavimo trukmė svyruoja nuo kelių minučių iki kelių valandų, o net ir nedidelis mechaninis sukrėtimas ar per didelis elektrinis potencialas gali sukelti negrįžtamą membranos plyšimą. Be to, šiai sistemai reikalinga dviejų elektrodų konfigūracija, kuri dar labiau riboja eksperimentinį lankstumą, o membranoje išliekantis organinio tirpiklio kiekis gali pakeisti jos storį ir elektrines savybes, palyginti su natūralia biologine membrana.[20]

1.4. Ant kieto paviršiaus palaikomos membranos (sBLM)

Siekiant padidinti membranų stabilumą, pradėtos kurti ant kieto pagrindo palaikomos membranos (angl. *solid-supported bilayer lipid membranes*, sBLM). Jos suteikė galimybę taikyti įvairius paviršiaus tyrimo metodus, tokius kaip atominės jėgos mikroskopija, kvarco mikrogravimetrijos matavimai ir elektrocheminė impedanso spektroskopija.[20]

sBLM paprastai formuojamos vienu iš dviejų būdų: naudojant Langmuir–Blodgett/Langmuir–Schaefer perkėlimo techniką, kai monosluoksniai nuosekliai perkeliami nuo oro–vandens sąlyčio paviršiaus ant kieto pagrindo, arba vezikulių fuzijos metodu, kai fosfolipidų vezikulės, priartėjusios prie hidrofilinio paviršiaus (pvz., stiklo, žėručio ar silicio oksido), spontaniškai suyra ir susilieja į ištisinį lipidų dvisluoksnį (Pav. 3). Tarp membranos ir kieto pagrindo išlieka tik labai plonas (~1–2 nm) vandens sluoksnis, kuris iš dalies izoliuoja lipidus nuo tiesioginio kontakto su paviršiumi, tačiau yra per plonas, kad jame galėtų tilpti didesni transmembraniniai baltymai ar jų funkciniai domenai.[20,27]

sBLM buvo atsparesnės už BLM, tačiau dėl glaudaus kontakto su paviršiumi jų lipidų judrumas buvo ribotas. Tai reiškė, kad sBLM buvo tinkamos ilgesniems tyrimams, tačiau negalėjo visiškai atkartoti biologinėms membranoms būdingo lankstumo. Šis trūkumas ypač ribojo galimybes į sBLM sėkmingai inkorporuoti didesnius integralinius membranų baltymus, kuriems reikalinga pakankama erdvė judėti ar keisti konformaciją. Todėl sBLM tapo naudingesnės tirti pačių lipidų sistemų fizikines savybes (fazinius virsmus, defektų susidarymą, elektroporacijos slenksčius) nei kaip funkcionalus membraninių baltymų inkorporavimo modelis.[28]



Pav. 3. Lipidų dvisluoksnės membranos formavimosi ant kieto pagrindo paviršiaus procesas, taikant Langmuir–Blodgett metodą ir pūslelių suliejimo procesą: *(**a**) substratas su vandens sluoksniu; (**b**) hidrofilinio substrato panardinimas ir ištraukimas per lipidų monosluoksnį; (**c**) pūslelė; (**d**) substratas su vienu lipidų monosluoksniu; (**e**) ant kieto pagrindo suformuota lipidų dvisluoksnė membrana (LBM). Pateikta pagal Khan, Dosoky ir Williams, Int. J. Mol. Sci. 2013, 14(11), 21561–21597, licencijuota pagal CC BY 3.0.*[24] *Paveiksle vartojami angliški terminai lietuviškai: Water layer – vandens sluoksnis; Substrate – substratas; Single phospholipid monolayer – vienas fosfolipidų monosluoksnis; Solid support – kietas pagrindas; Lipid bilayer membrane – lipidų dvisluoksnė membrana.*

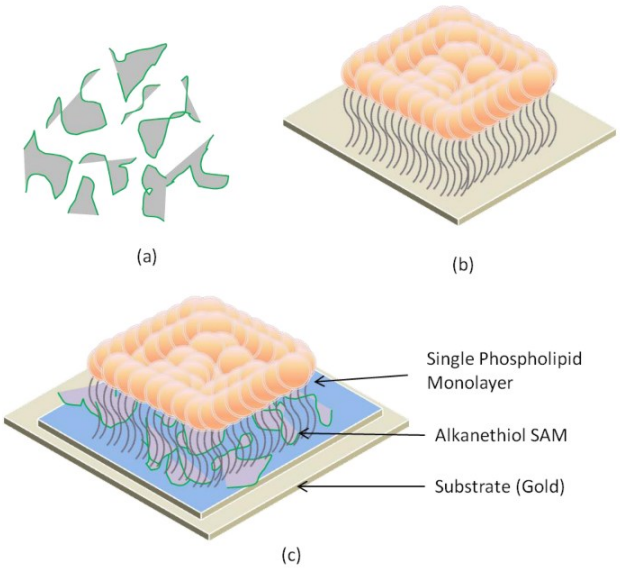
1.5. Hibridinės membranos (hBLM)

Kitas žingsnis buvo hibridinių membranų (angl. *hybrid bilayer lipid membranes*, hBLM) sukūrimas. Ši sistema sudaryta iš savitvarkio monosluoksnio (SAM), pritvirtinto prie paviršiaus, ir ant jo suformuoto fosfolipidų sluoksnio. Tokia struktūra suteikia žymiai didesnį mechaninį ir elektrinį stabilumą nei BLM ar sBLM, tačiau jos biologinis lankstumas išlieka ribotas.[29]

hBLM koncepcija grindžiama asimetrine dvisluoksnio architektūra: vieną membranos sluoksnį sudaro kovalentiškai prie paviršiaus prijungtos alkilo grandinės (dažniausiai alkantioliai ant aukso arba alkilsilanai, pvz., oktadeciltrichlorsilanas, ant metalų oksidų), o kitą – natūralių fosfolipidų monosluoksnis, susiformuojantis ant hidrofobinio SAM paviršiaus vezikulių fuzijos būdu arba taikant Langmuir–Blodgett techniką (Pav. 4).[29] Toks dizainas iš dalies imituoja natūraliai membranai būdingą vidinio ir išorinio

sluoksnių asimetriją, tačiau, skirtingai nei natūralioje membranoje, apatinis sluoksnis yra fiksuotas ir neturi lipidų judrumo. Gerai suformuota hBLM pasižymi didele specifine elektrine varža (dažnai 10^5–10^7 Ω·cm^2 eilės) ir santykinai stabilia elektrine talpa. Šie parametrai, registruojami elektrocheminės impedanso spektroskopijos būdu, tampa jautriais membranos vientisumo ir defektų indikatoriais.[30]

hBLM privalumas yra ir tai, kad SAM sluoksnio elektrinės izoliacijos savybės leidžia tarp membranos ir laidaus pagrindo registruoti itin mažus srovės pokyčius. Dėl šios priežasties tokios sistemos plačiai naudojamos kuriant biosensorius, jautrius membranos pralaidumo pokyčiams (pvz., toksinų ar detergentų poveikiui nustatyti). Vis dėlto būtent apatinio sluoksnio nejudrumas riboja hBLM gebėjimą atkurti visavertę, savaime besitvarkančią biologinę membraną.[30,31]



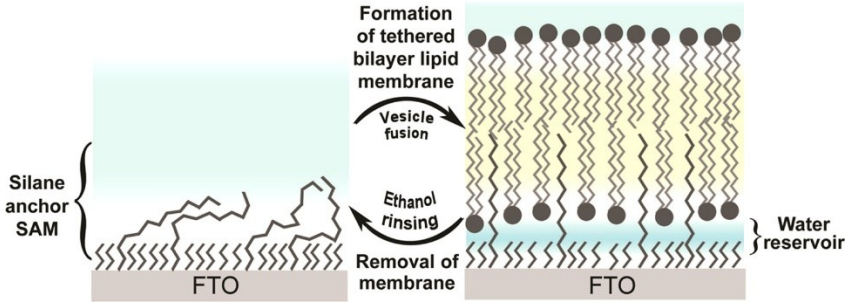
Pav. 4. Hibridinės lipidinės membranos iliustracija: *(**a**) alkanetiolio SAM sluoksnis; (**b**) vienas fosfolipidų monosluoksnis ant substrato paviršiaus; (**c**) alkanetiolio SAM sluoksniai išsidėsto ant aukso paviršiaus ir sudaro sąlygas lipidų monosluoksniui prisitvirtinti. Pateikta pagal Khan, Dosoky ir Williams, Int. J. Mol. Sci. **2013**, 14(11), 21561–21597, licencijuota pagal CC BY 3.0.[24] Paveiksle vartojami angliški terminai lietuviškai: Single phospholipid monolayer – vienas fosfolipidų monosluoksnis; Alkanethiol SAM – alkantiolio savitvarkis monosluoksnis; Substrate (gold) – substratas (auksas).*

1.6. Tvirtinamos membranos (tBLM)

Šiuolaikiniai tyrimai vis dažniau remiasi tvirtinamomis membranomis (angl. *tethered bilayer lipid membranes*, tBLM). Jose fosfolipidai yra

pritvirtinti prie paviršiaus per lanksčius inkarinius jungiklius, o tarp paviršiaus ir lipidų sluoksnio išlieka 1–2 nm storio vandeninis rezervuaras (Pav. 5).[18] tBLM dizainas turi keletą svarbių pranašumų: i) jos pasižymi dideliu elektriniu ir mechaniniu stabilumu; ii) išlaiko biologinėms membranoms būdingą lankstumą; iii) submembraninis rezervuaras imituoja citoplazminę aplinką; iv) leidžia tirti membranos atsaką į ilgalaikį elektrinį poveikį.[32]

„Inkaravimo“ jungikliai paprastai yra tiolipidai arba polimerinės-lipidinės hibridinės molekulės (pvz., WC14 tipo inkarai), kurių viename gale yra funkcinė grupė (dažniausiai tiolio), leidžianti prisijungti prie aukso ar kito laidaus paviršiaus, o kitame – hidrofobinė uodegėlė, integruojama į lipidų dvisluoksnį.[33] Tarp inkaro ir paties membranos sluoksnio dažnai naudojamas hidrofilinis (pvz., polietilenglikolio) tarpiklis, kuris suformuoja submembraninį vandeninį rezervuarą. Šis rezervuaras yra funkciškai itin svarbus: jis suteikia pakankamai erdvės transmembraniniams baltymams (jonų kanalams, receptoriams) inkorporuoti, nevaržant jų konformacinio judrumo. Tokios savybės neturi nei sBLM, nei hBLM, kuriose membrana glaudžiai priglunda prie kieto pagrindo arba turi standų apatinį sluoksnį.[18]



Pav. 5. Tvirtinamos lipidinės membranos (tBLM) formavimo ant silanizuoto fluoru legiruoto alavo oksido (FTO) paviršiaus schema. *Kairėje pavaizduotas silano inkarų savitvarkis monosluoksnis (SAM), suformuotas ant FTO paviršiaus. Vezikulių fuzijos būdu ant SAM sluoksnio susidaro tBLM, kurios apatiniame sluoksnyje tarp lipidinės membranos ir kieto pagrindo išlieka vandeninis rezervuaras (dešinėje paveikslo pusėje, mėlyna sritis). Plaunant etanoliu, susiformavusi membrana gali būti pašalinta, atidengiant pradinį SAM paviršių ir sudarant galimybę procesą pakartoti. Šaltinis: Gabriūnaitė, I.; Valinčius, G.; Žilinskas, A.; Valiūnienė, A. Tethered Bilayer Membrane Formation on Silanized Fluorine Doped Tin Oxide Surface. Journal of the Electrochemical Society* ***2022****, 169, 037515. © The Electrochemical Society. Atkurta gavus IOP Publishing Ltd. leidimą. Visos teisės saugomos.*[32] *Paveiksle vartojami angliški terminai lietuviškai: Silane anchor SAM – silano inkaro savitvarkis monosluoksnis; Formation of tethered bilayer lipid membrane – tvirtinamos lipidinės membranos formavimasis; Vesicle fusion – vezikulių fuzija; Ethanol rinsing – plovimas etanoliu; Removal of membrane – membranos pašalinimas; Water reservoir – vandeninis rezervuaras*.

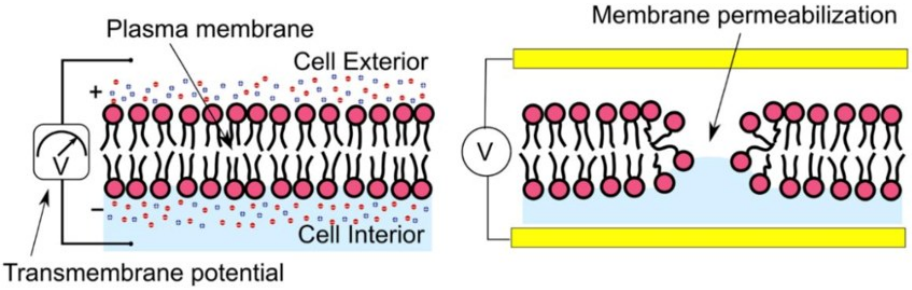
2. ELEKTROPORACIJA: MECHANIZMAI IR TAIKYMO SRITYS

2.1. Elektroporacijos fenomeno samprata

Elektroporacija – tai fizikinis procesas, kurio metu, veikiant ląstelės arba dirbtinės membranos fosfolipidų dvisluoksnį stipriu elektriniu lauku, jame susidaro laikinos arba nuolatinės poros. Šios struktūros padidina membranos pralaidumą įvairioms molekulėms ir jonams, kurie įprastomis sąlygomis negalėtų prasiskverbti pro lipidinį barjerą. Reiškinys yra universalus – jis stebimas tiek dirbtinėse membranose, pavyzdžiui, liposomose ar hibridiniuose dvisluoksniuose, tiek gyvose ląstelėse, įskaitant bakterijas, mieles ir žinduolių ląsteles.[14]

Pagrindinis molekulinis mechanizmas grindžiamas transmembraninio potencialo samprata. Kai elektrinis laukas membranoje indukuoja pakankamą potencialų skirtumą, viršijantį kritinę ribą (dažniausiai 0,2–1 V lipidiniams dvisluoksniams), fosfolipidų molekulės persitvarko ir susidaro hidrofilinės poros. Šios poros leidžia vandeniui bei ištirpusioms medžiagoms patekti į ląstelę arba pasišalinti iš jos. Šis procesas laikomas energetiškai aktyvuotu: membranoje spontaniškai susidarantys maži defektai, veikiami elektrinio lauko, gali plėstis ir pereiti į laidžią hidrofilinės poros būseną (Pav. 6).[19]

Kiekybiškai šį procesą aprašo I. G. Abidoro ir bendraautorių 1979 m. pasiūlytas „vandeninių porų formavimosi modelis“ (angl. *Aqueous Pore Formation Model*), kuris iki šiol laikomas vienu pagrindinių teorinių elektroporacijos aprašymo modelių.[19] Pagal šį modelį pora gali egzistuoti dviem energetiškai konkuruojančiomis būsenomis: hidrofobine (pereinamąja, defekto tipo) ir hidrofiline (visiškai susiformavusia, vandeniu užpildyta) būsena. Bendroji poros energija apibūdinama kaip dviejų priešingų dedamųjų suma: linijinio krašto įtempio (angl. *line tension*) energijos, kuri didėja proporcingai poros spinduliui ir skatina porą užsiverti, bei elektrinio lauko ir paviršiaus įtempio sąveikų sukeliamos energijos, kuri didėja proporcingai spindulio kvadratui ir skatina poros plėtimąsi. Šių dviejų dedamųjų pusiausvyra lemia kritinį poros spindulį: mažesnės už kritinį dydį poros savaime užsiveria, o jį viršijančios gali sparčiai plėstis, kol membrana suyra arba pora stabilizuojasi ties pusiausvyros dydžiu, priklausančiu nuo taikomo potencialo.[17,19] Šis modelis paaiškina, kodėl elektroporacija yra slenkstinis, o ne tolydus reiškinys, ir kodėl net nedidelis potencialo padidėjimas virš kritinės vertės gali lemti iš esmės skirtingą membranos elgseną.



Pav. 6. Elektroporacija. Scheminė diagrama, vaizduojanti plazminės membranos pažeidimo procesą, pagrįstą elektroporacijos principu. **Pateikta pagal** Zhang, K. S.; Nadkarni, A. V.; Paul, R. ir kt. Microfluidic Surgery in Single Cells and Multicellular Systems. Chem. Rev. **2022**, 122(7), 7097–7141, licencijuota pagal CC BY-NC-ND 4.0.[34] *Paveiksle vartojami angliški terminai lietuviškai: Plasma membrane – plazminė membrana; Cell exterior/interior – ląstelės išorė/vidus; Transmembrane potential – transmembraninis potencialas; Membrane permeabilization – membranos pralaidumo didinimas.*

Laiko atžvilgiu porų susidarymas vyksta itin sparčiai: pirminiai hidrofobiniai defektai membranoje atsiranda per keliasdešimt nanosekundžių nuo elektrinio lauko poveikio pradžios, o jų virtimas stabiliomis hidrofilinėmis poromis trunka nuo dešimčių iki šimtų mikrosekundžių.[14,35] Tai reiškia, kad net trumpi nanosekundinės trukmės impulsai (vadinamieji nsPEF, angl. *nanosecond pulsed electric fields*) gali sukelti membranos pralaidumo pokyčius. Tačiau tokiu atveju dažniausiai susidaro daugybė mažesnių porų, o ne keletas didelių, todėl molekulių pernašos selektyvumas skiriasi nuo poveikio, sukeliamo ilgesnės trukmės mikrosekundiniais ar milisekundiniais impulsais.[36]

2.2. Grįžtama ir negrįžtama elektroporacija

Priklausomai nuo elektrinio impulso parametrų ir membranos savybių, elektroporacija gali būti grįžtama arba negrįžtama.[14]

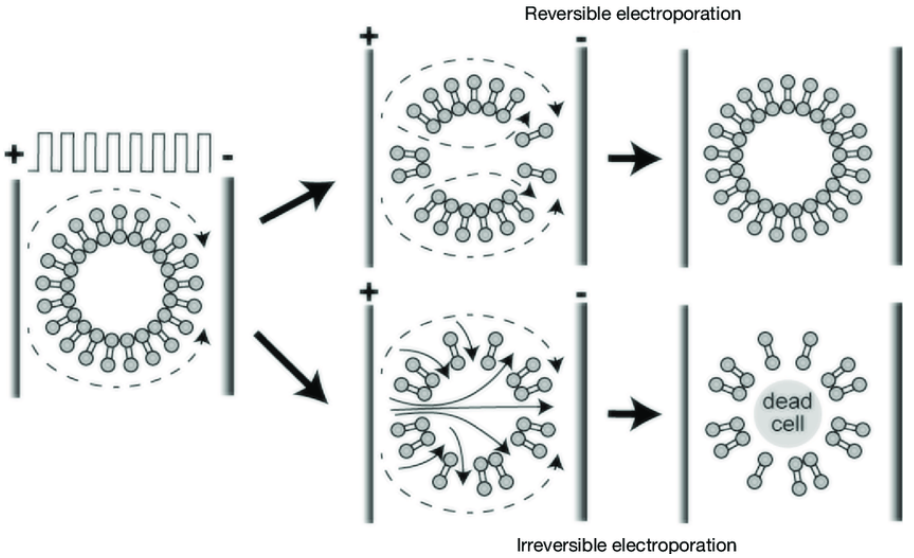
Grįžtamos elektroporacijos metu susidariusios poros laikui bėgant užsiveria, o membranos vientisumas atsistato. Šis procesas leidžia į ląsteles įnešti įvairias medžiagas – nuo mažų molekulių iki didelių baltymų ar nukleorūgščių. Dėl šios savybės grįžtama elektroporacija yra vienas svarbiausių metodų genų inžinerijoje ir vaistų pernašoje, nes ji leidžia trumpam padidinti membranos pralaidumą nesukeliant ilgalaikės žalos ląstelei.[14,37]

Membranos atsistatymas po grįžtamos elektroporacijos vyksta ne vienu homogenišku procesu, o keliais nuosekliais etapais, kurių trukmė gali skirtis

keliomis eilėmis.[38] Pirmasis etapas – staigus porų dydžio sumažėjimas, trunkantis trumpiau nei 1 sekundę ir susijęs su greita elektrinio lauko poveikio sukeltų įtempių bei energijos pokyčių relaksacija nutraukus impulsą. Antrasis etapas – lėtas, difuzijos kontroliuojamas porų mažėjimas, trunkantis nuo kelių iki keliolikos minučių, kurio metu lipidų molekulės palaipsniui grįžta į energetiškai palankią uždaros membranos konfigūraciją. Trečiasis, galutinis etapas – visiškas porų išnykimas ir membranos elektrinių savybių (varžos, talpos) atsistatymas iki pradinio lygio. Šis procesas gali trukti ilgiau nei 10 minučių, o kai kuriais atvejais – ir kelias valandas, priklausomai nuo membranos tipo bei elektrinio impulso intensyvumo.[38,39] Ši trifazė dinamika yra svarbi metodologiniu požiūriu, nes rodo, kad membranos vientisumo vertinimas praėjus tik kelioms sekundėms ar minutėms po impulso gali klaidingai rodyti negrįžtamą pažeidimą, nors atsistatymo procesas dar nėra pasibaigęs.

Negrįžtama elektroporacija pasireiškia tada, kai poros tampa per didelės arba jų susidaro tiek daug, kad membrana praranda barjerinę funkciją ir ląstelė žūsta.[40] Šis reiškinys naudojamas tais atvejais, kai siekiama selektyviai sunaikinti nepageidaujamas ląsteles, pavyzdžiui, navikinius audinius, arba inaktyvuoti mikroorganizmus maisto ir aplinkosaugos pramonėje. Klinikinėje praktikoje negrįžtama elektroporacija (angl. *Irreversible Electroporation*, IRE) per pastarąjį dešimtmetį tapo pripažintu minimaliai invaziniu navikų abliacijos metodu (Pav. 7), ypač taikomu tais atvejais, kai šiluminės abliacijos metodų (radiodažninės abliacijos, krioabliacijos) galimybės yra ribotos dėl šalia esančių stambių kraujagyslių ar tuščiavidurių organų (pvz., gydant kasos vėžį). Kadangi IRE mechanizmas yra nešiluminis, jis pažeidžia ląstelių membranas, tačiau leidžia išsaugoti kolageninį jungiamojo audinio karkasą bei stambesnes kraujagysles.[41]

Svarbu pažymėti, kad riba tarp grįžtamos ir negrįžtamos elektroporacijos nėra griežtai fiksuota konstanta. Ji priklauso nuo konkretaus elektrinio impulso parametrų derinio (lauko stiprio, trukmės ir jų sąveikos), taip pat nuo ląstelės tipo bei membranos savybių. Todėl vienas esminių metodologinių iššūkių yra tiksliai nustatyti šią ribą kiekvienai tiriamai sistemai atskirai.[42]



Pav. 7. Negrįžtamai ir grįžtamai elektroporuotų zonų išsidėstymo po negrįžtamos elektroporacijos (IRE) abliacijos procedūros schema. *Negrįžtamos elektroporacijos zonoje įvyksta visiška ląstelių žūtis, o periferinėje zonoje esančios ląstelės pažeidžiamos minimaliai ir po IRE abliacijos procedūros gali atsikurti.* ***Pateikta pagal*** *Eresen, A.; Yang, J.; Scotti, A. ir kt. Combination of Natural Killer Cell-Based Immunotherapy and Irreversible Electroporation for the Treatment of Hepatocellular Carcinoma. Ann. Transl. Med.* ***2021****, 9(13), 1089, licencijuota pagal CC BY-NC-ND 4.0.*[43] *Paveiksle vartojami angliški terminai lietuviškai: Reversible/irreversible electroporation – grįžtama/negrįžtama elektroporacija; dead cell – negyva ląstelė.*

2.3. Elektroporacijos parametrus lemiantys veiksniai

Elektroporacijos rezultatas priklauso nuo daugelio tarpusavyje susijusių parametrų, kuriuos galima suskirstyti į fizinius, cheminius ir biologinius veiksnius.[14]

Svarbiausi fiziniai parametrai yra elektrinio lauko stipris, impulso trukmė ir forma, impulsų skaičius bei elektrodo geometrija. Lauko stipris (V/cm) tiesiogiai lemia indukuojamo transmembraninio potencialo dydį: didesnis elektrinis laukas skatina spartesnį porų susidarymą. Impulso trukmė (nuo nanosekundžių iki milisekundžių) turi įtakos tam, ar susidariusios poros išliks mažos ir trumpalaikės, ar taps didesnės bei stabilesnės. Impulso forma (stačiakampė, eksponentinė, bipolinė) veikia membranos įkrovimo dinamiką ir elektrinio lauko pasiskirstymą. Impulsų skaičius gali sustiprinti poveikį, nes kartotiniai elektriniai stimulai didina porų susidarymo tikimybę.[42] Galiausiai, elektrodo dydis, forma ir atstumas iki membranos yra ypač svarbūs lokalizuotos elektroporacijos atveju: mažesni ir tinkamai sukonfigūruoti elektrodai leidžia suformuoti labiau apribotas poveikio zonas, o didesni

elektrodai dažniausiai sukuria platesnį, tačiau mažiau lokalizuotą elektrinį lauką.[14]

Svarbūs yra ir impulso poliškumas bei pasikartojimo dažnis. Bipoliniai impulsai (kai naudojamos priešingos poliškumo fazės) vis dažniau taikomi klinikinėje IRE praktikoje, nes gali sumažinti nepageidaujamą raumenų susitraukimą procedūros metu.[44] Tačiau jų poveikis porų susidarymo efektyvumui priklauso nuo konkrečių impulso parametrų, įskaitant dažnį ir trukmę, todėl gali skirtis nuo vienpolių impulsų sukeliamo poveikio. Be to, eksperimento metu membranos temperatūra yra reikšmingas, tačiau dažnai nepakankamai įvertinamas veiksnys. Aukštesnė temperatūra didina lipidų dvisluoksnio takumą, todėl gali sumažinti kritinį pramušimo potencialą ir pagreitinti porų atsistatymą. Dėl to tas pats elektrinis impulsas skirtingomis temperatūros sąlygomis gali sukelti iš esmės skirtingą rezultatą – grįžtamą arba negrįžtamą membranos pažeidimą.[6,44]

Membranos reakcija į elektroporaciją priklauso nuo aplinkos terpės sudėties, t. y. nuo cheminių veiksnių. Jonų koncentracija ir terpės laidumas lemia srovės pasiskirstymą bei galimus šiluminius efektus. Skirtingas pH gali paveikti lipidų įkrovą ir porų stabilumą. Osmosinis slėgis reguliuoja vandens judėjimą per membraną, todėl gali didinti arba mažinti ląstelės jautrumą elektriniam poveikiui. Taip pat svarbus redokso tarpininkų buvimas: kai kurie iš jų gali palengvinti srovės tekėjimą, tačiau kartu inicijuoti šalutinius cheminius procesus, keičiančius membranos savybes.[14]

Kiekviena ląstelė pasižymi specifiniu dydžiu, forma ir membranos sudėtimi – šiuos veiksnius galima apibendrintai vadinti biologiniais parametrais. Pavyzdžiui, didesnės ląstelės kritinį transmembraninį potencialą pasiekia esant silpnesniam elektriniam laukui, nes pagal $\Delta\Psi m = 1{,}5 \cdot E \cdot R \cdot \cos\theta$ formulę indukuojamas transmembraninis potencialas yra proporcingas ląstelės spinduliui.[14] Lipidų sudėtis, ypač cholesterolio kiekis, daro didelę įtaką membranos standumui ir pralaidumo slenksčiui: didesnis cholesterolio kiekis paprastai didina membranos atsparumą elektriniam poveikiui. Membraninių baltymų buvimas taip pat gali pakeisti elektroporacijos eigą – jie gali sudaryti papildomus laidumo kelius arba, priešingai, sustiprinti barjerinę membranos funkciją.[45] Todėl elektroporacija yra procesas, stipriai priklausantis nuo ląstelės tipo ir jos fiziologinės būklės.

Be to, formulėje $\Delta\Psi m = 1{,}5 \cdot E \cdot R \cdot \cos\theta$ esantis kampinis narys $\cos\theta$ atskleidžia dar vieną svarbų, dažnai nepakankamai įvertinamą aspektą – elektroporacijos priklausomybę nuo ląstelės orientacijos elektrinio lauko atžvilgiu. Didžiausias transmembraninis potencialas indukuojamas tose vietose, kur ląstelės paviršiaus normalė yra lygiagreti elektrinio lauko krypčiai ($\theta = 0\,°$ arba $180\,°$, t. y. „poliuose“ elektrinio lauko atžvilgiu), o ties „pusiaujo“

sritimi ($\theta = 90\ °$) potencialas artėja prie nulio.[46] Todėl net ir vienalyčiame elektriniame lauke ta pati ląstelė patiria erdviškai nevienodą poveikį, o porų susidarymas dažniausiai inicijuojamas tose paviršiaus srityse, kuriose indukuojamas didžiausias transmembraninis potencialas. Nesferinės formos ląstelėms (pavyzdžiui, pailgoms bakterijoms ar pumpuruojančioms mielėms) šis geometrinis efektas tampa dar sudėtingesnis, nes vietinis kreivumo spindulys skirtingose ląstelės vietose skiriasi. Dėl to vien ląstelės forma gali lemti nevienodą jautrumą elektroporacijai skirtinguose jos regionuose.[14,42]

2.4. Elektroporacijos taikymo sritys

Elektroporacija, iš pradžių tirta kaip fundamentinis biofizikinis reiškinys, šiandien yra plačiai taikoma technologija, apimanti biomedicinos, biotechnologijos, maisto pramonės ir aplinkosaugos sritis. Jos universalumas grindžiamas gebėjimu kontroliuojamai keisti ląstelių membranų pralaidumą, todėl elektroporacija gali būti naudojama tiek medžiagų pernašai į ląsteles, tiek jų inaktyvacijai ar struktūriniam pažeidimui.[14]

Biomedicinoje elektroporacija tapo svarbiu įrankiu, taikomu vaistų ir genetinės medžiagos pernašai į ląsteles. Elektrochemoterapijoje elektriniai impulsai derinami su chemoterapiniais preparatais, siekiant padidinti jų patekimą į ląsteles ir sustiprinti gydomąjį poveikį.[37] Genų terapijoje elektroporacija leidžia į ląsteles įvesti nukleorūgštis nenaudojant virusinių vektorių, o vakcinologijoje ji taikoma nukleorūgščių vakcinų kūrimui ir imuninių ląstelių genetiniam modifikavimui.[37] Ypač svarbi šiuolaikinė elektroporacijos taikymo kryptis yra negrįžtama elektroporacija (IRE), naudojama onkologijoje kaip minimaliai invazinis, nešiluminis navikų abliacijos metodas.[40,44] Kadangi IRE poveikis nėra grindžiamas intensyviu audinių kaitinimu, ši technologija gali būti taikoma šalia stambių kraujagyslių, tulžies latakų ir kitų temperatūrai jautrių anatominių struktūrų, kuriose šiluminiai abliacijos metodai, tokie kaip radiodažninė ar mikrobangų abliacija, gali būti riboti dėl aplinkinių audinių pažeidimo rizikos.[41]

Biotechnologijoje elektroporacija plačiai naudojama mikroorganizmų genetinei transformacijai. Ji sudaro galimybę efektyviai į bakterijas, mieles ir kitus mikroorganizmus įvesti genetinę medžiagą, todėl yra svarbi kuriant rekombinantinių baltymų gamybos sistemas bei genetiškai modifikuotus pramoninės biotechnologijos mikroorganizmų kamienus.[47] Tokie kamienai naudojami fermentų, organinių rūgščių, biokuro ir kitų biotechnologiškai vertingų produktų gamybai. Elektroporacija taip pat tiriama biosensorių kūrimo srityje, kur kontroliuojamas membranos pralaidumo pokytis gali būti panaudojamas kaip signalinis mechanizmas. Pramoniniuose

biotechnologiniuose procesuose transformacijos efektyvumas yra vienas iš veiksnių, lemiančių tolesnio proceso našumą ir ekonominį efektyvumą.[39]

Maisto pramonėje elektroporacijos principai dažniausiai realizuojami taikant impulsinius elektrinius laukus (angl. Pulsed Electric Field, PEF). Ši technologija naudojama skysčių apdorojimui, mikroorganizmų inaktyvacijai ir žaliavų struktūros modifikavimui. Kadangi PEF procesai gali būti vykdomi santykinai žemoje temperatūroje, jie leidžia sumažinti terminio apdorojimo poveikį maisto produktų jutiminėms ir maistinėms savybėms, kartu užtikrinant reikiamą mikrobiologinį stabilumą. Elektroporacija taip pat gali būti taikoma siekiant pagerinti sulčių ekstrakciją, palengvinti bioaktyviųjų junginių išskyrimą ir intensyvinti tam tikrus fermentacijos procesus. Dėl šių savybių PEF technologijos yra tiriamos ir taikomos įvairių skystų bei augalinės kilmės maisto produktų apdorojimui.[48]

Aplinkosaugos srityje elektroporacija tiriama kaip priemonė mikroorganizmų inaktyvacijai, nuotekų apdorojimui, biomasės paruošimui ir biologinių procesų efektyvinimui. Elektrinis poveikis, sukeliantis ląstelių membranų pralaidumo padidėjimą arba jų pažeidimą, gali palengvinti intraceliulinių komponentų išsiskyrimą ir taip pagerinti tolesnius biologinius ar cheminius procesus. Ypač daug dėmesio skiriama elektroporacijos taikymui mikrodumblių biomasės perdirbimo procesuose, kai ląstelių struktūrų pažeidimas gali palengvinti lipidų ir kitų vertingų komponentų ekstrakciją. Tokiu būdu elektroporacija gali būti naudojama kaip alternatyva cheminiams ląstelių ardymo metodams, potencialiai mažinant cheminių reagentų poreikį ir proceso poveikį aplinkai.[49]

Taigi, elektroporacijos taikymo sričių įvairovę lemia galimybė kontroliuoti membranos pralaidumą ir, priklausomai nuo elektrinio poveikio parametrų, sukelti grįžtamus arba negrįžtamus jos struktūros pokyčius. Dėl to elektroporacija yra reikšminga ne tik praktinėse technologijose, bet ir fundamentiniuose membranų biofizikos tyrimuose, kuriuose siekiama nustatyti ryšį tarp elektrinio lauko parametrų, membranos struktūros ir jos atsako. Ši sąsaja ypač svarbi kuriant lokalizuoto elektrinio poveikio metodus, leidžiančius kontroliuoti elektroporacijos mastą erdvėje ir laike.[14]

2.5. Dirbtinių fosfolipidinių membranų vaidmuo elektroporacijos tyrimuose

Nors elektroporacija jau seniai taikoma praktikoje, jos molekulinis mechanizmas vis dar nėra iki galo išaiškintas. Gyvos ląstelės yra heterogeniškos sistemos – jų membranų sudėtyje yra ne tik lipidų, bet ir baltymų, citoskeleto elementų bei įvairių kitų struktūrinių komponentų. Dėl

šios priežasties eksperimentiniai duomenys dažnai yra sudėtingi interpretuoti.[50]

Šis interpretacijos sudėtingumas kyla dėl to, kad gyvoje ląstelėje registruojamas elektrinis ar elektrocheminis atsakas atspindi ne vien lipidų dvisluoksnio savybes, bet visos ląstelės, kaip sudėtingos bioelektrocheminės sistemos, elgseną. Plazminė membrana elektriniu požiūriu veikia kartu su citoskeletu, kuris gali mechaniškai stabilizuoti membraną ir riboti porų augimą, su organelių membranomis, kurios taip pat gali būti veikiamos elektrinio lauko, bei su aktyviais jonų transporto mechanizmais (siurbliais ir kanalais), kurie reaguoja į membranos potencialo pokyčius ir siekia atkurti joninę pusiausvyrą.[51] Todėl tiesiogiai iš gyvų ląstelių eksperimentų nustatyti elektroporacijos parametrai – kritinis potencialas, porų dydis ar atsistatymo trukmė – negali būti vienareikšmiškai priskirti vien lipidų dvisluoksnio savybėms, nes jie atspindi kelių tarpusavyje susijusių procesų bendrą rezultatą.

Dėl šios priežasties itin svarbu taikyti modelines membranų sistemas, tokias kaip hibridinės (hBLM) ir tvirtinamosios (tBLM) membranos, kurios leidžia kontroliuojamomis sąlygomis tirti elektroporacijos slenksčius, porų formavimosi dinamiką ir atsistatymo procesus. Šios sistemos leidžia sumažinti biologinio sudėtingumo įtaką ir sutelkti dėmesį į fundamentines lipidų dvisluoksnio fizikines savybes.[16] Metodologiniu požiūriu dirbtinių membranų taikymas atitinka klasikinį biofizikos principą „nuo paprasto prie sudėtingo“: pirmiausia elektroporacijos dėsningumai nustatomi kontroliuojamoje ir gerai apibrėžtoje sistemoje (dirbtinėje membranoje), o vėliau šie rezultatai lyginami su duomenimis, gautais vis sudėtingesnėse biologinėse sistemose (gyvose ląstelėse, audiniuose).

Elektroporacija mielių ląstelėse yra žinoma literatūroje. A. Stirkės ir bendraautorių darbuose parodyta, kad nanosekundinės trukmės didelės galios elektriniai impulsai gali padidinti *Saccharomyces cerevisiae* ląstelių sienelės pralaidumą ir taip sudaryti sąlygas didelės molekulinės masės organiniams junginiams patekti į ląsteles.[52] Vėlesniame tos pačios grupės darbe nagrinėta sąsaja tarp mielių ląstelių sienelės akytumo ir plazminės membranos pralaidumo po impulsinio elektrinio lauko (PEF) poveikio.[53] Šiuose tyrimuose naudota dviejų elektrodų sistema, kurioje elektrinis poveikis taikytas visai ląstelių populiacijai.

3. SKENUOJANČIOJI ELEKTROCHEMINĖ MIKROSKOPIJA (SECM) IR ELEKTROCHEMINĖ IMPEDANSO SPEKTROSKOPIJA (EIS)

3.1. SECM metodo atsiradimas ir veikimo principai

Skenuojančioji elektrocheminė mikroskopija (angl. *Scanning Electrochemical Microscopy*, SECM) yra modernus elektroanalitinis metodas, sukurtas 1989 m. A. J. Bardo grupėje. SECM atsiradimas laikomas svarbiu lūžiu elektrochemijos srityje, nes šis metodas sujungė klasikinę elektroanalizę su skenuojančiųjų zondų mikroskopijos principais.[54-57]

Metodologiškai SECM ištakos siejamos su 1981–1982 m. sukurta skenuojančiąja tuneline mikroskopija (STM), kuri parodė, kad itin mažas zondas gali būti naudojamas lokalioms paviršiaus savybėms tirti.[54,58] Vis dėlto SECM, priešingai nei STM ar vėliau sukurta atominės jėgos mikroskopija (AFM), nėra pagrįsta tunelinės srovės ar mechaninės sąveikos registravimu. SECM atveju pagrindinis informacijos šaltinis yra Faradėjaus srovė, kylanti dėl elektrocheminių krūvio pernašos procesų.[55] Todėl metodas gali būti taikomas skystoje terpėje ir suteikia tiesiogiai su vietiniais cheminiais bei elektrocheminiais procesais susijusią informaciją, o ne vien topografinį paviršiaus vaizdą.[59] Ši savybė ypač svarbi biologinių sistemų tyrimuose, kuriuose matavimai turi būti atliekami vandeninėje terpėje, artimoje fiziologinėms sąlygoms, o tiriamieji objektai dažnai yra minkšti, deformuojami ir elektrochemiškai aktyvūs.[56,59-61]

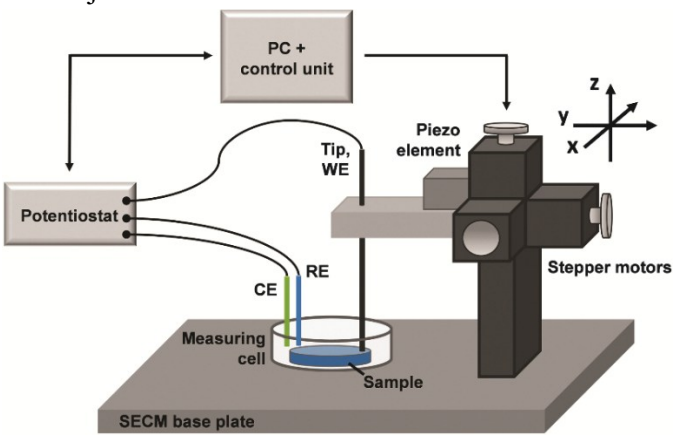
SECM veikimo principas pagrįstas ultramikroelektrodo (UME), veikiančio kaip elektrocheminio zondo, skenavimu virš tiriamo paviršiaus. UME dažniausiai yra diskinės geometrijos, o jo matmenys gali siekti nuo kelių dešimčių mikrometrų iki submikrometrinio dydžio. Dėl mažo elektrodo paviršiaus ploto UME registruojamos nedidelės srovės, todėl galima tirti lokalizuotus elektrocheminius procesus ir pasiekti didelę erdvinę skiriamąją gebą.[54-56,59,62] UME elektrocheminis elgesys iš esmės skiriasi nuo makroskopinių elektrodų: mažėjant elektrodo matmenims, vis didesnę reikšmę įgyja radialinė medžiagos pernaša, todėl difuzijos srautas į elektrodo paviršių tampa nebe vien planarinis. Dėl tokios difuzijos geometrijos mikro- ir ultramikroelektroduose galima greitai pasiekti pastoviosios būsenos (angl. *steady-state*) srovę.[62] Pastoviosios būsenos srovė diskinio UME atveju priklauso nuo elektrodo spindulio, elektroaktyviosios medžiagos koncentracijos ir difuzijos koeficiento; idealiomis difuzijos kontroliuojamos reakcijos sąlygomis ji aprašoma ryšiu:

$$I_{ss}=4nFDCr \quad (1)$$

kur n yra perduodamų elektronų skaičius, F – Faradėjaus konstanta, D – difuzijos koeficientas, C – elektroaktyviosios medžiagos koncentracija, o r – elektrodo disko spindulys.[63] Tokia pastoviosios būsenos charakteristika yra viena svarbiausių UME savybių, leidžiančių atlikti kiekybinius, jautrius ir gerai atkuriamus elektrocheminius matavimus bei tirti greitus lokalizuotus elektrocheminius procesus.[62,64]

UME paprastai naudojamas trijų elektrodų elektrocheminėje sistemoje, kurią sudaro darbo elektrodas (UME), palyginamasis elektrodas, pavyzdžiui, Ag/AgCl, ir pagalbinis elektrodas, dažniausiai platinos viela (Pav. 8). Potenciostatas palaiko nustatytą darbo elektrodo potencialą, o UME tekančios srovės pokyčiai registruojami priklausomai nuo elektrodo padėties, atstumo iki tiriamo paviršiaus ir jame vykstančių elektrocheminių procesų.[55,62]

Toks veikimo principas leidžia SECM naudoti ne tik paviršiaus elektrocheminėms savybėms charakterizuoti, bet ir medžiagų pernašos procesams, reakcijų kinetikai bei lokaliam elektrocheminiam aktyvumui tirti. Be to, kontroliuojant UME potencialą, galima lokalizuotai inicijuoti arba modifikuoti elektrocheminius procesus pasirinktose paviršiaus srityse.[59] Galimybė vienoje sistemoje derinti lokalų elektrocheminio aktyvumo matavimą ir kontroliuojamą elektrinį poveikį paviršiui yra ypač perspektyvi tiriant procesus, kurių eigą lemia elektrinis laukas ir kuriems svarbi tiksli poveikio lokalizacija.[61,65]



Pav. 8. SECM įrenginio schema. Šaltinis: *Ventosa ir Schuhmann, Phys. Chem. Chem. Phys.* ***2015****, 17(43), 28441–28450, licencijuota pagal CC BY 3.0.*[66] *Paveiksle vartojami angliški terminai lietuviškai: PC + control unit – kompiuteris ir valdymo blokas; Potentiostat – potenciostatas; Piezo element – pjezoelementas; Stepper motors – žingsniniai varikliai; Tip, WE – zondas (darbinis elektrodas); CE – pagalbinis elektrodas; RE – palyginamasis elektrodas; Measuring cell – matavimo celė; Sample – mėginys; SECM base plate – SECM pagrindo plokštė.*

3.2. SECM veikimo režimai

SECM gali būti taikoma skirtingais veikimo režimais, leidžiančiais gauti įvairaus pobūdžio informaciją apie tiriamąją sistemą. Grįžtamojo ryšio režimu (angl. feedback mode) ultramikroelektrodas (UME) priartinamas prie tiriamo paviršiaus ir registruojamas srovės pokytis, priklausantis nuo elektrodo ir paviršiaus sąveikos. Jei paviršius yra elektrochemiškai aktyvus arba gali regeneruoti redokso tarpininką, oksiduotos ar redukuotos rūšys atkuriamos ant paviršiaus, todėl registruojama srovė padidėja ir stebimas teigiamas grįžtamasis ryšys. Priešingai, jei paviršius yra nelaidus arba riboja elektrocheminę sąveiką, redokso rūšies regeneracija nevyksta, difuzijos srautas sumažėja ir registruojama srovė mažėja, todėl pasireiškia neigiamas grįžtamasis ryšys. Šis režimas dažniausiai naudojamas paviršiaus elektrocheminiam aktyvumui, laidumui ir defektams tirti. Grįžtamojo ryšio principu taip pat registruojamos artėjimo kreivės (angl. approach curves), parodančios srovės priklausomybę nuo UME ir paviršiaus atstumo. Tokios kreivės yra ypač naudingos vertinant membranos vientisumą ir heterogeniškumą.[54-57,59]

Generavimo–surinkimo režimu (angl. generation/collection mode) viena elektrocheminė sistema generuoja tiriamąją rūšį, o jos susidarymas arba transportas registruojamas kitame elektrode ar substrato paviršiuje. Šis režimas leidžia tirti reakcijų kinetiką, fermentinį aktyvumą ir medžiagų pernašos procesus. Atsižvelgiant į tai, kuris elektrodas generuoja, o kuris surenka tiriamą redokso rūšį, išskiriami substrato generavimo–zondo surinkimo (angl. substrate generation/tip collection, SG/TC) ir zondo generavimo–substrato surinkimo (angl. tip generation/substrate collection, TG/SC) režimai. Toks eksperimentinės geometrijos pasirinkimas ypač svarbus tiriant biologines sistemas, kai siekiama atskirti biologinį signalą nuo galimo paties zondo poveikio.[54-57,59]

Tiesioginiu režimu (angl. direct mode) UME naudojamas kaip pagalbinis elektrodas, o tiriamasis paviršius tampa darbo elektrodu. Tokiu būdu tarp UME ir substrato sukuriamas lokalus elektrinis laukas, leidžiantis selektyviai modifikuoti paviršių, pavyzdžiui, atlikti vietinį ėsdinimą ar medžiagų nusodinimą. Nors šis režimas daugiausia buvo taikomas medžiagotyroje ir paviršių mikrofabrikavime, jo principas – lokalizuoto elektrinio lauko sukūrimas tarp UME ir substrato – gali būti pritaikomas ir tikslinei membranos elektroporacijai. Tokiu atveju UME tampa lokalizuotu elektrinio poveikio šaltiniu virš nepoliarizuoto ir su išorine elektrine grandine tiesiogiai nesujungto ląstelių ar membranos sluoksnio.[54-57,59]

Pastovaus aukščio režimu (angl. constant height mode) UME skenuoja paviršių x ir y kryptimis, išlaikydamas apytiksliai pastovų atstumą nuo tiriamo objekto. Šis režimas leidžia sudaryti elektrocheminį paviršiaus žemėlapį ir nustatyti defektus, heterogeniškumą bei lokalius elektrocheminio aktyvumo skirtumus. Erdvinė skiriamoji geba šiuo atveju yra glaudžiai susijusi su UME ir paviršiaus atstumu: siekiant jautriai registruoti lokalius paviršiaus pokyčius, šis atstumas paprastai turi būti panašus į UME skersmenį arba už jį mažesnis.[54-57,59]

Šių režimų derinimas leidžia gauti išsamesnę informaciją apie tiriamąją sistemą – nuo lokalios elektrocheminės veiklos iki erdvinio paviršiaus heterogeniškumo.[54-57,59]

3.3. SECM privalumai ir ribojimai

SECM turi keletą esminių privalumų, dėl kurių ji yra ypač tinkama biologinių sistemų tyrimams. Eksperimentai gali būti atliekami skystoje terpėje, todėl metodas gali būti pritaikytas biologinėms sistemoms artimomis sąlygomis ir leidžia tirti elektrochemiškai aktyvius procesus jų natūralioje arba fiziologiškai artimoje aplinkoje.[61,65] Be to, dėl ultramikroelektrodo (UME) mažų matmenų ir galimybės tiksliai kontroliuoti jo padėtį tiriamo paviršiaus atžvilgiu, SECM pasižymi didele erdvine skiriamąja geba ir leidžia analizuoti lokalius pavienių ląstelių bei jų paviršiaus procesus.[64] Ši savybė ypač svarbi tais atvejais, kai siekiama ne tik nustatyti bendrą biologinės sistemos atsaką, bet ir lokalizuoti elektrocheminio aktyvumo ar membranos savybių pokyčius konkrečioje paviršiaus srityje. SECM taip pat gali būti derinama su kitais skenuojančiosios mikroskopijos ir bioanalitiniais metodais, pavyzdžiui, atominės jėgos mikroskopija (AFM), skenuojančiąja jonų laidumo mikroskopija (SICM) ar optiniais metodais, taip suteikiant galimybę susieti elektrocheminę informaciją su struktūriniais ir funkciniais tiriamos sistemos pokyčiais.[61,65] Svarbus SECM privalumas yra ir tai, kad elektrocheminiam signalui registruoti nereikalingas fluorescencinis ar kitas optinis žymėjimas. Dėl to metodas gali būti taikomas gyvoms ląstelėms, išvengiant papildomo žymenų poveikio tiriamai sistemai, o tinkamai parinkus eksperimento sąlygas galima pakartotinai stebėti biologinio objekto elektrocheminę veiklą ir jos kitimą laike.[64]

Nepaisant šių privalumų, SECM turi ir tam tikrų metodologinių apribojimų. Vienas svarbiausių jų yra santykinai ribotas erdvinio skenavimo greitis. Ypač tiriant didesnius paviršiaus plotus arba atliekant didelės erdvinės raiškos matavimus, skenavimo trukmė gali reikšmingai pailgėti, nes ją lemia skenuojamo ploto dydis, žingsnio dydis, pasirinktas darbo režimas ir atstumo

kontrolės metodas. Dėl šios priežasties SECM tradicinis skenavimo režimas yra ribotai tinkamas labai greitai, sekundžių ar milisekundžių skalėje, vykstantiems procesams tiesiogiai vaizduoti. Šis apribojimas ypač aktualus tiriant gyvas ląsteles, kurių paviršius yra nelygus ir dinamiškas, todėl didesnę erdvinę raišką dažnai tenka derinti su mažesniu skenavimo greičiu.[67]

Kitas svarbus aspektas yra ultramikroelektrodo mechaninis trapumas ir jautrumas netyčiniam kontaktui su tiriamuoju paviršiumi. Kadangi SECM matavimai dažnai atliekami labai mažu atstumu tarp UME ir substrato, ypač taikant didelės erdvinės raiškos arba pastovaus atstumo režimus, net nedidelis elektrodo arba mėginio padėties pokytis gali sukelti zondo kontaktą su paviršiumi ir pažeisti tiek UME, tiek tiriamą objektą. Ši problema ypač aktuali biologinių sistemų tyrimuose, kuriuose tiriamieji objektai yra minkšti, nelygūs ir deformuojami. Todėl patikimam SECM taikymui dažnai būtinos tikslios atstumo kontrolės sistemos ir kruopštus eksperimento parametrų optimizavimas.[54,55,57,67]

Reikšmingą iššūkį SECM taikymui sudaro ir eksperimentinių duomenų interpretavimas, nes registruojamas signalas priklauso nuo daugelio tarpusavyje susijusių parametrų, įskaitant elektrodo geometriją ir matmenis, UME–paviršiaus atstumą, redokso tarpininko savybes, difuzijos procesus bei tiriamojo paviršiaus elektrocheminį aktyvumą. Todėl patikimai kiekybinei analizei būtina tiksliai kontroliuoti eksperimentines sąlygas ir įvertinti jų įtaką registruojamam signalui. Ypač svarbus yra tikslus absoliutaus atstumo tarp UME ir tiriamojo paviršiaus nustatymas, t. y. vadinamosios nulinės padėties apibrėžimas. Šis parametras yra kritiškai svarbus interpretuojant artėjimo kreives, nes net ir nedidelė atstumo nustatymo paklaida gali lemti reikšmingus registruojamos srovės pokyčius ir dėl to paveikti iš kreivių apskaičiuojamus kiekybinius parametrus. Tai ypač aktualu tiriant membranas, kurių elektrocheminis atsakas gali būti jautrus net nedideliems UME–paviršiaus geometrijos pokyčiams.[55-57] Taigi, nors SECM suteikia išskirtines galimybes lokaliai tirti biologinių sistemų elektrochemines savybes, patikimų ir tarpusavyje palyginamų kiekybinių rezultatų gavimas reikalauja tikslios elektrodo padėties kontrolės, stabilios eksperimentinės sąrangos, kruopštaus matavimo parametrų parinkimo ir adekvataus elektrocheminių duomenų modeliavimo.

3.4. Elektrocheminė impedanso spektroskopija (EIS)

Elektrocheminė impedanso spektroskopija (angl. *Electrochemical Impedance Spectroscopy*, EIS) yra vienas svarbiausių elektrocheminių metodų, taikomų membranų elektrinėms savybėms tirti. Metodas pagrįstas sistemos atsako į mažos amplitudės sinusinį kintamosios srovės signalą registravimu plačiame dažnių diapazone, paprastai nuo milihercų iki megahercų. Keičiant sužadinimo signalo dažnį, galima įvertinti skirtingų elektrocheminėje sistemoje vykstančių procesų indėlį į bendrą jos impedansą.[68]

Tipinis EIS matavimo rezultatas pateikiamas Nyquisto diagramoje, kurioje vaizduojamos realioji ir menamoji impedanso dedamosios. Gauti duomenys interpretuojami taikant ekvivalentines elektrines grandines, leidžiančias įvertinti pagrindinius sistemos parametrus, tokius kaip tirpalo varža, dvigubojo elektrinio sluoksnio talpa, krūvio pernašos varža ir difuzijos procesų charakteristikos.[69] Membranų tyrimuose dažnai taikoma supaprastinta Randleso tipo ekvivalentinė grandinė, sudaryta iš neskompensuotos tirpalo varžos ir lygiagrečiai sujungtų krūvio pernašos varžos bei talpinio elemento. Kadangi realių elektrocheminių sistemų elektrinis atsakas dažnai nukrypsta nuo idealaus kondensatoriaus elgsenos, talpiniam atsakui aprašyti praktikoje dažnai naudojamas pastoviosios fazės elementas (angl. *Constant Phase Element*, CPE).[68,69]

CPE ypač aktualus tiriant biologines ir dirbtines membranas, nes realūs paviršiai paprastai nėra idealiai homogeniški. CPE apibūdinamas dydžio ir eksponentiniu fazės parametrais, o jo eksponentinis parametras *n*, kintantis nuo 0 iki 1, nusako sistemos elektrinio atsako nukrypimą nuo idealaus kondensatoriaus elgsenos. Kai *n* artėja prie 1, sistemos atsakas labiau atitinka idealaus kondensatoriaus elgseną, o mažesnės *n* vertės paprastai siejamos su didesniu paviršiaus elektrinių savybių nevienalytiškumu.[70] Todėl CPE parametrai gali būti naudojami kaip papildomi paviršiaus heterogeniškumo ir membranos struktūros pokyčių rodikliai, tačiau jų interpretacija turi būti grindžiama visos ekvivalentinės grandinės ir eksperimentinės sistemos kontekstu.[68,70,71]

Vis dėlto tradicinės EIS matavimo konfigūracijos pasižymi vienu svarbiu apribojimu – registruojamas integruotas viso elektrodo arba tiriamo paviršiaus elektrinis atsakas. Todėl vien iš impedanso spektro paprastai neįmanoma nustatyti, kurioje konkrečioje paviršiaus vietoje įvyko elektrocheminis pokytis. Kitaip tariant, EIS pasižymi dideliu jautrumu elektrinių parametrų pokyčiams, tačiau pati savaime nesuteikia jų erdvinės lokalizacijos.[72] Dėl šios priežasties EIS gali būti derinama su erdvinę informaciją teikiančiais

metodais, tokiais kaip skenuojančioji elektrocheminė mikroskopija (SECM). Toks metodų derinys leidžia papildyti kiekybinę informaciją apie membranos elektrinių savybių pokyčius jų erdvine lokalizacija ir taip išsamiau charakterizuoti lokalizuoto elektrinio poveikio sukeltus membranos pokyčius.[55,56,68,72]

3.5. SECM ir EIS kombinacija

Pastaraisiais Pastaraisiais metais vis daugiau dėmesio skiriama skenuojančiosios elektrocheminės mikroskopijos (SECM) ir elektrocheminės impedanso spektroskopijos (EIS) deriniui, kuris suteikia galimybę erdvinę elektrocheminę informaciją papildyti kiekybiniu sistemos elektrinių savybių vertinimu. Toks metodų derinys yra ypač aktualus biologinių membranų ir ląstelių tyrimuose, kuriuose vien lokalizuoto elektrocheminio signalo nepakanka membranos struktūriniams ir funkciniams pokyčiams apibūdinti.[72] SECM leidžia nustatyti dominančią paviršiaus sritį, lokalizuotai paveikti pasirinktą objektą ir įvertinti elektrocheminio aktyvumo pokyčių erdvinį pasiskirstymą, tuo tarpu EIS suteikia galimybę kiekybiškai apibūdinti šių pokyčių įtaką sistemos elektrinėms savybėms.[60]

Šio metodų derinio potencialą biologinių sistemų tyrimuose iliustruoja literatūroje aprašyti darbai. Pavyzdžiui, tiriant aktyvių ir inaktyvuotų *Saccharomyces cerevisiae* mielių elektrocheminį aktyvumą, SECM kartu su greitosios Furjė transformacijos elektrocheminės impedanso spektroskopijos (FFT-EIS) metodu buvo panaudota mielių metaboliniam aktyvumui ir deguonies suvartojimui įvertinti. Nustatyta, kad mielių elektrocheminis aktyvumas ir vadinamasis „kvėpavimas“, susijęs su ištirpusio deguonies vartojimu, gali būti registruojami, kai atstumas tarp ultramikroelektrodo (UME) ir mielių ląstelių paviršiaus yra 0–25 μm; autoriai nurodė, kad apie 25 μm yra didžiausias atstumas, tinkamas efektyviam mielių aktyvumo tyrimui FFT-SEIM režimu. Tyrime taip pat įvertinta aktyvių ir inaktyvuotų mielių krūvio pernašos varža, parodant, kad SEIM gali būti naudojama skirtingos fiziologinės būklės mielių ląstelių elektrocheminiams skirtumams lokalizuotai charakterizuoti.[73]

SECM ir impedansinių metodų derinys taip pat pritaikytas fermentinių biointerfeisų tyrimams. Imobilizuotos gliukozės oksidazės (GOx) atveju buvo tiriami gliukozės fermentinės oksidacijos metu susidarančios gliukono rūgšties koncentracijos pokyčiai ir jų poveikis tirpalo impedansui lokalioje aplinkoje prie ultramikroelektrodo (UME). Nustatyta, kad lokaliai išmatuojama impedansa priklauso nuo gliukono rūgšties koncentracijos bei jonų difuzijos, o šie parametrai kinta priklausomai nuo UME padėties GOx

modifikuoto paviršiaus atžvilgiu ir laikui bėgant. Šie rezultatai parodė, kad SEIM gali būti naudojama fermentinių reakcijų produktų susidarymui ir pernašai lokalioje zondo aplinkoje tirti bei fermentais modifikuotiems biointerfeisams charakterizuoti, taip pat atskleidė metodo potencialą biosensorių ir biokuro elementų tyrimuose.[74]

Praktiniu požiūriu SECM ir EIS derinimas leidžia tyrimą organizuoti keliais nuosekliais etapais. Pirmiausia SECM naudojama tiriamo paviršiaus padėčiai, jo elektrocheminiam aktyvumui ar dominančiai sričiai nustatyti. Nustačius tinkamą UME padėtį, galima registruoti lokalų elektrocheminį atsaką arba, priklausomai nuo pasirinktos eksperimentinės konfigūracijos, sukurti lokalizuotą elektrocheminį poveikį. Tada pasirinktoje padėtyje atliekamas EIS matavimas, leidžiantis kiekybiškai įvertinti lokalios sistemos elektrinių parametrų pokyčius. Tokia metodika leidžia susieti erdvinę elektrocheminio aktyvumo informaciją su kiekybiniais impedanso parametrais. Kartojant matavimus skirtingais laiko momentais arba skirtingose paviršiaus vietose, galima įvertinti ne tik lokalizuoto poveikio mastą, bet ir sukeltų pokyčių dinamiką bei jų grįžtamumą.[72,75]

Toks metodologinis derinys potencialiai yra ypač tinkamas elektroporacijos tyrimams. SECM gali sudaryti prielaidas lokalizuotai indukuoti elektroporaciją, kontroliuojant UME padėtį, atstumą nuo tiriamo paviršiaus ir elektrinio poveikio parametrus, o EIS gali būti naudojama elektroporacijos sukeltų membranos elektrinių savybių pokyčiams kiekybiškai įvertinti. Tokiu atveju membranos varžos pokyčiai galėtų būti siejami su jos joninio pralaidumo pokyčiais, o talpos ir CPE parametrų kitimas galėtų suteikti papildomos informacijos apie membranos struktūros ir sąsajos elektrinių savybių pokyčius. Pakartotiniai impedanso matavimai skirtingais laiko intervalais taip pat galėtų būti taikomi šių pokyčių dinamikai ir galimam membranos atsistatymui įvertinti. Šios metodologinės galimybės sudaro prielaidas SECM ir EIS derinį taikyti lokalizuotos elektroporacijos procesų tyrimams, o konkrečių parametrų pokyčiai ir jų interpretacija priklauso nuo tiriamos membranos sistemos bei eksperimentinių sąlygų.

Svarbus šio metodologinio derinio privalumas yra tai, kad SECM ir EIS sprendžia dvi skirtingas, tačiau viena kitą papildančias elektroporacijos tyrimų problemas. SECM suteikia erdvinę informaciją ir galimybę lokalizuoti elektrinį poveikį, tačiau vien SECM signalas ne visada leidžia kiekybiškai įvertinti membranos elektrinių parametrų pokyčius. EIS, priešingai, yra jautri membranos elektrinės varžos, talpos ir krūvio pernašos pokyčiams, tačiau pati savaime nesuteikia informacijos apie jų erdvinę lokalizaciją. Todėl šių metodų derinimas galėtų sudaryti prielaidas susieti paveiktą membranos sritį su joje vykstančiais elektrinių savybių pokyčiais.

Atsižvelgiant į šių metodų papildomumą, SECM ir EIS derinys gali būti perspektyvus kontroliuojamos elektroporacijos tyrimų metodologinis pagrindas. SECM galėtų būti naudojama lokalizuotam elektriniam poveikiui sukurti, jo erdviniam mastui įvertinti ir lokaliam membranos ar ląstelių elektrocheminiam atsakui registruoti, o EIS – šio poveikio sukeltų elektrinių savybių pokyčiams kiekybiškai charakterizuoti. Pakartotiniai EIS matavimai taip pat galėtų suteikti galimybę įvertinti šių pokyčių kitimą laike ir membranos atsistatymo procesus. Tokia metodologinė prieiga sudarytų galimybę elektroporacijos procesą analizuoti vienu metu erdviniu, elektriniu ir dinaminiu aspektais, tačiau konkreti šio derinio taikymo vertė ir jo teikiamos informacijos apimtis turėtų būti įvertintos eksperimentiniais tyrimais.

4. SECM PRITAIKYMAI GYVŲ LĄSTELIŲ TYRIMUOSE

4.1. SECM reikšmė biologijoje

Gyvos ląstelės yra dinamiškos sistemos, kuriose nuolat vyksta biocheminiai ir biofiziniai procesai – nuo kvėpavimo ir metabolizmo iki signalų perdavimo bei tarpląstelinių sąveikų. Šių procesų supratimas yra svarbus biologijos, medicinos, farmakologijos ir biotechnologijos tyrimams. Tradiciniai ląstelių tyrimo metodai, tokie kaip fluorescencinė ir konfokalinė mikroskopija ar įvairios spektroskopinės technikos, suteikia daug vertingos informacijos, tačiau kai kuriais atvejais reikalauja fluorescuojančių žymenų arba kitų kontrastinių medžiagų. SECM suteikia galimybę tirti gyvas ląsteles elektrocheminiais metodais, dažnai nenaudojant išorinių fluorescencinių žymenų ir atliekant matavimus vandeninėje terpėje, todėl ši metodika yra ypač tinkama lokaliems biologinių sistemų elektrocheminiams procesams tirti.[61,64]

SECM registruoja elektrocheminį signalą, susidarantį ultramikroelektrodo (UME) paviršiuje, kai zondas priartinamas prie ląstelės. Priklausomai nuo naudojamo režimo ir redokso tarpininko, galima tirti ne tik ląstelės paviršiaus ypatumus, bet ir lokalius redokso procesus, metabolinį aktyvumą, medžiagų pernašą bei transmembraninius elektronų pernašos procesus. Tai sudaro galimybę tirti pavienes ląsteles ir įvertinti jų elektrocheminio aktyvumo heterogeniškumą.[76]

SECM taikymas gyvų ląstelių tyrimuose taip pat leidžia derinti elektrocheminę informaciją su erdvine informacija apie tiriamą objektą. Pavyzdžiui, SECM buvo naudojama skirtingo tipo žmogaus krūties ląstelių kultūrų vaizdinimui ir jų atskyrimui pagal elektrocheminį aktyvumą. Tyrime SECM signalas buvo derinamas su optinės ir fluorescencinės mikroskopijos duomenimis, taip parodant metodo potencialą lokalizuotai tirti ląstelių heterogeniškumą ir redokso aktyvumą.[77]

Metodologiniu požiūriu SECM skiriasi nuo invazinių elektrofiziologinių metodikų, tokių kaip pleistrinio įspaudimo (*patch-clamp*) metodas. Pastaruoju atveju būtinas tiesioginis elektrodo kontaktas su ląstelės membrana, tuo tarpu SECM matavimai gali būti atliekami UME laikant arti, tačiau nekontaktuojant su tiriamuoju paviršiumi. Tokia konfigūracija leidžia sumažinti mechaninio poveikio tiriamoms ląstelėms riziką ir suteikia galimybę jų elektrocheminį aktyvumą tirti lokalizuotai.[61,64]

4.2. Pagrindinės SECM taikymo sritys gyvų ląstelių tyrimuose

Vienas svarbiausių SECM pritaikymų yra pavienių ląstelių vaizdinimas ir jų elektrocheminio aktyvumo analizė. Grįžtamojo ryšio režimu registruojami srovės pokyčiai gali būti naudojami paviršiaus topografijai ir elektrocheminiam aktyvumui charakterizuoti, todėl galima atskleisti ne tik ląstelės morfologinius ypatumus, bet ir lokalius jos elektrocheminio aktyvumo skirtumus. UME matmenys yra vienas svarbių parametrų, lemiančių SECM vaizdinimo kokybę: mažesni elektrodai gali sumažinti zondo reakcijos poveikį tiriamai sistemai ir sudaryti prielaidas detalesniam pavienės ląstelės elektrocheminiam vaizdinimui. Tai buvo parodyta tiriant pavienes *Saccharomyces cerevisiae* ląsteles, kur mažesnio skersmens zondai leido tiksliau atlikti generavimo–surinkimo režimu pagrįstą vaizdinimą.[78]

Tobulėjant SECM zondams, skenavimo strategijoms ir mikrofluidinėms sistemoms, atsirado galimybė SECM taikyti ne tik pavienių ląstelių charakterizavimui, bet ir didesnio skaičiaus ląstelių analizei. Pavyzdžiui, Shi ir kt. sukūrė programuojamos SECM ir mikrošulinėlių matricos derinį, leidusį atlikti didelio našumo, žymenų nereikalaujančią pavienių ląstelių analizę ir įvertinti šarminės fosfatazės aktyvumo heterogeniškumą atskirų ląstelių lygmeniu.[79]

SECM taip pat plačiai taikoma ląstelių kvėpavimo ir metaboliniam aktyvumui tirti. Registruojant deguonies suvartojimą galima lokalizuotai įvertinti ląstelių kvėpavimo aktyvumą ir jo pokyčius veikiant įvairiems cheminiams ar farmakologiniams dirgikliams. Tokia prieiga buvo pritaikyta tiek pavienių HeLa ląstelių kvėpavimo aktyvumui, tiek mikroorganizmų metaboliniam aktyvumui tirti, nustatant lokalius deguonies koncentracijos pokyčius aplink ląsteles.[80] SECM taip pat gali būti naudojama reaktyviųjų deguonies rūšių, pavyzdžiui, vandenilio peroksido (H_2O_2), išskyrimui iš pavienių ląstelių kiekybiškai nustatyti. Naujesni tyrimai parodė, kad tokiu būdu galima gauti erdviškai lokalizuotą informaciją apie ekstraląstelinio H_2O_2 išsiskyrimą iš pavienių ląstelių.[81] Be to, SECM pagrįsti matavimai gali būti naudojami ląstelių atsakui į metabolizmą ar kvėpavimą veikiančius junginius vertinti, todėl metodas yra tinkamas ne tik baziniam ląstelių aktyvumui charakterizuoti, bet ir ankstyviems funkciniams pokyčiams stebėti.[80] Vis dėlto kiekybinis metabolinio aktyvumo vertinimas pavienių ląstelių lygmeniu išlieka metodologiškai sudėtingas, nes registruojami signalai yra labai maži, o matavimo rezultatams įtakos gali turėti zondo reakcijos kinetika, UME–ląstelės atstumas ir difuziniai procesai.[82]

Kita svarbi SECM taikymo kryptis – jonų pernašos, ląstelių transporto procesų ir jų atsako į įvairius cheminius junginius analizė. Naudojant jonams

selektyvius ultramikroelektrodus galima lokalizuotai stebėti jonų koncentracijos pokyčius bei jų patekimą į ląsteles arba pašalinimą iš jų. Pavyzdžiui, Zhan ir kt. panaudojo Ag^+ jonams selektyvų SECM zondą ir realiuoju laiku tyrė Ag^+ pasisavinimą bei išskyrimą iš gyvų fibroblastų ląstelių, taip pat įvertino jonų kanalų blokatoriaus poveikį šiam procesui.[83] SECM taip pat gali būti naudojama membraninių transporto baltymų funkciniam aktyvumui vertinti. Polcari ir kt. parodė, kad SECM galima nustatyti su daugybiniu atsparumu vaistams susijusio baltymo MRP1 funkcinį aktyvumą pavienių vėžinių ląstelių lygmeniu, taip suteikiant galimybę susieti membraninio transporterio aktyvumą su ląstelės fenotipu.[84] Be jonų pernašos, SECM gali būti pritaikyta ir lokaliems ląstelių mikroaplinkos pokyčiams, pavyzdžiui, pH kitimui, registruoti. Selva ir kt. sukūrė potenciometrinį mikrojutiklį, integruotą į SECM sistemą, ir panaudojo jį realiuoju laiku stebėti pH pokyčius šalia C2C12 ląstelių. Parodyta, kad ląstelių metabolizmo pokyčiai, sukelti kofeino poveikio, buvo susiję su lokaliu aplinkos parūgštėjimu, kurį buvo galima registruoti kelių mikrometrų atstumu nuo ląstelės paviršiaus.[85] Šie tyrimai rodo, kad SECM gali būti naudojama ne tik bendrai ląstelių elektrocheminei būklei apibūdinti, bet ir lokaliai tirti jonų pernašą, membraninių transporto sistemų funkcinį aktyvumą bei ląstelių mikroaplinkos pokyčius, taip suteikiant papildomos informacijos apie ląstelių atsaką į cheminius ir farmakologinius dirgiklius.[86]

SECM taip pat gali būti naudojama lokaliems medžiagų pernašos procesams ir ląstelių sąveikai su jų mikroaplinka tirti. Derinant SECM su nanopipetiniais zondais ar kitais skenuojančiaisiais metodais, galima vienu metu registruoti paviršiaus topografiją, elektrochemiškai aktyvių rūšių srautus ir lokalius molekulių pernašos procesus. Pavyzdžiui, SECM ir skenuojančiosios jonų laidumo mikroskopijos (SICM) derinys buvo panaudotas erdviniam ląstelės membranos pralaidumo ir jonų koncentracijos pasiskirstymui apibūdinti, taip pat lokalizuotai molekulių pernašai ir jų pasisavinimui gyvose ląstelėse tirti. Tokie metodai suteikia galimybę analizuoti cheminės mikroaplinkos heterogeniškumą, medžiagų pernašą bei pavienių ląstelių atsaką lokalioje erdvėje.[87]

4.3. Išvados apie SECM taikymą gyvoms ląstelėms

Skenuojančioji elektrocheminė mikroskopija (SECM) suteikia galimybę gyvas ląsteles tirti lokalizuotai ir minimaliai invaziškai, išlaikant jų funkcinį aktyvumą matavimo metu. Skirtingai nuo metodų, registruojančių integruotą visos ląstelių populiacijos atsaką, SECM leidžia analizuoti pavienių ląstelių elektrocheminį aktyvumą ir įvertinti jų funkcinį heterogeniškumą. Keičiant

ultramikroelektrodo padėtį ląstelės atžvilgiu ir kontroliuojant atstumą iki jos paviršiaus, galima lokalizuoti elektrochemiškai aktyvias sritis bei stebėti jų pokyčius laike. Todėl SECM gali būti taikoma ne tik ląstelių metaboliniam aktyvumui ir medžiagų pernašai tirti, bet ir jų atsakui į įvairius cheminius bei fizikinius dirgiklius vertinti.

Literatūroje SECM taikoma įvairiems gyvų ląstelių procesams tirti, įskaitant metabolinį aktyvumą, vaistinių medžiagų poveikį ir pernašą, lokalizuotus ląstelės paviršiaus elektrocheminius procesus bei ląstelių mikroaplinkos pokyčius. Metodo informatyvumą galima dar labiau išplėsti jį derinant su kitais elektrocheminiais ir neelektrocheminiais metodais. Toks metodų derinimas leidžia susieti lokalų elektrocheminį signalą su papildoma struktūrine ar funkcine informacija ir taip išsamiau apibūdinti tiriamos biologinės sistemos būklę.

Apibendrinant literatūros duomenis, vienas svarbiausių SECM privalumų tiriant gyvas ląsteles yra galimybė susieti lokalų elektrocheminį atsaką su konkrečia ląstelės ar jos paviršiaus sritimi. Tai ypač svarbu biologinėms sistemoms, pasižyminčioms dideliu erdviniu ir funkciniu heterogeniškumu, nes lokalizuoti matavimai leidžia išvengti dalies apribojimų, būdingų makroskopiniams metodams, kai registruojamas vidutinis visos ląstelių populiacijos atsakas. Taigi SECM sudaro tinkamą metodologinį pagrindą gyvų ląstelių funkciniam aktyvumui, lokaliems membranos procesams ir jų atsakui į išorinius poveikius tirti.

Šios SECM savybės yra ypač aktualios elektroporacijos tyrimuose, kuriuose svarbu ne tik nustatyti bendrą membranos atsaką į elektrinį lauką, bet ir įvertinti jo erdvinį pasiskirstymą. Galimybė tiksliai kontroliuoti ultramikroelektrodo padėtį ląstelės atžvilgiu ir sukurti lokalizuotą elektrinį poveikį sudaro prielaidas elektroporaciją nagrinėti kaip lokalų membranos procesą. Dėl šių priežasčių, SECM ir EIS kombinacija toliau disertacijoje taikoma elektroporacijos tyrimams, apimantiems tiek dirbtines membranas, tiek gyvas *Saccharomyces cerevisiae* ląsteles.

5. LITERATŪROS APIBENDRINIMAS

Biologinės membranos yra sudėtingos ir dinamiškos sistemos, kurių struktūra ir funkcinės savybės lemia daugelį gyvybiškai svarbių ląstelės procesų. Elektroporacija yra vienas iš svarbiausių membranos pralaidumo moduliavimo būdų, plačiai taikomas biomedicinoje, biotechnologijoje, maisto pramonėje ir aplinkosaugos technologijose. Nepaisant ilgalaikių šio reiškinio tyrimų, daugelis molekulinių elektroporacijos mechanizmų ir juos lemiančių veiksnių vis dar nėra visiškai išaiškinti.

Siekiant atskirti fundamentinius membranos procesus nuo sudėtingo biologinio konteksto, elektroporacijos tyrimuose plačiai naudojamos dirbtinės lipidinės membranos. Jos leidžia kontroliuojamomis sąlygomis tirti porų susidarymą, membranos atsistatymą ir elektrinių parametrų pokyčius. Vis dėlto dauguma tradicinių elektroporacijos metodų pagrįsti visą tiriamą sistemą veikiančio elektrinio lauko sudarymu, todėl jų galimybės lokalizuoti elektrinį poveikį ir kontroliuoti elektroporaciją pavienės ląstelės ar atskiros membranos srities mastu yra ribotos.

Skenuojančioji elektrocheminė mikroskopija (SECM) suteikia galimybę lokaliai tirti paviršių elektrochemines savybes ir, kontroliuojant ultramikroelektrodo (UME) padėtį bei potencialą, sukurti lokalizuotą elektrinį poveikį pasirinktoje paviršiaus srityje. SECM derinimas su elektrochemine impedanso spektroskopija (EIS) papildomai suteikia galimybę kiekybiškai vertinti elektrinių parametrų pokyčius po lokalizuoto poveikio ir stebėti jų raidą laike. Toks metodų derinys leidžia susieti elektrinio poveikio erdvinę lokalizaciją su jo sukeltu membranos elektriniu atsaku.

Literatūros analizė parodė, kad SECM plačiai taikoma pavienių ląstelių elektrocheminiam aktyvumui, metabolizmui, medžiagų pernašai ir biointerfeisams tirti. Tačiau jos taikymas kontroliuojamai lokalizuotai elektroporacijai, ypač derinant SECM lokalizuotam elektriniam poveikiui su EIS sukeltų membranos elektrinių pokyčių kiekybiniam vertinimui, išlieka ribotas. Ypač nedaug duomenų apie tokios metodikos taikymą skirtingos architektūros dirbtinėms lipidinėms membranoms ir gyvoms *Saccharomyces cerevisiae* ląstelėms. Todėl lokalizuotos elektroporacijos metodikos kūrimas ir jos taikymo skirtingoms biologinėms sistemoms įvertinimas yra aktualus tiek fundamentiniams membranų biofizikos tyrimams, tiek tolesniam lokalizuotų bioelektrinių metodų vystymui.

6. TYRIMŲ METODIKA

Šiame skyriuje apibendrinama eksperimentinė metodika, taikyta keturiuose disertaciją sudarančiuose moksliniuose straipsniuose. Nors atskirose publikacijose naudotos šiek tiek skirtingos eksperimentinės sąlygos (pvz., ultramikroelektrodo skersmuo, taikomas potencialas ar membranos tipas), visų tyrimų pagrindą sudarė ta pati elektrocheminė platforma – skenuojančioji elektrocheminė mikroskopija (SECM), derinama su elektrochemine impedanso spektroskopija (EIS) ir cikline voltamperometrija (CV).

6.1. Mielių ląstelių ir substrato paruošimas

Aktyvių mielių (*Saccharomyces cerevisiae*, kepimo mielės) suspensija (0,1 g/ml) ruošta sausas granuliuotas mieles suspenduojant dejonizuotame vandenyje ir inkubuojant 30 °C temperatūroje 30 min. Inaktyvuotos mielės, naudotos kontroliniams eksperimentams, paruoštos mielių suspensiją 2 val. laikant uždarame inde aukštesnėje kaip 80 °C temperatūroje. Kiekvienam eksperimentui buvo ruošiama nauja mielių suspensija.

Ląstelėms imobilizuoti naudotas fluoru legiruotu alavo oksidu (FTO) padengtas stiklas (paviršiaus varža ~7 Ω/sq). Prieš naudojimą FTO substratai buvo nuosekliai valomi ultragarsinėje vonelėje 2 % „Micro-90“ tirpale, dejonizuotame vandenyje ir 2-propanolyje (po 10 min. kiekviename tirpale), po to džiovinami azoto (N_2) srautu. Ant paruošto FTO paviršiaus buvo užlašinamas 0,1 % poli-L-lizino tirpalas, o vėliau – mielių suspensija. Abu sluoksniai palikti išdžiūti kambario temperatūroje, po to imobilizuotos ląstelės tris kartus plaunamos fosfatiniu buferiniu tirpalu (PBS; pH 7,1; 0,1 M NaCl ir 0,01 M NaH_2PO_4). Visų eksperimentų metu PBS tirpale buvo palaikoma 10 mmol gliukozės koncentracija, siekiant užtikrinti aktyvų mielių metabolizmą.

6.2. Hibridinės membranos (hBLM) paruošimas

Hibridinės lipidinės membranos (hBLM) buvo formuojamos dviem etapais. Pirmiausia ant išvalyto FTO paviršiaus suformuotas oktadeciltrichlorsilano (OTS) savitvarkis monosluoksnis (SAM), FTO plokštelę 1 val. inkubuojant 2,5 mM OTS tirpale heptane 60 °C temperatūroje. Po silanizavimo paviršius buvo plaunamas heptanu ir džiovinamas N_2 srautu.

Antrajame etape ant silanizuoto paviršiaus vezikulių fuzijos metodu suformuota lipidų dvisluoksnio dalis. 1,2-dioleoil-*sn*-glicero-3-fosfocholino (DOPC) ir cholesterolio mišinys (molinis santykis 6:4) buvo ištirpintas chloroforme, tirpiklis pašalintas azoto srautu, o susidaręs lipidų sluoksnis

resuspenduotas fosfatiniame buferyje (pH 4,6) iki 1 mM bendros lipidų koncentracijos. Silanizuotas paviršius su lipidų vezikulių suspensija kontaktavo 1 val., po to tirpalas pakeistas PBS (pH 7,1), kuriame atlikti tolesni elektrocheminiai matavimai.

6.3. Tvirtinamos membranos (tBLM) paruošimas

tBLM buvo formuojamos ant FTO paviršiaus, prieš tai jį nuosekliai valant Alconox® ploviklio tirpale ultragarsinėje vonelėje, koncentruotoje sieros rūgštyje (95 %, 1 val.) ir per naktį laikant dejonizuotame vandenyje.

Savitvarkis monosluoksnis buvo formuojamas naudojant trichloro(3-(oktadeciltio)propil)silaną (TOPS) ir aliltrichlorsilaną (ATS) 1:1 moliniu santykiu heptane, FTO plokštelę inkubuojant 1 val. 60 °C temperatūroje. Po silanizavimo paviršius plaunamas heptanu ir džiovinamas N_2 srautu.

Ant modifikuoto paviršiaus vezikulių fuzijos metodu suformuotas DOPC ir cholesterolio (6:4 molinis santykis, bendra koncentracija 1 mM) lipidų dvisluoksnis, resuspenduotas fosfatiniame buferyje (pH 4,6). Po 1 val. inkubacijos tirpalas pakeistas PBS (pH 7,1), kuriame atlikti elektrocheminiai matavimai.

Skirtingai nei hBLM, kurių vidinį sluoksnį sudaro hidrofobinis SAM sluoksnis, tBLM sistemoje tarp lipidų dvisluoksnio ir kieto paviršiaus išlieka maždaug 1–2 nm storio submembraninis joninis rezervuaras, imituojantis citoplazmos sąlygas.

6.4. Ultramikroelektrodų (UME) paruošimas ir SECM/EIS sąranga

Eksperimentuose naudoti diskiniai aukso (Au, Ø 10 μm) ir platinos (Pt, Ø 25 μm) ultramikroelektrodai (Sensolytics, Bochumas, Vokietija). Prieš kiekvieną matavimą elektrodai buvo valomi dviem etapais: mechaniškai, poliruojant 0,3 μm grūdėtumo abrazyvine medžiaga, ir elektrochemiškai, registruojant 10–50 ciklinių voltamperogramų 0,5 M H_2SO_4 tirpale (potencialo ribos 0–1,7 V, skenavimo greitis 0,2 V/s), kol voltamperogramos tapdavo stabilios ir nebelikdavo pašalinių redokso smailių.

Visi elektrocheminiai matavimai atlikti naudojant standartinę trijų elektrodų sistemą: darbo elektrodą (UME), pagalbinį platinos elektrodą ir sotųjį Ag/AgCl palyginamąjį elektrodą. Matavimai atlikti potenciostatu/galvanostatu „Autolab PGSTAT 30“ (EcoChemie, Utrechtas, Nyderlandai), sujungtu su „Sensolytics“ (Bochumas, Vokietija) SECM sistema.

Darbinis potencialas kiekvienam eksperimentui buvo parenkamas remiantis ciklinės voltamperometrijos duomenimis, pasirenkant potencialo sritį, kurioje vyksta deguonies redukcijos reakcija ($O_2 + 4H^+ + 4e^- \rightarrow 2H_2O$), tačiau dar neprasideda intensyvus vandenilio išsiskyrimas. Visi šiame darbe nurodomi potencialai pateikiami sočiojo Ag/AgCl, Cl^-_{sat} palyginamojo elektrodo atžvilgiu, nebent nurodyta kitaip.

UME ir tiriamojo paviršiaus atstumas buvo nustatomas registruojant grįžtamojo ryšio režimo artėjimo kreives (*approach curves*). Elektroporuotos srities dydžiui įvertinti atlikti pastovaus aukščio horizontalūs SECM skenavimai prieš ir po elektroporacijos ta pačia kryptimi, naudojant 10 µm žingsnį ir 10 µm/s skenavimo greitį.

6.5. Elektroporacijos protokolai

Grįžtamajai mielių ląstelių elektroporacijai naudotas Au-UME (Ø 10 µm) arba Pt-UME (Ø 25 µm), kuris buvo pozicionuojamas 20 µm atstumu nuo ląstelių paviršiaus. Šiuose eksperimentuose taikyti 1,0–2,0 V potencialai yra gerokai mažesni nei įprastinėse dviejų elektrodų elektroporacijos sistemose naudojamos šimtų ar tūkstančių voltų įtampos. Tokį skirtumą lemia elektrodų geometrija ir atstumas tarp jų. Elektrinio lauko stipris priklauso nuo potencialų skirtumo ir atstumo, kuriame šis potencialų skirtumas pasiskirsto. Įprastose elektroporacijos kiuvetėse atstumas tarp elektrodų siekia kelis milimetrus ar centimetrus, todėl norint sukurti elektroporacijai reikalingą elektrinio lauko stiprį naudojamos didelės įtampos. SECM sistemoje UME yra pozicionuojamas vos kelių–keliasdešimties mikrometrų atstumu nuo tiriamo paviršiaus, todėl nedidelis potencialų skirtumas gali sukurti didelio stiprio lokalų elektrinį lauką. Pavyzdžiui, 1 V potencialų skirtumas 10 µm atstumu, apskaičiuojant pagal $E = U/d$, atitinka 1 kV/cm elektrinio lauko stiprį. Taigi SECM sistemoje nedidelė taikoma įtampa leidžia sukurti stiprų, tačiau erdviškai lokalizuotą elektrinį poveikį.

Prieš elektroporaciją ląstelės 5 min buvo stabilizuojamos, esant −0,2 V potencialui (Ag/AgCl, Cl^-_{sat}). Po stabilizacijos potencialas buvo padidintas iki 1,0 arba 2,0 V ir palaikytas 120 s. Negrįžtamajai mielių ląstelių elektroporacijai naudotas Ø 25 µm Pt-UME, taikant 2,0 V potencialą 120 s.

Hibridinių membranų (hBLM) elektroporacijai naudotas Ø 10 arba 25 µm Pt-UME, kuris buvo pozicionuojamas 4–10 µm atstumu nuo membranos paviršiaus. Taikytas 1,0 V potencialas, naudojant vieną 1–2 min trukmės impulsą arba pertraukiamą impulsų režimą (2 × 90 s, tarp impulsų darant 60 s pertrauką), priklausomai nuo siekiamo elektroporacijos pobūdžio.

Tvirtinamų membranų (tBLM) elektroporacijai naudotas Ø 25 µm Pt-UME, kuris buvo pozicionuojamas 5 µm atstumu nuo membranos paviršiaus. Taikytas 2,0 V potencialas: 2 min trukmės impulsas naudotas grįžtamajai, o 5 min trukmės impulsas – negrįžtamajai elektroporacijai sukelti. Siekiant išvengti pakartotinių elektrinių impulsų kumuliacinio poveikio, kiekvienas eksperimentas atliktas naudojant naują tBLM bandinį.

6.6. Elektrocheminės impedanso spektroskopijos (EIS) matavimai ir duomenų analizė

Membranų elektrinių savybių pokyčiams kiekybiškai nustatyti EIS spektrai registruoti prieš elektroporaciją ir praėjus 1, 30 bei 60 min po jos. Matavimų metu ultramikroelektrodas (UME) buvo išlaikomas toje pačioje padėtyje, kurioje buvo atlikta elektroporacija.

Matavimai atlikti potenciostatiniu režimu, naudojant 10 mV amplitudės kintamosios įtampos trikdymo signalą ir 0,1 Hz–100 kHz dažnių diapazoną. Gauti impedanso spektrai pateikti Nyquisto diagramomis, kuriose realioji impedanso dalis (Z') vaizduojama priklausomai nuo menamosios impedanso dalies su priešingu ženklu (-Z''). Spektrai analizuoti naudojant programinę įrangą „ZView“.

Eksperimentiniai duomenys aproksimuoti ekvivalentinėmis elektrinėmis grandinėmis, kurių struktūra parinkta atsižvelgiant į tiriamą sistemą ir eksperimentiniuose spektruose stebimus impedanso atsakus. Naudotos grandinės apėmė neskompensuotą tirpalo varžą R_0 ir vieną arba dvi varžos bei talpinio elemento šakas. Šiose šakose naudota ideali dvigubojo elektrinio sluoksnio talpa (Rct_1 ir CD) arba pastoviosios fazės elementas (CPE), aprašantis neidealų talpinį atsaką. Modelio parametrams nustatyti taikytas netiesinių mažiausiųjų kvadratų metodas. Aproksimacijos paklaida visais atvejais neviršijo maždaug 7 %.

Krūvio pernašos varža (R_{ct}, angl. *charge-transfer resistance*) apibūdina pasipriešinimą Faradėjiniam krūvio pernašos procesui per elektrodo ir elektrolito sąsają. Esant kitoms vienodoms sąlygoms, didesnė R_{ct} vertė rodo lėtesnę krūvio pernašos reakcijos kinetiką. Šio parametro vertė nustatyta aproksimuojant eksperimentinius EIS spektrus pasirinkta ekvivalentine elektrine grandine. Paprastesnėse sistemose krūvio pernašos varža gali būti siejama su Nyquisto diagramos pusapskritimio skersmeniu. Tačiau, kai spektrai apima kelis persidengiančius procesus, parametro vertė nustatoma aproksimuojant visą atitinkamą spektrą arba jo pasirinktą dalį pagal taikomą modelį. Todėl R_{ct} fizinė interpretacija priklauso nuo konkrečios ekvivalentinės grandinės ir eksperimentinės geometrijos.

Ekvivalentinės grandinės struktūra buvo parenkama atsižvelgiant į tiriamą sistemą, eksperimentinę geometriją ir tai, kiek skirtingų laiko konstantų galima išskirti EIS spektruose. Atsižvelgiant į šiuos kriterijus, disertacijos pagrindą sudarančiuose darbuose naudotos skirtingos ekvivalentinės grandinės.

1. Gyvų mielių ląstelių elektroporacija naudojant Ø 10 µm Au UME ir 1 V arba 2 V potencialo impulsus, kurių trukmė – 120 s.[88] Naudota dviejų varžos ir talpinio elemento šakų grandinė: $R_0 + (R_{ct1} \| C_D) + (R_{ct2} \| CPE)$. Ji pasirinkta todėl, kad Nyquisto diagramose buvo stebimi du persidengiantys pusapskritimiai, siejami su skirtingomis laiko konstantomis. Pirmasis priskirtas UME ir elektrolito sąsajos atsakui, o antrasis – elektrocheminiam atsakui sistemoje, kurioje mielių ląstelės buvo imobilizuotos ant FTO pagrindo. CPE naudotas vietoje idealios talpos, nes šio elemento rodiklis (n) buvo 0,72–0,74, rodantis neidealų talpinį atsaką. Aproksimacijos paklaida neviršijo 7 %. Grandinės schema pateikta Pav. 11 D.

2. Negrįžtamas gyvų mielių ląstelių pažeidimas naudojant Ø 25 µm Pt UME.[89] EIS spektrai registruoti esant −0,75 V potencialui prieš elektroporaciją ir praėjus 1, 30 bei 60 min po jos. Duomenims aproksimuoti naudota viena varžos ir talpinio elemento šaka, t. y. supaprastinta Randles tipo grandinė: $R_0 + (R_{ct} \| CPE)$. Nors spektruose buvo matomi keli pusapskritimiai, aproksimacijai pasirinkta aukštų dažnių sritis, apimanti pirmąjį pusapskritimį. Taip buvo siekiama aprašyti šioje dažnių srityje išskiriamą impedanso atsaką, naudojant supaprastintą modelį. Todėl gauta (R_{ct}) vertė interpretuota atsižvelgiant į aproksimuotą spektrą ir taikytos grandinės ribas. Grandinės schema pateikta Pav. 13 B.

3. Tvirtinamųjų lipidinių membranų (tBLM) ant FTO pagrindo elektroporacija naudojant Ø 25 µm Pt UME ir 2 V potencialo impulsus, kurių trukmė – 2 min (grįžtamosios elektroporacijos sąlygos) arba 5 min (negrįžtamosios elektroporacijos sąlygos).[90] Naudota dviejų varžos ir talpinio elemento šakų grandinė: $R_1 + (R_2 \| CPE_1) + (R_3 \| CPE_2)$. Čia R_1 apibūdino neskompensuotą tirpalo varžą, R_2 ir CPE_1– Pt UME ir PBS sąsajos atsaką, o (R_3) ir CPE_2 – tBLM ir elektrolito sistemos atsaką. Tokia grandinė pasirinkta atsižvelgiant į SECM geometriją, kai UME yra pozicionuojamas tirpale virš membranos, o FTO pagrindas nėra poliarizuojamas. Pirmojoje šakoje naudotas CPE, o ne ideali talpa, siekiant aprašyti neidealų UME ir elektrolito sąsajos talpinį atsaką. CPE taikymas leidžia atsižvelgti į nuo idealios talpos nukrypstantį elgesį, kuris gali būti susijęs su paviršiaus nehomogeniškumu ir kitais relaksacijos procesų pasiskirstymą lemiančiais veiksniais. Šioje sistemoje elektroporacijos poveikis analizuotas pagal

ekvivalentinės grandinės parametrų pokyčius, ypač atsižvelgiant į tBLM sąsają apibūdinančius parametrus.

Apibendrinant, ekvivalentinės grandinės struktūra buvo parenkama atsižvelgiant į tiriamą sistemą, eksperimentinę geometriją, spektruose išskiriamų laiko konstantų skaičių ir modelio tinkamumą eksperimentiniams duomenims aprašyti. Taigi vienos arba dviejų varžos ir talpinio elemento šakų naudojimą lėmė EIS spektrų ypatybės ir pasirinktas analizės modelis, o ne tiesiogiai elektroporacijos grįžtamumas. Elementų žymėjimas ir jų fizinė interpretacija kiekvienu atveju siejami su atitinkamame straipsnyje naudota ekvivalentine grandine.

6.7. Naudoti reagentai ir įranga

Eksperimentuose naudoti šie pagrindiniai reagentai ir medžiagos:

1. Sausos granuliuotos kepimo mielės (*Saccharomyces cerevisiae*);
2. Dejonizuotas vanduo;
3. Fluoru legiruotu alavo oksidu (FTO) padengtas stiklas (paviršiaus varža ~7 Ω/sq);
4. 2 % „Micro-90“ ploviklio tirpalas, 2-propanolis, azoto (N_2) dujos (substrato valymui ir džiovinimui);
5. Poli-L-lizino tirpalas (0,1 %) (ląstelių imobilizavimui);
6. NaCl ir NaH_2PO_4 (fosfatinio buferinio tirpalo, PBS, pH 7,1, ruošimui) bei gliukozė (10 mmol, mielių metabolizmui palaikyti);
7. Oktadeciltrichlorsilanas (OTS) ir heptanas (hBLM savitvarkio monosluoksnio formavimui);
8. 1,2-dioleoil-sn-glicero-3-fosfocholinas (DOPC), cholesterolis ir chloroformas (lipidų dvisluoksnio formavimui);
9. Alconox® ploviklio tirpalas ir koncentruota sieros rūgštis (H_2SO_4, 95 %) (tBLM substrato valymui);
10. Trichloro(3-(oktadeciltio)propil)silanas (TOPS) ir aliltrichlorsilanas (ATS) (tBLM savitvarkio monosluoksnio formavimui);
11. 0,5 M H_2SO_4 tirpalas (ultramikroelektrodų elektrocheminiam valymui).

Pagrindinė naudota įranga:

12. Diskiniai aukso (Au, Ø 10 µm) ir platinos (Pt, Ø 25 µm) ultramikroelektrodai bei skenuojantysis elektrocheminis mikroskopas (Sensolytics, Bochumas, Vokietija);

13. Potenciostatas/galvanostatas Autolab PGSTAT 30 (EcoChemie, Utrechtas, Nyderlandai);
14. Platinos pagalbinis elektrodas ir sotusis Ag/AgCl, Cl^-sat palyginamasis elektrodas;
15. Ultragarsinė vonelė (substratų valymui);
16. EIS duomenų analizės programinė įranga ZView.

7. PAGRINDINIŲ REZULTATŲ APIBENDRINIMAS: DIRBTINIŲ MEMBRANŲ (HBLM, TBLM) IR MIELIŲ LĄSTELIŲ ELEKTROPORACIJA

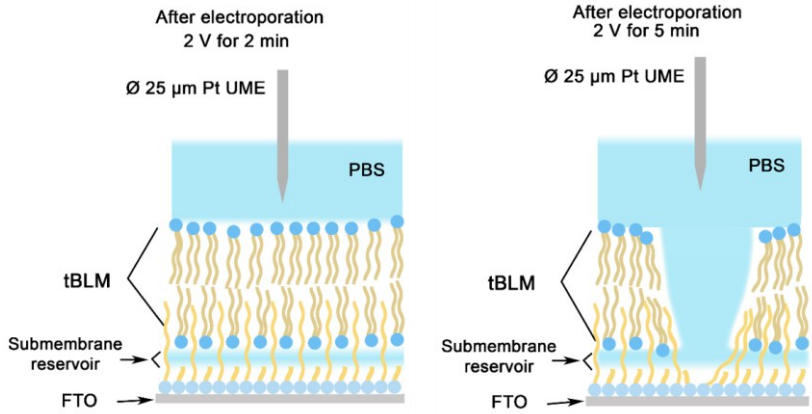
Šioje disertacijoje atlikti tyrimai nuosekliai plėtojo lokalizuotos elektroporacijos, indukuojamos skenuojančiąja elektrochemine mikroskopija (SECM), koncepciją – nuo dirbtinių membranų modelių iki gyvų mielių ląstelių. Pagrindinis šių tyrimų tikslas buvo nustatyti, ar SECM gali būti naudojama ne tik lokaliam elektriniam poveikiui sukelti, bet ir jo rezultatams kiekybiškai įvertinti, taip susiejant elektroporacijos indukavimą su tiesioginiu membranos elektrinių savybių pokyčių stebėjimu. Tam buvo derinama SECM, elektrocheminės impedanso spektroskopijos (EIS) ir ciklinės voltamperometrijos metodika.

Pirmiausia, kaip lyginamasis pagrindas šiame darbe naudoti ankstesni hibridinių lipidinių membranų (hBLM) elektroporacijos tyrimai, atlikti autorės magistrantūros studijų metu, dar prieš pradedant šios disertacijos rengimą[91]. Šie tyrimai parodė, kad SECM ultramikroelektrodu galima lokaliai indukuoti elektroporaciją ribotoje membranos srityje ir kad proceso baigtis priklauso nuo elektrinio poveikio sąlygų. Taikant 1,0 V potencialą 1 minutę, UME laikant 10 μm atstumu, membranos priartėjimo kreivės būdingas bruožas (pastovios srovės sritis, ~20 μm) liko praktiškai nepakitęs. Tačiau taikant tą pačią 1,0 V įtampą 2 minutes, UME laikant tik 5 μm atstumu, membrana buvo pažeista negrįžtamai – susiformavo ~400 μm skersmens paveikta sritis (~20 kartų didesnė už 20 μm UME skersmenį), kuri neatsistatė net po 11 val. Tuo tarpu naudojant pertraukiamą protokolą (du 90 s impulsai su 60 s pertrauka tarp jų, 4 μm atstumu), pasiekta pilna, grįžtama elektroporacija – membranos priartėjimo kreivės būdingas bruožas (30 ± 9 μm) atsistatė per ~18 min. Šie rezultatai buvo svarbūs ne tik kaip lokalizuotos elektroporacijos koncepcijos įrodymas, bet ir kaip pagrindas tolesniam klausimui: kaip membranos struktūra ir jos architektūra lemia atsparumą elektriniam laukui?

Šiam klausimui nagrinėti hBLM buvo palygintos su tvirtinamosiomis lipidinėmis membranomis (tBLM),[90,91] kurių struktūroje tarp lipidų dvisluoksnio ir kieto pagrindo išlieka submembraninis vandeninis jonų rezervuaras. Palyginimas parodė esminį šių dviejų modelių elgsenos skirtumą: tomis pačiomis sąlygomis (1,0 V, 2 min), kuriomis hBLM buvo pažeidžiama negrįžtamai, tBLM elektroporacijos požymių iš viso neparodė. Padidinus potencialą iki 2,0 V, 2 minučių trukmės impulsas sukėlė tik grįžtamus tBLM pokyčius (Pav. 9): sąsajos varža R_3 sumažėjo nuo 14,7 iki 5,3 $\Omega \cdot cm^2$ ir

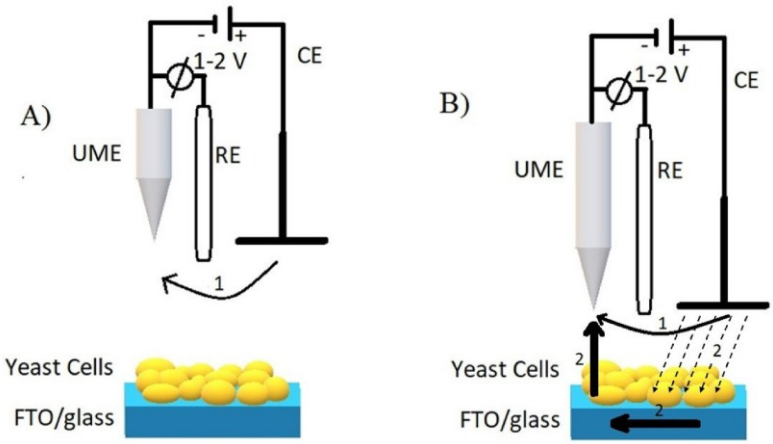
atsistatė iki 6,8 Ω·cm^2 per 60 min, o SECM pastovios srovės sritis (~100 µm, maždaug penkis kartus platesnė nei hBLM atveju) po pradinio nedidelio išsiplėtimo taip pat pilnai atsistatė. Tik pailginus impulsą iki 5 minučių pasiekta negrįžtamos tBLM elektroporacijos riba (R_3 nukrito iki 0,20 Ω·cm^2 ir neatsistatė net po 12 val.). Šie rezultatai rodo, kad submembraninio rezervuaro buvimas reikšmingai keičia membranos atsaką į lokalų elektrinį lauką ir veikia kaip papildomas struktūrinis elementas, mažinantis membranos pažeidžiamumą.

Svarbus šių tyrimų rezultatas buvo ir tai, kad elektroporacijos baigtis galėjo būti vertinama ne vien pagal tiesioginį elektrocheminį signalą, bet ir kiekybiškai analizuojant membranos elektrines savybes EIS metodu, taikant dviejų nuosekliai sujungtų RC grandžių ekvivalentinę schemą. Po lokalizuoto elektrinio poveikio stebėti krūvio pernašos varžos ir talpos pokyčiai suteikė informacijos apie membranos pralaidumo pokyčius ir jų atsistatymą. Taigi SECM ir EIS derinys leido susieti erdviškai lokalizuotą elektroporacijos indukavimą su kiekybiniu jos pasekmių apibūdinimu.



Pav. 9. Tvirtinamos lipidinės membranos (tBLM) būklė po elektroporacijos, taikant 2 V potencialą 2 minutėms (kairėje, grįžtama elektroporacija — membrana išlieka vientisa) ir 2 V potencialą 5 minutėms (dešinėje, negrįžtama elektroporacija — matomas aiškus poros susiformavimas membranoje ir submembraniniame rezervuare). Naudotas Ø 25 µm Pt ultramikroelektrodas. *Adaptuota (sujungtos originalios 4 ir 7 paveikslų dalys) iš Poderytė, M.; Gabriūnaitė, I.; Valiūnienė, A. Electroporation and Structural Integrity Analysis of Tethered Bilayer Lipid Membranes on Fluorine-Doped Tin Oxide Surface. Journal of Electroanalytical Chemistry* ***2026****, 1000, 119608. https://doi.org/10.1016/j.jelechem.2025.119608. © 2025 Elsevier B.V. Naudojama pagal autorės teisę pakartotinai panaudoti savo paskelbto straipsnio turinį daktaro disertacijoje (Elsevier autoriaus teisių politika).*[90]

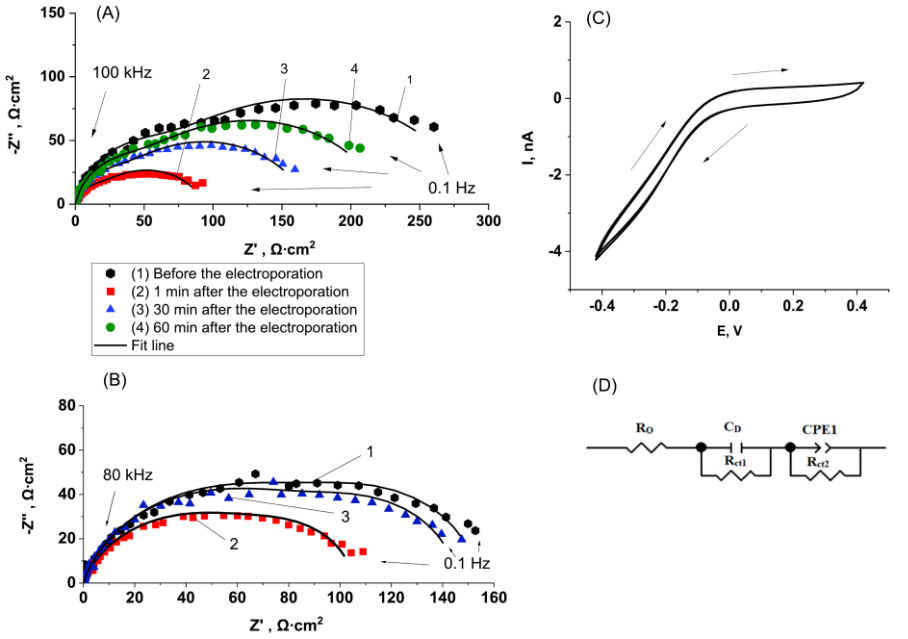
Kitas tyrimų etapas buvo skirtas nustatyti, ar tokia lokalizuota elektroporacija gali būti pritaikyta gyvoms Saccharomyces cerevisiae ląstelėms[88,89]. Mielės pasirinktos kaip tinkamas tarpinis modelis tarp supaprastintų dirbtinių membranų ir sudėtingesnių žinduolių ląstelių sistemų. Jos leidžia išlaikyti biologinės membranos kompleksiškumą, tačiau kartu pasižymi santykinai paprasta ir eksperimentams patogia organizacija. SECM taikymas šiame etape leido elektros poveikį apriboti lokalizuota ląstelės paviršiaus sritimi (Pav. 10), o EIS – stebėti po impulso vykstančius membranos elektrinių parametrų pokyčius.



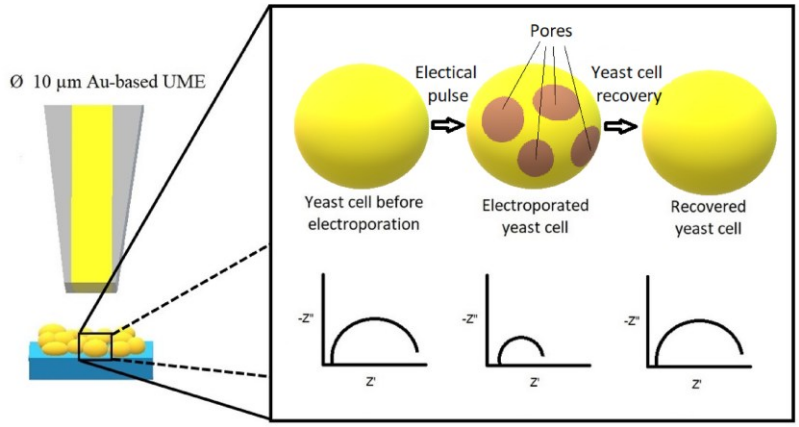
Pav. 10. Srovės tekėjimo kelias trijų elektrodų sistemoje: **A** — kai UME yra santykinai toli nuo mielių ląstelėmis modifikuoto paviršiaus, srovė teka tiesiogiai per elektrolito tirpalą tarp UME ir pagalbinio elektrodo (CE) (kelias 1); **B** — kai UME laikomas itin mažu atstumu nuo paviršiaus, atsiranda papildomas srovės kelias, kertantis nepoliarizuotą, su išorine grandine tiesiogiai nesujungtą mielių ląstelių sluoksnį (keliai 1 ir 2). *UME — ultramikroelektrodas, RE — palyginamasis elektrodas, CE — pagalbinis elektrodas. Šaltinis: Poderytė, M.; Valiūnienė, A.; Ramanavičius, A. Scanning electrochemical microscope as a tool for the electroporation of living yeast cells. Biosensors and Bioelectronics* ***2022****, 205, 114096. https://doi.org/10.1016/j.bios.2022.114096. © 2022 Elsevier B.V. Naudojama pagal autorės teisę pakartotinai panaudoti savo paskelbto straipsnio turinį daktaro disertacijoje (Elsevier autoriaus teisių politika).*[88]

Mielių ląstelių tyrimai parodė, kad SECM gali būti naudojama kontroliuojamai grįžtamai elektroporacijai sukelti.[88] Taikant 10 µm skersmens auksinį UME bei 2,0 V potencialą 120 s, po elektroporacijos registruotas krūvio pernašos varžos sumažėjimas: bendra varža (R_{ct1}+R_{ct2}) sumažėjo nuo 294 iki 94 $\Omega \cdot cm^2$ jau po vienos minutės, tačiau per 60 min beveik visiškai atsistatė iki pradinės vertės (Pav. 11). SECM paviršiaus skenavimas parodė, kad paveiktos srities skersmuo siekė apie 250 µm, t. y. maždaug 25 kartus

daugiau nei elektrodo skersmuo (Pav. 12). Toks rezultatų pobūdis – varžos sumažėjimas ir jos atsistatymas – patvirtino, kad membranos pažeidimas buvo laikinas, o pagrindinė šio pokyčio priežastis – iš ląstelių į aplinką išsiskyrę elektroaktyvūs jonai (K^+, Na^+, Ca^{2+}). Be to, silpnesnis, 1,0 V, impulsas sukėlė švelnesnį ir greičiau (per ~30 min) atsistatantį atsaką, o tai patvirtina, kad lokalizuota SECM elektroporacija gali būti ne tik indukuojama, bet ir reguliuojama keičiant elektrinio poveikio parametrus.[88]

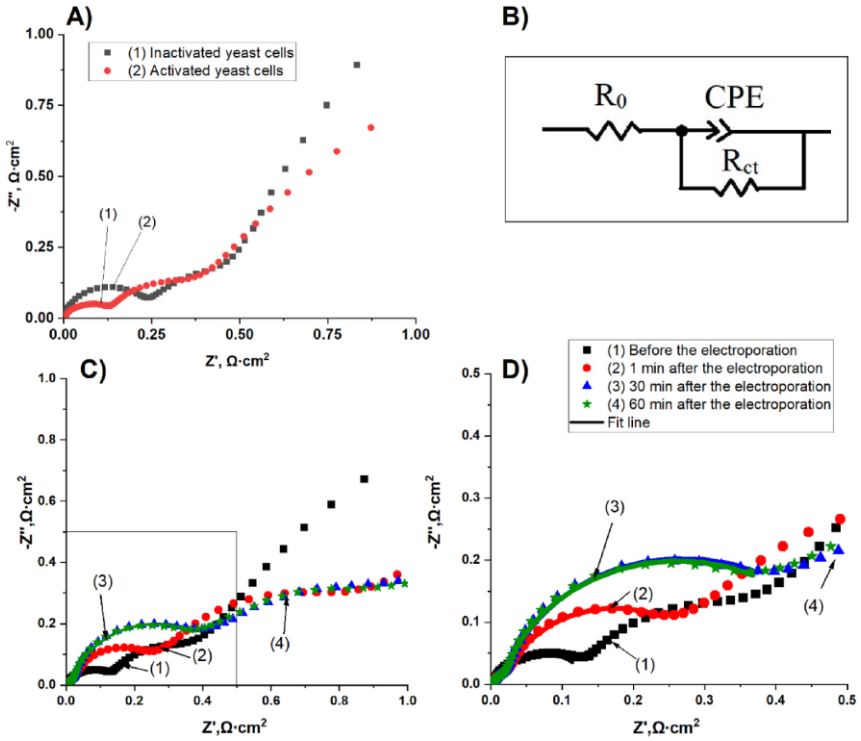


Pav. 11. Aktyvių mielių ląstelių elektrocheminio atsako pokyčiai po grįžtamos elektroporacijos, taikant skirtingus potencialus, bei šiam vertinimui naudoti kontroliniai matavimai. A ir **B** — EIS spektrai, registruoti virš aktyvių mielių ląstelių, taikant –0,2 V potencialą Ag/AgCl, Cl^-_{sat} elektrodo atžvilgiu, prieš elektroporaciją ir po jos skirtingu laiku. Aktyvių mielių ląstelių elektroporacija atlikta fosfatiniame buferiniame tirpale (pH 7,1) su 10 mmol gliukozės, taikant Au-UME potencialo šuolį: **A** — nuo –0,2 V iki 2,0 V Ag/AgCl, Cl^- prisotinto elektrodo atžvilgiu, potencialą palaikant 120 s; **B** — nuo –0,2 V iki 1,0 V Ag/AgCl, Cl^- prisotinto elektrodo atžvilgiu, potencialą palaikant 120 s. **C** — Ø 10 µm Au ultramikroelektrodo ciklinė voltamperograma buferiniame tirpale (pH 7,1) su 10 mmol gliukozės, esant 10 $mV \cdot s^{-1}$ potencialo kitimo greičiui. **D** — ekvivalentinės grandinės modelis, naudotas EIS duomenims aproksimuoti: R_0 — neskompensuota tirpalo varža; R_{ct1} ir CD — krūvio pernašos varža ir elektrinio dvigubo sluoksnio (EDL) talpa ties Au-UME/elektrolito tirpalo sąsaja; Rct_2 ir CPE_1 — krūvio pernašos varža ir talpa ties mielių ląstelių/elektrolito tirpalo sąsaja. *Šaltinis: Margarita Poderytė, Aušra Valiūnienė, Arūnas Ramanavičius. Scanning electrochemical microscope as a tool for the electroporation of living yeast cells. Biosensors and Bioelectronics, 205 (2022), 114096. https://doi.org/10.1016/j.bios.2022.114096. © 2022 Elsevier B.V. Naudojama pagal autorės teisę pakartotinai panaudoti savo paskelbto straipsnio turinį daktaro disertacijoje (Elsevier autoriaus teisių politika).*[88]



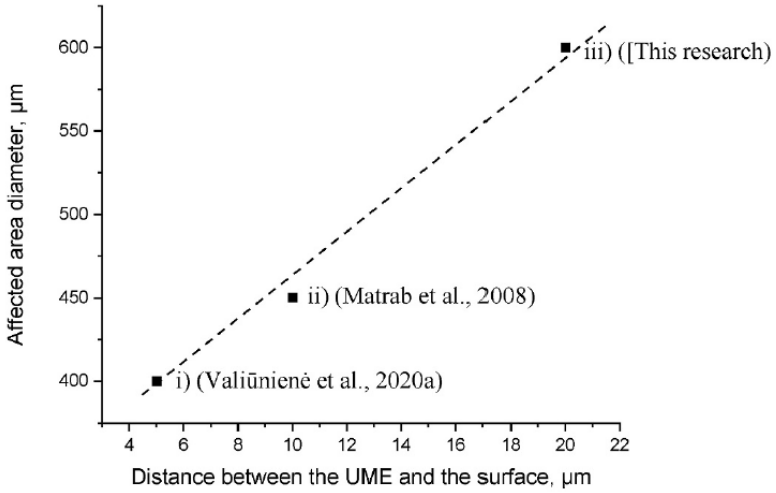
Pav. 12. Grįžtamos mielių ląstelės elektroporacijos proceso, naudojant Ø 10 µm skersmens auksinį ultramikroelektrodą, vizualizacija. Elektrinio impulso metu ląstelės membranoje susiformuoja poros, dėl kurių sumažėja Nyquisto diagramos pusapskritimio dydis (susijęs su krūvio pernašos varža); ląstelei atsistačius, poros užsiveria ir impedanso spektras grįžta į pradinę formą. *Šaltinis: Poderytė, M.; Valiūnienė, A.; Ramanavičius, A. Scanning electrochemical microscope as a tool for the electroporation of living yeast cells. Biosensors and Bioelectronics* ***2022****, 205, 114096. https://doi.org/10.1016/j.bios.2022.114096. © 2022 Elsevier B.V. Naudojama pagal autorės teisę pakartotinai panaudoti savo paskelbto straipsnio turinį daktaro disertacijoje (Elsevier autoriaus teisių politika).*[88]

Toliau buvo nagrinėjama priešinga – negrįžtama elektroporacija, naudojant didesnio, 25 µm, skersmens Pt-UME ir taikant 2,0 V potencialą 120 s.[89] Šiuo atveju krūvio pernašos varža po impulso ne sumažėjo, o padidėjo – nuo 0,15 iki 0,32 $\Omega \cdot cm^2$ po vienos minutės, ir toliau didėjo, kol nusistovėjo ties 0,50 $\Omega \cdot cm^2$ po 30 min, tokia išlikdama iki 60 min (Pav. 13). Šis priešingos krypties pokytis aiškinamas kitu mechanizmu: suirusios membranos baltymai ir lipidai adsorbuojasi ant elektrodo paviršiaus ir mažina jo efektyvų elektrochemiškai aktyvų plotą, per kurį gali vykti Faradėjinė reakcija. SECM skenavimai parodė, kad paveiktos srities skersmuo šiuo atveju siekė apie 500–600 µm (~20 kartų didesnis už elektrodo skersmenį). Tai patvirtino, kad lokalizuotas elektroporacijos procesas nėra apribotas vien tiesiogiai po elektrodu esančia sritimi, o jo erdvinį mastą lemia elektrinio lauko pasiskirstymas aplink ultramikroelektrodą.[89]



Pav. 13. Aktyvių ir inaktyvintų mielių ląstelių elektrocheminio atsako palyginimas bei negrįžtamos elektroporacijos, atliktos Ø 25 µm Pt UME, poveikio įvertinimas elektrocheminės impedanso spektroskopijos (EIS) metodu. **A** — elektrocheminės impedanso spektroskopijos (EIS) spektrai, gauti naudojant Ø 25 µm Pt UME, pozicionuotą 20 µm atstumu nuo aktyvių (1) ir inaktyvintų (2) mielių ląstelių. Matavimai atlikti buferiniame tirpale (pH 7,1), turinčiame 10 mM gliukozės. Taikytas –0,75 V potencialas Ag/AgCl, Cl^-_{sat} elektrodo atžvilgiu; dažnių intervalas – 0,1 Hz–100 kHz. **B** — EIS duomenims aproksimuoti naudotas ekvivalentinės grandinės modelis. **C** — aktyvių mielių ląstelių elektroporacija atlikta naudojant Ø 25 µm Pt UME, taikant 2 V potencialą 120 s. EIS spektrai, užregistruoti pozicionavus UME virš mielių ląstelių: prieš elektroporaciją (1 kreivė), praėjus 1 min (2 kreivė), 30 min (3 kreivė) ir 60 min (4 kreivė) po elektroporacijos. Matavimai atlikti buferiniame tirpale (pH 7,1) su 10 mM gliukozės, taikant –0,75 V potencialą Ag/AgCl, Cl^-_{sat} elektrodo atžvilgiu; dažnių intervalas – 0,1 Hz–100 kHz. **D** — padidinta duomenų sritis, apimanti 0,5 Ω·cm² intervalą abiejose ašyse ir atvaizduojanti atitinkamai Z′ ir –Z″ duomenis, aproksimuotus ekvivalentinės grandinės modeliu. *Šaltinis: Margarita Poderytė, Arūnas Ramanavičius, Aušra Valiūnienė. Scanning electrochemical microscopy based irreversible destruction of living cells. Biosensors and Bioelectronics, 216 (2022), 114621. https://doi.org/10.1016/j.bios.2022.114621. © 2022 Elsevier B.V. Naudojama pagal autorės teisę pakartotinai panaudoti savo paskelbto straipsnio turinį daktaro disertacijoje (Elsevier autoriaus teisių politika).*[89]

Bendras dirbtinių membranų ir gyvų mielių ląstelių rezultatų vertinimas parodė, kad elektroporacijos baigtį galima kontroliuoti keliais tarpusavyje susijusiais parametrais – ultramikroelektrodo skersmeniu, jo atstumu nuo tiriamo paviršiaus, taikomo potencialo verte ir impulso trukme. Visose trijose tirtose sistemose (hBLM, tBLM ir mielių ląstelėse) paveiktos srities skersmuo buvo maždaug 18–25 kartus didesnis už elektrodo skersmenį – šis sistemingas santykis rodo, kad elektrodo geometrija gali būti naudojama kaip papildomas kontrolės parametras, leidžiantis reguliuoti ne tik elektrinio poveikio intensyvumą, bet ir paveiktos srities erdvinį mastą (Pav. 14).



Pav. 14. Elektroporuotos srities skersmens priklausomybė nuo atstumo tarp UME elektrodo ir mėginio paviršiaus. Taškas ties 400 µm: Ø 25 µm Pt UME buvo laikomas 5 µm atstumu nuo hibridinės dvisluoksnės membranos paviršiaus; elektroporacija atlikta taikant 1,0 V potencialą 2 min, todėl susidarė 400 µm skersmens elektroporuota sritis (Valiūnienė ir kt., 2020) [i]. Taškas ties 450 µm: Ø 25 µm Pt pagrindo UME buvo laikomas 8 µm atstumu nuo organiniais junginiais modifikuoto aukso paviršiaus, todėl paveiktos srities skersmuo siekė 450 µm (Matrab ir kt., 2008) [ii]. Taškas ties 600 µm: Ø 25 µm Pt UME buvo laikomas 20 µm atstumu nuo mielių ląstelių paviršiaus; elektroporacija atlikta taikant 2,0 V potencialą 2 min, todėl susidarė 600 µm skersmens elektroporuota sritis (šis tyrimas). *Šaltinis: Margarita Poderytė, Arūnas Ramanavičius, Aušra Valiūnienė. Scanning electrochemical microscopy based irreversible destruction of living cells. Biosensors and Bioelectronics, 216 (2022), 114621. https://doi.org/10.1016/j.bios.2022.114621. © 2022 Elsevier B.V. Naudojama pagal autorės teisę pakartotinai panaudoti savo paskelbto straipsnio turinį daktaro disertacijoje (Elsevier autoriaus teisių politika).*[89]

Svarbu tai, kad šiame darbe elektroporacija buvo vertinama dviem tarpusavyje papildančiais aspektais. SECM suteikė galimybę tiksliai lokalizuoti elektrinio poveikio vietą, indukuoti elektroporaciją ir stebėti jos

erdvinį pasiskirstymą, o EIS leido kiekybiškai apibūdinti po elektroporacijos vykstančius membranos elektrinių savybių pokyčius ir jų atsistatymo dinamiką. Todėl šių metodų derinys suteikė daugiau informacijos nei vien atskiras elektroporacijos indukavimo arba galutinės ląstelės būklės įvertinimas. Ypač svarbu, kad EIS leido stebėti ne tik galutinį membranos pažeidimo rezultatą, bet ir jo raidą laike, todėl atsirado galimybė atskirti trumpalaikius, grįžtamus membranos pokyčius nuo negrįžtamo struktūrinio pažeidimo.

Apibendrinant visą tyrimų eigą: hBLM tyrimai[91] buvo svarbus pradinis metodologinis etapas, parodęs lokalizuotos SECM indukuojamos elektroporacijos galimybę; tBLM tyrimai[90] leido įvertinti membranos architektūros reikšmę jos atsparumui elektriniam laukui; o mielių ląstelių tyrimai[88,89] parodė, kad sukurta metodologinė prieiga gali būti taikoma ne tik supaprastintoms membranų sistemoms, bet ir gyviems biologiniams objektams. Šią tyrimų seką nuo dirbtinių membranų iki gyvų ląstelių apibendrinantis apžvalginis straipsnis[92] patvirtino, kad SECM ir EIS derinys yra perspektyvi ir plačiai pritaikoma platforma lokalizuotiems elektrocheminiams membranų tyrimams.

Šių rezultatų visuma rodo, kad SECM ir EIS derinys gali būti vertinamas kaip perspektyvi platforma lokalizuotai elektroporacijai indukuoti ir jos dinamikai kiekybiškai charakterizuoti. Nustatytas ryšys tarp elektrinio poveikio parametrų, UME geometrijos ir elektroporacijos baigties sudaro pagrindą tolesniam šios metodikos vystymui, siekiant tiksliau kontroliuoti paveiktos srities dydį, elektroporacijos grįžtamumą ir membranos atsistatymo procesus. Tokia prieiga potencialiai gali būti pritaikoma ne tik fundamentiniams membranų biofizikos tyrimams, bet ir kuriant lokalizuoto poveikio bioelektronines bei biomedicinines technologijas. Svarbu pažymėti, kad visi šie rezultatai pasiekti taikant vos 1–2 V potencialus – šimtus ar net tūkstančius kartų mažesnius nei įprastose dviejų elektrodų elektroporacijos sistemose naudojamos įtampos. Toks skirtumas susijęs su SECM geometrija, kai elektrinis poveikis koncentruojamas mažoje erdvinėje srityje prie mikroelektrodo. Todėl lokalizuota, SECM pagrįsta elektroporacija leidžia sukelti stiprų elektrinį poveikį tik pasirinktoje mėginio srityje, kartu sumažinant nepageidaujamą poveikį likusiai, nepaveiktai mėginio daliai. Tai yra vienas iš praktinių šio metodo pranašumų, palyginti su tradiciniais elektroporacijos metodais, kai elektrinis poveikis taikomas visam mėginio tūriui.

IŠVADOS

1. Hibridinės (hBLM) ir tvirtinamos (tBLM) lipidinės membranos, naudotos kaip dirbtiniai plazminės membranos modeliai, pasižymi skirtingu atsparumu lokalizuotam elektriniam poveikiui. hBLM buvo jautri elektriniams impulsams jau esant 1,0 V potencialui ir, taikant pertraukiamą impulsų protokolą, po elektroporacijos atsistatė per maždaug 18 min. TBLM, priešingai, neparodė elektroporacijos požymių taikant 1,0 V, 2 min protokolą, kuris hBLM sukėlė negrįžtamą pažeidimą, ir išliko funkciškai vientisa taikant 2,0 V, 2 min impulsą. Šiuo atveju sąsajos varža R_3 grįžtamai sumažėjo nuo 14,7 iki 5,3 $\Omega \cdot cm^2$ ir per 60 min atsistatė iki 6,8 $\Omega \cdot cm^2$. Negrįžtamas tBLM pažeidimas nustatytas tik pailginus 2,0 V impulso trukmę iki 5 min – R3 sumažėjo iki 0,20 $\Omega \cdot cm^2$ ir neatsistatė net po 12 val. Šie rezultatai rodo, kad tBLM šiuose eksperimentuose pasižymėjo didesniu atsparumu lokalizuotam elektriniam poveikiui nei hBLM ir yra tinkamas modelis elektroporacijos procesams tirti ilgesniais stebėjimo laikotarpiais.
2. Lokalizuotos elektroporacijos grįžtamumą lemia taikomo elektrinio poveikio parametrai, tarp jų potencialas, impulso trukmė ir ultramikroelektrodo skersmuo. Tiek dirbtinėse membranose, tiek gyvose mielių ląstelėse elektroporacijos baigtis priklausė nuo šių parametrų: tBLM atveju, esant 2,0 V potencialui, 2 min trukmės impulsas sukėlė grįžtamus membranos elektrinių savybių pokyčius, o pailginus impulso trukmę iki 5 min nustatytas negrįžtamas pažeidimas. Mielių ląstelių atveju, taikant 2,0 V potencialą 120 s, Ø10 µm UME sukėlė grįžtamą, o Ø25 µm UME – negrįžtamą elektroporaciją.
3. Sukurta ir eksperimentiškai pritaikyta SECM pagrįsta lokalizuotos membranų elektroporacijos indukavimo metodika, leidžianti naudojant 1–2 V potencialo impulsus sukelti lokalizuotą membranų elektroporaciją. EIS leidžia kiekybiškai nustatyti elektroporacijos sukeltus membranos elektrinių savybių, įskaitant krūvio pernašos varžos ir talpinio elemento parametrų, pokyčius bei jų kitimą laike. SECM priartėjimo kreivės papildomai parodė membranos struktūrinio ir barjerinio vientisumo pokyčius toje pačioje vietoje, kurioje buvo sukeltas elektrinis poveikis.
4. SECM ir EIS metodų derinys pritaikytas gyvų Saccharomyces cerevisiae ląstelių lokalizuotai elektroporacijai tirti. Nustatyta, kad elektroporacijos baigtis priklauso nuo ultramikroelektrodo skersmens: naudojant Ø10 µm UME, sukeliama grįžtama elektroporacija, kurios metu membranos elektrinės savybės atsistato per 30–60 min, o naudojant Ø25 µm UME, tomis pačiomis 2,0 V ir 120 s sąlygomis, sukeliama negrįžtama elektroporacija. Pastaruoju atveju padidėjusi varža per stebėjimo

laikotarpį neatsistatė; šis pokytis siejamas su elektroporacijos metu išsiskyrusių arba atsiskyrusių membranos komponentų kaupimusi ir elektrodo paviršiaus blokavimu.

5. Lokalizuotos elektroporacijos paveiktos srities dydis priklauso nuo ultramikroelektrodo geometrijos ir jo atstumo nuo tiriamo paviršiaus. Mielių ląstelių ir hBLM tyrimuose nustatytas ryšys tarp UME skersmens ir susidariusios paveiktos srities dydžio, o mielių ląstelių atveju paveiktos srities skersmuo buvo maždaug 20–25 kartus didesnis už UME skersmenį. Rezultatai taip pat parodė, kad keičiant UME–paviršiaus atstumą galima keisti elektrinio poveikio erdvinį pasiskirstymą. Tai rodo, kad UME geometrija ir jo padėtis paviršiaus atžvilgiu yra svarbūs parametrai, leidžiantys kontroliuoti lokalizuotos elektroporacijos paveiktos srities dydį.

Pagrindinė išvada, darbo apribojimai ir perspektyvos

Pagrindinė disertacijos išvada – sukurta ir eksperimentiškai patikrinta metodika, leidžianti skenuojančiąja elektrochemine mikroskopija (SECM) sukelti lokalizuotą elektroporaciją, o elektrocheminės impedanso spektroskopijos (EIS) metodu kiekybiškai analizuoti po jos vykstančius membranų elektrinių savybių pokyčius. Metodika pritaikyta dirbtinėms lipidinėms membranoms (hBLM ir tBLM) bei gyvoms *Saccharomyces cerevisiae* mielių ląstelėms. Nustatyta, kad elektroporacijos grįžtamumas priklauso nuo taikomo potencialo, impulso trukmės ir ultramikroelektrodo skersmens, o paveiktos srities dydžiui įtakos turi elektrodo geometrija ir atstumas iki tiriamo paviršiaus.

Vertinant rezultatus, svarbu atsižvelgti į kelis tyrimo apribojimus. Eksperimentai atlikti su imobilizuotomis mielių ląstelėmis ir makroskopinėmis dirbtinėmis lipidinėmis membranomis, todėl gauti rezultatai neapibūdina elektroporacijos procesų pavienės ląstelės ar nanometrinio membranos lopinėlio lygmeniu. Be to, mielių ląstelių modelio pritaikomumą žinduolių ląstelėms riboja jų struktūriniai skirtumai, ypač mieles gaubianti standi ląstelės sienelė. Taip pat nebuvo atskirai įvertintas elektrodo medžiagos ir jo skersmens poveikis, todėl šių veiksnių indėlio į elektroporacijos rezultatus negalima vienareikšmiškai atskirti.

Tolesniuose tyrimuose numatoma pritaikyti metodiką pavienių ląstelių tyrimams, išbandyti ją su žinduolių ląstelių linijomis ir sudėtingesnėmis trimatėmis, audinių savybes imituojančiomis sistemomis. Taip pat būtų tikslinga sistemingai atskirti elektrodo medžiagos, geometrijos ir elektrodo–paviršiaus atstumo įtaką elektroporacijos rezultatams. Šie tyrimai padėtų geriau apibrėžti metodikos galimybes ir apribojimus bei įvertinti jos perspektyvas ateityje, pavyzdžiui, kuriant lokalizuotos vaistų pernašos ar tikslinio poveikio audiniams metodus.

LITERATŪROS SĄRAŠAS

1 Singer, S. J. & Nicolson, G. L. The Fluid Mosaic Model of the Structure of Cell Membranes. *Science* **175**, 720-731 (1972). https://doi.org:doi:10.1126/science.175.4023.720

2 Nicolson, G. L. The Fluid—Mosaic Model of Membrane Structure: Still relevant to understanding the structure, function and dynamics of biological membranes after more than 40years. *Biochimica et Biophysica Acta (BBA) - Biomembranes* **1838**, 1451-1466 (2014). https://doi.org:https://doi.org/10.1016/j.bbamem.2013.10.019

3 van Meer, G., Voelker, D. R. & Feigenson, G. W. Membrane lipids: where they are and how they behave. *Nature Reviews Molecular Cell Biology* **9**, 112-124 (2008). https://doi.org:10.1038/nrm2330

4 Israelachvili, J. N., Mitchell, D. J. & Ninham, B. W. Theory of self-assembly of hydrocarbon amphiphiles into micelles and bilayers. *Journal of the Chemical Society, Faraday Transactions 2: Molecular and Chemical Physics* **72**, 1525-1568 (1976). https://doi.org:10.1039/f29767201525

5 Yeagle, P. L. Cholesterol and the cell membrane. *Biochimica et Biophysica Acta (BBA) - Reviews on Biomembranes* **822**, 267-287 (1985). https://doi.org:https://doi.org/10.1016/0304-4157(85)90011-5

6 Papahadjopoulos, D., Jacobson, K., Nir, S. & Isac, I. Phase transitions in phospholipid vesicles Fluorescence polarization and permeability measurements concerning the effect of temperature and cholesterol. *Biochimica et Biophysica Acta (BBA) - Biomembranes* **311**, 330-348 (1973). https://doi.org:https://doi.org/10.1016/0005-2736(73)90314-3

7 Leventis, P. A. & Grinstein, S. The Distribution and Function of Phosphatidylserine in Cellular Membranes. *Annual Review of Biophysics* **39**, 407-427 (2010). https://doi.org:https://doi.org/10.1146/annurev.biophys.093008.131234

8 Simons, K. & Ikonen, E. Functional rafts in cell membranes. *Nature* **387**, 569-572 (1997). https://doi.org:10.1038/42408

9 Reigada, R. Electroporation of heterogeneous lipid membranes. *Biochimica et Biophysica Acta (BBA) - Biomembranes* **1838**, 814-821 (2014). https://doi.org:https://doi.org/10.1016/j.bbamem.2013.10.008

10 Demel, R. A. & De Kruyff, B. The function of sterols in membranes. *Biochimica et Biophysica Acta (BBA) - Reviews on Biomembranes* **457**, 109-132 (1976). https://doi.org:https://doi.org/10.1016/0304-4157(76)90008-3

11 Engelman, D. M. Membranes are more mosaic than fluid. *Nature* **438**, 578-580 (2005). https://doi.org:10.1038/nature04394

12 Chen, T. *et al.* Designing energy-efficient separation membranes: Knowledge from nature for a sustainable future. *Advanced Membranes* **2**, 100031 (2022). https://doi.org:https://doi.org/10.1016/j.advmem.2022.100031

13 Nagle, J. F. & Tristram-Nagle, S. Structure of lipid bilayers. *Biochimica et Biophysica Acta (BBA) - Reviews on Biomembranes* **1469**, 159-195 (2000). https://doi.org:https://doi.org/10.1016/S0304-4157(00)00016-2

14 Kotnik, T., Rems, L., Tarek, M. & Miklavčič, D. Membrane Electroporation and Electropermeabilization: Mechanisms and Models. *Annual Review of Biophysics* **48**, 63-91 (2019). https://doi.org:https://doi.org/10.1146/annurev-biophys-052118-115451

15 Filice, F. P. & Ding, Z. Analysing single live cells by scanning electrochemical microscopy. *Analyst* **144**, 738-752 (2019). https://doi.org:10.1039/C8AN01490F

16 Chan, Y. H. & Boxer, S. G. Model membrane systems and their applications. *Curr Opin Chem Biol* **11**, 581-587 (2007). https://doi.org:10.1016/j.cbpa.2007.09.020

17 Weaver, J. C. & Chizmadzhev, Y. A. Theory of electroporation: A review. *Bioelectrochemistry and Bioenergetics* **41**, 135-160 (1996). https://doi.org:https://doi.org/10.1016/S0302-4598(96)05062-3

18 Raguse, B. *et al.* Tethered Lipid Bilayer Membranes: Formation and Ionic Reservoir Characterization. *Langmuir* **14**, 648-659 (1998). https://doi.org:10.1021/la9711239

19 Abidor, I. G. *et al.* Electric breakdown of bilayer lipid membranes: I. The main experimental facts and their qualitative discussion. *Journal of Electroanalytical Chemistry and Interfacial Electrochemistry* **104**, 37-52 (1979). https://doi.org:https://doi.org/10.1016/S0022-0728(79)81006-2

20 Castellana, E. T. & Cremer, P. S. Solid supported lipid bilayers: From biophysical studies to sensor design. *Surface Science Reports* **61**, 429-444 (2006). https://doi.org:https://doi.org/10.1016/j.surfrep.2006.06.001

21 Mueller, P., Rudin, D. O., Ti Tien, H. & Wescott, W. C. Reconstitution of Cell Membrane Structure in vitro and its Transformation into an Excitable System. *Nature* **194**, 979-980 (1962). https://doi.org:10.1038/194979a0

22 Mueller, P., Rudin, D. O., Tien, H. T. & Wescott, W. C. METHODS FOR THE FORMATION OF SINGLE BIMOLECULAR LIPID MEMBRANES IN AQUEOUS SOLUTION. *The Journal of Physical Chemistry* **67**, 534-535 (2002). https://doi.org:10.1021/j100796a529

23 Hanai, T., Haydon, D. A. & Taylor, J. The variation of capacitance and conductance of bimolecular lipid membranes with area. *Journal of Theoretical Biology* **9**, 433-443 (1965). https://doi.org:https://doi.org/10.1016/0022-5193(65)90042-1

24 Khan, M. S., Dosoky, N. S. & Williams, J. D. Engineering Lipid Bilayer Membranes for Protein Studies. *International Journal of Molecular Sciences* **14**, 21561-21597 (2013).

25 Hladky, S. B. & Haydon, D. A. Discreteness of Conductance Change in Bimolecular Lipid Membranes in the Presence of Certain Antibiotics. *Nature* **225**, 451-453 (1970). https://doi.org:10.1038/225451a0

26 Neher, E. & Sakmann, B. Single-channel currents recorded from membrane of denervated frog muscle fibres. *Nature* **260**, 799-802 (1976). https://doi.org:10.1038/260799a0

27 Sackmann, E. Supported Membranes: Scientific and Practical Applications. *Science* **271**, 43-48 (1996). https://doi.org:doi:10.1126/science.271.5245.43

28 Tanaka, M. & Sackmann, E. Polymer-supported membranes as models of the cell surface. *Nature* **437**, 656-663 (2005). https://doi.org:10.1038/nature04164

29 Plant, A. L. Supported Hybrid Bilayer Membranes as Rugged Cell Membrane Mimics. *Langmuir* **15**, 5128-5135 (1999). https://doi.org:10.1021/la981662t

30 Gabriunaite, I., Valiūnienė, A. & Valincius, G. Formation and properties of phospholipid bilayers on fluorine doped tin oxide electrodes. *Electrochimica Acta* **283**, 1351-1358 (2018). https://doi.org:https://doi.org/10.1016/j.electacta.2018.04.160

31 Gabriunaite, I., Valiūnienė, A., Sabirovas, T. & Valincius, G. Mixed Silane-based Self-assembled Monolayers Deposited on Fluorine Doped Tin Oxide as Model System for Development of Biosensors for Toxin Detection. *Electroanalysis* **33**, 1315-1324 (2021). https://doi.org:https://doi.org/10.1002/elan.202060578

32 Gabriunaite, I., Valincius, G., Žilinskas, A. & Valiūnienė, A. Tethered Bilayer Membrane Formation on Silanized Fluorine Doped Tin Oxide Surface. *Journal of The Electrochemical Society* **169**, 037515 (2022). https://doi.org:10.1149/1945-7111/ac5c96

33 Cornell, B. A. *et al.* A biosensor that uses ion-channel switches. *Nature* **387**, 580-583 (1997). https://doi.org:10.1038/42432

34 Zhang, K. S., Nadkarni, A. V., Paul, R., Martin, A. M. & Tang, S. K. Y. Microfluidic Surgery in Single Cells and Multicellular Systems. *Chemical Reviews* **122**, 7097-7141 (2022). https://doi.org:10.1021/acs.chemrev.1c00616

35 Tarek, M. Membrane Electroporation: A Molecular Dynamics Simulation. *Biophysical Journal* **88**, 4045-4053 (2005). https://doi.org:10.1529/biophysj.104.050617

36 Pakhomov, A. G. *et al.* Lipid nanopores can form a stable, ion channel-like conduction pathway in cell membrane. *Biochemical and Biophysical Research Communications* **385**, 181-186 (2009). https://doi.org:https://doi.org/10.1016/j.bbrc.2009.05.035

37 Gehl, J. Electroporation: theory and methods, perspectives for drug delivery, gene therapy and research. *Acta Physiologica Scandinavica* **177**, 437-447 (2003). https://doi.org:https://doi.org/10.1046/j.1365-201X.2003.01093.x

38 Kotnik, T., Kramar, P., Pucihar, G., Miklavcic, D. & Tarek, M. Cell membrane electroporation- Part 1: The phenomenon. *IEEE Electrical*

Insulation Magazine **28**, 14-23 (2012). https://doi.org:10.1109/MEI.2012.6268438

39 Kotnik, T. *et al.* Electroporation-based applications in biotechnology. *Trends in Biotechnology* **33**, 480-488 (2015). https://doi.org:10.1016/j.tibtech.2015.06.002

40 Davalos, R. V., Mir, L. M. & Rubinsky, B. Tissue Ablation with Irreversible Electroporation. *Annals of Biomedical Engineering* **33**, 223-231 (2005). https://doi.org:10.1007/s10439-005-8981-8

41 Martin, R., McFarland, K., Ellis, S. & Velanovich, V. Irreversible Electroporation Therapy in the Management of Locally Advanced Pancreatic Adenocarcinoma. *Journal of the American College of Surgeons* **215**, 361-369 (2012). https://doi.org:10.1016/j.jamcollsurg.2012.05.021

42 Rems, L. & Miklavčič, D. Tutorial: Electroporation of cells in complex materials and tissue. *Journal of Applied Physics* **119** (2016). https://doi.org:10.1063/1.4949264

43 Eresen, A. *et al.* Combination of natural killer cell-based immunotherapy and irreversible electroporation for the treatment of hepatocellular carcinoma. *Annals of Translational Medicine* **9**, 1089 (2021).

44 Arena, C. B. *et al.* High-frequency irreversible electroporation (H-FIRE) for non-thermal ablation without muscle contraction. *BioMedical Engineering OnLine* **10**, 102 (2011). https://doi.org:10.1186/1475-925X-10-102

45 Koronkiewicz, S. & Kalinowski, S. Influence of cholesterol on electroporation of bilayer lipid membranes: chronopotentiometric studies. *Biochimica et Biophysica Acta (BBA) - Biomembranes* **1661**, 196-203 (2004). https://doi.org:https://doi.org/10.1016/j.bbamem.2004.01.005

46 Kinosita, K., Jr. *et al.* Electroporation of cell membrane visualized under a pulsed-laser fluorescence microscope. *Biophys J* **53**, 1015-1019 (1988). https://doi.org:10.1016/s0006-3495(88)83181-3

47 Dower, W. J., Miller, J. F. & Ragsdale, C. W. High efficiency transformation of E.coli by high voltage electroporation. *Nucleic Acids Research* **16**, 6127-6145 (1988). https://doi.org:10.1093/nar/16.13.6127

48 Toepfl, S., Heinz, V. & Knorr, D. High intensity pulsed electric fields applied for food preservation. *Chemical Engineering and Processing: Process Intensification* **46**, 537-546 (2007). https://doi.org:https://doi.org/10.1016/j.cep.2006.07.011

49 Goettel, M., Eing, C., Gusbeth, C., Straessner, R. & Frey, W. Pulsed electric field assisted extraction of intracellular valuables from microalgae. *Algal Research* **2**, 401-408 (2013). https://doi.org:https://doi.org/10.1016/j.algal.2013.07.004

50 Teissie, J., Golzio, M. & Rols, M. P. Mechanisms of cell membrane electropermeabilization: a minireview of our present (lack of ?) knowledge. *Biochim Biophys Acta* **1724**, 270-280 (2005). https://doi.org:10.1016/j.bbagen.2005.05.006

51 Rols, M.-P. & Teissié, J. Experimental evidence for the involvement of the cytoskeleton in mammalian cell electropermeabilization. *Biochimica et Biophysica Acta (BBA) - Biomembranes* **1111**, 45-50 (1992). https://doi.org:https://doi.org/10.1016/0005-2736(92)90272-N

52 Stirke, A. *et al.* Permeabilization of yeast Saccharomyces cerevisiae cell walls using nanosecond high power electrical pulses. *Applied Physics Letters* **105**, 253701 (2014). https://doi.org:10.1063/1.4905034

53 Stirke, A. *et al.* The link between yeast cell wall porosity and plasma membrane permeability after PEF treatment. *Scientific Reports* **9**, 14731 (2019). https://doi.org:10.1038/s41598-019-51184-y

54 Bard, A. J., Fan, F. R. F., Kwak, J. & Lev, O. Scanning electrochemical microscopy. Introduction and principles. *Analytical Chemistry* **61**, 132-138 (1989). https://doi.org:10.1021/ac00177a011

55 Bard, A. J., Fan, F. R. F., Kwak, J. & Lev, O. Scanning electrochemical microscopy. Introduction and principles. *Analytical Chemistry* **61**, 132-138 (2002). https://doi.org:10.1021/ac00177a011

56 Bard, A. J., Li, X. & Zhan, W. Chemically imaging living cells by scanning electrochemical microscopy. *Biosensors and Bioelectronics* **22**, 461-472 (2006). https://doi.org:https://doi.org/10.1016/j.bios.2006.04.028

57 Kai, T., Zoski, C. G. & Bard, A. J. Scanning electrochemical microscopy at the nanometer level. *Chemical Communications* **54**, 1934-1947 (2018). https://doi.org:10.1039/C7CC09777H

58 Binnig, G., Rohrer, H., Gerber, C. & Weibel, E. Surface Studies by Scanning Tunneling Microscopy. *Physical Review Letters* **49**, 57-61 (1982). https://doi.org:10.1103/PhysRevLett.49.57

59 Amemiya, S., Bard, A. J., Fan, F.-R. F., Mirkin, M. V. & Unwin, P. R. Scanning Electrochemical Microscopy. *Annual Review of Analytical Chemistry* **1**, 95-131 (2008). https://doi.org:https://doi.org/10.1146/annurev.anchem.1.031207.112938

60 Beaulieu, I., Kuss, S., Mauzeroll, J. & Geissler, M. Biological scanning electrochemical microscopy and its application to live cell studies. *Anal Chem* **83**, 1485-1492 (2011). https://doi.org:10.1021/ac101906a

61 Huang, L. *et al.* Recent Advances in Scanning Electrochemical Microscopy for Biological Applications. *Materials (Basel)* **11** (2018). https://doi.org:10.3390/ma11081389

62 Aoki, K. Theory of ultramicroelectrodes. *Electroanalysis* **5**, 627-639 (1993). https://doi.org:https://doi.org/10.1002/elan.1140050802

63 Britz, D., Poulsen, K. & Strutwolf, J. Reference values of the diffusion-limited current at a microdisk electrode. *Electrochimica Acta* **50**, 107-113 (2004). https://doi.org:https://doi.org/10.1016/j.electacta.2004.07.019

64 Bergner, S., Vatsyayan, P. & Matysik, F.-M. Recent advances in high resolution scanning electrochemical microscopy of living cells – A review. *Analytica Chimica Acta* **775**, 1-13 (2013). https://doi.org:https://doi.org/10.1016/j.aca.2012.12.042

65 Roberts, W. S., Lonsdale, D. J., Griffiths, J. & Higson, S. P. J. Advances in the application of scanning electrochemical microscopy to bioanalytical systems. *Biosensors and Bioelectronics* **23**, 301-318 (2007). https://doi.org:https://doi.org/10.1016/j.bios.2007.06.020

66 Ventosa, E. & Schuhmann, W. Scanning electrochemical microscopy of Li-ion batteries. *Physical Chemistry Chemical Physics* **17**, 28441-28450 (2015). https://doi.org:10.1039/c5cp02268a

67 Conzuelo, F., Schulte, A. & Schuhmann, W. Biological imaging with scanning electrochemical microscopy. *Proc Math Phys Eng Sci* **474**, 20180409 (2018). https://doi.org:10.1098/rspa.2018.0409

68 Macdonald, J. R. & Johnson, W. B. in *Impedance Spectroscopy* 1-20 (2018).

69 Lazanas, A. C. & Prodromidis, M. I. Electrochemical Impedance Spectroscopy-A Tutorial. *ACS Meas Sci Au* **3**, 162-193 (2023). https://doi.org:10.1021/acsmeasuresciau.2c00070

70 Brug, G. J., van den Eeden, A. L. G., Sluyters-Rehbach, M. & Sluyters, J. H. The analysis of electrode impedances complicated by the presence of a constant phase element. *Journal of Electroanalytical Chemistry and Interfacial Electrochemistry* **176**, 275-295 (1984). https://doi.org:https://doi.org/10.1016/S0022-0728(84)80324-1

71 Zhang, W., Wang, P., Ma, J., Wang, Z. & Liu, H. Investigations on electrochemical properties of membrane systems in ion-exchange membrane transport processes by electrochemical impedance spectroscopy and direct current measurements. *Electrochimica Acta* **216**, 110-119 (2016). https://doi.org:https://doi.org/10.1016/j.electacta.2016.09.018

72 Ballesteros Katemann, B., Schulte, A., Calvo, E. J., Koudelka-Hep, M. & Schuhmann, W. Localised electrochemical impedance spectroscopy with high lateral resolution by means of alternating current scanning electrochemical microscopy. *Electrochemistry Communications* **4**, 134-138 (2002). https://doi.org:https://doi.org/10.1016/S1388-2481(01)00294-6

73 Valiūnienė, A., Petronienė, J., Dulkys, M. & Ramanavičius, A. Investigation of Active and Inactivated Yeast Cells by Scanning Electrochemical Impedance Microscopy. *Electroanalysis* **32**, 367-374 (2020). https://doi.org:https://doi.org/10.1002/elan.201900414

74 Morkvenaite-Vilkonciene, I., Genys, P., Ramanaviciene, A. & Ramanavicius, A. Scanning electrochemical impedance microscopy for investigation of glucose oxidase catalyzed reaction. *Colloids and Surfaces B: Biointerfaces* **126**, 598-602 (2015). https://doi.org:https://doi.org/10.1016/j.colsurfb.2015.01.007

75 Morkvenaite-Vilkonciene, I., Valiūnienė, A., Petroniene, J. & Ramanavicius, A. Hybrid system based on fast Fourier transform electrochemical impedance spectroscopy combined with scanning electrochemical microscopy. *Electrochemistry Communications* **83**, 110-112 (2017). https://doi.org:https://doi.org/10.1016/j.elecom.2017.08.020

76 Cai, C., Liu, B., Mirkin, M. V., Frank, H. A. & Rusling, J. F. Scanning electrochemical microscopy of living cells. 3. Rhodobacter sphaeroides. *Anal Chem* **74**, 114-119 (2002). https://doi.org:10.1021/ac010945e

77 Feng, W., Rotenberg, S. A. & Mirkin, M. V. Scanning Electrochemical Microscopy of Living Cells. 5. Imaging of Fields of Normal and Metastatic Human Breast Cells. *Analytical Chemistry* **75**, 4148-4154 (2003). https://doi.org:10.1021/ac0343127

78 Nagamine, K., Takahashi, Y., Ino, K., Shiku, H. & Matsue, T. Influence of Tip Size on Single Yeast Cell Imaging Using Scanning Electrochemical Microscopy. *Electroanalysis* **23**, 1168-1174 (2011). https://doi.org:https://doi.org/10.1002/elan.201000595

79 Shi, M. *et al.* High-Content Label-Free Single-Cell Analysis with a Microfluidic Device Using Programmable Scanning Electrochemical Microscopy. *Analytical Chemistry* **93**, 12417-12425 (2021). https://doi.org:10.1021/acs.analchem.1c02507

80 Kaya, T., Torisawa, Y.-s., Oyamatsu, D., Nishizawa, M. & Matsue, T. Monitoring the cellular activity of a cultured single cell by scanning electrochemical microscopy (SECM). A comparison with fluorescence viability monitoring. *Biosensors and Bioelectronics* **18**, 1379-1383 (2003). https://doi.org:https://doi.org/10.1016/S0956-5663(03)00083-6

81 Zhao, X., Zhu, R., Anikovskiy, M., Wu, Q. & Ding, Z. Profiling H(2)O(2) from single COS-7 cells by means of scanning electrochemical microscopy. *Biosens Bioelectron* **227**, 115123 (2023). https://doi.org:10.1016/j.bios.2023.115123

82 Nebel, M., Grützke, S., Diab, N., Schulte, A. & Schuhmann, W. Visualization of Oxygen Consumption of Single Living Cells by Scanning Electrochemical Microscopy: The Influence of the Faradaic Tip Reaction. *Angewandte Chemie International Edition* **52**, 6335-6338 (2013). https://doi.org:https://doi.org/10.1002/anie.201301098

83 Zhan, D., Fan, F. R. & Bard, A. J. The Kv channel blocker 4-aminopyridine enhances Ag+ uptake: a scanning electrochemical microscopy study of single living cells. *Proc Natl Acad Sci U S A* **105**, 12118-12122 (2008). https://doi.org:10.1073/pnas.0805286105

84 Polcari, D., Hernández-Castro, J. A., Li, K., Geissler, M. & Mauzeroll, J. Determination of the Relationship between Expression and Functional Activity of Multidrug Resistance-Associated Protein 1 using Scanning Electrochemical Microscopy. *Analytical Chemistry* **89**, 8988-8994 (2017). https://doi.org:10.1021/acs.analchem.7b01601

85 Selva, J. S. G., Voltarelli, V. A., Brum, P. C. & Bertotti, M. SECM investigation on pH changes in cellular environment induced by caffeine. *Electrochimica Acta* **444**, 142015 (2023). https://doi.org:https://doi.org/10.1016/j.electacta.2023.142015

86 Polcari, D., Dauphin-Ducharme, P. & Mauzeroll, J. Scanning Electrochemical Microscopy: A Comprehensive Review of Experimental

Parameters from 1989 to 2015. *Chemical Reviews* **116**, 13234-13278 (2016). https://doi.org:10.1021/acs.chemrev.6b00067

87 Takahashi, Y. *et al.* 3D electrochemical and ion current imaging using scanning electrochemical–scanning ion conductance microscopy. *Physical Chemistry Chemical Physics* **19**, 26728-26733 (2017). https://doi.org:10.1039/c7cp05157c

88 Poderyte, M., Valiūnienė, A. & Ramanavicius, A. Scanning electrochemical microscope as a tool for the electroporation of living yeast cells. *Biosensors and Bioelectronics* **205**, 114096 (2022). https://doi.org:https://doi.org/10.1016/j.bios.2022.114096

89 Poderyte, M., Ramanavicius, A. & Valiūnienė, A. Scanning electrochemical microscopy based irreversible destruction of living cells. *Biosensors and Bioelectronics* **216**, 114621 (2022). https://doi.org:https://doi.org/10.1016/j.bios.2022.114621

90 Poderyte, M., Gabriunaite, I. & Valiūnienė, A. Electroporation and structural integrity analysis of tethered bilayer lipid membranes on fluorine-doped tin oxide surface. *Journal of Electroanalytical Chemistry* **1000**, 119608 (2026). https://doi.org:https://doi.org/10.1016/j.jelechem.2025.119608

91 Valiūnienė, A., Gabriunaite, I., Poderyte, M. & Ramanavicius, A. Electroporation of a hybrid bilayer membrane by scanning electrochemical microscope. *Bioelectrochemistry* **136**, 107617 (2020). https://doi.org:10.1016/j.bioelechem.2020.107617

92 Poderyte, M., Ramanavicius, A. & Valiūnienė, A. Exploring the Living Cell: Applications and Advances of Scanning Electrochemical Microscopy. *Critical Reviews in Analytical Chemistry* **55**, 956-967 (2025). https://doi.org:10.1080/10408347.2024.2328135

SUMMARY

Investigation of Living Cells and Their Membrane Modification Using Electrochemical Methods

Plasma membrane electroporation is a biophysical phenomenon in which external electric fields induce the formation of temporary or permanent pores in the lipid bilayer, thereby increasing membrane permeability. This process has become one of the key tools in biomedicine, biotechnology, and food processing, being widely applied for drug delivery, gene therapy, electrochemotherapy, microbial inactivation, and biosensor development. Despite its broad applicability, electroporation remains only partially controllable, and the precise mechanisms underlying pore formation and resealing are still incompletely understood. In conventional two-electrode electroporation systems, the electric field is essentially homogeneous throughout the sample volume, so every cell present is exposed to the same field regardless of its position, and there is no possibility of restricting the affected region in space or of monitoring the process in real time.

Scanning electrochemical microscopy (SECM), in which an ultramicroelectrode (UME) acts as a spatially confined field source whose position can be controlled with micrometre precision, offers a way to overcome this limitation: the electric field can be focused on a chosen location on a cell or membrane without affecting the surrounding area, and the same UME can immediately afterwards be used as a sensor. Combined with electrochemical impedance spectroscopy (EIS), which quantifies changes in membrane charge-transfer resistance and capacitance, this approach allows electroporation to be induced and its outcome to be evaluated with the same instrument, at the same location, in real time.

Theoretically, electroporation is described by the transmembrane potential ($\Delta\Psi m$) concept: when the potential difference induced by an external electric field across the membrane exceeds a critical threshold (typically in the range of 0.2 to 1 V, depending on lipid composition, temperature, and pulse duration), microscopic hydrophobic defects spontaneously present in the lipid bilayer become thermodynamically favourable and expand into hydrophilic pores. Because $\Delta\Psi m$ is proportional to the electric field strength and to the radius of the cell (or surface point) and depends on the angular position of that point relative to the field direction ($\Delta\Psi m = 1.5 \cdot E \cdot R \cdot \cos\theta$), the same external field necessarily affects different points of a membrane unequally, with the strongest stimulation occurring at the membrane poles facing the field and negligible stimulation at the equator. In conventional two-electrode

electroporators the field is nearly homogeneous throughout the sample volume, so every cell and membrane region present is stimulated identically; such a method is adequate for bulk transfection or sterilization but is unsuitable whenever only a single cell or a defined membrane region must be targeted while the surrounding tissue remains untouched, as required for targeted drug delivery, gene therapy, and the selective destruction of tumour cells while sparing healthy tissue.

A broader review of the literature shows that SECM combined with EIS (an approach also referred to as scanning electrochemical impedance microscopy, SEIM) has already been successfully applied to related membrane-permeability phenomena - for example, to the Triton X-100-induced permeabilization of HeLa cell membranes, where hydrophilic-molecule permeability was found to increase already at a detergent concentration of approximately 0.17 mM, and to the early stages of ferroptosis, an iron-dependent, lipid-peroxidation-driven form of cell death, in single hepatocellular carcinoma cells. However, most of these studies remain phenomenological and do not offer a systematic, quantitative model directly linking electrode geometry (diameter), electrode-to-surface distance, and membrane type (artificial or living, hybrid or tethered) to the electroporation outcome - its reversibility, the size of the affected area, and the membrane recovery time. Revealing precisely these systematic relationships was the central aim of the present dissertation.

Aim: The aim of this dissertation was to develop and experimentally evaluate a methodology for controlled, localized electroporation based on the combination of scanning electrochemical microscopy (SECM) and electrochemical impedance spectroscopy (EIS), and to apply this methodology to artificial lipid membranes and living yeast cells.

Objectives

1. To evaluate and compare the resistance of hBLM and tBLM membranes to localized electrical stimulation.
2. To determine the conditions for reversible and irreversible electroporation with respect to the parameters of the electrical stimulus.
3. To develop and experimentally evaluate a methodology for inducing localized membrane electroporation using SECM.
4. To apply the combination of SECM and EIS to the study of localized electroporation of living Saccharomyces cerevisiae cells.

5. To evaluate the influence of ultramicroelectrode geometric parameters and electrode-to-surface distance on the results of localized electroporation.

Scientific novelty

The novelty of this work lies in the development and experimental validation of a methodology for inducing localized electroporation with SECM; the systematic comparison of the response of hBLM and tBLM membranes, which differ in architecture, to localized electrical stimulation; the evaluation of how ultramicroelectrode diameter and electrode-to-surface distance influence the outcome of localized electroporation; the application of the SECM-EIS combination to the quantitative, time-resolved evaluation of electroporation-induced changes in membrane electrical properties; and the extension of this methodological approach to the localized electroporation of living Saccharomyces cerevisiae cells.

Practical significance

The methodology developed in this work can be applied to fundamental studies of the electrical response and electroporation of biological membranes, as well as to the further development of localized electrochemical interventions in biological systems. The SECM-EIS combination makes it possible to control the location of the electrical stimulus and to quantitatively evaluate the resulting changes in membrane electrical properties. This methodological approach may prove useful for improving localized cell manipulation techniques, biosensors, and other bioelectrochemical measurement systems.

Methodology

Two types of artificial phospholipid membranes were investigated: hybrid bilayer lipid membranes (hBLM), formed by combining a self-assembled octadecyltrichlorosilane (OTS) monolayer with a DOPC/cholesterol (6:4 molar ratio) lipid layer deposited by vesicle fusion, and tethered bilayer lipid membranes (tBLM), formed using a TOPS/ATS-based self-assembled monolayer as a flexible molecular anchor, leaving a sub-membrane aqueous ionic reservoir (~1-2 nm thick) between the lipid bilayer and the fluorine-doped tin oxide (FTO) support. Living Saccharomyces cerevisiae cells were immobilized on poly-L-lysine-coated FTO/glass substrates and kept

metabolically active with 10 mM glucose in phosphate-buffered saline (pH 7.1). All electrochemical measurements were carried out in a standard three-electrode configuration (Au or Pt ultramicroelectrode as the working electrode, a saturated Ag/AgCl reference electrode, and a Pt wire counter electrode) combined with an SECM system (Sensolytics) and an Autolab PGSTAT 30 potentiostat/galvanostat. Localized electroporation was induced by holding the UME at a fixed potential for a defined period at a controlled distance from the surface, determined beforehand from SECM approach curves. Before and after electroporation, EIS spectra (0.1 Hz-100 kHz, 10 mV perturbation) were recorded at the same electrode position and fitted with an equivalent circuit consisting of uncompensated solution resistance together with two series-connected RC elements, describing the UME/electrolyte interface and the membrane-or-cell/electrolyte interface respectively; SECM approach curves and horizontal surface scans were used independently to evaluate the size and recovery of the affected area.

Results: hybrid bilayer lipid membranes (hBLM)

Hybrid bilayer lipid membranes (hBLMs), studied in prior work carried out during the author's Master's studies and used here as a comparative baseline, proved to have a comparatively low electroporation threshold, and their electroporation outcome depended critically on pulse duration and electrode distance: a 1 V pulse applied for 1 min at a 10 µm distance left the SECM approach-curve signature essentially unchanged, whereas a 2 min pulse at a 5 µm distance caused irreversible disruption, with a ~400 µm-diameter affected area (~20× the 20 µm UME diameter) that failed to recover even after 11 h. A pulsed protocol (two 90 s pulses separated by a 60 s open-circuit interval, 4 µm distance), however, produced fully reversible electroporation, with the membrane's characteristic constant-current feature in the SECM approach curve (found at 30 ± 9 µm) re-emerging within ~18 min. These results show that hBLM can tolerate only narrow, carefully chosen stimulation windows before undergoing permanent structural damage.

Results: tethered bilayer lipid membranes (tBLM)

Tethered bilayer lipid membranes (tBLMs) were, by contrast, characterized by superior dielectric stability and closer resemblance to natural plasma membranes, attributable to the presence of the 1-2 nm sub-membrane aqueous reservoir. Strikingly, tBLM showed no measurable electroporation at all under the very same 1 V/2 min protocol that irreversibly destroyed hBLM,

evidence attributed to the ionic reservoir providing an alternative current path that dissipates the field before it can rupture the bilayer. At higher voltage, tBLM tolerated a 2 V, 2-minute pulse with only minor, fully reversible changes: the interfacial resistance R3 dropped from 14.7 to 5.3 $\Omega \cdot cm^2$ after 1 min, recovering to 6.8 $\Omega \cdot cm^2$ by 60 min, while the ~100 μm-wide SECM constant-current plateau (roughly 5× wider than hBLM's ~20 μm) was fully restored. Only a prolonged 2 V, 5-minute pulse produced irreversible membrane breakdown: R_3 collapsed from 14.7 to 0.20 $\Omega \cdot cm^2$ and never recovered above 0.4 $\Omega \cdot cm^2$, while the SECM exclusion plateau vanished permanently, persisting even 12 h post-pulse, with the resulting pore expected to be roughly 20-fold wider than the 25 μm UME used. These findings demonstrate that tBLM constitutes a substantially more robust model of the natural plasma membrane than hBLM, and is therefore more suitable for long-term and applied electroporation studies.

Results: living yeast cells (Saccharomyces cerevisiae)

Living yeast cells were used as a robust biological system for investigating electroporation with SECM. It was found that the electroporation outcome depends strongly on the diameter of the ultramicroelectrode used. A 10 μm gold UME (1-2 V, 120 s, 20 μm distance) induced reversible electroporation, with charge-transfer resistance dropping from 294 to 94 $\Omega \cdot cm^2$ and recovering within 60 min, over an affected area (~250 μm in diameter) roughly 25 times larger than the electrode diameter itself, a pattern consistent with the release of electroactive ions (K^+, Na^+, Ca^{2+}) from the electroporated cells into solution. A 25 μm platinum UME (2.0 V, 120 s) instead caused irreversible electroporation and cell death: resistance did not decrease but instead rose steadily and remained permanently elevated, a pattern explained by detached membrane proteins and lipids adsorbing onto and blocking the electrode surface, over an affected zone (~500-600 μm) about 20× the electrode diameter. This directionally opposite resistance response - decreasing for reversible, increasing for irreversible electroporation - provided an independent electrochemical signature for distinguishing the two outcomes.

SECM and EIS as a combined platform

Across all three systems studied (hBLM, tBLM, and yeast cells), the diameter of the electroporation-affected area was consistently about 18-25 times larger than the diameter of the ultramicroelectrode used and increased further with increasing electrode-to-surface distance. This provides direct,

quantitative evidence that electrode geometry, membrane architecture (the presence or absence of a sub-membrane reservoir), and local electric field distribution jointly determine the balance between reversible and irreversible outcomes. The combination of SECM with EIS thus provides a unique methodological platform: SECM enables localized application of electrical pulses with micrometre precision, while EIS allows quantitative, real-time evaluation of membrane resistance, capacitance, and pore-formation dynamics at the same location where the stimulus was applied. Together, these methods bridge the gap between theoretical electroporation models and practical applications, offering an approach for investigating pore nucleation, growth, and resealing in both artificial membranes and living cells without the need for optical labels or destructive assays.

In the equivalent circuit used to fit the EIS data, the first RC element (charge-transfer resistance and double-layer capacitance at the UME/electrolyte interface) served as an internal control, since its values remained essentially unchanged throughout every experiment, confirming that the electrode itself was not the source of the observed changes. All electroporation-related changes were instead captured by the second RC element, representing the membrane-or-cell/electrolyte interface: a resistance decrease indicated ion leakage through newly formed, still-resealable pores (as observed for reversibly electroporated tBLM and for yeast cells with a small-diameter electrode), a resistance increase indicated detached membrane material blocking the electrode surface after severe, irreversible membrane rupture (as observed for yeast cells electroporated with a large-diameter electrode), and the associated constant-phase-element exponent shifting toward unity indicated a loss of the distributed, heterogeneous capacitive behaviour characteristic of an intact bilayer in favour of simpler, defect-dominated conduction. This distinct electrochemical signature, rather than the absolute magnitude of the resistance change alone, provided the principal basis for distinguishing reversible from irreversible electroporation throughout this work.

The present dissertation, prepared on the basis of 4 scientific publications, thereby provides new, quantitative insight into the electroporation of hybrid and tethered bilayer membranes as well as yeast cells using SECM and EIS. The results highlight the importance of model-membrane choice, electrode geometry, and methodological integration for the development of controlled, localized electroporation technologies, of fundamental significance for membrane biophysics and of potential value for applied research in medicine, biotechnology, and bioelectronics.

Statements presented for defence

1. Hybrid and tethered lipid bilayer membranes exhibit different resistance to localized electrical stimulation and different electroporation conditions.
2. The outcome of localized reversible and irreversible electroporation can be controlled by varying ultramicroelectrode geometry, electrode-to-surface distance, and the parameters of the electrical stimulus.
3. Electrochemical impedance spectroscopy allows quantitative evaluation of electroporation-induced changes in membrane electrical properties and their evolution over time.
4. SECM can be applied to induce localized electroporation of living Saccharomyces cerevisiae cells and to evaluate its spatial extent.
5. The combination of SECM and EIS allows the spatial localization of the electrical stimulus to be linked to the membrane electrical property changes occurring during and after electroporation.

Key conclusions:

1. Hybrid (hBLM) and tethered (tBLM) lipid bilayer membranes, used as artificial models of the plasma membrane, show fundamentally different resistance to localized electrical stimulation: hBLM is sensitive to electrical pulses already at 1 V and recovers only slowly (~18 min under a pulsed protocol), whereas tBLM showed no electroporation at all under the same 1 V/2 min protocol that irreversibly damaged hBLM, and remained intact under a 2 V/2 min pulse (interfacial resistance R3 dropped reversibly from 14.7 to 5.3 Ω·cm² and recovered to 6.8 Ω·cm² within 60 min); irreversible damage occurred only after extending the pulse to 5 min (R3 fell to 0.20 Ω·cm² and did not recover even after 12 h), making tBLM the more suitable model for long-term and applied electroporation studies.
2. The reversibility of localized electroporation is governed by a combination of parameters - potential, pulse duration, and electrode diameter - rather than any single one: the same potential can produce reversible or irreversible damage depending on pulse duration (tBLM: 2 min reversible vs. 5 min irreversible at 2.0 V) or electrode diameter (yeast cells: Ø10 µm reversible vs. Ø25 µm irreversible at 2.0 V/120 s).
3. An SECM-based methodology for inducing localized membrane electroporation was developed and experimentally validated, in which EIS quantitatively evaluates electroporation-induced changes in

membrane charge-transfer resistance and capacitance over time, while SECM approach curves independently confirm changes in membrane structural integrity at the same location where the stimulus was applied.

4. The combination of SECM and EIS was successfully applied to the localized electroporation of living Saccharomyces cerevisiae cells: the outcome depends strongly on ultramicroelectrode diameter, with a smaller (10 μm) electrode producing reversible electroporation (charge-transfer resistance and capacitance fully recovering within 30-60 min) and a larger (25 μm) electrode producing irreversible electroporation, in which resistance remains permanently elevated due to membrane components blocking the electrode surface.
5. Ultramicroelectrode geometry and electrode-to-surface distance directly determine the size of the localized electroporation-affected area: across all systems studied (hBLM, tBLM, and yeast cells), the affected-area diameter was consistently about 18-25 times larger than the electrode diameter, and this ratio increased with electrode-to-surface distance. This systematic relationship demonstrates that the SECM-EIS combination allows not only the localization but also the quantitative prediction of electroporation effects, providing a basis for the future design of targeted electroporation systems.

Some limitations of the present work should be noted. The experiments were performed on populations of immobilized cells or on macroscopically formed artificial membranes rather than at the level of a single cell or a single nanoscale membrane patch, so the reported values reflect an averaged response. Yeast cells, possessing a rigid cell wall, do not fully represent the behaviour of wall-less mammalian cells, and the relative contributions of electrode material versus electrode diameter were not separated as independent variables. Future work will focus on extending the developed methodology to single-cell measurements, to mammalian cell lines, and to more complex, tissue-like three-dimensional environments, as well as on separating the roles of electrode material and geometry, in order to move the present findings closer to practical, targeted biomedical applications such as selective drug delivery and localized tissue treatment.

Prior to each electroporation experiment, the electrode-to-surface distance was established from SECM approach curves recorded in feedback mode, and the working potential was selected from cyclic voltammetry data to lie within the region where oxygen reduction generates a stable Faradaic current without significant hydrogen evolution, ensuring that the measured signal reliably reflected the state of the membrane rather than artefacts of the measurement itself.

PADĖKA

Nuoširdžiai dėkoju savo mokslinei vadovei prof. dr. Aušrai Valiūnienei už vadovavimą visų doktorantūros studijų metu, kantrybę, pagalbą sprendžiant iškilusius klausimus ir malonius, įkvepiančius pokalbius, kurie ne kartą padėjo pažvelgti į tyrimus iš naujos perspektyvos. Dėkoju dr. Ingai Gabriūnaitei už vertingus patarimus, didelę pagalbą ruošiant membranų mėginius, bendradarbiavimą rengiant mokslines publikacijas ir eksperimentų metu. Dėkoju dr. Povilui Virbickui už atidų disertacijos recenzavimą, konstruktyvias pastabas, buvimą geru kolega ir visada pasirengusiu padėti. Dėkoju kolegei Gabijai už tai, kad buvo gera kolegė ir kartu išgyventą doktorantūros kelią. Dr. Ievai Agnei Misiūnei — ačiū už visą šitą vienuolikos metų kelionę kartu, nuo pačios pirmos bakalauro dienos. Sunku išreikšti žodžiais. Kas būtų pagalvojęs, kad ši diena ateis.

Dėkoju visai Vilniaus universiteto Chemijos ir geomokslų fakulteto Fizinės chemijos katedros bendruomenei už sudarytas sąlygas atlikti tyrimus bei draugišką darbo aplinką. Ypač dėkoju Aleksandrai Prichodko už neįkainojamą pagalbą tvarkant doktorantūros formalumus ir administracinius reikalus viso proceso metu.

DALYVAVIMAS MOKSLINIUOSE RENGINIUOSE

Disertacijos autorė dalyvavo šiuose tarptautiniuose moksliniuose renginiuose, kuriuose pristatyti jos mokslinių tyrimų rezultatai:

1. EuChemS Chemistry Congress (8-asis), Lisabona, Portugalija, 2022 m. rugpjūčio 28 d. – rugsėjo 1 d. Pranešimas: „CO_2-mediated monoacylation of symmetric diamines“ (kartu su J. M. V. Lauridsen, J.-W. Lee).
2. TOKS (Træf for Organisk Kemi-Studerende), Danija, 2023 m. Pranešimas: „Monoacylation of symmetrical diamines using CO_2“.

GYVENIMO IR MOKSLINĖS BEI KŪRYBINĖS VEIKLOS APRAŠYMAS

Margarita Poderytė 2015–2019 m. studijavo nanomedžiagų chemiją Vilniaus universitete ir bakalauro studijas baigė aukščiausiu įvertinimu (10/10), parengusi baigiamąjį darbą „Hibridinio fosfolipidų dvisluoksnio paviršiaus tyrimas skenuojančiuoju elektrocheminiu mikroskopu“, vadovaujant prof. dr. Aušrai Valiūnienei. 2019–2021 m. tame pačiame universitete ir toje pačioje programoje ji įgijo magistro laipsnį, taip pat įvertintą aukščiausiu pažymiu (10/10, diplomas Magna Cum Laude), tęsdama tyrimus su skenuojančiuoju elektrocheminiu mikroskopu kaip elektroporacijos proceso tyrimo įrankiu.

2021 m. Margarita Poderytė pradėjo chemijos mokslo krypties daktaro studijas Vilniaus universiteto Chemijos ir geomokslų fakultete. Vadovaujant prof. dr. Aušrai Valiūnienei, ji atliko šioje disertacijoje pristatomus tyrimus, susijusius su gyvų ląstelių ir dirbtinių lipidinių membranų elektroporacija, derindama skenuojančiąją elektrocheminę mikroskopiją (SECM) su elektrochemine impedanso spektroskopija (EIS). Disertacijos tyrimų rezultatai paskelbti keturiuose moksliniuose straipsniuose aukšto lygio tarptautiniuose leidiniuose – Biosensors and Bioelectronics, Critical Reviews in Analytical Chemistry ir Journal of Electroanalytical Chemistry – kuriuose visuose ji yra pirmoji autorė.

2023–2024 m. ji stažavosi Kopenhagos universitete (Danija), organinės chemijos srityje, vadovaujant prof. Jiwoong Lee, kur tyrė polietileno tereftalato (PET) plastiko atliekų panaudojimo anglies dioksido surišimui galimybes. Nuo 2026 m. balandžio mėn. ji dirba mokslo darbuotoja (podoktorantūros tyrėja) Kopenhagos universiteto Chemijos katedroje, tęsdama su anglies dioksido surišimo technologijomis susijusius tyrimus ir jų pritaikymą pramoniniu mastu.

Be mokslinio darbo, Margarita Poderytė aktyviai dalyvauja mokslo populiarinimo, inovacijų ir mokslo bendruomenės veikloje: nuo 2023 m. yra Kopenhagos universiteto Chemijos katedros įvairovės, lygybės ir įtraukties (DEI) komiteto narė. Jos vykdomi moksliniai tyrimai, susiję su anglies dioksido surišimo technologijomis, buvo pristatyti ir tarptautiniu mastu pripažinti keliuose mokslo bei inovacijų konkursuose ir programose.

Margarita Poderytė laisvai kalba lietuviškai (gimtoji kalba) ir angliškai, taip pat moka danų ir rusų kalbas.

PUBLIKACIJŲ SĄRAŠAS

1. **Margarita Poderytė**, Aušra Valiūnienė, Arūnas Ramanavičius. Scanning electrochemical microscope as a tool for the electroporation of living yeast cells. Biosensors and Bioelectronics, 205 (2022), 114096. https://doi.org/10.1016/j.bios.2022.114096
Autorės indėlis: eksperimentų planavimas ir atlikimas, duomenų analizė, straipsnio teksto rengimas.

2. **Margarita Poderytė**, Arūnas Ramanavičius, Aušra Valiūnienė. Scanning electrochemical microscopy based irreversible destruction of living cells. Biosensors and Bioelectronics, 216 (2022), 114621. https://doi.org/10.1016/j.bios.2022.114621
Autorės indėlis: eksperimentų planavimas ir atlikimas, duomenų analizė, straipsnio teksto rengimas.

3. **Margarita Poderytė**, Arūnas Ramanavičius, Aušra Valiūnienė. Exploring the Living Cell: Applications and Advances of Scanning Electrochemical Microscopy. Critical Reviews in Analytical Chemistry, 55(5) (2025), 956–967. https://doi.org/10.1080/10408347.2024.2328135
Autorės indėlis: literatūros šaltinių analizė, straipsnio teksto rengimas.

4. **Margarita Poderytė**, Inga Gabriūnaitė, Aušra Valiūnienė. Electroporation and Structural Integrity Analysis of Tethered Bilayer Membranes on Fluorine-Doped Tin Oxide Surfaces. *Journal of Electroanalytical Chemistry*, 1000 (2026), 119608. https://doi.org/10.1016/j.jelechem.2025.119608
Autorės indėlis: eksperimentų planavimas ir atlikimas, duomenų analizė, straipsnio teksto rengimas.

*5. Papildomas straipsnis (nesudaro disertacijos pagrindo): Jerik Mathew Valera Lauridsen+, **Margarita Poderytė+**, Ji-Woong. Lee. Taming diamines and acyl chlorides by carbon dioxide in selective mono-acylation reactions. Green Chemistry, 25 (2023), 1834–1841. https://doi.org/10.1039/D2GC04478A. Pastaba: J. M. V. Lauridsen ir M. Poderytė yra lygiaverčiai pirmieji autoriai (co-first authors). Šis straipsnis į disertaciją sudarančių publikacijų sąrašą neįtrauktas, kadangi jo tematika (organinė chemija, selektyvus monoacilinimas naudojant CO_2) skiriasi nuo disertacijos temos (elektrochemija, lokalizuota elektroporacija). Straipsnis parengtas doktorantūros studijų metu atliktos mokslinės stažuotės Kopenhagos universitete rezultatų pagrindu.*

PUBLIKACIJŲ KOPIJOS

Journal of Electroanalytical Chemistry 1000 (2026) 119608

Contents lists available at ScienceDirect

Journal of Electroanalytical Chemistry

journal homepage: www.elsevier.com/locate/jelechem

Electroporation and structural integrity analysis of tethered bilayer lipid membranes on fluorine-doped tin oxide surface

Margarita Poderyte [a], Inga Gabriunaite [a], Aušra Valiūnienė [a,b,*]

[a] Institute of Chemistry, Faculty of Chemistry and Geosciences, Vilnius University, Naugarduko 24, Vilnius, LT 03225, Lithuania
[b] State Research Institute Center for Physical Sciences and Technology, Sauletekio ave. 3, LT-10257, Vilnius, Lithuania

ARTICLE INFO

Keywords:
Electroporation
Tethered bilayer lipid membrane (tBLM)
Scanning electrochemical microscopy (SECM)
Electrochemical impedance spectroscopy (EIS)
Fluorine-doped tin oxide (FTO)

ABSTRACT

Tethered bilayer lipid membranes (tBLMs) represent a robust model for mimicking cellular membranes in bioelectrochemical applications. In this study, we investigate the electroporation behavior and structural resilience to electrical impulses of tBLMs formed on fluorine-doped tin oxide surfaces. The tBLMs were composed of 60% 1,2-dioleoyl-sn-glycero-3-phosphocholine and 40% cholesterol, closely resembling mammalian plasma membranes. Using scanning electrochemical microscope (SECM) in a three-electrode configuration, we applied localized voltage pulses to induce electroporation on uncharged tBLM while monitoring structural changes via electrochemical impedance spectroscopy (EIS). A 2 V, 2 min pulse caused only minor and fully reversible alterations in impedance and SECM approach curves, suggesting reorganization without membrane disruption. In contrast, a prolonged 5 min pulse at the same 2 V voltage led to irreversible membrane breakdown, determined by a permanent decrease in interfacial resistance and loss of the SECM approach curve defined exclusion zone. These results demonstrate the utilization of SECM and EIS as complementary tools for analysis and electroporation dynamics in bilayer membrane structures and highlight the superior dielectric stability of tBLMs compared to hybrid bilayer systems.

1. Introduction

Electroporation is the formation of reversible or irreversible pores in plasma membranes of the cells. This process could be applied for introduction of various drugs or foreign DNA into mammalian, bacterial or other cells mainly for therapeutic purposes [1]. Electroporation occurs when an external electric field raises the transmembrane potential above a critical threshold (~0.2–1 V for lipid bilayers), lowering the energy barrier for pore nucleation and enabling transient or permanent aqueous pore formation; the process is thermally activated and influenced by field strength, duration, and membrane composition [2–5]. The activation energy for electroporation depending on the temperature and the type of lipids in the membrane, is around 23–34 kJ·mol^{-1} [6].

Over the years, most studies concerning electroporation were carried out as dynamic simulation models [7,8]. Even though theoretical models have been shown to depict real systems quite accurately [4,5], they cannot fully substitute for laboratory experiments. Recent findings indicate that theoretical models of lipid bilayer electroporation do not always correlate with experimental results [6]. Therefore, further studies are essential to understand the mechanisms of electroporation of different membranes and how the architecture of the membrane could influence the occurring processes. In practice, electroporation could be applied in vitro [9,10] and in vivo [10,11]. Moreover, electroporation could be used in model lipid membrane systems, as it is a convenient tool to investigate various processes occurring in the membranes [12–15].

Different models of lipid membranes were designed and investigated since the middle of 20th century, such as black lipid membranes (BLMs) [16–18] (often called planar lipid bilayers), solid supported bilayer lipid membranes (sBLMs) [19–21] also known as a supported lipid bilayers (SLBs) [22,23], hybrid bilayer lipid membranes (hBLMs) [24–26] also known as a hybrid supported lipid bilayers hSLBs [22,27] and tethered bilayer lipid membranes (tBLMs) [28–30]. BLMs and sBLMs are the least stable forms of lipid membranes, while hBLM is much more robust. However, hBLM contains less biologically relevant fluidity [25], that is necessary for all biological systems. This limitation arises from the structural differences between hBLM and tBLM. The inner leaflet of the hBLM is primarily composed of hydrophobic units from a self-assembled monolayer (SAM). Such hydrophobic environment prevents the formation of a submembrane ionic reservoir between the membrane and the solid support, which is necessary for the membrane to become relevant.

* Corresponding author at: Institute of Chemistry, Faculty of Chemistry and Geosciences, Vilnius University, Naugarduko 24, Vilnius, LT 03225, Lithuania
E-mail address: ausra.valiuniene@chf.vu.lt (A. Valiūnienė).

https://doi.org/10.1016/j.jelechem.2025.119608
Received 12 July 2025; Received in revised form 20 October 2025; Accepted 28 October 2025
Available online 1 November 2025
1572-6657/© 2025 Elsevier B.V. All rights are reserved, including those for text and data mining, AI training, and similar technologies.

This limitation can be altered by using different types of SAMs [31,32], however, the inner leaflet remains predominantly hydrophobic, as it must interact with hydrophobic parts of phospholipids to form a uniform bilayer membrane. tBLM is notably the most stable model of synthetic membranes and closely reassembles plasma membrane of the cell. The outer layer of tBLMs is surrounded by a large amount of electrolyte solution that resembles extracellular fluid. Meanwhile, the inner leaflet of the tBLM is separated from the solid support by a submembrane ionic reservoir that is 1–2 nm thick and mimics the cytosol [33]. This submembrane ionic reservoir makes tBLMs suitable for incorporating transmembrane proteins. These include pore-forming toxins [34] and many non-channel-forming membrane proteins [31,35].

Electroporation has been investigated in black lipid membranes [36], as it is a convenient platform to form the membrane and apply the electric field from both sides of the membrane in a two-electrode setup. Such platform is also convenient to investigate occurring processes. However, results obtained with BLM would be difficult to apply to experiments in vivo or in vitro. While BLMs can mimic membrane composition, their fragility and the need for electrode placement on both sides limit their applicability in vivo and complicate in vitro use with intact cells or tissues. Solid-supported membranes, including tBLMs, allow single-sided access, making them more representative of clinical or physiological conditions. A better understanding of electroporation phenomena could be achieved by examining the other types of membranes (sBLM, hBLM and tBLM) formed on solid support in different architectures. If the solid support, that membrane was formed on is conductive, then it is possible to polarize the membrane from both sides, as it was shown for tBLMs [14,15]. Even though this method allows the voltage to be applied evenly across the membrane, it would require a more complex setup to implement it in practical approaches for in vitro or in vivo by using two electrodes in both sides of the target. Additionally, electroporation of tBLM should give the best understanding of how the plasma membrane of the cell could be permeated by electric field because, the structure of tBLM best resembles plasma membrane while the inner submembrane ionic reservoir resembles the cytosol. The authors propose that the most practical approach for investigating electroporation is to apply an external electric field in a three-electrode setup - using working, reference, and counter electrodes - by approaching the membrane from only one side [12,13]. The reference electrode ensures the stability of the applied voltage, while current flows between the working and counter electrodes. The use of scanning electrochemical microscopy (SECM) allows the working electrode to be positioned as close as a few nanometers from the membrane, maximizing the efficiency of electroporation. This setup enables targeted electroporation with minimal invasiveness and without damaging surrounding cells or tissues [37,38]. This approach has been investigated in hBLMs, which lack a submembrane ionic reservoir, demonstrating both reversible and irreversible electroporation [12]. However, investigations involving tBLMs could provide a more detailed understanding of how the submembrane ionic reservoir affects the electroporation process.

In this study, we investigated the electroporation phenomena in tBLMs using scanning electrochemical microscopy. The tBLM was formed on fluorine doped tin oxide (FTO) modified with trichloro(3-(octadecylthio)propyl)silane (TOPS) and allyltrichlorosilane (ATS) self-assembled monolayer (SAM). The tBLM contained 60% 1,2-dioleoyl-sn-glycero-3-phosphocholine (DOPC) and 40% cholesterol (Chol), because this lipid composition mimics most mammalian cell membranes [39,40]. The findings would provide insights into the structural differences, electroporation thresholds, and recovery behavior of the membranes, suggesting significant distinctions in their performance and stability under similar experimental conditions.

The novelty of this research lies in combining scanning electrochemical microscopy (SECM) with a Pt ultramicroelectrode (UME) to perform spatially localized electroporation of tethered bilayer lipid membranes (tBLMs) while simultaneously characterizing the membrane in situ at micrometer-scale. This configuration enables interrogation of electroporation effects with spatial and temporal resolution not achievable in conventional bulk-electrode setups. Unlike previous studies that apply electric fields across the entire membrane, our approach delivers controlled disruption to a defined area and allows immediate post-pulse impedance measurements within the affected zone. These capabilities advance the field by enabling mechanistic studies of localized membrane permeabilization processes relevant to nanopore formation, targeted drug delivery, and modulation of membrane protein function.

2. Materials and methods

2.1. Formation of the tethered bilayer lipid membranes (tBLMs)

The glass slide, coated with a thin film of fluorine doped tin oxide (Sigma-Aldrich), was cleaned in Alconox® (Sigma-Aldrich) detergent solution in an ultrasonic bath, then rinsed with deionized water, incubated in concentrated sulphuric acid (95%, Chempur) for 1 h, rinsed with deionized water and incubated in deionized water overnight. Then, self-assembled monolayer (SAM) consisting of trichloro(3-(octadecylthio)propyl)silane (TOPS) and allyltrichlorosilane (ATS, Sigma-Aldrich) was formed. The synthesis of TOPS is described in reference [41], the procedure results in 1:1 M ratio ready-to-use silanization mixture of TOPS:ATS. 30 μL of silane mixture were added to 20 mL of heptane (HPLC grade, Honeywell), heated to 60 °C and clean FTO sample was immersed and incubated in silane solution for 1 h, at 60 °C. After, the electrode was rinsed with heptane and dried in a stream of nitrogen.

The tBLM formation was carried out via vesicle fusion method. The multilamellar vesicles contained a 6:4 M ratio of 1,2-dioleoyl-sn-glycero-3-phosphocholine (DOPC, Avanti) and cholesterol (Chol, Avanti) with a total lipid concentration of 1 mM in phosphate-buffered saline (PBS) (pH 4.6) containing 0.1 M NaCl and 0.01 M NaH_2PO_4 (both Reachem Slovakia, p.a.). Lipid solutions in chloroform were prepared at a concentration of 10 mM. Then, the desired amounts of DOPC and Chol solutions in chloroform were placed in a glass vial and evaporated in a stream of nitrogen gas until a dry film of lipids is formed at the bottom of the vial. Then, the lipids were rehydrated in PBS at pH 4.6 by performing several aspiration cycles using an automatic pipette until a whitish solution was achieved. The preparation of the vesicle solution described in [42], results in neutral vesicles with a zeta potential of approximately 0 mV, a diameter of 500–1100 nm, and a narrow polydispersity (see the Supporting material in [43]). The vesicle solution was poured over FTO modified with SAM, left for 1 h to incubate, and then rinsed with PBS pH 7.1. The tBLM covered FTO electrode was immediately used for electrochemical experiments.

The vesicle fusion and tBLM formation were performed at room temperature (~22 °C), where DOPC is in the liquid-disordered phase. The addition of 40 mol% cholesterol promotes formation of a liquid-ordered phase, increasing bilayer packing and bending modulus [44]. While a higher bending modulus can reduce the risk of spontaneous rupture, the tethering chemistry used in this study encourages vesicle fusion and bilayer formation, even at an elevated cholesterol content, as confirmed by previous studies [45,46]. In this study, tBLM was formed from a mixture of 60 mol% 1,2-dioleoyl-sn-glycero-3-phosphocholine (DOPC) and 40 mol% cholesterol (Chol). It has been demonstrated that this composition mimics the structure and mechanical properties of mammalian plasma membranes [39,40].

2.2. Electrochemical measurements

Electroporation experiments were conducted using a 25 μm diameter platinum (Pt) ultramicroelectrode (UME) in neutral PBS at pH 7.1. Localized electrical pulses were applied exclusively via the UME at a distance of 5 μm from non-polarised and unconnected surface of

tethered bilayer lipid membranes (tBLMs) using scanning electrochemical microscopy (SECM) in a three-electrode configuration with the Pt UME as the working electrode, a Pt wire as the counter electrode, and an Ag/AgCl/$Cl^-_{sat.}$ electrode as the reference electrode. In this three-electrode configuration, the applied potential is maintained by the potentiostat, ensuring a continuous current path between the working and counter electrodes. This avoids the isolated capacitive decay observed in two-electrode arrangements and enables precise, targeted electroporation without the need to charge the entire membrane support. Electroporation was completed using SECM by holding a Pt-based UME at a potential of 2.0 V vs Ag/AgCl/$Cl^-_{sat.}$ for 2 min or 5 min. The effect of this potential on tBLM was then evaluated by measuring the electrochemical impedance spectra of the platinum UME at a potential of −0.75 V in the same three-electrode configuration used for the SECM measurements. Tethered bilayer lipid membranes formed on FTO substrates remained electrically unpolarized during electroporation.

SECM measurements were performed in feedback mode. This allows the UME to measure Faradaic current of occurring redox reaction, which is influenced by approaching different types of surfaces [47]. The electrochemical activity of the tBLM was evaluated by approaching the membrane surface in the *Z*-direction and recording the current response as a function of distance, generating approach curves. These measurements were used to assess changes in membrane integrity before and after electroporation. The schematic representation of the setup is shown in Fig. 1.

Electrochemical impedance spectroscopy (EIS) was used to monitor changes in the electrochemical characteristics of the membrane before and after electroporation. EIS experiments were carried out in potentiostatic mode over a frequency range of 0.1 Hz to 100 kHz using a Ø 25 μm Pt UME as the working electrode biased at −0.75 V (vs. Ag/AgCl/$Cl^-_{sat.}$). The peak-to-peak amplitude of the perturbation voltage was 10 mV. Electrochemical impedance spectra were analyzed using *ZView* software and fitted to selected equivalent circuit models to extract electrochemical parameters. The equivalent circuit models were selected to reflect the specific SECM geometry used here, in which the Pt UME approaches the tBLM from solution while the FTO support remains unbiased; this configuration alters the distribution of capacitive and resistive elements compared to models developed for planar tethered bilayers on biased substrates. The results are presented as Nyquist plots, where the real part of impedance (Z') is plotted on the x-axis and the imaginary part (Z") on the y-axis. Nyquist plots were selected for the main text because they allow for straightforward visual comparison of membrane resistance (semicircle diameter) before and after electroporation, which is our primary parameter of interest. Corresponding Bode magnitude and phase plots, which provide complementary information on system heterogeneity, are provided in the Supplementary Material (Fig. S1).

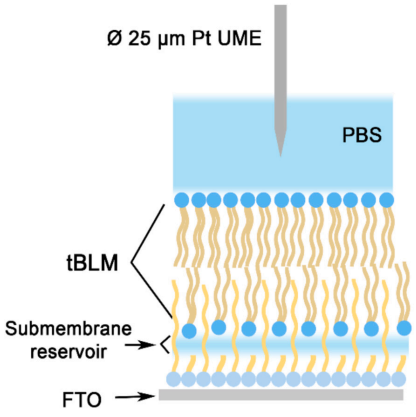


Fig. 1. Schematic representation of pristine tBLM before approaching its surface with Ø 25 μm Pt UME recording the current response as a function of distance.

3. Results

3.1. Stability of the tBLM to an electrical impulse

In this study, SECM was employed to monitor electroporation processes. The method is based on measuring Faradaic current between the ultramicroelectrode (UME) and the counter electrode. Although redox mediators are typically employed to amplify the Faradaic signal, this study opted for a mediator-free approach to prevent the potentially unfavorable impact of additional ions on the sensitive tBLM system.

Instead, the electroporation proceeds at a higher applied voltage (vide infra), where the Faradaic current arises from the onset of the oxygen evolution reaction. This ensures that, after the initiation of the potentiostatic pulse, the charging of the electrical double layer is followed by the continuous residual current flow through the UME. The effect of such electroporation procedure was evaluated by the EIS performed at −0.75 V (vs. Ag/AgCl/$Cl^-_{sat.}$), where the hydrogen ion reduction at the UME-PBS interface starts [12]. The choice of this potential was made because the hydrogen reduction, a kinetically fast process, ensures minimal contribution of this process to the measured impedance of the system.

The conditions for electroporation of tBLM using SECM by holding a Pt-based UME at a potential of 1.0 V vs Ag/AgCl/$Cl^-_{sat.}$ for 2 min were selected similar to previously investigated electroporation of hBLM [12], however, for tBLM no electroporation was observed (data not shown). This could be explained by the existence of submembrane ionic reservoir and natural defects inside the tBLM. The electric current, as it approaches the tBLM, flows through natural defects inside tBLM, reaches submembrane reservoir and continues to flow in the reservoir between membrane and solid surface. As compared to hBLM, where no submembrane ionic reservoir exists, even if the same natural defects exist, the current has no path to flow between membrane and solid support, which leads to destruction of the hBLM.

Further experiments with tBLMs involved applying a voltage of 2 V for the electroporation of the membrane. The effect of this voltage on the tBLM was then evaluated by measuring the EIS of the Pt UME at a potential of −0.75 V vs Ag/AgCl/$Cl^-_{sat.}$. When the UME is positioned in close proximity to an unconnected, unpolarised tBLM surface, the tBLM can be AC coupled with the counter electrode due to a large interfacial capacitance [48]. Alternating current can flow directly through the electrolyte solution between the counter electrode and the Pt UME, and it can cross the tBLM-electrolyte solution interface to flow from the counter electrode to the Pt UME.

Fig. 2 A shows the impedance response of a tBLM after a 2 min 2 V pulse was applied via the Ø 25 μm Pt UME. Only a slight decrease in resistance (Fig. 2 A inset, red circles) appears 1 min after the electrical stimulation, indicating a minor increase in ion permeability. This subtle change could suggest the formation of small, transient pores or slight membrane perturbation. However, a measurement taken 30 min later (Fig. 2 A inset, blue triangles) showed that the impedance spectrum had returned to a similar shape that was recorded before the electroporation. The fitting data obtained using model in Fig. 2 B and presented in the Table 1 show that the parameter R2, which is designated as the interfacial resistance between the UME and the tBLM, remains nearly constant throughout the experiment, with values consistently around 0.2 Ω·cm^2. A slight decrease observed 1 min after the pulse (from 0.23 Ω·cm^2 to 0.18 Ω·cm^2) can be attributed to the immediate effect of the sudden potential impulse slightly influencing the current flow between the UME and the membrane surface. However, the change is minimal

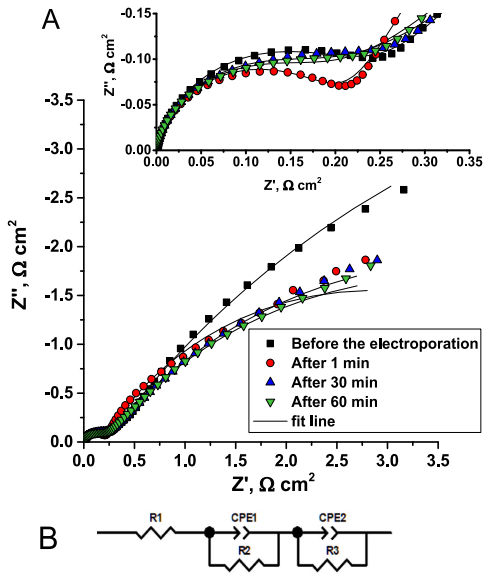


Fig. 2. A - electrochemical impedance spectra before and after the electroporation of tBLMs. 2 min 2 V pulse was applied. Inset – zoomed in part of the impedance spectra. Measurements were performed using a three-electrode system with Ø 25 μm Pt UME, biased at −0.75 V. **B** - equivalent circuit model used for the fitting of EIS data, where: R1 – uncompensated solution resistance; R2 and CPE1 – the charge transfer resistance at the interface Pt UME/PBS and the constant phase element of the electric double layer, respectively. R3 and CPE2 – the charge transfer resistance and the capacitance at the interface tBLM/PBS, respectively. CPE elements were used to represent non-ideal capacitive behavior at the Pt UME/electrolyte interface, arising from electrode curvature, surface roughness, and local heterogeneity in double-layer structure, which introduce a distribution of relaxation times rather than a single ideal capacitance.

and quickly stabilizes (0.20 Ω·cm^2 after 30 min), suggesting that no significant or lasting electroporation has occurred. Such a small and transient drop in resistance is unlikely to reflect pore formation within the bilayer, since electroporation typically results in substantial decrease in membrane resistance due to the formation of conductive pore, defects or pathways [12].

Parameter R3 associated with the larger semicircle in the Nyquist plot (Fig. 2 A), is interpreted as the resistance affecting ion transport through the 1–2 nm thick submembrane ionic reservoir between the membrane and solid support and, potentially, across the bilayer itself. This element is consistent with previously described models in which the total current is distributed between two parallel pathways: one involving ionic conduction along the solid support and another through the thin aqueous layer beneath the membrane [49]. The occurring drop in R3 from 14.7 Ω·cm^2 before the electroporation to 5.3 Ω·cm^2 1 min after the pulse, followed by partial recovery to 6.8 Ω·cm^2 60 min after the pulse, may reflect changes in ion distribution, local conductivity, or dielectric properties within the submembrane region, rather than direct formation of membrane-spanning pores. Similar current distribution behavior and its sensitivity to electric field-induced structural rearrangements have been reported in studies of tBLM systems using SECM and EIS, particularly in response to mechanical or electrochemical perturbation [14,49]. Thus, slight shifts in R3 are interpreted as local structural changes rather than large-scale membrane failure. Overall, these EIS results indicate that the applied 2 min 2 V pulse induces only minimal and reversible changes in the tBLM and does not lead to significant electroporation or compromise of membrane integrity.

Fig. 3 presents the SECM approach curves recorded before the electroporation at 2 V for 2 min, and at 1 min and 60 min after the electroporation. The constant current region - indicative of the distance at which the membrane impedes redox mediator access to the electrode - has been observed as previously described in literature [12,13]. The constant current region of the tBLM is several times longer than that in hybrid bilayer lipid membranes (hBLMs), reaching approximately 100 μm (Fig. 3, black squares) compared to only ~20 μm for hBLMs [12]. This difference arises because tBLMs are both more electrically insulating and structurally thicker than hBLMs. 1 min after the electroporation pulse, the constant current region expanded by approximately 20 μm, (Fig. 3 inset, red circles) suggesting an increase in membrane thickness and/or dielectric properties. This correlates with the drop in CPE2 after 1 min (see Table 1), which also indicates an increase in the thickness of the tBLM. The slight expansion of the constant current region can be explained by the localized reorganising or compacting of the lipid bilayer, which is induced by the applied electric field. This slight expansion can be explained by localized reorganization or compaction

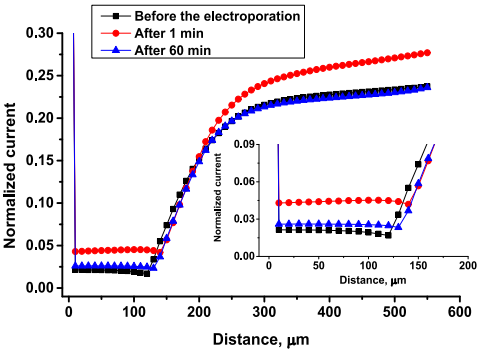


Fig. 3. SECM approach curves recorded while approaching the tBLM surface before electroporation, and 1 min and 60 min after electroporation, with 2 V applied to the Pt UME for 2 min. Inset shows the zoomed in part of the same approach curves at distances between 0 and 200 μm. Measurements were performed using a three-electrode system with Ø 25 μm Pt UME as the working electrode, biased at −0.75 V.

Table 1
Fitting data of electrochemical impedance spectra obtained before and after the electroporation of the tBLM by applying 2 min 2 V pulse (showed in Fig. 2 A). The data were fitted according to equivalent scheme showed in Fig. 2 B.

	χ^2	CPE1, mF·cm^{-2}	n (CPE1)	R2, Ω·cm^2	CPE2, F·cm^{-2}	n (CPE2),	R3, Ω·cm^2
Before the electroporation	$6.6\cdot10^{-4}$	2.85	0.88	0.23	0.25	0.62	14.7
After 1 min	$8.3\cdot10^{-4}$	2.93	0.88	0.18	0.23	0.67	5.3
After 30 min	$1.1\cdot10^{-3}$	3.29	0.88	0.20	0.27	0.59	7.4
After 60 min	$9.4\cdot10^{-4}$	2.90	0.89	0.18	0.26	0.59	6.8

of the lipid bilayer induced by the applied electric field. Electric fields are known to cause structural rearrangements in supported lipid systems, including dipolar reorientation and enhanced lipid packing, especially in the presence of cholesterol [50,51]. This enhanced packing could temporarily increase the effective membrane thickness and its dielectric barrier, thereby extending the region in which the redox mediator is excluded from the electrode. Furthermore, the tethered structure of tBLM and the submembrane ionic reservoir (~1–2 nm thick) likely contribute to this behavior by offering a buffer zone that supports reversible deformation without structural failure [33].

Although 2 V is considered an intense local stimulus in electroporation literature – especially at small electrode distances - it appears that the tBLM provided sufficient structural integrity to either resist or rapidly recover from such perturbation according to the SECM data (Fig. 3), combined with electrochemical impedance spectroscopy (Fig. 2). Fig. 4 shows a schematic representation of the tBLM after 2 min of electroporation at 2 V. In this case, negligible changes in the tBLM were observed without pore formation. This level of robustness is particularly relevant in applications involving biosensors or bioelectronic devices, where membrane-coated electrodes must resist to pulsed electric fields without losing functional integrity.

3.2. Irreversible electroporation and membrane breakdown

To further study the electroporation and determine the stability threshold of the tBLM, the 2 V electroporation pulse was extended from 2 min to 5 min. The 2 min and 5 min electroporation experiments were performed on separate tBLM samples to avoid cumulative effects from repeated pulses. In the three-electrode configuration used here, the applied potential and current flow are sustained for the entire pulse duration, enabling a controlled comparison of different electroporation times. The recorded data is presented in Figs. 5 and 6. The electrochemical impedance spectra recorded after applying a 5 min 2 V pulse (Fig. 5 A) show a substantial change in both spectral shape and absolute values of fitted parameters (Table 2) compared to 2 min 2 V pulse (Fig. 2 and Table 1), reflecting clear evidence of irreversible electroporation. The most notable shift is in the R2 value (Fig. 5 C and D, showed by the arrows), which drops from ~0.2 Ω·cm^2 before the pulse to ~1.3 ·10^{-2} Ω·cm^2 after 1 min. This sharp decrease suggests the formation of a conductive pore that effectively bypasses the insulating barrier of the membrane. Interestingly, R2 increases slightly to ~3.8·10^{-2} Ω·cm^2 after 30 and 60 min (Fig. 5 E and F, arrows and Table 2), which may indicate that the tBLM attempts to reseal the pore or restore its functional architecture. However, the resistance does not return to baseline, suggesting the pore remains permanently formed, with slightly increased hindrance to ion flow.

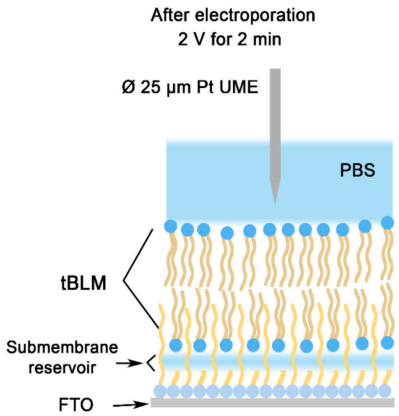


Fig. 4. Schematic representation of tBLM after 2 min 2 V electroporation with Ø 25 µm Pt UME. The electroporation yielded only negligible changes to the tBLM.

The changes in R3 associated with the second, larger semicircle in the Nyquist plot (Fig. 5 A), reflecting ion flow across the membrane, also reflect significant membrane changes. Prior to electroporation, R3 is approximately 14.7 Ω·cm^2, but it drops to 0.2 Ω·cm^2 post-pulse and remains below 0.4 Ω·cm^2 at all subsequent time points. This dramatic loss of resistance indicates that the bilayer has lost its integrity as an insulating barrier, allowing direct ionic conduction and short-circuiting of the electrode interface.

In terms of spectral shape, the disappearance of well-defined semicircles and the emergence of flattened arcs or distorted shapes in the Nyquist plots suggest increased heterogeneity and possibly mixed conduction pathways at the membrane–electrode interface (Fig. 5 A). Moreover, the constant phase elements (CPE1 and CPE2), also change significantly after electroporation. The increase in CPE1 (from 2.85 to 9.11 mF·cm^{-2}) and the decrease in CPE2 (from 24.9 to 19.1 mF·cm^{-2}) together with the shift in n values for CPE2 (from 0.62 to 0.81), indicate that electroporation introduces more conductive pathways while reducing the distributed capacitance associated with the intact bilayer.

These trends are consistent with literature reports [14,52] showing that electroporation disrupts membrane uniformity, resulting in more distributed capacitance behavior due to defects, surface roughness, and uneven charge distribution.

Supporting this, the SECM approach curves (Fig. 6) showed a dramatic and irreversible collapse of the constant current region following the 5 min 2 V electroporation pulse. Before electroporation, the tBLM displayed a wide constant current plateau ~100 µm (Fig. 6, black squares), indicating an intact, highly insulating membrane that effectively blocked mediator access to the conductive surface. After the pulse, this plateau nearly disappeared, and the approach curves shifted to a steep positive feedback response - clearly showing that the redox mediator could now freely reach the electrode. This confirms permanent pore formation and loss of membrane integrity. The fact that this change persisted at 1 min, 60 min, and even 12 h post-pulse (Fig. 6, red circles, blue and green triangles) highlights the irreversible nature of the damage. The disappearance of the constant current region reflects not only increased permeability but also the breakdown of the bilayer's barrier function.

Fig. 7 shows a schematic representation of the 5 min 2 V irreversible electroporation of the tBLM and the formation of a pore inside tBLM. The diameter of the pore is expected to be approx. 20 fold wider compared to the diameter of the UME according to the literature [12,53]. These observations demonstrate that the constant current region observed in the approach curve is a sensitive indicator of the state of the membrane, with contraction of this region marking the shift from an insulating to a conductive interface.

Together, EIS and SECM are complementary and powerful tools for evaluating the electroporation threshold and structural resilience of model membranes. Prolonged or excessive electrical stimulation leads to irreversible electroporation and full breakdown of the tBLM. The duration of the pulse plays a critical role - a shorter 2 min pulse may result in no disruption, while a 5 min pulse causes permanent membrane failure.

3.3. Discussion

Our current findings on the electroporation behavior of tBLMs can be directly compared to our previous work on hBLMs, where similar SECM approach curve methodology was applied [12]. The glass/FTO surface was functionalized with octadecyltrochlorosilane (OTS) self-assembling monolayer (SAM). This created hydrophobic surface. Then, using vesicle solution of the same composition (DOPC:Chol 60:40) the hybrid bilayer

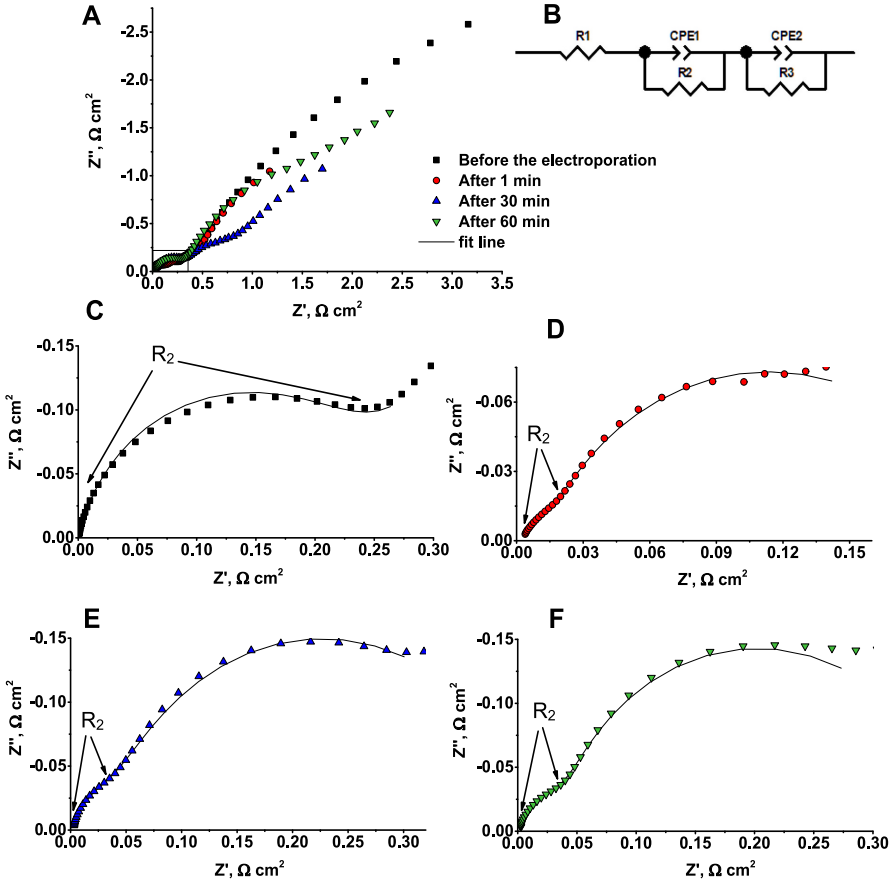


Fig. 5. Electroporation of the tBLM by 2 V pulse applied for 5 min to the Ø 25 μm Pt UME. **A** - impedance spectra recorded before the electroporation, and after 1 min, 30 min and 60 min after the electroporation. The square in **A** shows the approximate part of spectra that is zoomed in and showed in C, D, E and F. **B** - equivalent circuit model used for the fitting of EIS data, where: R1 – uncompensated solution resistance; R2 and CPE1 – the charge transfer resistance at the interface Pt UME/PBS and the constant phase element of the electric double layer, respectively. R3 and CPE2 – the charge transfer resistance and the capacitance at the interface tBLM/PBS, respectively. **C** – zoomed in part of the impedance spectrum recorded before electroporation. **D** – zoomed in part of impedance spectrum recorded 1 min after the electroporation. **E** – zoomed in part of impedance spectrum recorded 30 min after the electroporation. **F** – zoomed in part of the impedance spectrum recorded 60 min after the electroporation. The arrows in C, D, E and F show the semicircle that represents R2 in the equivalent scheme in B.

was formed. The hBLM consisted of two different leaflets: one is the hydrophobic OTS layer, and the other is the phospholipid bilayer with hydrophilic heads facing outwards. The main difference between tBLM and hBLM, is that hBLM lacks the submembrane ionic reservoir because there is not enough or not at all hydrophilic spacers and/or molecular anchors, making the tBLM superior choice for investigating different properties of lipid bilayers. However, the more convenient method for preparation of hBLM and commercial availability of silane-based anchors might be a suitable approach as well, for instance, creating biosensors.

Previous studies [12] have shown that hBLMs formed on glass/FTO surfaces have a relatively low electroporation threshold. Irreversible membrane disruption occurs at just 1 V for 2 min, with only partial recovery even after 60 min. In contrast, reversible electroporation in hBLMs was possible under a carefully pulsed 1 V protocol (90 s ON / 60 s OFF / 90 s ON), with gradual recovery observed over 15–18 min [12].

In the present study, tBLMs required higher voltage and longer duration to achieve comparable disruption. As shown in Fig. 2, a 2 min 2 V electroporation pulse resulted in only a slight and possibly reversible change in electrochemical impedance spectra, which returned to baseline after 30 min. This contrasts with hBLMs, where even a 1 V pulse caused lasting damage. Only when the tBLM was exposed to a prolonged 5 min 2 V pulse, we observed irreversible membrane breakdown, indicated by a sustained drop in impedance and significant changes in SECM approach curves (Figs. 5 and 6).

In the three-electrode configuration used in this research, the potentiostat maintains the applied potential between the Pt UME (working electrode) and Pt wire (counter electrode) for the full pulse duration, so after the initial μs double-layer charging at the UME, a steady field is sustained in the UME–surface gap. The tBLM/FTO stack

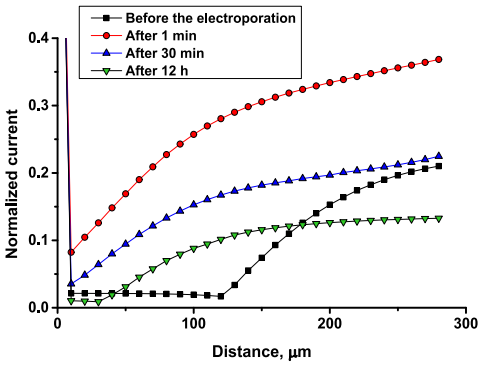


Fig. 6. SECM approach curves measured before the 5 min 2 V electroporation, and at 1 min, 60 min, and 12 h after the pulse. Measurements were performed using a three-electrode system with Ø 25 μm Pt UME as the working electrode, biased at −0.75 V.

behaves as series capacitors (double layer at UME | bulk electrolyte gap | lipid core | submembrane water layer (~1–2 nm) | FTO side). Because the capacitance per area of the submembrane water layer and double layers exceeds that of the lipid core, the local potential drop partitions predominantly across the lipid. When the pulse is turned on, interfacial polarization and ion redistribution lower the free-energy barrier for aqueous defect nucleation within the lipid. In tBLMs enriched with cholesterol, line tension and order are high, so small pores tend to re-seal quickly when the driving field is removed - unless the field acts long enough to push some defects past the critical size. For 2 min pulses, defects remain sub-critical and reseal upon field removal due to lipid mobility and line tension. This matches our data: minimal, transient changes in R2 and R3, drop in CPE2 that recovers, and SECM constant-current region that returns (Figs. 2 and 3, Table 1). For 5 min pulses, the sustained field increases the time-integrated nucleation/growth probability. This allows some pores to exceed the critical radius, coalesce, and/or induce local lipid depletion. These defects cannot reseal once the pulse ends. This was observed in irreversible electroporation experiments, which showed a step-change and only partial recovery in R2, a persistent collapse of R3, a decrease in CPE2 with $n \rightarrow 1$ (less distributed capacitance of an intact bilayer), and a permanent loss of the SECM exclusion plateau (Figs. 5 and 6 and Table 2).

These findings highlight that tBLMs possess a significantly higher electroporation threshold than hBLMs, requiring more intense or prolonged stimuli to cause irreversible damage. Although vesicle fusion and electroporation both involve transient aqueous pore formation, the underlying mechanisms are different. Vesicle fusion is thermodynamically driven by lipid rearrangements that minimize curvature stress [54], whereas electroporation is driven by an external electric field reducing the pore nucleation energy barrier [55,56]. In the DOPC:Chol 60:40 bilayer, cholesterol increases packing order and stabilizes transient defects, facilitating both processes under their respective driving conditions. The longer blocking distance observed in SECM approach curves for intact tBLMs (up to 100 μm) compared to hBLMs (approx. 20 μm) also indicates a denser and more stable bilayer, better at resisting ion and probe permeation. These characteristics align with literature reports that tBLMs provide enhanced mechanical and electrochemical stability due to their more compact lipid packing and the existence of submembrane ionic reservoir [14,29,49,57]. From an application point of view, the robustness of tBLMs makes them highly suitable for biosensor platforms, membrane protein studies, and other biotechnological uses where long-term membrane stability and integrity are critical. On the other hand, hBLMs - while less stable - may offer advantages in scenarios requiring temporary permeability, such as controlled drug release or transient molecular transport. The ability to tune membrane performance based on structure and composition provides a versatile toolkit for designing membrane-based systems tailored to specific functional needs.

Unlike conventional whole-membrane electroporation, the SECM–Pt UME configuration enables spatially confined pulse application while the conductive FTO support remains unbiased. This allows immediate near-field impedance probing and localized electroporation without global charging of the substrate, potentially opening avenues for selective disruption of targeted membranes or cell layers.

4. Conclusions and outlook

Using SECM and EIS, we showed that tBLMs remain stable under a 2 min 2 V pulse, exhibiting only minor and potentially reversible changes. Irreversible membrane disruption occurred only after prolonged

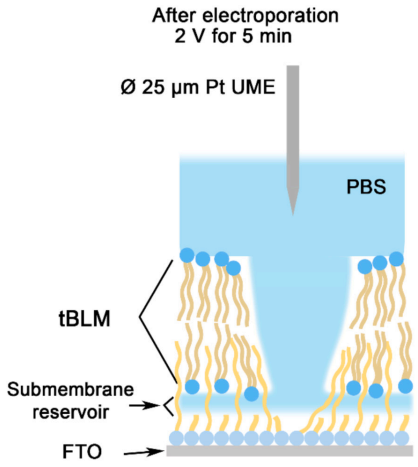


Fig. 7. Schematic representation of tBLM after 5 min 2 V electroporation with Ø 25 μm Pt UME. The electroporation yielded a clear pore formation inside the tBLM.

Table 2
Fitting data of electrochemical impedance spectra obtained before and after electroporation of the tBLM by applying 2 V pulse for 5 min (showed in Fig. 5). The data were fitted according to equivalent scheme showed in Fig. 5 B.

	χ^2	CPE1, mF·cm^{-2}	n (CPE1)	R2, mΩ·cm^2	CPE2, mF·cm^{-2}	n (CPE2)	R3, Ω·cm^2
Before the electroporation	$6.7{\cdot}10^{-4}$	2.85	0.88	220	24.9	0.62	14.7
After 1 min	$3.3{\cdot}10^{-4}$	9.11	0.82	13	19.1	0.81	0.20
After 30 min	$6.2{\cdot}10^{-4}$	5.31	0.86	38	12.6	0.84	0.38
After 60 min	$6.1{\cdot}10^{-4}$	3.69	0.89	39	9.9	0.91	0.33

exposure (5 min at 2 V), as evidenced by a sustained drop in impedance and permanent alterations in SECM approach curves. When comparing to similar SECM-based studies in the literature, hBLMs were shown to undergo irreversible disruption after just 2 min at 1 V, with only partial recovery observed even after extended time periods [12]. While this responsiveness to lower voltages may be advantageous in systems designed for controlled and transient permeability (e.g., drug delivery), it limits their use in applications requiring structural resilience. tBLMs, on the other hand, demonstrate superior robustness and insulating properties, owing to their tightly packed lipid structure and sub-membrane ionic reservoir. These features make tBLMs particularly suitable for long-term applications such as biosensing, membrane protein reconstitution, and bioelectronic devices, where membrane integrity under electrical or mechanical stress is essential.

A key advantage of our approach is the use of SECM combined with ultramicroelectrodes, which enables highly localized, targeted electroporation with precise control over electrode positioning and stimulus delivery. This allows us to induce electroporation in well-defined areas without affecting the entire membrane, making it particularly valuable for investigating spatially resolved membrane behavior or for applications requiring localized membrane access, such as single-cell electroporation, nanoscale biosensing, or localized drug release. This platform can be extended to study the effects of membrane composition, tethering chemistry, and environmental conditions (e.g., ionic strength, pH) on electroporation dynamics. Ultimately, the combination of SECM and EIS offers a powerful and versatile toolkit for developing and characterizing advanced membrane-based technologies. Future work will focus on extending localized SECM electroporation to investigate membrane resealing kinetics in diverse lipid compositions and ionic conditions, as well as targeted probing electroporation effects on membranes with embedded proteins or receptors.

CRediT authorship contribution statement

Margarita Poderyte: Writing – review & editing, Writing – original draft, Validation, Methodology, Investigation, Formal analysis, Data curation, Conceptualization. **Inga Gabriunaite:** Writing – review & editing, Writing – original draft, Visualization, Validation, Formal analysis. **Aušra Valiūnienė:** Writing – review & editing, Writing – original draft, Validation, Supervision, Resources, Project administration, Formal analysis, Conceptualization.

Funding

This research did not receive any specific grant from funding agencies in the public, commercial, or not-for-profit sectors.

Declaration of competing interest

The authors declare that they have no known competing financial interests or personal relationships that could have appeared to influence the work reported in this paper.

Appendix A. Supplementary data

Supplementary data to this article can be found online at https://doi.org/10.1016/j.jelechem.2025.119608.

References

[1] E. Neumann, M. Schaefer-Ridder, Y. Wang, P.H. Hofschneider, Gene transfer into mouse lyoma cells by electroporation in high electric fields, EMBO J. 1 (1982) 841–845, https://doi.org/10.1002/J.1460-2075.1982.TB01257.X.
[2] S. Koronkiewicz, S. Kalinowski, Influence of cholesterol on electroporation of bilayer lipid membranes: chronopotentiometric studies, Biochim. Biophys. Acta Biomembr. 1661 (2004) 196–203, https://doi.org/10.1016/J.BBAMEM.2004.01.005.
[3] J. Gehl, Electroporation: theory and methods, perspectives for drug delivery, gene therapy and research, Acta Physiol. Scand. 177 (2003) 437–447, https://doi.org/10.1046/J.1365-201X.2003.01093.X.
[4] J.C. Weaver, Molecular basis for cell membrane Electroporationa, Ann. N. Y. Acad. Sci. 720 (1994) 141–152, https://doi.org/10.1111/J.1749-6632.1994.TB30442.X.
[5] E. Neumann, S. Kakorin, K. Tœnsing, Fundamentals of electroporative delivery of drugs and genes, Bioelectrochem. Bioenerg. 48 (1999) 3–16, https://doi.org/10.1016/S0302-4598(99)00008-2.
[6] A.K. Majhi, S. Kanchi, V. Venkataraman, K.G. Ayappa, P.K. Maiti, Estimation of activation energy for electroporation and pore growth rate in liquid crystalline and gel phases of lipid bilayers using molecular dynamics simulations, Soft Matter 11 (2015) 8632–8640, https://doi.org/10.1039/C5SM02029H.
[7] L. Delemotte, M. Tarek, Molecular dynamics simulations of lipid membrane electroporation, J. Membr. Biol. 245 (2012) 531–543, https://doi.org/10.1007/S00232-012-9434-6.
[8] M. Tarek, Membrane electroporation: a molecular dynamics simulation, Biophys. J. 88 (2005) 4045–4053, https://doi.org/10.1529/BIOPHYSJ.104.050617.
[9] T. Matsuda, C.L. Cepko, Electroporation and RNA interference in the rodent retina in vivo and in vitro, Proc. Natl. Acad. Sci. USA 101 (2004) 16–22, https://doi.org/10.1073/PNAS.2235688100.
[10] T. Muramatsu, A. Nakamura, H.M. Park, In vivo electroporation: a powerful and convenient means of nonviral gene transfer to tissues of living animals (review), Int. J. Mol. Med. 1 (1998) 55–62, https://doi.org/10.3892/IJMM.1.1.55.
[11] B. Al-Sakere, F. André, C. Bernat, E. Connault, P. Opolon, R.V. Davalos, B. Rubinsky, L.M. Mir, Tumor ablation with irreversible electroporation, PLoS One 2 (2007) e1135, https://doi.org/10.1371/JOURNAL.PONE.0001135.
[12] A. Valiūnienė, I. Gabriunaite, M. Poderyte, A. Ramanavicius, Electroporation of a hybrid bilayer membrane by scanning electrochemical microscope, Bioelectrochemistry 136 (2020) 107617, https://doi.org/10.1016/J.BIOELECHEM.2020.107617.
[13] I. Gabriunaite, A. Valiūnienė, M. Poderyte, A. Ramanavicius, Silane-based self-assembled monolayer deposited on fluorine doped tin oxide as model system for pharmaceutical and biomedical analysis, J. Pharm. Biomed. Anal. 177 (2020) 112832, https://doi.org/10.1016/J.JPBA.2019.112832.
[14] C.G. Cranfield, B.A. Cornell, S.L. Grage, P. Duckworth, S. Carne, A.S. Ulrich, B. Martinac, Transient potential gradients and impedance measures of tethered bilayer lipid membranes: pore-forming peptide insertion and the effect of electroporation, Biophys. J. 106 (2014) 182–189, https://doi.org/10.1016/J.BPJ.2013.11.1121.
[15] W. Hoiles, V. Krishnamurthy, C.G. Cranfield, B. Cornell, An engineered membrane to measure electroporation: effect of tethers and bioelectronic Interface, Biophys. J. 107 (2014) 1339–1351, https://doi.org/10.1016/J.BPJ.2014.07.056.
[16] P. Mueller, D.O. Rudin, H. Ti Tien, W.C. Wescott, Reconstitution of cell membrane structure in vitro and its transformation into an excitable system, Nat 1962 1944832. 194 (1962) 979–980. Doi: https://doi.org/10.1038/194979a0.
[17] M. Winterhalter, Black lipid membranes, Curr. Opin. Colloid Interface Sci. 5 (2000) 250–255, https://doi.org/10.1016/S1359-0294(00)00063-7.
[18] M. Tsemperouli, E. Amstad, N. Sakai, S. Matile, K. Sugihara, Black lipid membranes: challenges in simultaneous quantitative characterization by electrophysiology and fluorescence microscopy, Langmuir 35 (2019) 8718–8757, https://doi.org/10.1021/ACS.LANGMUIR.9B00673.
[19] E. Sackmann, Supported membranes: Scientific and practical applications, Science (80-.). 271 (1996) 43–48. Doi: https://doi.org/10.1126/science.271.5245.43.
[20] J. Kurniawan, J.F. Ventrici De Souza, A.T. Dang, G.Y. Liu, T.L. Kuhl, Preparation and characterization of solid-supported lipid bilayers formed by Langmuir-Blodgett deposition: a tutorial, Langmuir 34 (2018) 15622–15639, https://doi.org/10.1021/ACS.LANGMUIR.8B03504.
[21] E. Labbé, O. Buriez, Electrode-supported and free-standing bilayer lipid membranes: formation and uses in molecular electrochemistry, Electrochem. Sci. Adv. 2 (2022) e2100170, https://doi.org/10.1002/ELSA.202100170.
[22] L. Bar, M.E. Villanueva, C. Martín, A.V. Ramirez, J. Goole, F.U. Renner, P. Losada-Pérez, Stability of supported hybrid lipid bilayers on chemically and topographically-modified surfaces, Colloids Surfaces A Physicochem. Eng. Asp. 664 (2023) 131125, https://doi.org/10.1016/J.COLSURFA.2023.131125.
[23] V. Kiessling, S.T. Yang, L.K. Tamm, Supported lipid bilayers as models for studying membrane domains, Curr. Top. Membr. 75 (2015) 1–23, https://doi.org/10.1016/BS.CTM.2015.03.001.
[24] V.I. Silin, H. Wieder, J.T. Woodward, G. Valincius, A. Offenhausser, A.L. Plant, The role of surface free energy on the formation of hybrid bilayer membranes, J. Am. Chem. Soc. 124 (2002) 14676–14683, https://doi.org/10.1021/ja026585+.
[25] I. Gabriunaite, A. Valiūnienė, G. Valincius, Formation and properties of phospholipid bilayers on fluorine doped tin oxide electrodes, Electrochim. Acta 283 (2018) 1351–1358, https://doi.org/10.1016/j.electacta.2018.04.160.
[26] A.L. Plant, Supported hybrid bilayer membranes as rugged cell membrane mimics, Langmuir 15 (1999) 5128–5135, https://doi.org/10.1021/la981662t.
[27] E.A. Schafer, E. Davis, Z. Manzer, S. Daniel, J. Rivnay, Hybrid supported lipid bilayers for bioinspired bioelectronics with enhanced stability, ACS Appl. Mater. Interfaces 15 (2023) 24638–24647, https://doi.org/10.1021/ACSAMI.3C0105.
[28] S.A. Glazier, D.J. Vanderah, A.L. Plant, H. Bayley, G. Valincius, J.J. Kasianowicz, Reconstitution of the pore-forming toxin α-Hemolysin in phospholipid/18-Octadecyl-1-thiahexa(ethylene oxide) and phospholipid/n-Octadecanethiol supported bilayer membranes, Langmuir 16 (2000) 10428–10435, https://doi.org/10.1021/la000690k.
[29] T. Sabirovas, M. Talaikis, R. Tamulytė, A. Polita, V. Pudzaitis, G. Niaura, D. J. Vanderah, G. Valincius, Molecular engineering of tethered bilayer lipid

membranes for impedimetric detection of pore-forming toxins, Electrochim. Acta 508 (2024) 145226, https://doi.org/10.1016/j.electacta.2024.145226.
[30] B.A. Cornell, G. Krishna, P.D. Osman, R.D. Pace, L. Wieczorek, Tethered-bilayer lipid membranes as a support for membrane-active peptides, Biochem. Soc. Trans. 29 (2001) 613–617, https://doi.org/10.1042/BST0290613.
[31] I. Gabriunaite, A. Valiūnienė, T. Sabirovas, G. Valincius, Mixed silane-based self-assembled monolayers deposited on fluorine doped tin oxide as model system for development of biosensors for toxin detection, Electroanalysis 33 (2021) 1315–1324, https://doi.org/10.1002/elan.202060578.
[32] T. Sabirovas, A. Valiūnienė, I. Gabriunaite, G. Valincius, Mixed hybrid bilayer lipid membranes on mechanically polished titanium surface, Biochim. Biophys. Acta Biomembr. 1862 (2020), https://doi.org/10.1016/j.bbamem.2020.183232.
[33] B. Raguse, V. Braach-Maksvytis, B.A. Cornell, L.G. King, P.D.J. Osman, R.J. Pace, L. Wieczorek, Tethered lipid bilayer membranes: formation and ionic reservoir characterization, Langmuir 14 (1998) 648–659, https://doi.org/10.1021/la9711239.
[34] R. Budvytyte, M. Pleckaityte, A. Zvirbliene, D.J. Vanderah, G. Valincius, Reconstitution of cholesterol-dependent vaginolysin into tethered phospholipid bilayers: implications for bioanalysis, PLoS One 8 (2013) 1–13, https://doi.org/10.1371/journal.pone.0082536.
[35] J.G. Bollinger, K. Diraviyam, F. Ghomashchi, D. Murray, M.H. Gelb, Interfacial binding of bee venom secreted phospholipase A2 to membranes occurs predominantly by a nonelectrostatic mechanism, Biochemistry 43 (2004) 13293–13304, https://doi.org/10.1021/bi049390i.
[36] R. Benz, F. Beckers, U. Zimmermann, Reversible electrical breakdown of lipid bilayer membranes: a charge-pulse relaxation study, J. Membr. Biol. 48 (1979) 181–204, https://doi.org/10.1007/BF01872858.
[37] M. Poderyte, A. Valiūnienė, A. Ramanavicius, Scanning electrochemical microscope as a tool for the electroporation of living yeast cells, Biosens. Bioelectron. 205 (2022) 114096, https://doi.org/10.1016/J.BIOS.2022.114096.
[38] M. Poderyte, A. Ramanavicius, A. Valiūnienė, Scanning electrochemical microscopy based irreversible destruction of living cells, Biosens. Bioelectron. 216 (2022) 114621, https://doi.org/10.1016/J.BIOS.2022.114621.
[39] S. Chakraborty, M. Doktorova, T.R. Molugu, F.A. Heberle, H.L. Scott, B. Dzikovski, M. Nagao, L.R. Stingaciu, R.F. Standaert, F.N. Barrera, J. Katsaras, G. Khelashvili, M.F. Brown, R. Ashkar, How cholesterol stiffens unsaturated lipid membranes, Proc. Natl. Acad. Sci. USA 117 (2020) 21896–21905, https://doi.org/10.1073/PNAS.2004807117.
[40] K. Pinkwart, F. Schneider, M. Lukoseviciute, T. Sauka-Spengler, E. Lyman, C. Eggeling, E. Sezgin, Nanoscale dynamics of cholesterol in the cell membrane, J. Biol. Chem. 294 (2019) 12599–12609, https://doi.org/10.1074/JBC.RA119.009683.
[41] I. Gabriunaite, G. Valincius, A. Žilinskas, A. Valiūnienė, Tethered bilayer membrane formation on Silanized fluorine doped tin oxide surface, J. Electrochem. Soc. 169 (2022) 037515, https://doi.org/10.1149/1945-7111/ac5c96.
[42] A. Valiūnienė, Ž. Margarian, I. Gabriūnaitė, V. Matulevičiūtė, T. Murauskas, G. Valinčius, Cadmium stannate films for immobilization of phospholipid bilayers, J. Electrochem. Soc. 163 (2016) H762–H767, https://doi.org/10.1149/2.0331609jes.
[43] T. Ragaliauskas, M. Mickevicius, B. Rakovska, T. Penkauskas, D.J. Vanderah, F. Heinrich, G. Valincius, Fast formation of low-defect-density tethered bilayers by fusion of multilamellar vesicles, Biochim. Biophys. Acta Biomembr. 2017 (1859) 669–678, https://doi.org/10.1016/j.bbamem.2017.01.015.
[44] M.W. Lee, S. Chakraborty, N.W. Schmidt, R. Murgai, S.H. Gellman, G.C.L. Wong, Two interdependent mechanisms of antimicrobial activity allow for efficient killing in nylon-3-based polymeric mimics of innate immunity peptides, Biochim. Biophys. Acta Biomembr. 2014 (1838) 2269–2279, https://doi.org/10.1016/J.BBAMEM.2014.04.007.
[45] R.A. Cooper, Influence of increased membrane cholesterol on membrane fluidity and cell function in human red blood cells, J. Supramol. Cell. Biochem. 8 (1978) 413–430, https://doi.org/10.1002/JSS.400080404.
[46] N. Monteiro, A. Martins, R.L. Reis, N.M. Neves, Liposomes in tissue engineering and regenerative medicine, J. R. Soc. Interface 11 (2014), https://doi.org/10.1098/RSIF.2014.0459.
[47] A.J. Bard, F.R.F. Fan, J. Kwak, O. Lev, Scanning electrochemical microscopy. Introduction and principles, Anal. Chem. 61 (1989) 132–138, https://doi.org/10.1021/AC00177A011.
[48] A.S. Baranski, P.M. Diakowski, Application of AC impedance techniques to scanning electrochemical microscopy, J. Solid State Electrochem. 8 (2004) 683–692, https://doi.org/10.1007/S10008-004-0533-X.
[49] G. Valincius, T. Meškauskas, F. Ivanauskas, Electrochemical impedance spectroscopy of tethered bilayer membranes, Langmuir 28 (2012) 977–990, https://doi.org/10.1021/la204054g.
[50] F. Leeb, L. Maibaum, Spatially resolving the condensing effect of cholesterol in lipid bilayers, Biophys. J. 115 (2018) 2179–2188, https://doi.org/10.1016/j.bpj.2018.10.024.
[51] A. Radhakrishnan, H.M. McConnell, Electric field effect on cholesterol-phospholipid complexes, Proc. Natl. Acad. Sci. USA 97 (2000) 1073–1078, https://doi.org/10.1073/PNAS.97.3.1073.
[52] G. Valincius, M. Mickevicius, T. Penkauskas, M. Jankunec, Electrochemical impedance spectroscopy of tethered bilayer membranes: an effect of heterogeneous distribution of defects in membranes, Electrochim. Acta 222 (2016) 904–913, https://doi.org/10.1016/j.electacta.2016.11.056.
[53] T. Matrab, C. Combellas, F. Kanoufi, Scanning electrochemical microscopy for the direct patterning of a gold surface with organic moities derived from iodonium salt, Electrochem. Commun. 10 (2008) 1230–1234, https://doi.org/10.1016/J.ELECOM.2008.06.006.
[54] G. Van Meer, D.R. Voelker, G.W. Feigenson, Membrane lipids: where they are and how they behave, Nat. Rev. Mol. Cell Biol. 9 (2008) 112–124, https://doi.org/10.1038/NRM2330;KWRD=LIFE+SCIENCES.
[55] S. Kalinowski, G. Ibron, K. Bryl, Z. Figaszewski, Chronopotentiometric studies of electroporation of bilayer lipid membranes, Biochim. Biophys. Acta Biomembr. 1369 (1998) 204–212, https://doi.org/10.1016/S0005-2736(97)00222-8.
[56] G. Blumrosen, A. Abazari, A. Golberg, M.L. Yarmush, M. Toner, Single-step electrical field strength screening to determine electroporation induced transmembrane transport parameters, Biochim. Biophys. Acta Biomembr. 2016 (1858) 2041–2049, https://doi.org/10.1016/J.BBAMEM.2016.05.022.
[57] D. Dziubak, S. Sek, Physicochemical characterization of sparsely tethered bilayer lipid membranes: structure of submembrane water and nanomechanical properties, ChemElectroChem 8 (2021) 2564–2571, https://doi.org/10.1002/CELC.202100721.

Biosensors and Bioelectronics 205 (2022) 114096

Contents lists available at ScienceDirect

Biosensors and Bioelectronics

journal homepage: www.elsevier.com/locate/bios

Scanning electrochemical microscope as a tool for the electroporation of living yeast cells

Margarita Poderyte [a], Aušra Valiūnienė [a,**], Arunas Ramanavicius [a,b,*]

[a] Vilnius University, Faculty of Chemistry and Geosciences, Institute of Chemistry, Naugarduko 24, Vilnius, LT-03225, Lithuania
[b] Laboratory of Nanotechnology, State Research Institute Centre of Physical Sciences and Technology, Sauletekio ave. 3, LT-10257, Vilnius, Lithuania

ARTICLE INFO

Keywords:
Cell treatment
Drug delivery
Yeast cells
Scanning electrochemical microscope
Reversible electroporation
Impedance spectroscopy
Ultramicroelectrode

ABSTRACT

In this study, a scanning electrochemical microscope (SECM) was for the first time adapted to perform the electroporation process of living yeast cells. We have demonstrated that relatively low voltage pulses of 1–2 V vs. Ag/AgCl,Cl^-_{sat} applied to gold-based ultramicroelectrode (Au-UME) are performing reversible electroporation of yeast cells immobilized on fluorine-doped tin oxide (FTO)/glass surface. SECM and electrochemical impedance spectroscopy (EIS) were used for the determination of quantitative electrochemical characteristics before and after the electroporation. The electrochemical impedance spectroscopy (EIS) illustrated significant electrochemical changes of electroporated yeast cells, while SECM feedback mode surface vertical scan current-distance curves showed that the diameter of the area affected by the electrical pulse is about 25 times larger than the diameter of the Au-UME used for the electroporation process. The results presented in this research open up a possibility to develop a targeted electroporation system which will affect only the selected area of tissue or some other cell-covered surface. Such model is promising for the selective treatment of selected cells in tissues and/or other sensitive biological systems while selecting the location and size of electroporated areas.

1. Introduction

Electroporation is a physical method in which cells are exposed to a strong electrical field pulse (about 1 kV cm^{-1}), as a result of which temporary or permanent pores are formed in the phospholipid layer. It is an increasingly relevant technique in biomedicine, biotechnology, food science and technology, and environmental science. In different fields of application, this technique is referred to as electropermeabilization, electroporation, electropulsation, or PEF (pulsed electric field) treatment (Kotnik et al., 2019; Stirke et al., 2014, 2019).

Electroporation is a probabilistic process. The number and size of pores in the membrane are highly dependent on the basic physical parameters: electrical pulse intensity; pulse shape; pulse duration; number of pulses. Cell electroporation begins when electric field intensity is greater than the permeabilization threshold (Lee et al., 2009). Increasing the strength of the electric field above the threshold increases the number of pores formed during electroporation. Moreover, there are chemical and biological factors affecting electroporation in particular cell size and form, membrane molecular structure, osmotic pressure, ionic medium composition, electrode material, temperature (Chen et al., 2006).

An important feature of electroporation, which determines its wide range of applications, is that when the parameters of the electric field are properly selected, the pores disappear after a certain period of time and the cell remains viable. This phenomenon is known as reversible electroporation enabling the treated cells to have been restored to their initial state and survived (Zand et al., 2021). After the electroporation, cell membrane recovers in a few milliseconds or microseconds, and the final recovery of viability can take several seconds, minutes, or even several hours (Kotnik et al., 2012). Depending on the size of the pores, there are three stages of their disappearance: sudden decrease of the pore (<1 s), slow decrease of the pore (~2–10 min), complete disappearance of the pore (>10 min) (Kotnik et al., 2015). The reversible electroporation is widely used in medicine to insert into living cells substances that do not naturally pass through the cell membrane, namely drugs, proteins, enzymes, antibodies, nucleotides, DNA, RNA, and even small organs (Sweeney et al., 2018). At present, in biomedicine great importance has targeted drug delivery i.e., the selective introduction of drugs into selected cells using various drug carriers (e.g., liposomes, microcapsules, nanocapsules), which are directed to the

* Corresponding author. Vilnius University, Faculty of Chemistry and Geosciences, Institute of Chemistry, Naugarduko 24, Vilnius, LT-03225, Lithuania.
** Corresponding author.
E-mail addresses: ausra.valiuniene@chf.vu.lt (A. Valiūnienė), arunas.ramanavicius@chf.vu.lt (A. Ramanavicius).

https://doi.org/10.1016/j.bios.2022.114096
Received 30 November 2021; Received in revised form 8 February 2022; Accepted 11 February 2022
Available online 20 February 2022
0956-5663/© 2022 Elsevier B.V. All rights reserved.

required organs (Caramazza et al., 2020; Gholami et al., 2020; Jain Editor, n.d.; Liu et al., 2020). Reversible electroporation induced by chip-based devices could be applied during the design of cell-based biosensors for monitoring microphysiological systems (Ferrari et al., 2020; Xu et al., 2019). Although the technology of filling cells with various compounds using electroporation is efficient and already used in practice, the process conditions are still not optimized. The conventional methods proposed for determining the size of the pores formed in cell membranes, the loading time of the molecules, and the lifespan of the pores are not always efficient (Nakamura and Funahashi, 2013).

For several decades *Saccharomyces cerevisiae* (a eukaryotic unicellular microbe) has been investigated as a model system for the assessment of eukaryote cell action because these cells have a true nucleus that is separated from the cytoplasm by a phospholipid-based membrane (Galao et al., 2007). The basic processes such as gene expression, protein translation, signal transduction, and metabolism are resembling between yeast and higher eukaryotes (Daum, 2000). They are rather resistant to the environment (significant pH changes, can survive under both anaerobic and aerobic conditions), their maintenance and disposal are simple, and yeast cells are much cheaper compared to more complex eukaryotic cells. These reasons determine the attractiveness and applicability of yeast for complicated biological studies (Gencturk et al., 2020; Rodriguez et al., 2004). Even though the yeast cells are highly investigated, there is still rather little information on the effects of the electric field on yeast cell components. As early as 1989, T. Tomov and I. Tsoneva showed that under the influence of a pulsed electric field, the yeast wall changes the charge due to the ions leaving the cell (Tomov and Tsoneva, 1989). However, there is still no clear mechanism explaining why the charge on the yeast wall changes during and/or after electroporation, (Mattar et al., 2014). Some of our previous researches illustrated the electroporation of yeast cell membrane and even cell wall (Mikoliunaite et al., 2011) and delivery of large molecular weight organic compounds into yeast cells using a two-electrode system (Stirke et al., 2014, 2019). However, the application of a three-electrode system for the electroporation of yeast cells immobilized on an unpolarized substrate has not yet been presented. The advantage of three-electrode systems in yeast cell electroporation is that the working electrode held above the surface of unpolarized yeast cells can be used to induce an electrical pulse that may cause the formation of differently sized pores depending on the electrode diameter, and moreover, electroporation could be achieved by affecting only a particular area by placing the electrode above cell surface. Scanning electrochemical microscopy (SECM) is the most promising method for the investigation of the electroporation process because it has already been proved that while forming modifications on a substrate with SECM, the affected area size depends upon the diameter of the electrode used (Malel et al., 2010; Matrab et al., 2008; Valiūnienė et al., 2020).

SECM is a technology in which a current flowing through a very small electrode (an ultramicroelectrode (UME) with a working surface diameter of 25 μm or less) is used to assess the properties of a substrate (analyte) immersed in a solution (Bard et al., 1989). SECM is a frequently used tool in biomedical research because the experimental environment can be easily biocompatible (Edwards et al., 2006). The most common mode of SECM operation is the feedback mode, where only the tip current is monitored. In the feedback mode, the tip current depends on the distance (d) between the analyte and the electrode and whether the analyte is a conductor or an insulator. When the distance (d) is very large (about 10 times larger than the electrode diameter), the current reaches a steady-state, yet the basis of scanning electrochemical microscopy relies on measurements made at very low distances from the surface. When the distance is small enough, the electrode current begins to be affected by the substrate, and a surface electrochemical scan can be performed. The best resolution scan is performed when the constant distance is not higher than 1–2 radii of the ultramicroelectrode applied for the measurement. However, working at very low distances, increases the possibility to contaminate the Au-UME surface, especially while working with biological systems (Morkvenaite-Vilkonciene et al., 2019).

In this research, a controlled model of the *Saccharomyces cerevisiae* cells electroporation phenomenon was developed and investigated by using the method of SECM. Avoiding undesired damage to the biological system being investigated, the electroporation experiments were performed by using a three-electrode electrochemical cell that enables the application of relatively low electrical pulses to the not-connected, thus, unpolarized, surface of the yeast cells. For the determination of quantitative electrochemical characteristics of the investigated system, electrochemical impedance spectroscopy was performed simultaneously with SECM measurements. The main purpose of this study was (i) to demonstrate the applicability of SECM for localized electroporation and (ii) to evaluate the area of cell culture affected by SECM-based electroporation. Our research is particularly important in biomedicine due to a possible further application of electroporation for very selective tissue treatment. Therefore, the development and application of SECM for a controlled electroporation model for yeast cells can pave a way for targeted drug delivery and/or treatment of some cancer forms.

2. Materials and methods

This section describes chemicals and experimental details. It starts by depicting how active yeast cells suspension was prepared and immobilized on fluorine-doped tin oxide (FTO)/glass surface followed by preparation of ultramicroelectrode for electrochemical measurements and finally a description of electroporation experiments. Evaluation of electroporated area size and electrochemical impedance spectroscopy measurements to capture changes of electrochemical parameters before and after the electroporation of yeast cells are described, respectively.

2.1. Yeast cell preparation and immobilization

Active yeast cell suspension (0.1 g ml^{-1}) was prepared by adding 0.050 g of yeast (*Saccharomyces cerevisiae*, commonly known as baker's yeast, which were purchased in granular form from food supplier LALLEMAND (Lublin, Poland)) to 0.5 ml of deionized water (with initial conductivity of 0.05 μS). The resulting suspension was shaken for about 5 min and stored at 30 °C for 30 min, as it was described in our previous research (Valiūnienė et al., 2020). For each electroporation experiment, new batch of active yeast cells was prepared.

For the immobilization of the cells, the surface of FTO (surface resistivity ~7 X/sq, Sigma Aldrich (Stockholm, Sweden) was cleaned with the following procedure described in our previous research (Gabriunaite et al., 2018). In detail: (i) sonication in 2% "Micro 90" solution from Sigma Aldrich (Stockholm, Sweden) for 10 min, (ii) rinsing and sonication in deionized water for 10 min, (iii) rinsing with deionized water and sonication in 2-propanol (99.5%, Honeywell) for 10 min, (iv) washing with deionized water and drying in a stream of N_2 gas. Afterward, 0.5 μm of poly-L-lysine (solution 0.1% (w/v) in H_2O – Sigma Aldrich (Stockholm, Sweden) was placed in the center of the FTO glass and left to dry. Then, 0.5 μm of yeast suspension was placed on the top of the dried poly-L-lysine and left to dry (Caloca et al., 2021). The immobilized yeast cells were then washed three times by the buffer solution.

FTO glass with immobilized yeast cells was then placed at the bottom of the Petri dish (made of poly (methyl-methacrylate), from Sigma Aldrich (Stockholm, Sweden). To keep active yeast cells active, a buffer solution (pH 7.1) containing 10 mmol of glucose from Carl Roth (Karlsruhe, Germany) was used for electrochemical experiments. The buffer solution was prepared by dissolving 0.1 $mol \cdot L^{-1}$ of NaCl (CAS No.: 7747-40-7; suprapur) and 0.01 M of $NaH_2PO_4 \cdot 2H_2O$ (CAS No.: 7558-80-7; S5011) in distilled water. The pH values were measured using a pH meter Mettler-Toledo 30130862, Sigma Aldrich (Stockholm, Sweden) and the required amount of NaOH dissolved in water was added until a pH of 7.1 was reached. For each experiment, 20 mL of buffer solution and 200 μL of 0.1 M glucose solution were used.

2.2. Electrochemical cell and ultramicroelectrode preparation

All electrochemical measurements were carried out in PBS buffer containing 0.1 M NaCl and 0.01 M NaH_2PO_4, pH 7.1. Potentiostat/galvanostat Autolab PGSTAT 30 from EcoChemie (Utrecht, The Netherlands) was used for cyclic voltammetry experiments. Scanning electrochemical microscope from Sensolytics (Bochum, Germany) combined with the potentiostat/galvanostat was used to perform electrochemical impedance spectroscopy (EIS)-based measurements over of surface of cell culture scan. All measurements were performed using conventional a three-electrode system consisting of a working electrode (Au-UME), Pt wire (99.99%) as a counter electrode, and Ag/AgCl,Cl^-_{sat} as a reference electrode. Disk-shaped flat Au-ultramicroelectrode has been purchased from Senslytics (Bochum, Germany) and used as it was in all the following experiments. The gold wire (purity 99,99%) is sealed in soda-lime glass, electrode length ca. 95–105 mm, outer glass diameter 1.5 mm, RG-value >10.

Before performing electrochemical experiments Au-UME with 10 μm diameter gold-based conducting part of electrode was cleaned in two stages: mechanically and electrochemically (Forster and Keyes, 2007). First, the Au-UME was washed with distilled water, then with ethanol (96%). Then, using special sandpaper (grain size 0.3 μm) moistened with ethanol (96%), the electrode was scrubbed in a circular motion holding it perpendicular to the sanding surface. After mechanical cleaning, the electrode was rinsed with distilled water and placed in an electrochemical cell with 0.5 mol L^{-1} H_2SO_4 solution. Cyclic voltammograms (CV) (10–50 cycles) were recorded in the potential range from 0 V to 1.7 V at a scan rate of 0.2 V s^{-1} until no reduction or oxidation peaks were observed. Then, the electrode was rinsed with distilled water and placed in the experimental cell.

2.3. Electroporation of yeast cells deposited on the surface of FTO-modified glass slide

Electroporation of active yeast cells was performed by holding the ø 10 μm Au-UME at a constant distance from the yeast surface. Two electroporation conditions were investigated in this research: i) applying the Au-UME preconditioning for 5 min at −0.2 V and then performing Au-UME potential step from −0.2 V to 2.0 V vs. Ag/AgCl,Cl^-_{sat} and holding it for 120 s ii) applying the Au-UME preconditioning for 5 min at −0.2 V and then performing Au-UME potential step from −0.2 V to 1.0 V vs. Ag/AgCl,Cl^-_{sat} and holding 1.0 V potential for 120 s.

For successful electroporation of active yeast cells, the most optimal constant distance between the Au-UME and yeast cell surface was selected by registering characteristic feedback mode approach curves (Fig. 1). It is known that UME current in feedback mode depends upon the distance (d) between the electrode and the analyte, and oxidation-reduction reactions that occur at the electrode (Ebejer et al., 2010; Lefrou and Cornut, 2010; Slim et al., 2018). Besides, the influence of the substrate is most tangible when the distance (d) is equal to 1–2 radii of the UME to the surface (Morkvenaite-Vilkonciene et al., 2019). Therefore, considering that Ø 10 μm Au-UME was used in our further experiments of electroporation, the distance of 5–10 μm theoretically could be the most suitable. However, the distance of 20 μm was chosen for the Au-UME positioning above the yeast cells because the approach curve in Fig. 1 shows that Au-UME current starts to decrease very rapidly at lower distances simultaneously increasing the risk of contamination and blocking of the Au-UME.

After registering approach curves, the electrode was cleaned mechanically and electrochemically as described in other research (Forster and Keyes, 2007) and then used for the electroporation experiments. Each electroporation experiment has been repeated at least 3 times and repeatability has been accomplished.

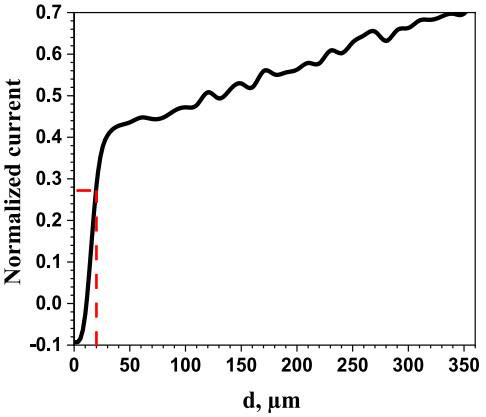


Fig. 1. Approach curve recorded while approaching active yeast cells. Measurement was performed with Au ultramicroelectrode of Ø 10 μm at −0.2 V potential vs. Ag/AgCl,Cl^-_{sat} in buffer solution (pH 7.1) with 10 mmol of glucose.

2.4. Scanning electrochemical microscope-based evaluation of yeast-modified surfaces

Measurements with SECM have been performed using feedback mode. The determination of the area damaged by electrical pulse was performed using a horizontal SECM scan, with a scan rate of 10 μm s^{-1} and a step of 10 μm. This experiment was carried out in three steps: i) the horizontal scan of active yeast cells was performed at a constant distance of 20 μm; ii) electroporation was performed at a position of the Au-UME selected by surface scan performed before the electroporation; iii) horizontal Au-UME scan has been repeated on the same line and direction as per scan before electroporation (i). Au-UME signals registered during scans before and after the electroporation were compared.

2.5. Electrochemical impedance spectroscopy (EIS) measurements

Electrochemical impedance spectroscopy has been used as a tool to determine electrochemical changes of yeast cells after they are exposed to electrical pulse induced by the Au-UME. Electrochemical impedance spectra were recorded in potentiostatic mode, and the range of alternating current frequencies varied from 0.1 Hz to 100 kHz. The peak-to-peak amplitude of the perturbation voltage was of 10 mV. Registered EIS spectra were evaluated by using EIS data acquisition software "ZView" according to the selected equivalent circuit model applied for the determination of electrochemical characteristics. In this research, EIS data are presented as Nyquist plots where x-axis represents the Z' (real impedance component), y-axis – Z'' (imaginary impedance component).

3. Results and discussion

The evidence of electroporation can be achieved by registering the changes in electrochemical characteristics that are changing due to the electroporation of yeast cells. These changes can be monitored by electrochemical impedance spectroscopy method; however, the appropriate experimental conditions should be considered prior to investigation. First, a suitable potential should be determined by analyzing cyclic voltammetry data and second, the best suited equivalent circuit model representing the investigated system should be determined and applied for the analysis of experimental EIS data. Besides, the registration of approach curves at appropriate potential in order to determine

the suitable distance between the UME and the surface of yeast cell is needed for the experiments of SECM-based electroporation. After achieving successful electroporation of yeast cells, one of the most important tasks is quantitative characterization of the electroporated area, i. e. determination of the diameter of electroporated area of yeast cells that can be achieved by applying the SECM feedback mode vertical scan above yeast cells. All these investigations enable to create an effective model for the electroporation of yeast cells, which can have significant importance in biomedicine because enables the selective treatment of selected cells in tissues and/or other biological systems.

3.1. Investigation of electroporation process of active yeast cells

Prior to electroporation experiments, cyclic voltammograms were performed in buffer solution (pH 7.1) containing 10 mmol of glucose (Fig. 2 C) to determine a suitable potential for further (i) SECM-based electroporation procedures, when registration of approach curves at appropriate potential is needed for the determination of the suitable distance between the Au-UME and the surface of yeast cell, and (ii) for EIS measurements at potentiostatic conditions. 10 mmol of glucose was added into buffer solution to keep yeast cells active. Yeast cells use glucose as one of the energy sources, hence the yeast cells' metabolism was active during all experiments. No redox mediators have been added to the system avoiding damage or other impacts to yeast cells, hence the reduction of oxygen on the Au-UME in the presence of hydrogen ions (H^+) has been assessed according to the equation:

$$O_2 + 4H^+ + 4e^- \rightarrow 2H_2O \quad (1)$$

It is seen in Fig. 2 C that CV shows no scattering of peaks or dots indicating that the electrode is clean, and no adverse electrochemical reaction occurs on the surface of Au-UME within the potential range from −0.1 V to 0.4 V. However, the SECM method is based on measuring Faradaic current that results from an electrochemical reaction at the Au-UME surface, thus the potential value for further EIS and SECM measurements has been selected from the CV area where the Faraday current is monitored on the Au-UME. Taking into consideration that under high cathodic potentials the unwanted formation of hydrogen bubbles can appear on the electrode (Valiūnienė et al., 2020; Valiuniene et al., 2019), a potential of −0.2 V vs. Ag/AglCl,Cl^-_{sat} was applied on the Au-UME of Ø 10 μm for further EIS and SECM measurements in this study.

The electroporation was performed with SECM by positioning the Au-UME at a 20 μm distance from the active yeast cells surface and by applying a constant potential of 2.0 V between the Au-UME and reference Ag/AglCl,Cl^-_{sat} electrode for 120 s. The aim of these experiments was to determine if such electroporation model using SECM and relatively low voltage is suitable for yeast cells electroporation. Nevertheless, it was used to determine if conditions of electrical pulse −0.2 V → 2.0 V applied between the Au-UME and reference Ag/AglCl,Cl^-_{sat} electrode for 120 s are suitable for the electroporation of yeast cells.

Since the charge-transfer properties of the Au-UME are dependent on the properties of the surface above it is fixed (Valiūnienė et al., 2019), we predict that electrical pulse applied to the UME positioned at a 20 μm distance from the active yeast cells may cause some changes in yeast cells, herewith some changes in the charge-transfer process may occur at the Au-UME/buffer solution interface. Therefore, to ascertain these changes the electrochemical impedance spectra of the Au-UME were measured: (i) before the electroporation (Fig. 2 A and B, curve 1); (ii) 1 min after the electroporation (Fig. 2 A and B, curve 2); (iii) 30 min after the electroporation (Fig. 2 A and B, curve 3); (iv) 60 min after the

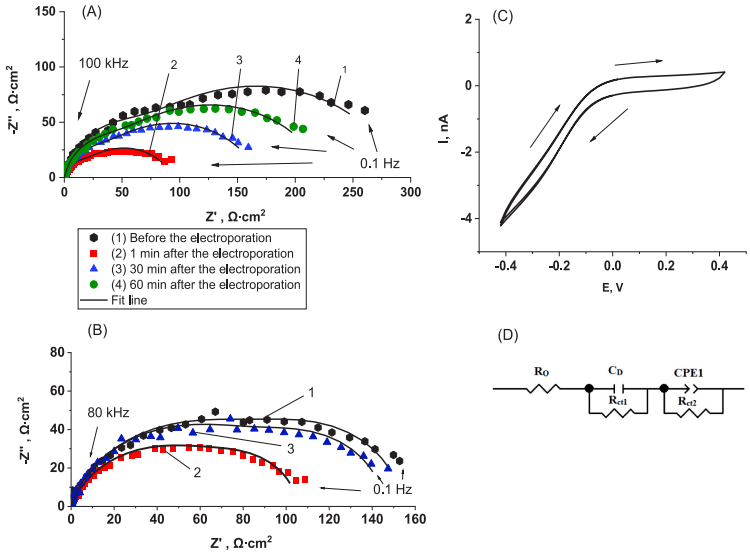


Fig. 2. A and **B** – EIS registered above active yeast cells at −0.2 V vs. Ag/AglCl,Cl^-_{sat} before the electroporation and after the electroporation at a different time. The electroporation of active yeast cells was performed in phosphate buffer solution, pH 7.1, with 10 mmol of glucose when applying the Au-UME potential step **A** from −0.2 V to 2.0 V vs. Ag/AglCl,Cl^-_{sat} and holding 2.0 V for 120 s; **B** – from −0.2 V to 1.0 V vs. Ag/AglCl,Cl^-_{sat} and holding 1.0 V for 120 s. **C** – cyclic voltammogram of the Ø 10 μm Au ultramicroelectrode in buffer solution (pH 7.1) with 10 mmol of glucose at potential sweep rate of 10 mV s^{-1}. **D** – equivalent circuit model used for the fitting of EIS data where: R_O – uncompensated solution resistance; R_{ct1} and C_D – the charge transfer resistance at the interface Au-UME/electrolyte solution and the capacitance of the electric double layer (EDL), respectively. R_{ct2} and *CPE*1 – the charge transfer resistance and the capacitance at the interface yeast cells/electrolyte solution, respectively.

electroporation (Fig. 2 A, curve 4). It can be seen in Fig. 2 that bell-shaped curves in Nyquist plot consist of two merging semicircles representing two different time constants i.e., two parallel *RC* elements, where *R* is circuit resistance and *C* is circuit capacitance. Systems that have more than one different resistance component are common not only in electrochemical systems but also in optical devices such as silicon optical sensor MOS (metal-oxide-semiconductor)-like device structure for gated emission (Xu, 2021).

Various interpretations of Nyquist plots, which were generated from experimental EIS measurements, consisting of one or two semicircles have been proposed in the literature, however, they are often contradictory (Mei et al., 2018; Schipper et al., 2016; Thangappan et al., 2016). Therefore, finding the best suited equivalent circuit model representing our investigated system was an important part of the scope of this study.

Assuming that Nyquist plots consist of two sequentially merged semicircles, we have analyzed experimentally registered EIS spectra (Fig. 2 A and B) by applying an equivalent circuit model (Fig. 2 D) consisting of uncompensated solution resistance, R_O, and two sequentially connected circuit elements: $C_D||R_{ct1}$ and $CPE1||R_{ct2}$ corresponding to compact layer at the interface Au-UME/electrolyte solution and diffuse layer, respectively. These two sequentially connected circuit elements ($C_D||R_{ct1}$ and $CPE1||R_{ct2}$) explain two possible ways of the flow of the current of the investigated system. First, alternating current flows between the counter electrode and Au-UME directly through the electrolyte solution, as it is shown in the scheme (Fig. 3 A). Second, while the Au-UME is positioned at very low distances to the investigative surface, another path of the current flow through the not-connected investigative surface is predicted (Fig. 3 B) (Baranski and Diakowski, 2004).

In our experiments one of the pathways (Fig. 3 B, 2nd pathway) of current flow can be attributed to the not-connected active yeast cells immobilized on the FTO/glass surface, thus current flows from the counter electrode to the Au-UME by crossing the yeast cell/electrolyte solution interface. Therefore, the equivalent circuit model (Fig. 2 D) consisting of sequentially connected elements of $C_D||R_{ct1}$ and $CPE1||R_{ct2}$ representing two ways of the flow of current was selected for the analysis of experimentally determined EIS in this work. Particularly, R_{ct1} and C_D represent the charge transfer resistance at the interface of Au-UME, which is affected by electrolyte solution and the capacitance of the electric double layer (EDL), respectively. R_{ct2} and *CPE*1 represent the charge transfer resistance and the capacitance at the interface yeast cells/electrolyte solution, respectively. The component of the EDL capacitance, C_D, may be used only for systems that represent homogeneous electrode surface (Chance et al., 1980). If the surface of the solid electrode is not enough equipotential, *CPE* should be introduced into the equivalent circuit (Valiūnienė et al., 2017). The impedance of *CPE* can be defined according to the equation:

$$Z_{CPE} = C_D^{-1}(jw)^{-n} \quad (2)$$

where *j* is an imaginary unit; *w* is the frequency; *n* is the exponential number, which shows the impedance phase shift describing the non-ideality of the EDL. When the electrode surface is homogenous, i.e., $n = 1$, Eq. (2) transforms into the simple double layer capacitor impedance equation:

$$Z_{CPE} = (C_D jw)^{-1} \quad (3)$$

By analyzing the impedance spectra of Ø 10 μm Au-UME (Fig. 2 A), while electroporation was performed by applying Au-UME potential step from −0.2 V to 2.0 V vs. Ag/AglCl,Cl^-_{sat} and holding it for 120 s, it was found that the exponential number (*n*) is very close to 1 ($0.98 \leq n \leq 1.00$). Therefore, according to equations *2* and *3*, *CPE* in the equivalent circuit representing capacitance of the EDL at the Au-UME/electrolyte interface turns into a conventional component of double-layer capacitance C_D (Fig. 2 D). However, it was obtained that the exponential number *n* in element *CPE*1 varied from 0.72 to 0.74 (Table 1), thus equation *2* does not transform into the simple double layer capacitor impedance equation *3*, and *CPE*1 should be introduced into the equivalent circuit.

The values of the equivalent circuit elements (Fig. 2 A and B, Fit line) match well with the experimental data (Fig. 2 A and B, symbols) indicating that the equivalent circuit model we used (Fig. 2 D) is well representative of the investigated process. The accuracy of the fitting was also monitored by checking the fit parameters and ensuring deviations do not exceed 7% (Table 1). The data in Fig. 2 and in Table 1 (Electroporation with 1 V electrical pulse) show that the values of R_{ct1} and R_{ct2} significantly decrease 1 min after the electroporation ($R_{ct1} + R_{ct2} = 94\ \Omega\ cm^2$) comparing to the result before the electroporation ($R_{ct1} + R_{ct2} = 294\ \Omega\ cm^2$), whereas the value of C_D increases after the electroporation from 415 to 966 μF cm^{-2}. The decrease of R_{ct1} and R_{ct2} after the electroporation can be explained by the fact that when the pores are formed in a plasma membrane – electroactive species such as ions (K^+, Na^+, Ca^{2+}, etc.) (Volkov, 2015; Batista Napotnik and Miklavčič, 2018) are released to the environment from yeast cells. As a result – the impedance of the system is decreased. Notably, before the electroporation *CPE*1 exhibited an unusually high value of 2048 μF cm^{-2}

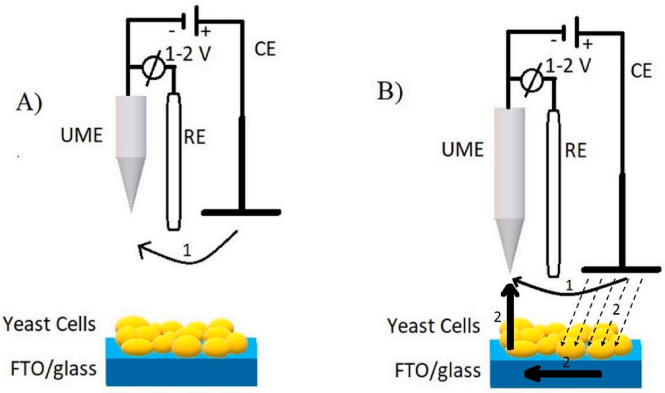


Fig. 3. Current flow pathway **A** – when working electrode is relatively far away from yeast cell modified surface; **B** – when working electrode is at very low distances from yeast cell modified surface.

Table 1
The values of the equivalent circuit (Fig. 2 D) obtained by analyzing EIS data of ⌀ 10 μm Au-UME (Fig. 2 A and B).

Electroporation of yeast cell by applying 2 V electrical pulse (Fig. 2 A).							
	R_0, Ω cm^2	C_D μF cm^{-2}	R_{ct1}, Ω cm^2	*CPE*1 μF cm^{-2}	*n* (*CPE*1)	R_{ct2}, Ω cm^2	$R_{ct1} + R_{ct2}$ Ω cm^2
Before the electroporation	0.017	415	50	2048	0.74	244	294
1 min after the electroporation	0.015	966	12	3819	0.72	82	94
30 min after the electroporation	0.012	577	23	2355	0.73	147	170
60 min after the electroporation	0.012	521	33	2161	0.74	194	227
Average Error value (%)	6.7	6.6	1.7	4.6	–	1.9	1.8
Electroporation of yeast cell by applying 1 V electrical pulse (Fig. 2 B).							
	R_0, Ω cm^2	C_D μF cm^{-2}	R_{ct1}, Ω cm^2	*CPE*1 μF cm^{-2}	*n* (*CPE*1)	R_{ct2}, Ω cm^2	$R_{ct1} + R_{ct2}$ Ω cm^2
Before the electroporation	0.029	970	56	8428	0.82	98	154
1 min after the electroporation	0.025	1299	31	13144	0.80	74	105
30 min after the electroporation	0.025	850	50	8955	0.83	96	146
Average Error value (%)	4.7	2.9	5.4	7.3	–	6.3	5.8

(Table 1 (Electroporation of yeast cell by applying 2 V electrical pulse)) because of the high heterogeneity of yeast cells surface and this finding coincides with the results obtained while EIS was registered above unpolarized graphite surface as it is reported in another research (Valiūnienė et al., 2020d). As can be expected, 1 min after the electroporation *CPE*1 increases up to 3819 μF cm^{-2} indicating significant changes in system heterogeneity after the pulse of 2.0 V that may cause the formation of pores in a plasma membrane of yeast cells. It is seen from the results of EIS (Fig. 2 A, curves 3 and 4 and Table 1 (Electroporation of yeast cell by applying 2 V electrical pulse)), that total system resistance increases over time because the pores in a plasma membrane begin to close and lower amount of the electroactive species is released from the yeast cells and diffused towards the surface of the Au-UME. 60 min after the electroporation the values of electrochemical characteristics are recovering almost to the same values, which were registered before the electroporation indicating that system is almost fully recovered after 1 h. This finding enables us to conclude that reversible electroporation of yeast cells can be performed by SECM when the pulse of 2.0 V vs. Ag/AgCl,Cl$^-_{sat}$ is applied to Ø 10 μm Au-UME positioned at a distance of 20 μm from unpolarized yeast cells surface.

After successfully performing electroporation by applying the 2.0 V electrical pulse, the same experiments were performed while applying a 1.0 V electrical pulse on the same yeast cell modified surface. Particularly similar results have been obtained while performing electroporation with 1.0 V voltage applied for 120 s to ⌀ 10 μm Au-UME (Fig. 2 B). As can be seen from Fig. 2 B, the total system resistance is fully restored after 30 min, since the data before electroporation (Fig. 2 B, curve 1) and 30 min after the electroporation (Fig. 2 B, curve 3) almost coincide. EIS data clearly showed that semicircle in Nyquist plot significantly decreases 1 min after the electroporation. This decrease in the total system resistance can be attributed to the formation of pores in a plasma membrane of yeast cells because through the pores some amount of the electroactive species can be released from the yeast cells causing the registered decrease in total system impedance. The main difference between electroporation processed with ⌀ 10 μm Au ultramicroelectrode by applying 2.0 V or 1.0 V for 120 s is that system recovery is achieved more quickly (within 30 min) when 1.0 V electrical pulse was applied in comparison to that when 2.0 V pulse (the recovery lasted for 60 min). Even though the reversible electroporation was achieved in both cases while applying 1.0 V or 2.0 V pulses on the yeast cells, it can be seen from the results in Fig. 2 A and B, that the pulse of 2.0 V causes more significant changes in the impedance (before and after electroporation) than the pulse of 1.0 V applied to the Au-UME.

Since electrical pulses of lower voltage during the electroporation of cells are inducing a much lower density of pores in the membrane (Mattiazzi et al., 2012), therefore, it is believed that this is the reason for a lower change in impedance. For further experiments to determine electroporated area size it was chosen to perform electroporation with 2.0 V pulse, for this reason, the results of electroporation become more evident.

Schematic representation of the reversible electroporation obtained in this study by using Ø 10 μm Au-UME is presented in Fig. 4. Assuming that yeast cells are characterized with a diameter from 1 to 10 μm, and the average size of active and ungrown cells is 4–5 μm (Dungrawala et al., 2012), the diameter of Ø 10 μm Au-UME is larger than the average size of yeast cells. As a result, not a single yeast cell, but all yeast cells that are in the area affected by the electrical pulse from the Au-UME, are electroporated. However, as each of the yeast cells has its own membrane, - pores are formed individually in each cell membrane. If the pores formed with Ø 10 μm Au-UME do not reach a critically big size and are able to reseal, then reversible electroporation should be achieved. The EIS data presented in this study (Fig. 2 A and B) indicate that electroporated yeast cells can reseal in 30 min or in 60 min after 1.0 V or 2.0 V electrical pulse is applied to Ø 10 μm Au-UME, respectively. Thus, these results indicate that the pores in yeast cells membrane do not reach critically sufficient large size and are able to reseal resulting in reversible electroporation (Fig. 4).

3.2. Determination of the diameter of electroporated area of deposited yeast cell area

The electroporation process can be applied to introduce various compounds (such as DNA, drugs, etc.) into the electroporated cells. Molecules with different structures are capable to penetrate pores of different sizes. One of the most important factors to create a controllable electroporation process is the ability to predict the size of the pores that will be formed. The electroporation process is being studied since it is desired to adapt SECM to treat some cancerous tissues. In this case, it is extremely important not only to predict the size of a pore but also the area, that is affected by the electroporation process, in order to minimize the influence of this treatment to healthy tissues. To determine the diameter of electroporated area of yeast cells, the SECM feedback mode vertical scan above yeast cells was carried out in this research before and after the electroporation. The active yeast cells were first scanned before performing the electroporation. Then the point where the electroporation will be performed was selected from the resulting curve (Fig. 5 A). The red dashed line in Fig. 5 represents the location where the yeast cell-coated area was electroporated. The electroporation was performed by applying 2.0 V vs. Ag/AgCl,Cl$^-_{sat}$ for 120 s to the Au-UME. After the electroporation, the electrode was returned to the initial scanning position and the surface scan was performed again. The surface scans registered are non-linear due to the yeast being immobilized irregularly on the FTO/glass and of their unequal size.

The results of electroporation and surface scan performed by using Ø 10 μm Au-UME (Fig. 5) show that the effect of the electrical pulse of 2.0 V (Fig. 5 B, a part of a current line that curves inward) is observed in the

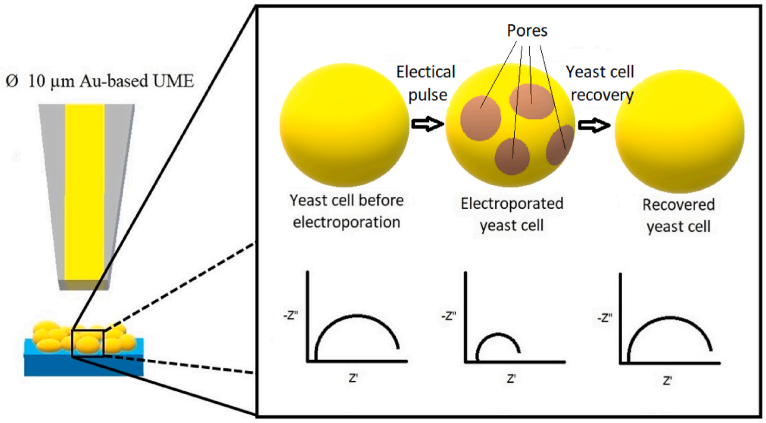


Fig. 4. Visualization of possible yeast cell electroporation process outcome by using Ø 10 µm Au ultramicroelectrode positioned directly over the surface of unpolarized yeast cells at the distance of 20 µm.

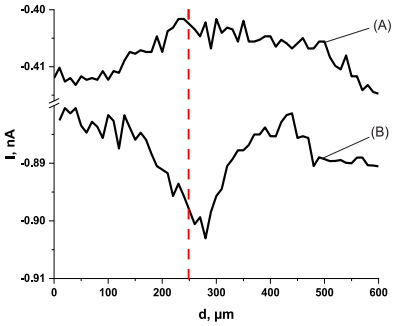


Fig. 5. Surface scan of immobilized yeast cells: **A** – before the electroporation and, **B** – after the electroporation. Red dashed line represents location where the electroporation was performed. The scan was performed at a constant distance of 20 µm from the surface. Measured with Ø 10 µm Au-UME. Au-UME potential of −0.2 V vs Ag/AglCl,Cl^-_{sat}., measurements were performed in buffer solution, pH 7.1, with 10 mmol of glucose. Electrode pitch – 10 µm, speed – 10 µm s^{-1}.

range from about ~150 µm–~400 µm, showing that the diameter of yeast cell covered area affected by the electroporation is approximately of 250 µm.

4. Conclusions

Results of this study show that the scanning electrochemical microscopy combined with electrochemical impedance spectroscopy is a suitable technology for reversible electroporation of yeast cells and for the determination of quantitative electrochemical characteristics of the investigated system. In contrary to usually applied strong electrical pulses, in this research pore formation was successfully performed by applying to the Au-UME single long-lasting (120 s) pulse of relatively low electrical pulse of 1.0 and/or 2.0 V vs. Ag/AglCl,Cl^-_{sat} in three electrode system. The diameter of the formed pore is approximately of 250 µm i.e., it is about 25 times larger than the diameter of conducting part of the Au-UME used for the electroporation. The procedure of reversible electroporation was carried out by using yeast cells immobilized on not-connected thus, unpolarized FTO/glass surface, avoiding possible damages to the investigated biological system and opening new possibilities to treat/investigate biological systems safely. We believe that such system can be applied to treat sensitive biological systems by the formation of affected cell areas and to predict the dimensions of affected areas, location, regeneration ability, and duration of regeneration. The development and the application of a controlled electroporation model for yeast cells can be effectively applied for biomedical purposes and paves the way for targeted drug delivery, very selective treatment of cancer cells, and/or some other biomedical and biotechnological applications.

CRediT authorship contribution statement

Margarita Poderyte: Methodology, Investigation, Formal analysis, Writing – original draft, Interpretation of data. **Aušra Valiūnienė:** Methodology, Investigation, Formal analysis, Writing – original draft, Supervision, Conceptualization, Interpretation of data, Formal analysis. **Arunas Ramanavicius:** Interpretation of data, Formal analysis, Supervision, Conceptualization, Writing – review & editing, Funding acquisition.

Declaration of competing interest

The authors declare that they have no known competing financial interests or personal relationships that could have appeared to influence the work reported in this paper.

Acknowledgement

This project has received funding from European Regional Development Fund (project No 01.2.2-LMT-K-718-01-0063) under grant agreement with the Research Council of Lithuania (LMTLT) by Prof. Habil. dr. Arunas Ramanavicius.

References

Baranski, A.S., Diakowski, P.M., 2004. Application of AC impedance techniques to scanning electrochemical microscopy. J. Solid State Electrochem. 8, 683–692. https://doi.org/10.1007/s10008-004-0533-x.

Bard, A.J., Fan, F.R.F., Kwak, J., Lev, O., 1989. Scanning electrochemical microscopy. Introduction and principles. Anal. Chem. 61, 132–138. https://doi.org/10.1021/ac00177a011.

Batista Napotnik, T., Miklavčič, D., 2018. In vitro electroporation detection methods – an overview. Bioelectrochemistry 120, 166–182. https://doi.org/10.1016/j.bioelechem.2017.12.005.

Caloca, B., Navarro, A., Canales-Torres, M., Le, B., Rosas, C., Sero, Z., Bachant, J., 2021. Comparison of Concanavalin A and Poly-L-lysine as Cell Adhesives for Routine Yeast Microscopy Applications. https://doi.org/10.1002/yea.3686. Yeast.

Caramazza, L., de Angelis, A., Nardoni, M., Paolicelli, P., Petralito, S., Apollonio, F., Liberti, M., 2020. Planning sine waves electroporation on liposomes for drug delivery application. In: 2020 IEEE MTT-S International Microwave Biomedical Conference, IMBioC 2020. Institute of Electrical and Electronics Engineers Inc. https://doi.org/10.1109/IMBioC47321.2020.9384905.

Chance, B., Mueller, P., De Vault, D., Powers, L., 1980. Biological membranes. Phys. Today 33, 32–38. https://doi.org/10.1063/1.2913788.

Chen, C., Smye, S.W., Robinson, M.P., Evans, J.A., 2006. Membrane electroporation theories: a review. Med. Biol. Eng. Comput. 44, 5–14. https://doi.org/10.1007/s11517-005-0020-2.

Daum, G., 2000. The yeast Saccharomyces cerevisiae, a eukaryotic model for cell biology. Microsc. Res. Tech. 51, 493–495. https://doi.org/10.1002/1097-0029(20001215)51:6<493:AID-JEMT1>3.0.CO;2-F.

Dungrawala, H., Hua, H., Wright, J., Abraham, L., Kasemsri, T., McDowell, A., Stilwell, J., Schneider, B.L., 2012. Identification of new cell size control genes in S. cerevisiae. Cell Div. 7 https://doi.org/10.1186/1747-1028-7-24.

Ebejer, N., Schnippering, M., Colburn, A.W., Edwards, M.A., Unwin, P.R., 2010. Localized high resolution electrochemistry and multifunctional imaging: scanning electrochemical cell microscopy. Anal. Chem. 82, 9141–9145. https://doi.org/10.1021/ac102191u.

Edwards, M.A., Martin, S., Whitworth, A.L., Macpherson, J.V., Unwin, P.R., 2006. Scanning electrochemical microscopy: principles and applications to biophysical systems. Physiol. Meas. 27 https://doi.org/10.1088/0967-3334/27/12/R01.

Ferrari, E., Palma, C., Vesentini, S., Occhetta, P., Rasponi, M., 2020. Integrating Biosensors in Organs-On-Chip Devices: A Perspective on Current Strategies to Monitor Microphysiological Systems. https://doi.org/10.3390/bios10090110. Biosensors.

Forster, R.J., Keyes, T.E., 2007. 6-Ultramicroelectrodes 6.1 BEHAVIOR of ULTRAMICROELECTRODES. Handbook of Electrochemistry. Elsevier, pp. 155–171.

Gabriunaite, I., Valiūnienė, A., Valincius, G., 2018. Formation and properties of phospholipid bilayers on fluorine doped tin oxide electrodes. Electrochim. Acta 283, 1351–1358. https://doi.org/10.1016/j.electacta.2018.04.160.

Galao, R.P., Scheller, N., Alves-Rodrigues, I., Breinig, T., Meyerhans, A., Díez, J., 2007. Saccharomyces cerevisiae: a versatile eukaryotic system in virology. Microb. Cell Factories 6, 1–9. https://doi.org/10.1186/1475-2859-6-32.

Gencturk, E., Ulgen, K.O., Mutlu, S., 2020. Thermoplastic microfluidic bioreactors with integrated electrodes to study tumor treating fields on yeast cells. Biomicrofluidics 14. https://doi.org/10.1063/5.0008462.

Gholami, A., Mousavi, S.M., Hashemi, S.A., Ghasemi, Y., Chiang, W.H., Parvin, N., 2020. Current trends in chemical modifications of magnetic nanoparticles for targeted drug delivery in cancer chemotherapy. Drug Metabol. Rev. https://doi.org/10.1080/03602532.2020.1726943.

Jain Editor, K.K., n.d. Drug Delivery Systems.

Kotnik, T., Frey, W., Sack, M., Haberl Meglič, S., Peterka, M., Miklavčič, D., 2015. Electroporation-based applications in biotechnology. Trends Biotechnol. 33, 480–488. https://doi.org/10.1016/j.tibtech.2015.06.002.

Kotnik, T., Kramar, P., Pucihar, G., Miklavčič, D., Tarek, M., 2012. Cell membrane electroporation - Part 1: the phenomenon. IEEE Electr. Insul. Mag. 28, 14–23. https://doi.org/10.1109/MEI.2012.6268438.

Kotnik, T., Rems, L., Tarek, M., Miklavcic, D., 2019. Membrane electroporation and electropermeabilization: mechanisms and models. Annu. Rev. Biophys. 48, 63–91. https://doi.org/10.1146/annurev-biophys-052118-115451.

Lee, W.G., Demirci, U., Khademhosseini, A., 2009. Microscale electroporation: challenges and perspectives for clinical applications. Integrative Biology 1, 242–251. https://doi.org/10.1039/b819201d.

Lefrou, C., Cornut, R., 2010. Analytical expressions for quantitative scanning electrochemical microscopy (SECM). ChemPhysChem 11, 547–556. https://doi.org/10.1002/cphc.200900600.

Liu, Z., Liang, X., Liu, H., Wang, Z., Jiang, T., Cheng, Y., Wu, M., Xiang, D., Li, Z., Wang, Z.L., Li, L., 2020. High-throughput and self-powered electroporation system for drug delivery assisted by microfoam electrode. ACS Nano 14, 15458–15467. https://doi.org/10.1021/acsnano.0c06100.

Malel, E., Ludwig, R., Gorton, L., Mandler, D., 2010. Localized deposition of Au nanoparticles by direct electron transfer through cellobiose dehydrogenase. Chem. Eur J. 16, 11697–11706. https://doi.org/10.1002/chem.201000453.

Matrab, T., Combellas, C., Kanoufi, F., 2008. Scanning electrochemical microscopy for the direct patterning of a gold surface with organic moities derived from iodonium salt. Electrochem. Commun. 10, 1230–1234. https://doi.org/10.1016/j.elecom.2008.06.006.

Mattar, J.R., Turk, M.F., Nonus, M., Lebovka, N.I., El Zakhem, H., Vorobiev, E., 2014. Stimulation of Saccharomyces cerevisiae cultures by pulsed electric fields. Food Bioprocess Technol. 7, 3328–3335. https://doi.org/10.1007/s11947-014-1336-4.

Mattiazzi, M., Petrovič, U., Križaj, I., 2012. Yeast as a model eukaryote in toxinology: a functional genomics approach to studying the molecular basis of action of pharmacologically active molecules. Toxicon. https://doi.org/10.1016/j.toxicon.2012.03.014.

Mei, B.A., Lau, J., Lin, T., Tolbert, S.H., Dunn, B.S., Pilon, L., 2018. Physical interpretations of electrochemical impedance spectroscopy of redox active electrodes for electrical energy storage. J. Phys. Chem. C 122, 24499–24511. https://doi.org/10.1021/acs.jpcc.8b05241.

Mikoliunaite, L., Makaraviciute, A., Suchodolskis, A., Ramanaviciene, A., Oztekin, Y., Stirke, A., Jurkaite, G., Ukanis, M., Carac, G., Cojocaru, P., Ramanavicius, A., 2011. Atomic force microscopy study of living baker's yeast cells. Adv. Sci. Lett. 4, 368–376. https://doi.org/10.1166/asl.2011.1236.

Morkvenaite-Vilkonciene, I., Ramanaviciene, A., Kisieliute, A., Bucinskas, V., Ramanavicius, A., 2019. Scanning electrochemical microscopy in the development of enzymatic sensors and immunosensors. Biosens. Bioelectron. https://doi.org/10.1016/j.bios.2019.111411.

Nakamura, H., Funahashi, J., 2013. Electroporation: past, present and future. Dev. Growth Differ. 55, 15–19. https://doi.org/10.1111/dgd.12012.

Rodriguez, C.E., Shinyashiki, M., Froines, J., Yu, R.C., Fukuto, J.M., Cho, A.K., 2004. An examination of quinone toxicity using the yeast Saccharomyces cerevisiae model system. Toxicology 201, 185–196. https://doi.org/10.1016/j.tox.2004.04.016.

Schipper, F., Dixit, M., Kovacheva, D., Talianker, M., Haik, O., Grinblat, J., Erickson, E. M., Ghanty, C., Major, D.T., Markovsky, B., Aurbach, D., 2016. Stabilizing nickel-rich layered cathode materials by a high-charge cation doping strategy: zirconium-doped LiNi0.6Co0.2Mn0.2O2. J. Mater. Chem. 4, 16073–16084. https://doi.org/10.1039/c6ta06740a.

Slim, C., Griveau, S., Bedioui, F., Bedioui Scanning Electrochemical Microscopy Paul Worsfold, F., Poole, C., Townshend, A., 2018. Scanning Electrochemical Microscopy, vol. 978. https://doi.org/10.1016/B978-0-12-409547-2.13947-2i.

Stirke, A., Celiesiute-Germaniene, R., Zimkus, A., Zurauskiene, N., Simonis, P., Dervinis, A., Ramanavicius, A., Balevicius, S., 2019. The link between yeast cell wall porosity and plasma membrane permeability after PEF treatment. Sci. Rep. 9 https://doi.org/10.1038/s41598-019-51184-y.

Stirke, A., Zimkus, A., Balevicius, S., Stankevic, V., Ramanaviciene, A., Ramanavicius, A., Zurauskiene, N., 2014. Permeabilization of yeast Saccharomyces cerevisiae cell walls using nanosecond high power electrical pulses. Appl. Phys. Lett. 105 https://doi.org/10.1063/1.4905034.

Sweeney, D.C., Douglas, T.A., Davalos, R.V., 2018. Characterization of cell membrane permeability in vitro part ii: computational model of electroporation-mediated membrane transport. Technol. Cancer Res. Treat. 17, 1–13. https://doi.org/10.1177/1533033818792490.

Thangappan, R., Kalaiselvam, S., Elayaperumal, A., Jayavel, R., Arivanandhan, M., Karthikeyan, R., Hayakawa, Y., 2016. Graphene decorated with MoS2 nanosheets: a synergetic energy storage composite electrode for supercapacitor applications. Dalton Trans. 45, 2637–2646. https://doi.org/10.1039/c5dt04832j.

Tomov, T.C., Tsoneva, I.C., 1989. Changes in the surface charge of cells induced by electrical pulses. J. Electroanal. Chem. 276, 127–133. https://doi.org/10.1016/0022-0728(89)87304-8.

Valiūnienė, A., Gabriunaite, I., Poderyte, M., Ramanavicius, A., 2020a. Electroporation of a hybrid bilayer membrane by scanning electrochemical microscope. Bioelectrochemistry 136. https://doi.org/10.1016/j.bioelechem.2020.107617.

Valiūnienė, A., Petronienė, J., Dulkys, M., Ramanavičius, A., 2020b. Investigation of active and inactivated yeast cells by scanning electrochemical impedance microscopy. Electroanalysis 32, 367–374. https://doi.org/10.1002/elan.201900414.

Valiūnienė, A., Petroniene, J., Morkvenaite-Vilkonciene, I., Popkirov, G., Ramanaviciene, A., Ramanavicius, A., 2019. Redox-probe-free scanning electrochemical microscopy combined with fast Fourier transform electrochemical impedance spectroscopy. Phys. Chem. Chem. Phys. 21, 9831–9836. https://doi.org/10.1039/c9cp00187e.

Valiūnienė, A., Rekertaitė, A.I., Ramanavičienė, A., Mikoliūnaitė, L., Ramanavičius, A., et al., 2017. Fast Fourier transformation electrochemical impedance spectroscopy for the investigation of inactivation of glucose biosensor based on graphite electrode modified by Prussian blue, polypyrrole and glucose oxidase. Colloids Surf. A Physicochem. Eng. Asp. 532, 165–171.

Valiūnienė, A., Sabirovas, T., Petronienė, J., Ramanavičius, A., 2020d. Towards the application of fast Fourier transform - scanning electrochemical impedance microscopy (FFT-SEIM). J. Electroanal. Chem. 864 https://doi.org/10.1016/j.jelechem.2020.114067.

Volkov, V., 2015. Quantitative description of ion transport via plasma membrane of yeast and small cells. Front. Plant Sci. 6, 1–20. https://doi.org/10.3389/fpls.2015.00425.

Xu, K., 2021. Silicon electro-optic micro-modulator fabricated in standard CMOS technology as components for all silicon monolithic integrated optoelectronic systems. J. Micromech. Microeng. 31 https://doi.org/10.1088/1361-6439/abf333.

Xu, K., Chen, Y., Okhai, T.A., Snyman, L.W., 2019. Micro optical sensors based on avalanching silicon light-emitting devices monolithically integrated on chips. Opt. Mater. Express 9, 3985. https://doi.org/10.1364/ome.9.003985.

Zand, E., Schottroff, F., Steinacker, E., Mae-Gano, J., Schoenher, C., Wimberger, T., Wassermann, K.J., Jaeger, H., 2021. Advantages and limitations of various treatment chamber designs for reversible and irreversible electroporation in life sciences. Bioelectrochemistry 141. https://doi.org/10.1016/j.bioelechem.2021.107841.

Biosensors and Bioelectronics 216 (2022) 114621

Contents lists available at ScienceDirect

Biosensors and Bioelectronics

journal homepage: www.elsevier.com/locate/bios

Scanning electrochemical microscopy based irreversible destruction of living cells

Margarita Poderyte, Arunas Ramanavicius, Aušra Valiūnienė *

Vilnius University, Faculty of Chemistry and Geosciences, Institute of Chemistry, Naugarduko 24, Vilnius, LT, 03225, Lithuania

ARTICLE INFO

Keywords:
Electrochemical tissue removal
Irreversible electroporation
Yeast cells
Scanning electrochemical microscope
Electrochemical impedance spectroscopy
Ultramicro-electrode

ABSTRACT

In this research, scanning electrochemical microscopy combined with electrochemical impedance spectroscopy has been applied to irreversible electroporation of active yeast cells by causing cell death. This finding is important for the development of irreversible electroporation technique, which could be suitable for the curing of cancerous tissues, because during this research cell death has been achieved using relatively low ultramicro-electrode (UME) voltage, precisely of 2.0 V *vs* Ag/AgCl,Cl⁻sat. It was determined that the irreversibly electroporated area of immobilized yeast cells was located directly below the UME and was of approximately 20 times larger width than the diameter of the UME, leaving undamaged cells out of this area. The ability of SECM to move the UME with high accuracy in x, y, and z directions and the ability to use electrodes of various diameters as well as the fact that the diameter of the electroporated area depends on the diameter of the UME and on the distance between the UME and the surface, what offers the possibility to establish targeted electroporation systems for selective treatment of tissues.

1. Introduction

Each living cell is surrounded by a plasma membrane that controls the exchange of substances and is involved in the transmission of signals from the environment (le Roux et al., 2019). In 1925 Gorter and Grendel showed that the membrane is composed of two layers of self-organized phospholipid molecules(Gorter and Grendel, 1925). These are amphiphilic molecules having a hydrophilic head consisting of a phosphate group and glycerol and a hydrophobic tail consisting of two long fatty acid chains connected *via* ester linkages to the first and second carbon atoms of the glycerol chain (Suetsugu et al., 2014). The membrane is stabilized by hydrophobic effects and van der Waals interactions. In an aqueous solution, the hydrophobic tails of phospholipids begin to self-organize in order to reduce interaction with water molecules and spontaneously form closed structures composed of a double layer based on lipid molecules. The polar heads face the water, and the hydrophobic tails is directed in the inside of the bilayer (Andersson Trojer and Brezesinski, 2016; Marsh, 2016).

Cell membranes possess selective permeability that can be modified and one of the modification methods is electroporation. It is a physical method in which cells are exposed to a strong electrical pulse (about 1 kV cm^{-1}), which results in the formation of temporary or permanent pores in the phospholipid layer (Kotnik et al., 2019). The first reports of transient permeability changes in vesicle membranes as a result of exposure to an external electric field were published in 1972. The procedure was called electroporation, and it was divided into two main branches: reversible electroporation, in which the treated cells have restored their initial state and survived, and irreversible electroporation, which resulted in cell death (Neumann and Rosenheck, 1972).

When cells are exposed to an electric field, a transmembrane potential ($\Delta\Psi m$) is induced in the plasma membrane of the cells, the magnitude of which depends on the strength of the external field and the radius of the cell, which can be defined with the formula (1):

$$\Delta\Psi m = 1.5\ E ext\ R\ \cos\theta \quad (1)$$

Where *E*ext is the strength of the external electric field; *R* – cell radius; cos*θ* – indicates the angular position of the cell with respect to the electric field vector.

A membrane is electroporated when its potential reaches a critical threshold from 200 mV up to 2.0 V, which is depending on the pulse duration (Batista Napotnik and Miklavčič, 2018; Delemotte and Tarek, 2012; Venslauskas and Šatkauskas, 2015).

Electroporation is a probabilistic process, therefore, the number and size of pores in the membrane is highly dependent on the basic physical

* Corresponding author.
E-mail address: ausra.valiuniene@chf.vu.lt (A. Valiūnienė).

https://doi.org/10.1016/j.bios.2022.114621
Received 10 June 2022; Received in revised form 18 July 2022; Accepted 2 August 2022
Available online 14 August 2022
0956-5663/© 2022 Elsevier B.V. All rights reserved.

parameters: pulse potential, pulse shape, pulse duration, and number of pulses (Bodénès et al., 2019; Demiryurek et al., 2015). High-potential long-term electrical impulses can completely collapse the integrity of the cell membrane because such pulses induce expanding pores beyond the critical size. The destruction of cell membrane causes its death (Bodénès et al., 2019; Thomson et al., 2015). Irreversible electroporation for quite a long time has been interpreted as a side effect and has only been investigated by setting cut-off values of the electric field at which cells remain viable. However, irreversible electroporation can be applied to the food industry – food and liquid sterilization. Up to 99.99% of bacteria are killed by a short pulse of a strong electric field when the bacterial suspension is exposed. The basis of such sterilization is the damage of cell membranes by a strong electric field (Kotnik et al., 2015; Saito et al., 2013). Research over the past few years has shown that irreversible electroporation can become an important and promising treatment method in recent biomedicine (Cohen et al., 2018; Geboers et al., 2020; Paiella et al., 2016). It has been found that the application of irreversible electroporation can successfully remove cancerous tissue or tumor without damaging healthy tissues. One of its most important advantages is that no drugs are used. In this case, one of the main aspects is the ability to precisely control the size of the electroporated area (Paiella et al., 2015; Wagstaff et al., 2016).

Scanning electrochemical microscope (SECM) can be applied for the investigation of living cells (Morkvenaite-Vilkonciene et al., 2016; Petroniene et al., 2020a, 2020b; Ramanavicius et al., 2017) and was applied the key tool for the development of a targeted cell-electroporation system (Poderyte et al., 2022). SECM is a useful tool for the investigation of complex and sensitive biological systems since while measuring, the analyte is not damaged in any way (Polcari et al., 2016). SECM signal is a current that is measured by ultramicro-electrode (UME), this current is induced by oxidation/reduction reaction that took place on the working surface of UME. The UME size can vary from the diameter of 25 μm down to a few nanometers and it can be moved in all three x-, y-, z-dimensions with the accuracy of 1 μm (Izquierdo et al., 2018; Zoski, 2016). It was already demonstrated in our previous research that SECM can be applied to electroporate living yeast cells (Poderyte et al., 2022) and artificial phospholipid bilayer membranes (Valiūnienė et al., 2020a). It has been shown that the size of electroporated area by SECM depends upon applied electrode diameter (Danieli and Mandler, 2013; Grisotto et al., 2011). The same correlation can also be seen during the application of SECM for the electroporation (Poderyte et al., 2022; Valiūnienė et al., 2020a).

In the light of these findings in this research, a scanning electrochemical microscope was successfully adapted to study the electroporation process of living yeast cells (Fig. 1). To the best of our knowledge, the applicability of SECM for electroporation process performance and its investigation has never been published by any other research groups

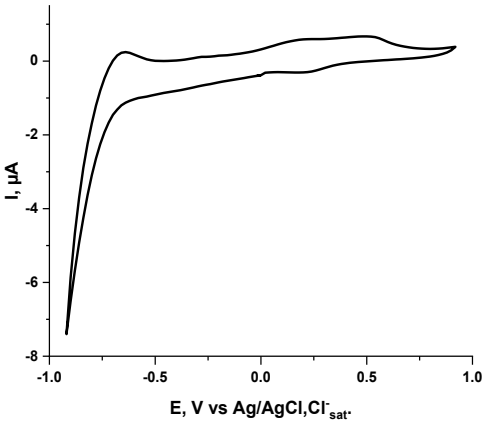


Fig. 2. Cyclic voltammetry curve of the ø 25 μm Pt ultramicro-electrode in buffer solution, pH 7.1, with 10 mM of glucose. Potential scan rate 10 mV s^{-1}.

excluding our group previous work (Poderyte et al., 2022). Considering that SECM is highlighted as a not invasive and not destructible technology, which can be applied for the assessment of sensitive biological systems (Morkvenaite-Vilkonciene et al., 2019). As we showed in our recent work (Poderyte et al., 2022) fully reversible electroporation can be obtained while only using SECM-based technology. Meanwhile, in this research we have shown that by the adjustment of proper system parameters, this SECM-based technology can also be applied for irreversible electroporation as well. The ability of SECM to move the UME in the x, y, and z directions with high accuracy, the ability to use electrodes of different diameters, and the dependence of the size of the formed pores on the diameter of the electrode used for the electroporation – has been adjusted in this research to create controlled irreversible electroporation model. The novelty of this research is the applicability of SECM to perform the electroporation process using a three-electrode system using relatively low voltage (2.0 V) pulses and to damage the cells only directly below the working electrode, leaving untouched these cells, which are out of this area. All these findings could lead to a breakthrough in developing targeted irreversible electroporation based treatment of cancerous tissue removal (see Fig. 2).

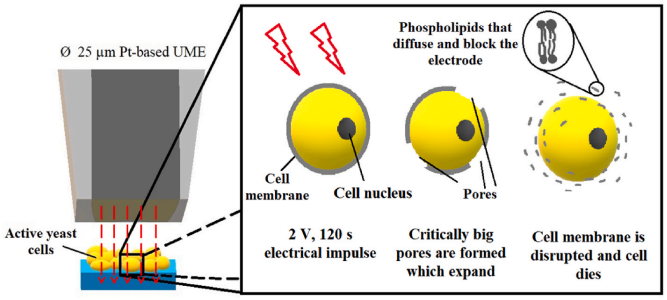


Fig. 1. Visualization of possible electroporation process by voltage of 2.0 V applied for 120 s to the Ø 25 μm UME, which is positioned at 20 μm distance above the surface of active yeast cells.

2. Experimental part

2.1. Ultramicro-electrode preparation

Before starting electrochemical measurement, ultramicro-electrode was cleaned carefully, since it is a very sensitive system, in which any impurities could cause contamination of the working area. The platinum UME of 25 μm diameter from Sensolytics (Bochum, Germany) was cleaned both mechanically and electrochemically. First of all, the electrode was rinsed with ethanol and then mechanically polished with sandpaper with a grain size of 0.3 μm while scrubbing it in a circular motion and holding it perpendicular to the sanding surface. After polishing, the electrode was washed with distilled water and placed in a three-electrode cell with 0.5 M H2SO4 solution where a Pt wire was used as the counter electrode, Ag/AgCl,Cl˙sat – as the reference electrode, and the UME – as the working electrode. To wash the electrode electrochemically, cyclic voltamperograms were recorded in the potential range from 0 V to 1.7 V at a scan rate of 0.2 V s^{-1} (10–50 cycles) until no undesired redox peaks occur.

The same three-electrode cell was used to determine the electrode potential suitable for further electrochemical measurements at potentiostatic mode. The cleaned UME was placed in an electrochemical cell far from the surface of interest (at least 1000 μm away) and cyclic voltamperograms were recorded in a 0.01 M phosphate-buffer, pH 7.1, in the potential range from −0.9 V to 0.9 V *vs* Ag/AgCl,Cl˙sat. The phosphate-buffered saline (PBS) solution was prepared by dissolving 0.1 M NaCl and 0.01 M NaH2PO4•2H2O in distilled water. Then it was adjusted with NaOH solution until a pH of 7.1 was reached.

2.2. Preparation and immobilization of active and inactivated yeast cells

The active yeast suspension has been made by adding 50 mg of dry yeast (*Saccharomyces cerevisiae*) and 0.5 ml of deionized water to the Eppendorf tube, shaken, and then stored at 30 °C for 30 min. To make an 'inactivated' yeast aliquot the suspension was stirred for 2 h in a covered beaker at a temperature of over 80 °C.

A glass slide, covered with semiconducting fluorine-doped tin oxide (FTO) thin film, was used as a substrate for the immobilization of the cells. Before using, FTO/glass has been cleaned following the procedure: (i) sonication in 2% "Micro 90" solution from Sigma Aldrich (Stockholm, Sweden) for 10 min, (ii) rinsing and sonication in deionized water for 10 min, (iii) rinsing with deionized water and sonication in 2-propanol (99.5%, Honeywell) for 10 min, (iv) washing with deionized water and drying in a stream of N2 gas.

For yeast cell immobilization on the FTO surface, poly-L-lysine was used since it improves the attachment of cells to the surfaces. A small drop of poly-L-lysine was placed in the middle of a clean FTO/glass plate and left to dry. Then, 0.5 μm of yeast suspension was placed on the top of the dried poly-L-lysine and left to dry. Afterward, immobilized yeast cells were washed with buffer solution three times to eliminate all the cells that were not immobilized on the surface.

2.3. Electroporation of immobilized cells and electrochemical impedance measurements

Electroporation of immobilized cells was performed by using chronoamperometry while applying 2 V for 120 s to the ⌀ 25 μm Pt UME. To avoid undesired cell damage and electrode contamination with yeast cells, electroporation has been performed while holding UME at a constant 20 μm distance from the surface of immobilized yeast cells.

To capture the electrochemical changes caused by electroporation of yeast cells the electrochemical impedance spectroscopy (EIS) measurements were made: (i) before the electroporation; (ii) 1 min after the electroporation; (iii) 30 min after the electroporation; (iv) 60 min after the electroporation. Registered data were evaluated using analysis software 'ZView' by applying a selected equivalent circuit model for the determination of electrochemical system characteristics. The impedance of the system has been registered with the same working electrode and in the same electrode position at which electroporation was performed. EIS spectra were measured in potentiostatic mode, and the range of alternating current frequencies varied from 0.1 Hz to 100 kHz. All the EIS spectra are presented as Nyquist plots, where x-axis represents the Z', which is real impedance component, and y-axis $-Z''$, which is imaginary impedance component.

2.4. The assessment of the electroporated area

To determine the electrical impulse affected area size, horizontal scans above the yeast cell surface have been recorded in SECM feedback mode: (i) before the electroporation; (ii) after the electroporation. Both scans have been performed in the same line and direction with a scan rate of 10 μm s-1 and a step of 10 μm at a constant 20 μm distance from the surface of yeast cells.

3. Results and Discussion

⌀ 25 μm Pt ultramicro-electrode has been chosen as a working electrode for the irreversible electroporation process since Pt is biocompatible, inert, and very stable metal (Vižintin et al., 2020), which already showed promising results in irreversible electroporation process for cancer treatment (Lim et al., 2021). Considering that SECM-based and EIS-based investigations of yeast cells can be successfully performed at appropriate potentiostatic conditions (Poderyte et al., 2022; Valiūnienė et al., 2020b), cyclic voltammetry curves were registered to determine a suitable potential value for further SECM and EIS experiments using Pt-based UME as a working electrode.

Cyclic voltammograms of the ⌀ 25 μm Pt ultramicro-electrode in buffer solution, pH 7.1, containing 10 mM of glucose (Fig. 1) show no redox peaks indicating that the electrode is clean, and any unwanted electrochemical reactions occur on the electrode in the potential range from −0.6 V to 0.9 V. Therefore, the potential value for further EIS and SECM measurements has been selected at the Faradaic region of measured current (−0.75 V) because: (i) SECM method is based on measuring the Faradaic current resulting from the electrochemical reaction at the UME; (ii) EIS registration at potentiostatic mode requires controlled potential in the Faradaic current zone as well.

3.1. The evaluation of active yeast cells and the efficiency of electroporation process by EIS-based measurement

To elucidate the possible effect of yeast cells viability on the electrochemical behaviour of the UME, the electrochemical impedance spectra have been recorded placing the ⌀ 25 μm Pt UME at the distance of 20 μm from both active and inactivated yeast cell surface. To keep yeast cells active, 10 mmol of glucose was added to the buffer solution. During all experiments with active yeast cells, glucose was used as an energy source, resulting in yeast cells' metabolism being active and traceable with EIS. The EIS data are presented in a Nyquist plot (Real impedance, Z' *vs* Imaginary impedance, Z'') in Fig. 3. The characteristic shape of semicircles appearing in the high-frequency range and representing charge transfer resistance indicates that the charge transfer resistance of the UME above active yeast cells is lower (Fig. 3A, spectrum 1) than the charge transfer resistance above inactivated yeast cells (Fig. 3A, spectrum 2). Thus, it can be concluded that the total impedance above active yeast cells significantly differs from the impedance above inactivated yeast cells. This difference may occur due to the load-bearing substances that are formed during metabolic processes in living (active) yeast cells. Inactivated yeast cells do not undergo metabolic processes, so there are fewer substances that can carry a charge directly to the UME surface (Valiūnienė et al., 2020b). Since it was considered that active yeast cells should generate a higher electrochemical signal after electroporation due to yeast habitual processes

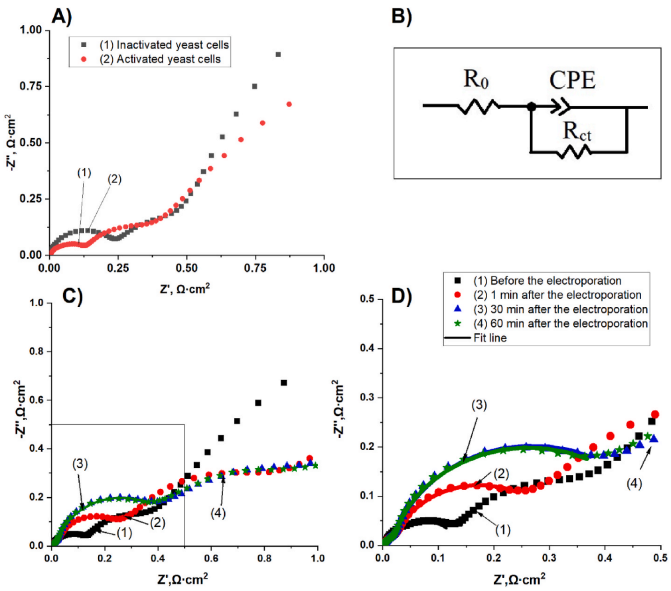


Fig. 3. A) Electrochemical impedance spectra of the ⌀ 25 μm Pt UME positioned at 20 μm distance from active (1) and inactivated (2) yeast cells, registered in buffer solution, pH 7.1, containing 10 mM of glucose. Applied potential: −0.75 V *vs* Ag/AgCl,Cl⁻sat electrode, frequency range 0.1 Hz–100 kHz. **B)** The equivalent circuit model used for the fitting of EIS data; **C)** Active yeast cells electroporation performed with ⌀ 25 μm Pt UME, while applying 2 V for 120 s; electrochemical impedance spectra registered placing UME over the yeast cells before the electroporation (curve 1); 1 min after the electroporation (curve 2); 30 min after the electroporation (curve 3); 60 min after the electroporation (curve 4). Measured in buffer solution, pH 7.1, with 10 mM of glucose. UME potential of −0.75 V *vs* Ag/AgCl,Cl⁻sat electrode, frequency range 0.1 Hz–100 kHz; **D)** Magnified data within the range of 0.5 Ω cm^2 on the x and y axis representing Z' and $-Z''$ data, respectively, that were fitted with the equivalent circuit model.

that could be interrupted by an electrical pulse, further yeast cell electroporation investigation has been performed only with active yeast cells. Also, electroporation can cause cell destruction or death, thus, during the experiments with initially inactivated yeast cells, significant electrochemical responses are not expected.

Contrary to the conventional electroporation model where cell membranes are affected by high voltage (approx. 1 kV cm^{-1}) induced in a two-electrode system (Rems and Miklavčič, 2016), in this research the surface of non-polarized yeast cells was affected by relatively low voltage (2.0 V *vs* Ag/AgCl,Cl⁻sat) of the UME in the three-electrode system. The electroporation was performed with SECM by fixing the UME at a 20 μm distance from the active yeast cells' surface and by applying a constant potential of 2.0 V between the UME and the reference Ag/AgCl,Cl⁻sat electrode for 120 s. The main advantage of selected experimental conditions is the possibility to avoid unwanted damage to active yeast cells that inevitably occurs at high UME voltage.

As can be seen in Fig. 3C, the shapes of obtained spectra of electrochemical impedance are composed of several semicircles. The simplest and the most common Randles equivalent circuit model was selected for the fitting of the data at the high-frequency range displaying the first semicircle (Fig. 3D), because the load transfer resistance is defined from the higher frequency range (Randviir and Banks, 2013). This equivalent circuit is presented in Fig. 3B) and it includes the electrolyte resistance (R_0), charge transfer resistance (R_{ct}) that represents the charge-transfer efficiency at the interface between the UME and the electrolyte, and constant phase element (*CPE*) that represents a capacitance related to the electric double layer (EDL). Since the experimental data (Fig. 3C and D, symbols) coincide well with the fitted data (Fig. 3 D, lines) it was concluded that values of the equivalent circuit elements (Table 1) are fitting appropriately.

Results presented in Table 1 illustrate that the *CPE* of the system resulted in extremely high values reaching 15 mF cm^2 1 min after the electroporation. The current between the UME and counter electrode is flowing through two main pathways: directly through the electrolyte solution and through the not-connected investigative surface (Baranski and Diakowski, 2004; Poderyte et al., 2022). As a result, the *CPE* represents not only electrical double layer capacitance at the UME-PBS interface but also a certain charge storage phenomenon of FTO/glass covered with the yeast cells resulting in high heterogeneity of the surface.

Table 1
The values of the equivalent circuit (Fig. 3B) registered by analyzing EIS data of ⌀ 25 μm Pt UME (Fig. 3D).

	R_0, Ω cm^2	CPE mF cm^2	n (CPE)	Rct, Ω cm^2
Before the electroporation	0.002	9.67	0.77	0.15
1 min after the electroporation	0.016	15.38	0.84	0.32
30 min after the electroporation	0.016	12.22	0.86	0.51
60 min after the electroporation	0.016	11.41	0.87	0.50

The most important observation of this research was determined by analyzing the values of charge transfer resistance before and after the electroporation procedure. The data determined before the electroporation illustrate (Table 1) that the value of R_{ct} was equal to 0.15 Ω cm^2, however, it increases up to 0.32 Ω cm^2 1 min after the electroporation and keeps increasing until it finally settles the value of 0.5 Ω cm^2 30 min after the electroporation. This observation suggests that irreversible electroporation of the yeast cells has been recorded since the system does not return to its original state, as opposed to the data obtained in previous research where reversible electroporation of the yeast cells was carried out using the Ø 10 μm Au UME (Poderyte et al., 2022). The irreversible increase in the impedance of the Ø 25 μm Pt UME indicates that electrical pulse of 2 V for 120 s resulted in irreversible electroporation of the yeast cells and caused the disruption of the plasma membrane. Contrary to our previous experiments of reversible electroporation when the ions from the yeast cells are released into the solution what is resulting into a decrease of charge transfer resistance, the experiments of this research indicate that proteins and membrane lipids are detached from the plasma membrane and block the surface of

the UME (Fig. 1.) resulting in an increase of charge transfer resistance (Table 1). Considering that affected area size while modifying the substrate with SECM depends upon used UME size (Danieli and Mandler, 2013; Grisotto et al., 2011; Matrab et al., 2008; Oswald et al., 2022; Valiūnienė et al., 2020a; Vaske et al., 2021), it is believed that by using the Ø 25 μm Pt UME the pores of critically large size are formed in the plasma membrane. Consequently, if the pores are formed of critically large size, they start to expand instead of resealing until the membrane is disrupted resulting in irreversible electroporation (Fig. 1). Meanwhile, our previous study (Poderyte et al., 2022) showed that if the pores in yeast cells membrane do not reach a critically large size, then they are able to reseal resulting in reversible electroporation.

3.2. The determination of the diameter of electroporated area of yeast cell modified surface

Irreversible electroporation of yeast cells is a very promising technology for biomedical applications, particularly, in cancerous tissue treatment. While performing irreversible electroporation – the cells of the tissue would be damaged/killed without any drugs and/or complicated medical surgery (Agnass et al., 2020; Kwon et al., 2021; Saini et al., 2019; Szlasa et al., 2020). During treatment of cancerous tissues, very often it is crucially important to control the affected area and protect from damages healthy tissues. For this reason, additional experiments to elucidate the diameter of the voltage-affected area have been performed in this research.

To determine the diameter of the UME affected area of yeast cells, the vertical scan above yeast cells was scanned before and after the electroporation procedure performed while applying to the Ø 25 μm Pt UME 2 V voltage for 120 s. The active yeast cells were first scanned before the electroporation (Fig. 4, curve 1). Then the location where the electroporation will be performed was selected from the resulting curve (Fig. 4, dashed line 3). After the electroporation, the UME was returned to the first scan position and the surface scanning was performed again (Fig. 4, curve 2). The surface scans obtained are non-linear due to the yeast being immobilized irregularly on the FTO/glass and their unequal size. Comparing the scan-line registered before (Fig. 4, curve 1) and the scan-line registered after the electroporation (Fig. 4, curve 2) a clear current drop is observed at the electroporated location. Although it is difficult to establish clear boundaries of the area affected by the electrical pulse, however, it is seen the curvature of the curve between ~200 μm and ~700 μm (Fig. 4, curve 2), is making the electroporated area with a width approximately of 500 μm. The changes in the surface scan current curve also can be used as proof of the successful electroporation process, since the current recorded above irreversibly electroporated cells was clearly lower than above active yeast cells. Such observations can be correlated to loss of metabolic processes after irreversible electroporation, which is causing yeast cell death.

Assuming the obtained results (Fig. 4, curves 1 and 2) the diameter of the affected area has been ~20 times larger than the diameter of the UME used for the electroporation. Similar results were obtained when a 25 μm diameter Pt-based UME was kept at 8 μm from the gold surface which was patterned with organic compounds, and the affected area resulted in 450 μm diameter (Matrab et al., 2008). Another comparable observation was made while electroporating FTO/glass modified with a hybrid bilayer membrane (Valiūnienė et al., 2020a) when Ø 25 μm Pt electrode was held at 5 μm and the electroporation was performed by applying 1 V for 90 s. This resulted in a formed pore with a diameter of 400 μm. Taking into consideration that a larger diameter of the electroporated area was obtained in this research (500 μm) by using Ø 25 μm Pt UME positioned at a constant distance of 20 μm above the surface, it can be concluded that the diameter of the electroporated area depends on both (i) the diameter of the UME and (ii) the distance between the UME and cell-modified surface (Fig. 5).

It can be concluded that the diameter of the electroporated area depends on both (i) the diameter of the UME applied for the electroporation and (ii) the distance between the UME and the surface. Both these findings are in agreement with previously published or (Valiūnienė et al., 2020a) and data reported by some other researchers (Matrab et al., 2008).

4. Conclusions

In this research irreversible electroporation of the yeast cells has been achieved by applying a 2.0 V (*vs* Ag/AgCl,Cl⁻sat) electrical pulse to the Ø 25 μm Pt UME positioned at a 20 μm distance from the surface of

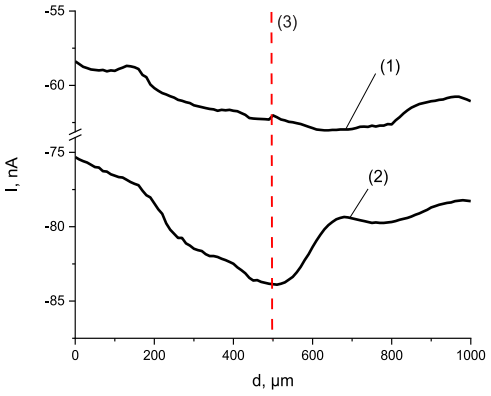


Fig. 4. Surface scan-line of immobilized yeast cells (curve 1) before the electroporation; (curve 2) scan-line after the electroporation. Curve 3 represents location where the electroporation was performed. The scan was performed by using ⌀ 25 μm Pt UME at a constant distance of 20 μm from the surface of yeast cells. UME potential of −0.75 V *vs* Ag/AgCl,Cl⁻sat. Measurements were made in buffer, pH 7.1, with 10 mM of glucose. Electrode pitch – 10 μm, horizontal movement speed – 10 μm s^{-1}.

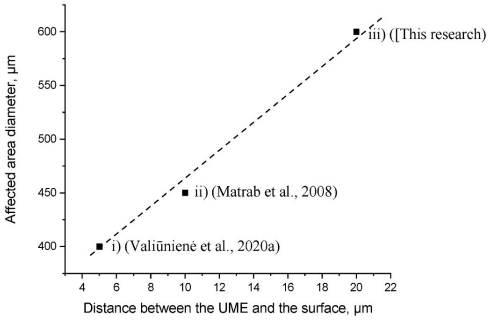


Fig. 5. The dependence of the diameter of the electroporated area on the distance between the UME and the sample: (i) point 400 μm – Ø 25 μm Pt UME was held at a distance of 5 μm from hybrid bilayer membrane and electroporation was performed by applying 1.0 V potential for 2 min – this resulted in a formed electroporated area with a diameter of 400 μm (Valiūnienė et al., 2020a); (ii) point at 450 μm – Ø 25 μm Pt-based UME was kept at a distance of 8 μm from the gold surface, which was patterned with organic compounds, in this case the affected area resulted in 450 μm diameter (Matrab et al., 2008); (iii) point at 600 μm – Ø 25 μm Pt UME was held at a distance of 20 μm from yeast surface and electroporation, which was performed by applying 2.0 V for 2 min, what resulted in a formation of electroporated area with a diameter of 600 μm (This research).

active yeast cells. The results of electrochemical impedance spectroscopy showed that the charge transfer resistance at the interface between the Ø 25 μm Pt UME and the electrolyte increases irreversibly after the electroporation procedure, which indicates that the surface of the UME was blocked by proteins and membrane lipids detached from the plasma membrane during the electroporation. An electrical pulse of 2.0 V lasting for 120 s causes the disruption of the plasma membrane and results in irreversible electroporation of the yeast cells making the electroporated area with a diameter of approximately 500 μm. The diameter of the electroporated area is ~20 times larger than the diameter of the UME used for the electroporation. It can be concluded that the diameter of the electroporated area depends on both (i) the diameter of the UME applied for the electroporation and (ii) the distance between the UME and the surface.

CRediT authorship contribution statement

Margarita Poderyte: Methodology, Investigation, Formal analysis, Writing – original draft, Interpretation of data, Formal analysis. **Arunas Ramanavicius:** Interpretation of data, Formal analysis, Supervision, Conceptualization, Writing – review & editing, Funding acquisition. **Aušra Valiūnienė:** Methodology, Investigation, Formal analysis, Writing – original draft, Interpretation of data, Formal analysis.

Declaration of competing interest

The authors declare the following financial interests/personal relationships which may be considered as potential competing interests: Ramanavicius reports financial support was provided by Research Council of Lithuania.

Data availability

Data will be made available on request.

Acknowledgement

This project has received funding from the Research Council of Lithuania (LMTLT), agreement No [S-MIP-20-18].

References

Agnass, P., van Veldhuisen, E., van Gemert, M.J.C., van der Geld, C.W.M., van Lienden, K.P., van Gulik, T.M., Meijerink, M.R., Besselink, M.G., Kok, H.P., Crezee, J., 2020. Mathematical modeling of the thermal effects of irreversible electroporation for in vitro, in vivo, and clinical use: a systematic review. Int. J. Hyperther. https://doi.org/10.1080/02656736.2020.1753828.

Andersson Trojer, M., Brezesinski, G., 2016. Self-assembly of lipid domains in the extracellular leaflet of the plasma membrane and models thereof. Curr. Opin. Colloid Interface Sci. https://doi.org/10.1016/j.cocis.2016.03.001.

Baranski, A.S., Diakowski, P.M., 2004. Application of AC impedance techniques to scanning electrochemical microscopy. J. Solid State Electrochem. 8, 683–692. https://doi.org/10.1007/s10008-004-0533-x.

Batista Napotnik, T., Miklavčič, D., 2018. In vitro electroporation detection methods – an overview. Bioelectrochemistry. https://doi.org/10.1016/j.bioelechem.2017.12.005.

Bodénès, P., Bensalem, S., Français, O., Pareau, D., le Pioufle, B., Lopes, F., 2019. Inducing reversible or irreversible pores in Chlamydomonas reinhardtii with electroporation: impact of treatment parameters. Algal Res. 37, 124–132. https://doi.org/10.1016/j.algal.2018.11.016.

Cohen, E.I., Field, D., Lynskey, G.E., Kim, A.Y., 2018. Technology of irreversible electroporation and review of its clinical data on liver cancers. Expet Rev. Med. Dev. https://doi.org/10.1080/17434440.2018.1425612.

Danieli, T., Mandler, D., 2013. Local surface patterning by chitosan-stabilized gold nanoparticles using the direct mode of scanning electrochemical microscopy (SECM). J. Solid State Electrochem. 17, 2989–2997. https://doi.org/10.1007/s10008-013-2194-0.

Delemotte, L., Tarek, M., 2012. Molecular dynamics simulations of lipid membrane electroporation. J. Membr. Biol. 245, 531–543. https://doi.org/10.1007/s00232-012-9434-6.

Demiryurek, Y., Nickaeen, M., Zheng, M., Yu, M., Zahn, J.D., Shreiber, D.I., Lin, H., Shan, J.W., 2015. Transport, resealing, and re-poration dynamics of two-pulse electroporation-mediated molecular delivery. Biochim. Biophys. Acta Biomembr. 1848, 1706–1714. https://doi.org/10.1016/j.bbamem.2015.04.007.

Geboers, B., Scheffer, H.J., Graybill, P.M., Ruarus, A.H., Nieuwenhuizen, S., Puijk, R.S., van den Tol, P.M., Davalos, R.v., Rubinsky, B., de Gruijl, T.D., Miklavčič, D., Meijerink, M.R., 2020. High-voltage electrical pulses in oncology: irreversible electroporation, electrochemotherapy, gene electrotransfer, electrofusion, and electroimmunotherapy. Radiology. https://doi.org/10.1148/radiol.2020192190.

Gorter, B.E., Grendel, F., 1925, On bimolecular layers of lipoids on the chromo-cytes of the blood. J Exp Med.; 41(4): 439–443. oi: 10.1084/jem.41.4.439.

Grisotto, F., Ghorbal, A., Goyer, C., Charlier, J., Palacin, S., 2011. Direct SECM localized electrografting of vinylic monomers on a conducting substrate. Chem. Mater. 23, 1396–1405. https://doi.org/10.1021/cm101563n.

Izquierdo, J., Knittel, P., Kranz, C., 2018. Scanning electrochemical microscopy: an analytical perspective. Anal. Bioanal. Chem. https://doi.org/10.1007/s00216-017-0742-7.

Kotnik, T., Frey, W., Sack, M., Haberl Meglič, S., Peterka, M., Miklavčič, D., 2015. Electroporation-based applications in biotechnology. Trends Biotechnol. https://doi.org/10.1016/j.tibtech.2015.06.002.

Kotnik, T., Rems, L., Tarek, M., Miklavčič, D., 2019. Annual Review of Biophysics Membrane Electroporation and Electropermeabilization: Mechanisms and Models. https://doi.org/10.1146/annurev-biophys-052118.

Kwon, W., Thomas, A., Kluger, M.D., 2021. Irreversible electroporation of locally advanced pancreatic cancer. Semin. Oncol. https://doi.org/10.1053/j.seminoncol.2021.02.004.

le Roux, A.L., Quiroga, X., Walani, N., Arroyo, M., Roca-Cusachs, P., 2019. The Plasma Membrane as a Mechanochemical Transducer. Philosophical Transactions of the Royal Society B: Biological Sciences. https://doi.org/10.1098/rstb.2018.0221.

Lim, B., Kim, H.B., Jeong, S., Kim, S.H., Kang, J.M., Park, Y., Won, D.S., Kim, J.W., Ryu, D.S., Kim, Y., Park, J.H., Kim, C.S., 2021. Novel platinum bipolar electrode for irreversible electroporation in prostate cancer: preclinical study in the beagle prostate. Sci. Rep. 11 https://doi.org/10.1038/s41598-021-96734-5.

Marsh, D., 2016. Equation of state for phospholipid self-assembly. Biophys. J. 110, 188–196. https://doi.org/10.1016/j.bpj.2015.11.012.

Matrab, T., Combellas, C., Kanoufi, F., 2008. Scanning electrochemical microscopy for the direct patterning of a gold surface with organic moities derived from iodonium salt. Electrochem. Commun. 10, 1230–1234. https://doi.org/10.1016/j.elecom.2008.06.006.

Morkvenaite-Vilkonciene, I., Ramanaviciene, A., Ramanavicius, A., 2016. 9,10-Phenanthrenequinone as a redox mediator for the imaging of yeast cells by scanning electrochemical microscopy. Sens. Actuators, B 228, 200–206. https://doi.org/10.1016/j.snb.2015.12.102.

Morkvenaite-Vilkonciene, I., Ramanaviciene, A., Kisieliute, A., Bucinskas, V., Ramanavicius, A., 2019. Scanning electrochemical microscopy in the development of enzymatic sensors and Immunosensors. Biosens. Bioelectron. 141, 111411 https://doi.org/10.1016/j.bios.2019.111411.

Neumann, E., Rosenheck, K., 1972. Permeability changes induced by electric impulses in vesicular membranes. J. Membr. Biol.

Oswald, E., Palanisamy, K., Kranz, C., 2022. Nanoscale surface modification via scanning electrochemical probe microscopy. Current Opinion in Electrochemistry 100965. https://doi.org/10.1016/j.coelec.2022.100965.

Paiella, S., Butturini, G., Frigerio, I., Salvia, R., Armatura, G., Bacchion, M., Fontana, M., D'Onofrio, M., Martone, E., Bassi, C., 2015. Safety and feasibility of irreversible electroporation (IRE) in patients with locally advanced pancreatic cancer: results of a prospective study. Dig. Surg. 32, 90–97. https://doi.org/10.1159/000375323.

Paiella, S., Salvia, R., Ramera, M., Girelli, R., Frigerio, I., Giardino, A., Allegrini, V., Bassi, C., 2016. Local ablative strategies for ductal pancreatic cancer (radiofrequency ablation, irreversible electroporation): a review. Gastroenterology Research and Practice. https://doi.org/10.1155/2016/4508376.

Petroniene, J., Morkvenaite-Vilkonciene, I., Miksiunas, R., Bironaite, D., Ramanaviciene, A., Mikoliunaite, L., Kisieliute, A., Rucinskas, K., Janusauskas, V., Plikusiene, I., Labeit, S., Ramanavicius, A., 2020a. Evaluation of redox activity of human myocardium-derived mesenchymal stem cells by scanning electrochemical microscopy. Electroanalysis 32, 1337–1345. https://doi.org/10.1002/elan.201900723.

Petroniene, J., Morkvenaite-Vilkonciene, I., Miksiunas, R., Bironaite, D., Ramanaviciene, A., Rucinskas, K., Janusauskas, V., Ramanavicius, A., 2020b. Scanning electrochemical microscopy for the investigation of redox potential of human myocardium-derived mesenchymal stem cells grown at 2D and 3D conditions. Electrochim. Acta 360. https://doi.org/10.1016/j.electacta.2020.136956.

Poderyte, M., Valiūnienė, A., Ramanavicius, A., 2022. Scanning electrochemical microscope as a tool for the electroporation of living yeast cells. Biosens. Bioelectron. 205, 114096 https://doi.org/10.1016/j.bios.2022.114096.

Polcari, D., Dauphin-Ducharme, P., Mauzeroll, J., 2016. Scanning electrochemical microscopy: a comprehensive review of experimental parameters from 1989 to 2015. Chem. Rev. https://doi.org/10.1021/acs.chemrev.6b00067.

Ramanavicius, A., Morkvenaite-Vilkonciene, I., Kisieliute, A., Petroniene, J., Ramanaviciene, A., 2017. Scanning electrochemical microscopy based evaluation of influence of pH on bioelectrochemical activity of yeast cells – Saccharomyces cerevisiae. Colloids Surf. B Biointerfaces 149, 1–6. https://doi.org/10.1016/j.colsurfb.2016.09.039.

Randviir, E.P., Banks, C.E., 2013. Electrochemical impedance spectroscopy: an overview of bioanalytical applications. Anal. Methods. https://doi.org/10.1039/c3ay26476a.

Rems, L., Miklavčič, D., 2016. Tutorial: electroporation of cells in complex materials and tissue. J. Appl. Phys. 119 https://doi.org/10.1063/1.4949264.

Saini, A., Breen, I., Alzubaidi, S., Pershad, Y., Sheth, R., Naidu, S., Knuttinen, M.G., Albadawi, H., Oklu, R., 2019. Irreversible electroporation in liver cancers and whole organ engineering. J. Clin. Med. https://doi.org/10.3390/jcm8010022.

Saito, K., Minamitani, Y., Komatsu, Y., 2013. Investigation of selective sterilization of unnecessary microorganisms on pulsed electric field sterilization. In: Digest of Technical Papers-IEEE International Pulsed Power Conference. https://doi.org/10.1109/PPC.2013.6627486.

Suetsugu, S., Kurisu, S., Takenawa, T., 2014. Phospholipids and membrane-deforming proteins. Physiol. Rev. 94, 1219–1248. https://doi.org/10.1152/physrev.00040.2013.-All.

Szlasa, W., Kiełbik, A., Szewczyk, A., Rembiałkowska, N., Novickij, V., Tarek, M., Saczko, J., Kulbacka, J., 2020. Oxidative effects during irreversible electroporation of melanoma cells-in vitro study. Molecules 26. https://doi.org/10.3390/molecules26010154.

Thomson, K.R., Kavnoudias, H., Neal, R.E., 2015. Introduction to irreversible electroporation-principles and techniques. Tech. Vasc. Intervent. Radiol. 18, 128–134. https://doi.org/10.1053/j.tvir.2015.06.002.

Valiūnienė, A., Gabriunaite, I., Poderyte, M., Ramanavicius, A., 2020a. Electroporation of a hybrid bilayer membrane by scanning electrochemical microscope. Bioelectrochemistry 136. https://doi.org/10.1016/j.bioelechem.2020.107617.

Valiūnienė, A., Petronienė, J., Dulkys, M., Ramanavičius, A., 2020b. Investigation of active and inactivated yeast cells by scanning electrochemical impedance microscopy. Electroanalysis 32, 367–374. https://doi.org/10.1002/elan.201900414.

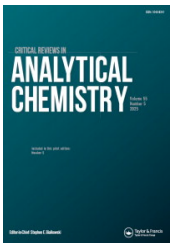
Vaske, B., Schaube, M., Meiners, F., Ross, J.H., Christoffers, J., Wittstock, G., 2021. Modification and patterning of self-assembled monolayers using electrogenerated etchants and homogeneous scavenging reactions in a scanning electrochemical microscope. Chemelectrochem 8, 3192–3202. https://doi.org/10.1002/celc.202100718.

Venslauskas, M.S., Šatkauskas, S., 2015. Mechanisms of transfer of bioactive molecules through the cell membrane by electroporation. Eur. Biophys. J. https://doi.org/10.1007/s00249-015-1025-x.

Vižintin, A., Vidmar, J., Ščančar, J., Miklavčič, D., 2020. Effect of interphase and interpulse delay in high-frequency irreversible electroporation pulses on cell survival, membrane permeabilization and electrode material release. Bioelectrochemistry 134. https://doi.org/10.1016/j.bioelechem.2020.107523.

Wagstaff, P.G.K., Buijs, M., van den Bos, W., de Bruin, D.M., Zondervan, P.J., de la Rosette, J.J.M.C.H., Laguna Pes, M.P., 2016. Irreversible Electroporation: State of the Art. OncoTargets and Therapy. https://doi.org/10.2147/OTT.S88086.

Zoski, C.G., 2016. Review—advances in scanning electrochemical microscopy (SECM). J. Electrochem. Soc. 163, H3088–H3100. https://doi.org/10.1149/2.0141604jes.



Critical Reviews in Analytical Chemistry

ISSN: 1040-8347 (Print) 1547-6510 (Online) Journal homepage: www.tandfonline.com/journals/batc20

Exploring the Living Cell: Applications and Advances of Scanning Electrochemical Microscopy

Margarita Poderyte, Arunas Ramanavicius & Aušra Valiūnienė

To cite this article: Margarita Poderyte, Arunas Ramanavicius & Aušra Valiūnienė (2025) Exploring the Living Cell: Applications and Advances of Scanning Electrochemical Microscopy, Critical Reviews in Analytical Chemistry, 55:5, 956-967, DOI: 10.1080/10408347.2024.2328135

To link to this article: https://doi.org/10.1080/10408347.2024.2328135

Published online: 01 Apr 2024.

Submit your article to this journal

Article views: 588

View related articles

Citing articles: 1 View citing articles

Full Terms & Conditions of access and use can be found at
https://www.tandfonline.com/action/journalInformation?journalCode=batc20

CRITICAL REVIEWS IN ANALYTICAL CHEMISTRY
2025, VOL. 55, NO. 5, 956–967
https://doi.org/10.1080/10408347.2024.2328135

Taylor & Francis
Taylor & Francis Group

Check for updates

Exploring the Living Cell: Applications and Advances of Scanning Electrochemical Microscopy

Margarita Poderyte[a], Arunas Ramanavicius[a,b], and Aušra Valiūnienė[a,c]

[a]Faculty of Chemistry and Geosciences, Institute of Chemistry, Vilnius University, Vilnius, Lithuania; [b]Laboratory of Nanotechnology, State Research Institute Centre of Physical Sciences and Technology, Vilnius, Lithuania; [c]State Research Institute Center for Physical Sciences and Technology, Vilnius, Lithuania

ABSTRACT

A living cell is a complex network of molecular, biochemical and physiological processes. Cellular activities, such as ion transport, metabolic processes, and cell-cell interactions can be determined electrochemically by detecting the electrons or ions exchanged in these processes. Electrochemical methods often are noninvasive, and they can enable the real-time monitoring of cellular processes. Scanning electrochemical microscopy (SECM) is an advanced scanning probe electroanalysis technique that can map the surface topography and local reactivity of a substrate with high precision at the micro- or nanoscale. By measuring electrochemical signals, such as redox reactions, ion fluxes, and pH changes, SECM can provide valuable insights into cellular activity. As a result of its compatibility with liquid medium measurements and its nondestructive nature, SECM has gained popularity in living cell research. This review aims to furnish an overview of SECM, elucidating its principles, applications, and its potential to contribute significantly to advancements in cell biology, electroporation, and biosensors. As a multidisciplinary tool, SECM is distinguished by its ability to unravel the intricacies of living cells and offers promising avenues for breakthroughs in our understanding of cellular complexity.

KEYWORDS

Living cell; electroporation; biosensors; electrochemical impedance spectroscopy; scanning electrochemical microscopy

Introduction

Living cells are highly complex systems. They are dynamic units of all living organisms based on complicated biochemical processes that enable them to perform essential functions. Understanding the complexity of living cells requires a multidisciplinary approach, such us fluorescence, spectrophotometry, chromatography, microscopy or electrochemistry.[1] Electrochemical analysis has been the preferred method for identifying cellular differences for decades due to its high sensitivity, good resolution, and ease of use.

One of the powerful electrochemical tools is scanning electrochemical microscopy (SECM) that enables detailed measurements at the micro- and nano- scales.[2,3] This technique combines the principles of scanning probe microscopy and electrochemistry. It uses a three electrode system where the working electrode (WE) is used as a probe to detect electrochemical processes at the surface of a sample, including living cells. Since the 1980s, when Bard's group established scanning electrochemical microscopy,[4] it has gained much attention in the scientific community. The fundamental origins of SECM can be traced back to scanning tunneling microscopy (STM),[5] however, it has a unique capability to probe the diffusion layer on an electrode surface, enabled by the use of an ultramicroelectrode (UME) with a diameter typically less than 25 μm. When the UME tip scans the immersed substrate, it records the resulting Faradic current response. By analyzing the changes in this current response, valuable information regarding the substrate's properties and characteristics can be obtained.[6] For instance, ultramicroelectrode can be positioned near the cell to measure various electrochemical signals, such as redox reactions, ion fluxes, or pH changes, providing valuable information about cellular activities and processes.[7,8]

SECM ability to scan the surface of a substrate works as a tool for quantifying local species concentrations and high-resolution imaging of surface topography in liquid environments.[9] SECM has found applications in diverse research fields such as biology,[10] corrosion,[11] kinetics,[12] and surface modification.[13] Particularly in the study of biological systems or their models, SECM is gaining popularity due to two main reasons: SECM measurements are conducted in a liquid medium, allowing for easy compatibility with biologically relevant conditions using physiological pH buffers and investigations often involve bringing the electrode close to the surface without physically touching or damaging it.[10,14] SECM offers four main measurement modes: feedback mode (FB), generation/collection (G/C) mode, direct mode, and constant height (surface scan) measurements.[15]

In feedback mode, which is one of the earliest and most informative methods, the UME moves vertically (z-axis) to the sample. The Faradic current dependence on the distance

CONTACT Aušra Valiūnienė ausra.valiuniene@chf.vu.lt Faculty of Chemistry and Geosciences, Institute of Chemistry, Vilnius University, Naugardukas str. 24, LT-03225 Vilnius, Lithuania

© 2024 Taylor & Francis Group, LLC

above the sample is recorded, enabling the determination of the substrate's conductivity. As the electrode moves away from the surface, uninterrupted diffusion occurs, and the current stabilizes. When the electrode approaches an insulating substrate, the diffusion of the redox species is physically blocked, resulting in a decrease of current. However, if the specimen surface is conductive, the diffusion of electroactive species toward the electrode is further sterically blocked, but the conductive surface oxidizes the reduced particles (or vice versa), leading to an increased flow of oxidizing particles toward the electrode. Reaching a substrate with the UME may result in a complete blockage of the electrode and then a drop to zero current or a sharp current jump is observed depending on weather substrate is insulating or conducting.[16–19]

The generation/collection (G/C) mode is another important operating principle of SECM, commonly used for kinetic parameter measurements or analytical detections. In this mode, the UME detects the current generated by reaction products. Unlike the feedback mode, the particles involved in the reduction or oxidation reactions are not in solution but are generated in the active region of the substrate and detected by the electrode, or vice versa. This mode can be classified as substrate generation/tip collection (SG/TC) or tip generation/substrate collection (TG/SC).[20,21]

The direct mode is a specific SECM method in which the UME serves as an auxiliary electrode while the substrate in the cell is functioning as the working electrode. Applying a specific potential creates a localized electric field between the probe and the substrate. This method is useful to perform modifications on the substrate, such as etching conductors or semiconductors, enzyme deposition, or micropatterning.[22,23]

Surface scan involves maintaining a constant UME height above the substrate while scanning it in the x- and y-coordinates at equal distances from the surface.[22,24] The resulting current response fluctuates due to surface irregularities or structures immobilized on the surface. The surface scan provides topographical data and an electrochemical map of the surface, facilitating the determination of the local surface activity of the analyte or the detection of defects.[22,25,26] The scan resolution depends on the tip-to-sample distance, and it is recommended to keep the distance between the analyte and the probe below the electrode diameter. However, when ultra-small electrodes are used for high-resolution imaging the risk of electrode breakage increases when scanning of uneven surfaces is performed. To overcome this challenge, methods such as integration of shear force have been developed. This technique equips the nanoelectrode with two piezo crystals, allowing for controlled vibration of the nanoelectrode tip. Near-surface shear forces cause amplitude and phase shifts, which are detected by the receiver, enabling nanometer-scale distance control without interfering with electrochemical experiments.[2,8]

SECM can also be combined with other techniques such as atomic force microscopy (AFM) and electrochemical impedance spectroscopy (EIS). The integration of SECM with AFM allows simultaneous topographical and electrochemical measurements, providing a more comprehensive understanding of the sample's properties.[27] The combination of SECM with electrochemical impedance spectroscopy enables measurements at specific locations on the analyte surface over a wide frequency range, resulting in a more accurate description of the electrochemical system and its processes. The permutation of these two techniques is known as scanning electrochemical impedance microscopy (SEIM). By performing SECM scans followed by impedance measurements at selected points on the surface, the appropriate equivalent circuit can be applied to calculate the parameters of the electrochemical system, which can be plotted in spatial coordinates.[28–30]

This review article focusses on diverse applications of scanning electrochemical microscopy in the study of living cells, covering key areas such as cellular imaging, cellular processes, drug uptake and release, cell-cell interactions, cell-based biosensors, electroporation, the integration of SECM with EIS, and future perspectives. The increasing volume of publications reflects SECM's growing research relevance. This review will also focus on new developments in electrical stimulation on cells, particularly relevant to medical applications, underlining the growing significance and potential of SECM in cell biology research and future technological innovations. It aims to fill gaps in current knowledge, offering an up-to-date and broad perspective on SECM's applications and future perspectives in cell biological research.

Discussion

SECM in living cell imaging

Scanning electrochemical microscopy has gained significant importance in the study of biological systems due to its unique capabilities and compatibility with liquid environments. When used to image living cells, SECM measures electrical currents resulting from chemical reactions near the UME tip, which is placed close to the biological sample.[18] When the tip moves across the cell's surface, it either collects or supplies electrons to the specimen, creating a map of local electrochemical activity. SECM technique is offering high resolution, can detect changes in cell surface activity, ion movements, and metabolic processes. Therefore, SECM provides a non-optical method to study the dynamic biochemical processes in living cells, offering high-resolution single cell imaging.[8,18,22,26]

In a study led by Kuniaki Nagamine and his team, the influence of tip reactions on the imaging of single yeast cells was investigated using the substrate generation and/or tip collection mode of SECM. Their study involved probe electrodes of various sizes in the micro- to nano-meter range. The motivation behind this research was to address concerns that tip reactions might disturb the concentration of intracellular enzyme reactants around the yeast cell. To address this challenge, the researchers conducted generation/collection mode measurements on single yeast cells, employing a dual mediator system comprising lipophilic menadione and hydrophilic ferricyanide. Their findings revealed that

reducing the tip size enabled quantitative SECM imaging of individual cells in GC mode while preserving the concentration profile of the mediator around the cell, minimizing disruptions caused by tip reactions.[31]

In another study, researchers introduced an innovative approach to address cellular heterogeneity and the limitations of label-based single-cell analysis. They combined programmable scanning electrochemical microscopy (P-SECM) with an addressable microwell array (Figure 1), significantly reducing the time needed for analysis. This method allowed for the rapid assessment of alkaline phosphatase (ALP) activity in 82 single cells, revealing higher ALP activity in cancer cells and a diverse distribution of ALP kinetics. This platform shows promise as a high-content, label-free single-cell analysis tool for large-scale applications.[32]

SECM for the study of cellular processes

To understand the complexities of cell metabolism and respiration, SECM has become an indispensable tool. Through its high-resolution and label-free approach, SECM can map electrochemical gradients directly on cell surfaces, providing insights into metabolic and respiratory processes in real time. SECM enables to track the consumption or production of electroactive substances like oxygen and hydrogen peroxide locally, as a result mapping hindered or facilitated metabolic or respiratory active regions. It provides crucial information about how cells process energy, how their mitochondria work[33–36], how they respond to different signals[8] – all-important aspects for understanding healthy and functioning cell activity.

Wolfgang Schuhmann and his group discuss the significance of detecting cellular respiratory activity and highlight the potential of SECM for single-cell measurements. The authors address common limitations in SECM-based respiration studies and propose a combination of potential pulse techniques in the redox competition mode of the SECM with shear force-based constant-distance positioning for the effective visualization of cell respiration activity.[37] While Tomokazu Matsue in their work presents the use of SECM to monitor the respiratory activities of cultured HeLa cells at the single-cell level. It compares SECM-based measurements with conventional fluorescence monitoring using Calcein-AM and demonstrates that SECM allows a more rapid detection of changes in cellular activity in response to respiration inhibitors like KCN and Antimycin A. This highlights the suitability of SECM for studying the cellular effects of such inhibitors.[38]

A study demonstrated the monitoring of ferroptosis, which is a form of cell death triggered by the buildup of damaging lipid peroxides due to iron imbalance, during the early stages in single living cancer cells using scanning electrochemical microscopy (SECM). This research focused on the investigation of HuH7 cells as a hepatocellular carcinoma model and Erastin as a ferroptosis inducer (Figure 2).

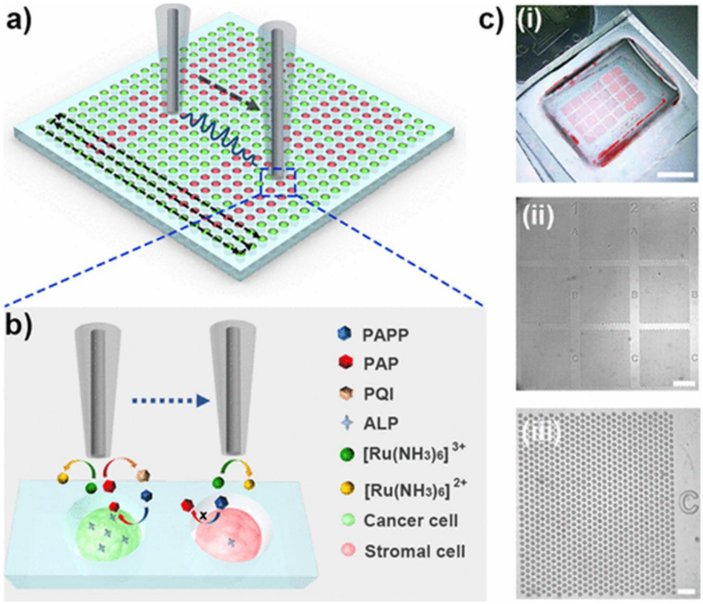


Figure 1. (a) A diagram showing extensive analysis of individual cells using a high-capacity microfluidic device that operates with programmable scanning electrochemical microscopy (P-SECM). (b) Evaluation of Alkaline Phosphatase (ALP) activity in individual cancer and stromal cells employing a dual-mediator mode in Variable Scan Mode (VSM)-SECM. (c) A microfluidic device designed for single-cell capture. (i) An image of the configurable microwell array filled with water-soluble dyes and topped with light mineral oil, featuring 24 sections (4 × 6) across an area of 1.7 cm^2 (scale bar: 0.5 cm). (ii) A zoomed-in view of a portion showing six sections (3 × 3) (scale bar: 500 μm). (iii) A close-up micrograph of a single section (scale bar: 100 μm).[32]

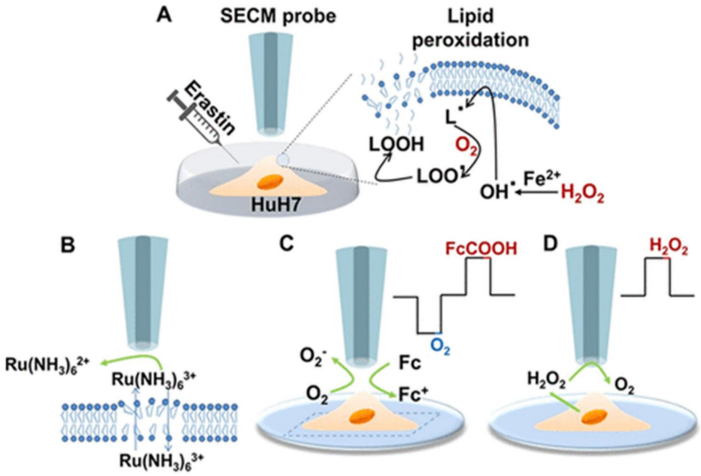


Figure 2. (A) A schematic representation of utilizing SECM for the in-situ analysis of the ferroptosis process in a single HuH7 cell treated with Erastin. (B) The use of SECM to track changes in membrane permeability of the HuH7 cell, employing $[Ru(NH_3)_6]^{3+}$ as the redox mediator. The schematic outlines the use of SECM with a programmable pulse potential mode for monitoring (C) the oxygen consumption and cellular topography, and (D) the H_2O_2 levels in a single HuH7 cell, using Ferocene carboxylic acid (FcCOOH), oxygen, and H_2O_2 as redox mediators within the SECM setup.[39]

SECM enabled the tracking of changes in cell membrane permeability, respiratory activity, and the determination of H_2O_2 levels. These findings unveiled insights into the initial stages of ferroptosis, demonstrating cell membrane structure degradation and increased oxidative stress. This work represents a significant advancement in the understanding of ferroptosis mechanisms, offering potential therapeutic insights for cancer treatment.[39]

Zhao Y et al. used UME probes to measure some metabolic activities of living cells, focucing mainly on the assessment of respiration rates, which is an important physiological parameter. These researchers faced sensitivity challenges in reported measurements, particularly in comparing cellular and UME fluxes and ensuring UME response stability over time. To address these issues, systematic analysis using scanning electrochemical microscopy with a platinum-based UME probe was conducted. A self-referencing measurement approach, a rarely used SECM technique, allowed periodic tracking of bulk UME responses while minimizing the impact of electrochemical processes on the cell. Through a combination of finite element method (FEM) modeling and SECM experiments, it was determined that the technique's current detection sensitivity is at or below the range of single-cell oxygen consumption rates (OCR) they investigated (1×10^{-18} to 1×10^{-16} mol s^{-1}). They suggest potential improvements for future measurements but stress the need for substantial enhancements in SECM stability and precision to achieve accurate single-cell OCR measurements.[40]

SECM for the study of drug uptake and release in cells

The ability of SECM to operate in conditions resembling the environment of a body makes it an impactful technology for studying drug behavior. It is possible to monitor the process of drugs (or their by-products) uptake and release in real-time. SECM's label-free approach ensures that the natural state of a cell remains unchanged during these investigations, offering insights into how cells respond to medications. Overall, SECM provides unmatched insights into drug dynamics, improving targeted therapies.

4-aminopyridine (4-AP) was explored as a blocker of voltage-sensitive potassium ion channels that affects silver ion (Ag^+) uptake in bacterial and mammalian cells. For this purpose, scanning electrochemical microscope with an Ag^+ ion-selective electrode was used for monitoring Ag^+ uptake and measurement of cell respiration rates. The results revealed that 4-AP significantly increased the quantity and rate of silver uptake, suggesting its potential application in enhancing silver's antimicrobial properties.[41]

In addition, some researchers assessed a multi-drug resistance (MDR) of cancer cells, which is a great challenge in chemotherapy. Researchers measured the activity of multidrug resistance-associated protein 1 (MRP1) at the single-cell level using SECM. Findings showed that MRP1 activity increases when cells adapt to specifically formed 'adhesive islands', offering a 30-minute measurement window. SECM imaging and MATLAB analysis provided insights into MDR mechanisms, particularly MRP1's role, as a robust indicator of cancer cell response to chemotherapy.[42]

In research led by Mauro Bertotti, a potentiometric microsensor for real-time pH monitoring induced by caffeine was developed using scanning electrochemical microscopy (SECM). The sensor, crafted through electrodeposition of an iridium oxide film on a dual-sensor with gold (Au) and platinum (Pt) microelectrodes, demonstrated a super Nernstian response. It accurately tracked pH changes induced by caffeine-induced metabolic shifts in the cells,

observing a notable decrease in pH. This emphasizes the localized nature of pH changes in biological systems, addressing challenges in in-vivo pH monitoring for understanding physiological phenomena such as muscle fatigue. The findings indicate that caffeine stimulates acidosis in C2C12 cells, with the dual SECM microsensor providing reliable monitoring of this process, which was observed within a few micrometers from the cell surface.[43]

SECM for the study of cell-cell interactions

Similar to drug uptake/release, SECM allows real-time tracking of the release and uptake of signalling molecules used in cell communication. These molecules, like neurotransmitters and ions, help cells synchronize their activities during vital processes. By capturing these processes, SECM enables researchers to understand how molecules mediate cell-cell interactions, real-time observation of the electroactive species involved in transport across cell junctions, the dynamics of molecular fluxes that sustain cellular coordination and homeostasis.[44] Operating in a natural environment ensures accurate observations, providing deep insights into the cell communication during various phases of cell development.[45,46]

In one of cell-cell interaction research a multifunctional dual-channel scanning probe nanopipet that combines scanning ion conductance microscopy (SICM) and SECM for mapping molecule uptake at living cells was introduced (Figure 3). One channel of the nanopipet is used for topographical feedback and local delivery of molecules of interest, while the other employs a solid carbon electrode to measure local concentration and flux. This setup enables precise differentiation of molecule uptake rates across various regions of single cells with nanoscale resolution and employs a "hopping mode" for self-referencing, critical for measurements in dynamic living systems. The versatility and quantitative capabilities of this technique offer potential applications in drug delivery, cytotoxicity screening, electrocatalysis, and various microscopy studies, making it a valuable addition to scanning electrochemical probe techniques.[47]

Another study that employs a combination of SECM and scanning ion-conductance microscopy (SICM) was developed to investigate cell-membrane permeability and ionic strength at nanoscale resolution. By using an ion current feedback system, the study effectively controls the probe-sample distance without physical contact, enabling the measurement of 3D chemical concentrations and the evaluation of chemical fluxes. This approach offers new possibilities for visualizing inhomogeneous chemical distribution and permeability on single cells, making it relevant for applications such as studying neurotransmitter concentration profiles and cell respiration activity. Additionally, it highlights the importance of electrode-sample distance control for improving SECM resolution and its potential in non-contact investigations of soft materials.[48]

SECM was also applied to investigate the complex relationship between calcium concentrations in osteoclasts and their resorptive activity. The researchers measured calcium release and found that osteoclasts are effective at removing calcium,

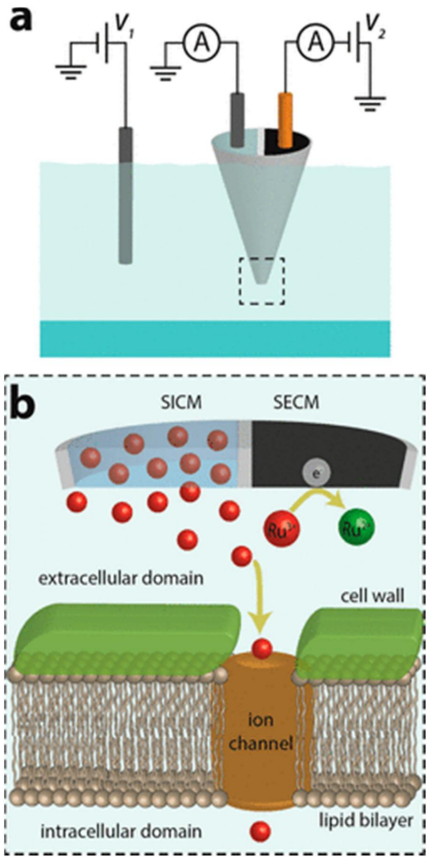


Figure 3. The experimental configuration of SICM-SECM for exploring cellular uptake: (a) A setup where current is measured between two Ag/AgCl Quasi-Reference Counter Electrodes (QRCEs) - one located in the bulk solution and another within the probe's open channel, employing a bias voltage, V1, for generating topographical feedback in a SICM setup. Additionally, a carbon electrode, operating at a bias of V2 - V1, is utilized for assessing the local concentration of specific species. (b) A diagram illustrating the movement of $[Ru(NH_3)_6]^{3+}$ from the SICM barrel to the area close to the cell. The current resulting from the reduction of $[Ru(NH_3)_6]^{3+}$ in the SECM channel is tracked as the probe nears the cell surface and is compared to the constant bulk current to evaluate uptake rates.[47]

maintaining low calcium levels in the immediate extracellular environment above the cell. Interestingly, they observed that an increase in intracellular calcium ($[Ca^{2+}]i$) could have various effects on osteoclast functions, indicating functional compartmentalization within the osteoclast that allows it to adapt and to maintain its resorptive activity even when exposed to elevated calcium levels within resorptive lacunae.[49]

Advanced electrochemical analysis of cell activity using SECM

SECM electrochemical capabilities can be enhanced by pairing it with electrochemical impedance spectroscopy (EIS).

SECM involves scanning a microelectrode across the surface of a sample, monitoring its electrochemical response at each point. When SECM is combined with EIS, it becomes possible to measure the local impedance of the sample at each scanning point, offering deeper insights into its electrochemical features. EIS works by applying a small alternating current to the sample and measuring the resulting voltage. This allows for the calculation of impedance, indicating how resistant the sample is to the current flow. The combination of SECM and EIS yields valuable information about a sample's local electrochemical and electrical properties, including changes in impedance as the SECM probe scans across it.[50–52]

One of the examples of scanning electrochemical impedance microscopy (SEIM), is research that explores a biointerface involving immobilized glucose oxidase (GOx). The study evaluates the production of gluconic acid during the enzymatic oxidation of glucose, focusing on its impact on the impedance of the solution near the ultramicroelectrode (UME) surface. The results demonstrate the potential of SEIM as a valuable tool for characterizing enzyme-modified surfaces in biosensors and biofuel cells, providing real-time insights into the behavior of these systems during operation.[53]

A novel technique called "fast Fourier transform - scanning electrochemical impedance microscopy (FFT-SEIM)," which combines SECM and fast Fourier transform - electrochemical impedance spectroscopy (FFT-EIS) was designed for evaluating and treating complex electrochemical systems, particularly in the context of biomedical research focused on identifying and treating unhealthy tissues at the cellular level. The study demonstrates that this technique can operate without the need of additional harmful redox probes and provides insights into improving the quality of FFT-SEIM signal acquisition. In particular, the use of extreme cathodic potential (−1.2 V vs. $Ag/AgCl/KCl_{sat}$) is highlighted to initiate Faradaic processes while avoiding the extensive formation of hydrogen bubbles. The research envisions that FFT-SEIM can be applied to investigate electrochemical activity in living cells, including the activity of redox enzymes and membrane permeability. Future developments aim to enhance synchronization between FFT-EIS and SECM equipment and to eliminate the "preconditioning" step during the mapping of cells.[54]

Another example of FFT-SEIM research offers the potential for investigation and treatment of tissues at the single-cell level. A key advancement is the development of a redox-probe-free FFT-SEIM, which enables the evaluation of conducting and non-conducting surfaces without the use of harmful redox mediators, making this method suitable for chemically sensitive samples such as tissues and living cells. The technique's ability to rapidly perform FFT-EIS experiments (in a few seconds) in the absence of redox probes holds great promise for various applications in bioelectrochemistry, biotechnology, and cell biology.[29]

Scanning electrochemical impedance microscopy was applied to investigate the electrochemical activity of active and inactivated yeast Saccharomyces cerevisiae cells. Electrochemical impedance spectrometer with a fast Fourier transform function (FFT-EIS) was employed in these SEIM-based experiments, enabling rapid observation of impedance spectra differences at various distances between the UME and yeast cell surfaces. The results indicated that electrochemical activity and oxygen consumption by yeast cells can be observed within a range of 0 μm to 25 μm, making 25 μm the maximum suitable distance for efficient investigation of yeast cell activity in FFT-SEIM mode. The studies also explored the redox efficiency of vitamin K1 and vitamin K3 as redox mediators, revealing faster redox efficiency when yeast cells were pretreated with these vitamins. Future research aims to apply FFT-SEIM for the evaluation of mammalian stem cells and tissues.[52]

SECM for the study of the effects of electrical stimulation on cells

SECM is primarily used as a noninvasive imaging and sensing technique, where the electrochemical probe tip scans over the surface of the cell or tissue sample to obtain spatially resolved chemical information. In contrast, electroporation involves the application of a high-voltage electric pulse to cells in order to temporarily disrupt their membranes and allow for the introduction of foreign molecules. SECM could potentially be used to monitor the effects of electroporation on cells, as it has been shown to track changes in the local redox environment or the release of electroactive species.[41,47–49] In addition, SECM could potentially be applied for electroporation to deliver electroactive species, such as redox mediators, directly to cells or tissues.[55]

One of the most noteworthy studies used SECM to investigate changes in HeLa cell morphology, membrane permeability, and viability induced by Triton X-100 (TX100), a non-ionic surfactant. It was found that membrane permeability, specifically for hydrophilic molecules like ferrocyanide, started at TX100 concentrations around 0.17 mM without affecting cell viability. The critical micelle concentration (CMC) of TX100 (around 0.19 to 0.20 mM) led to irreversible permeabilization of the cell membrane and structural collapse. SECM was instrumental in quantifying cell membrane permeability, with permeability estimated to be $6.5 \pm 2.0 \times 10^{-6}$ m^2/s at 0.17 mM TX100 for 32 min, demonstrating the potential of SECM for real-time tracking of electroporation processes and assessing cell viability and membrane permeability at the single-cell level.[56]

Despite the fact that SECM is a non-invasive technique, it has been demonstrated recently that it can be applied to the electroporation process and it's investigation. Our research team has introduced a groundbreaking approach to targeted electroporation of hybrid bilayer membranes (hBLMs) using SECM in a redox-probe-free system.[51] We have formed hBLMs on a glass substrate modified by fluorine-doped tin oxide and employed SECM to characterize and electroporate these membranes. A unique "constant-current region" at 1–30 µm distances between the ultramicroelectrode and the hBLM surface was identified, this region served as a distinctive feature for hBLM characterization (Figure 4). Depending on the applied potential-pulse

duration and UME-to-hBLM distance, the research achieved both irreversible and reversible electroporation of the hBLM. This pioneering work demonstrates the potential of SECM for electroporation studies and provides valuable insights into the phenomenon.[57]

The researchers also adapted SECM for the electroporation of living yeast cells, achieving reversible electroporation using low-voltage pulses (1–2 V vs. Ag/AgCl, Cl^-_{sat}) applied to a gold-based ultramicroelectrode (ø 10 µm Au-UME) on a fluorine-doped tin oxide (FTO)/glass surface (Figure 5). The combination of SECM and EIS allowed the quantification of electrochemical changes induced by the electroporation of yeast cells. Notably, the diameter of the affected area caused by the electrical pulse was approximately 25 times larger than the Au-UME's diameter, showcasing the potential for developing a targeted electroporation system for selective treatment of tissues and sensitive biological systems. This research opens new avenues for biomedical applications, including controlled drug delivery and selective cancer cell treatment.[55]

Another study focused on irreversible electroporation of active yeast cells, resulting in cell death at relatively low UME voltage, specifically 2.0 V vs. Ag/AgCl, Cl^-_{sat} (Figure 6). Notably, the electroporated area beneath the UME was approximately 20 times larger than the diameter of the UME, sparing surrounding cells from damage. SECM's precision in moving the UME and its potential to create targeted electroporation systems hold promise for selective tissue treatment, particularly in cancer therapy.[58]

While scanning electrochemical microscopy has great potential for electroporation and it's studies, it can also be used to study other effects of electrical stimulation on cells,

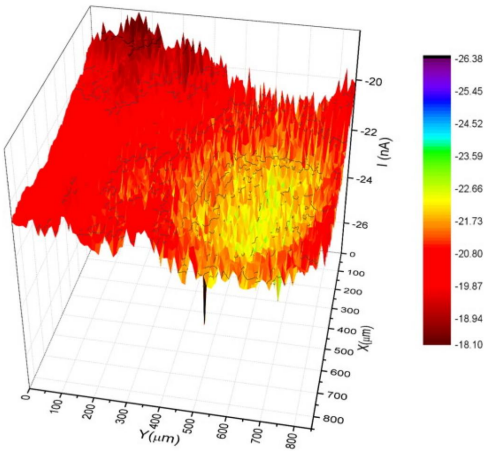


Figure 4. A glass/FTO/hBLM surface SECM topographical image captured following irreversible electroporation. Electroporation process involved applying 1 V between the Ultra-Microelectrode (UME) and a saturated Ag/AgCl reference electrode for 2 min, with the UME maintained at a 5 µm distance from the membrane surface. The image was recorded using a constant height mode, under the following conditions: a translation speed of 10 µm per second, a step size of 10 µm, a height setting of 40 µm, and a bias potential set at −0.75 V against a saturated Ag/AgCl electrode.[57]

such as tissue function[59,60], pH changes[61,62], stimulation.[60,63] An *in vitro* cardiac tissue model was developed on polyacrylamide gels, with pulsatile electrical fields applied to aid tissue maturation, which, similar to electroporation, involves the use of electrical stimuli to influence and modify cellular behavior and properties.[59] This model used a SECM setup with programmable pulse potentials to monitor key parameters such as respiratory activity, contraction frequency, and extracellular H_2O_2 levels in real time. These parameters were observed under normal conditions and with drugs such as isoproterenol and propranolol, with SECM detecting significant changes in these metrics, reflecting the metabolic and electrophysiological effects on cardiac tissues.[59] Additionally, another study used SECM to explore the impact of electric stimulation on cardiac tissue, demonstrating that oxygen consumption, cell membrane permeability, and contraction frequency are significantly affected by electrical energy. A thermal–electric model was devised to simulate electric field and temperature distributions, aiming to identify electric stimulation parameters that prevent thermal damage. Together, these studies offer valuable insights for advancing cardiac tissue engineering and refining electrotherapy practices.[59,60]

In pH measurements, studies have been conducted using dual UME in SECM to monitor extracellular pH changes in cells under electrical stimulation. One study developed a potentiometric SECM dual-microelectrode to observe pH variations in MCF-7 cells, employing a gold microelectrode to determine the electrode-cell distance and a polyaniline-modified Pt microelectrode for pH measurement. Similarly to electroporation studies,[55,58] this method demonstrated that pH decreased with increasing proximity to the cells and with increasing stimulation potential or duration, indicating increased cell membrane permeability.[61] These studies highlight SECM's effectiveness in exploring cell responses to environmental stimulation, particularly through changes in cell membrane permeability.[55,58–63]

Development of cell-based biosensors using SECM

SECM is widely used in the development of biosensors and bioanalytical assays. It can be integrated with functionalized microelectrodes or enzyme-modified electrodes to detect specific analytes or biomarkers, enabling applications in areas such as diagnostics, environmental monitoring, and biotechnology.[64] The technique provides real-time feedback on the performance of enzymatic reactions, antigen-antibody interactions, or DNA hybridization events on electrode surfaces, which are central to many biosensing modalities.[65] In addition, SECM can measure local redox activity and even image different surface details, which helps to assess the surface of microbe-modified structures and to improve the performance of biosensors. The detailed information provided by SECM, along with their ability to be applied in conditions similar to those, which are determined in the body, has been the most important in developing and testing new, high-precision biosensors and bioanalysis methods.[66,67]

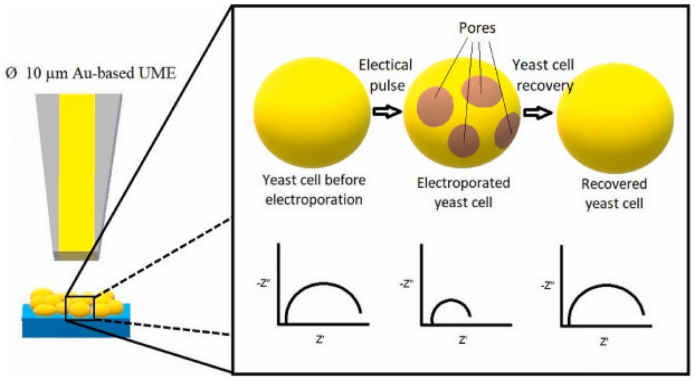


Figure 5. The potential outcomes of the yeast cell electroporation process visualization. The electroporation was performed with 10 µm diameter gold ultramicroelectrode while precisely positioning the electrode right above the surface of unpolarized yeast cells, maintaining a distance of 20 µm.[58]

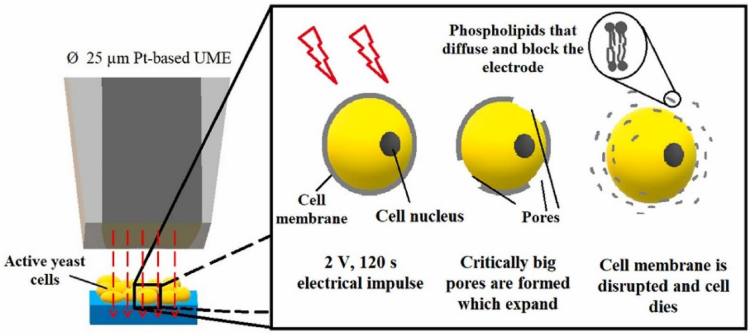


Figure 6. The potential outcomes of the electroporation process visualization by applying a voltage of 2.0 V for 120 s to a 25 µm diameter Ultra-Microelectrode (UME) while the electrode is strategically placed 20 µm above the surface of active yeast cells.[59]

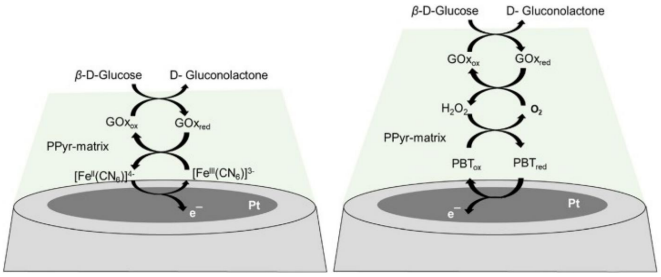


Figure 7. A schematic depiction illustrating the proposed reactions that occur in the detection of glucose using a micro-biosensor based on PPyr-GOx-PBT (polypyrrole-Glucose Oxidase-Polybenzothiophene).[70]

One of the research projects in this area presents a significant advance in the field of real-time *in situ* monitoring of nitric oxide (NO) in single cells using SECM. A novel SECM probe was designed with a platinum single nanoparticle (Pt NP) interface, enhanced by fluorinated self-assembled monolayers, resulting in high sensitivity (164.7 μA/μM cm^2) and excellent selectivity for NO detection. This modified probe successfully detected fluctuations in NO released by a single MCF-7 cell stimulated with cadmium (Cd), demonstrating its potential for SECM applications in single-cell analysis and providing insights into the design of ultramicro-interfaces, which are applied for future cellular studies.[68]

Quantitative determination of extracellular H_2O_2 released from individual COS-7 cells with high spatial resolution using scanning electrochemical microscopy was also

introduced. By employing depth scan imaging in the vertical x-z plane, the researchers obtained probe approach curves (PACs) at different positions on the cell membrane, allowing for the determination of H_2O_2 concentration at the membrane surface. Additionally, confocal microscopy was used to demonstrate intracellular H_2O_2 profiles. These complementary techniques shed light on H_2O_2 generation centered at the endoplasmic reticula and offer valuable insights into the assessment of physiological activity of single living cells.[69]

The development and application of a novel glucose micro-biosensor capable of reliable operation under hypoxic conditions, addressing a significant challenge in monitoring tumor metabolic activity is still highly relevant. The micro-biosensor, fabricated through a one-step synthesis, demonstrated improved sensitivity for glucose detection in hypoxic environments compared to normoxic conditions. When used in scanning electrochemical microscopy (Figure 7), the micro-biosensor successfully measured glucose uptake by breast metastatic adenocarcinoma cells, providing valuable insights into the glycolytic activity of single cancer cells under hypoxic conditions, which is relevant for tumor prognosis and cancer treatment strategy.[70]

Another SECM based biosensor research focuses on the development of miniaturized enzymatic biosensors for *in vitro* diagnostic applications, particularly for monitoring metabolites at the single-cell level. Glucose and lactate biosensors were created by immobilizing enzymes on 10 μm Pt ultramicroelectrodes, intending to use them as probes in scanning electrochemical microscopy for high-spatial-resolution electrochemical analysis. The study explores various enzyme immobilization techniques and compares their performance in terms of sensitivity, detection limit, response time, reproducibility, spatial resolution, efficiency, permeability, selectivity, and the ability to block interfering species. The goal is to optimize biosensor performance for specific applications, such as 2D imaging of metabolic activity in single living cells, with a focus on achieving high spatial resolution.[66]

Conclusions and future directions

Cellular surfaces, probe cell-substrate interactions, and its noninvasive nature make it a powerful tool for understanding the complex behavior of biological systems. SECM-based studies provide valuable insights into cellular processes, cell-substrate interactions, and the spatial distribution of analytes, contributing to fields as diverse as cell biology, neurobiology, biochemistry, and biomedical research. The unique capabilities of SECM to capture real-time, high-resolution electrochemical interactions at cellular interfaces have deepened our understanding of myriad cellular processes, from basic metabolic activities to intricate communication networks. The role of SECM in the development and optimization of biosensors and bioanalytical assays cannot be overstated, as it promises to bring precision and efficiency to future bioanalytical tools. Recently developed noninvasive electroporation model demonstrates that SECM has the potential to be used to remove cancerous tumours without the use of drugs. It can also be used to monitor the electroporation process in real time. As SECM gains recognition, collaborations between different fields, such as genetics, molecular biology, and systems biology, could offer a comprehensive understanding of cellular life.

While SECM offers valuable insights into the electrochemical properties of samples, it also has certain limitations. One major challenge is the relatively slow scanning speed compared to other microscopy techniques. This can be a limiting factor when studying dynamic processes or large areas. Additionally, the interpretation of SECM data requires careful analysis and understanding of the system's behavior, as well as consideration of possible artifacts that may arise during the measurement process. The tip-to-substrate distance in SECM is a critical parameter that affects the spatial resolution and sensitivity of the technique.[71–73] Maintaining an appropriate distance is crucial to obtain accurate results. However, it can be challenging to precisely control and maintain a constant distance, especially when scanning rough or uneven surfaces. Strategies such as feedback control or integration of shear force can help address this challenge.

One of the goals to make SECM even more applicable would be to create a simpler, user-friendly and compact setup of SECM so that it could be more easily used in university laboratories to teach advanced biochemical and bioelectrochemical chemistry concepts. This could help academic institutions and the biotech industry work together to develop SECM-based diagnostic biosensors for diseases such as diabetes. Nevertheless, a compact setup would open up the possibility of using SECM for real-time monitoring in areas such as environmental studies, where the effects of pollutants on microorganisms can be monitored *in situ*.

The combination of EIS and SECM demonstrated the possibility of developing a targeted electroporation model for more precise and advanced gene editing techniques, initiating the development of targeted gene therapies for genetic disorders. This technology also has a perspective to be applied in drug-free cancer treatment, that would suppress high risk of healthy organ damage during chemotherapies. Moreover, real-time monitoring of SECM can be helpful in studying tumor tissues and cancer cells providing information of tumor progression and metastasis.

SECM has a potential to be a valuable technology in pharmaceutical business. It could be applied for rapid screening of drug interactions at the cellular level. Machine learning algorithms are gaining a lot of researcher attention nowadays and it possibly could be combined with SECM to predict cellular responses to various stimuli, improving drug development processes. This would involve collecting and processing SECM data, focusing on the redox activities and other electrochemical properties of cells exposed to specific drug stimuli, and correlating specific electrochemical patterns with cellular behavior. Trained models then would be capable of predicting cellular reactions to new pharmaceutical compounds, offering a rapid, efficient for early-stage drug screening.

Overall, over the years, SECM has proven to be a valuable and recognizable technology for investigating living cells. While it currently faces some limitations, we believe that with ongoing improvements in sensitivity and resolution, SECM has large potential for future research. Looking ahead, the integration of SECM with emerging technologies such as machine learning will open new frontiers in cell biology and drug discovery, promising even more significant advances in our understanding of living cells.

Disclosure statement

No potential conflict of interest was reported by the author(s).

ORCID

Arunas Ramanavicius http://orcid.org/0000-0002-0885-3556
Aušra Valiūnienė http://orcid.org/0000-0003-0535-023X

References

[1] Liu, J.; Kim, Y. S.; Richardson, C. E.; Tom, A.; Ramakrishnan, C.; Birey, F.; Katsumata, T.; Chen, S.; Wang, C.; Wang, X.; et al. Genetically Targeted Chemical Assembly of Functional Materials in Living Cells, Tissues, and Animals. *Science* **2020**, *367*, 1372–1376. DOI: 10.1126/science.aay4866.

[2] Wahab, O. J.; Kang, M.; Unwin, P. R. Scanning Electrochemical Cell Microscopy: A Natural Technique for Single Entity Electrochemistry. *Curr. Opin. Electrochem.* **2020**, *22*, 120–128. DOI: 10.1016/j.coelec.2020.04.018.

[3] Ebejer, N.; Güell, A. G.; Lai, S. C. S.; McKelvey, K.; Snowden, M. E.; Unwin, P. R. Scanning Electrochemical Cell Microscopy: A Versatile Technique for Nanoscale Electrochemistry and Functional Imaging. *Annu Rev Anal Chem (Palo Alto Calif)* **2013**, *6*, 329–351. DOI: 10.1146/annurev-anchem-062012-092650.

[4] Bard, A. J.; Fan, F. R. F.; Kwak, J.; Lev, O. Scanning Electrochemical Microscopy. Introduction and Principles. *Anal. Chem.* **1989**, *61*, 132–138. DOI: 10.1021/ac00177a011.

[5] Bentley, C. L.; Edmondson, J.; Meloni, G. N.; Perry, D.; Shkirskiy, V.; Unwin, P. R. Nanoscale Electrochemical Mapping. *Anal. Chem.* **2019**, *91*, 84–108. DOI: 10.1021/acs.analchem.8b05235.

[6] Chen, H.; Kong, X.; Wang, D.; Zhang, M. Flexible Disk Ultramicroelectrode for High-Resolution and Substrate-Tolerable Scanning Electrochemical Microscopy Imaging. *Anal. Chem.* **2022**, *94*, 17320–17327. DOI: 10.1021/acs.analchem.2c04465.

[7] Roberts, W. S.; Lonsdale, D. J.; Griffiths, J.; Higson, S. P. J. Advances in the Application of Scanning Electrochemical Microscopy to Bioanalytical Systems. *Biosens. Bioelectron.* **2007**, *23*, 301–318. DOI: 10.1016/j.bios.2007.06.020.

[8] Filice, F. P.; Ding, Z. Analysing Single Live Cells by Scanning Electrochemical Microscopy. *Analyst* **2019**, *144*, 738–752. DOI: 10.1039/C8AN01490F.

[9] Santana, J. J.; Izquierdo, J.; Souto, R. M. Uses of Scanning Electrochemical Microscopy [SECM] for the Characterization with Spatial and Chemical Resolution of Thin Surface Layers and Coating Systems Applied on Metals: A Review. *Coatings* **2022**, *12*, 637. DOI: 10.3390/coatings12050637.

[10] Zhou, Y.; Takahashi, Y.; Fukuma, T.; Matsue, T. Scanning Electrochemical Microscopy for Biosurface Imaging. *Curr. Opin. Electrochem.* **2021**, *29*, 100739. DOI: 10.1016/j.coelec.2021.100739.

[11] Traxler, I.; Singewald, T. D.; Schimo-Aichhorn, G.; Hild, S.; Valtiner, M. Scanning Electrochemical Microscopy Methods [SECM] and Ion-Selective Microelectrodes for Corrosion Studies. *Corrosion Reviews* **2022**, *40*, 515–542. [acccessed 2023-11-04]. DOI: 10.1515/corrrev-2021-0104.

[12] Preet, A.; Lin, T.-E. A Review: Scanning Electrochemical Microscopy [SECM] for Visualizing the Real-Time Local Catalytic Activity. *Catalysts* **2021**, *11*, 594. DOI: 10.3390/catal11050594.

[13] Oswald, E.; Palanisamy, K.; Kranz, C. Nanoscale Surface Modification via Scanning Electrochemical Probe Microscopy. *Curr. Opin. Electrochem.* **2022**, *34*, 100965. DOI: 10.1016/j.coelec.2022.100965.

[14] Gwon, H. J.; Lim, D.; Ahn, H. S. Bioanalytical Chemistry with Scanning Electrochemical Microscopy. *Bulletin Korean Chem. Soc.* **2021**, *42*, 1400–1410. DOI: 10.1002/bkcs.12383.

[15] Polcari, D.; Dauphin-Ducharme, P.; Mauzeroll, J. Scanning Electrochemical Microscopy: A Comprehensive Review of Experimental Parameters from 1989 to 2015. *Chem. Rev.* **2016**, *116*, 13234–13278. DOI: 10.1021/acs.chemrev.6b00067.

[16] Dauphin-Ducharme, P.; Kuss, C.; Rossouw, D.; Payne, N. A.; Danis, L.; Botton, G. A.; Mauzeroll, J. Corrosion Product Formation Monitored Using the Feedback Mode of Scanning Electrochemical Microscopy with Carbon Microelectrodes. *J. Electrochem. Soc.* **2015**, *162*, C677–C683. DOI: 10.1149/2.0701512jes.

[17] Kai, T.; Zoski, C. G.; Bard, A. J. Scanning Electrochemical Microscopy at the Nanometer Level. *Chem. Commun. (Camb)***2018**, *54*, 1934–1947. 101039/C7CC09777H. DOI: 10.1039/C7CC09777H.

[18] Bard, A. J.; Li, X.; Zhan, W. Chemically Imaging Living Cells by Scanning Electrochemical Microscopy. *Biosens. Bioelectron.* **2006**, *22*, 461–472. DOI: 10.1016/j.bios.2006.04.028.

[19] Gabriunaite, I.; Valiūnienė, A.; Poderyte, M.; Ramanavicius, A. Silane-Based Self-Assembled Monolayer Deposited on Fluorine Doped Tin Oxide as Model System for Pharmaceutical and Biomedical Analysis. *J. Pharm. Biomed. Anal.* **2020**, *177*, 112832. DOI: 10.1016/j.jpba.2019.112832.

[20] Cannan, S.; Cervera, J.; Steliaros, R. J.; Bitziou, E.; Whitworth, A. L.; Unwin, P. R. Scanning Electrochemical Microscopy [SECM] Studies of Catalytic EC′ Processes: Theory and Experiment for Feedback, Generation/Collection and Imaging Measurements. *Phys. Chem. Chem. Phys.* **2011**, *13*, 5403–5412. DOI: 10.1039/C0CP02530E.

[21] Morkvenaite-Vilkonciene, I.; Ramanaviciene, A.; Ramanavicius, A. Redox Competition and Generation-Collection Modes Based Scanning Electrochemical Microscopy for the Evaluation of Immobilised Glucose Oxidase-Catalysed Reactions. *RSC Adv* **2014**, *4*, 50064–50069. 101039/C4RA08697J. DOI: 10.1039/C4RA08697J.

[22] Bergner, S.; Vatsyayan, P.; Matysik, F.-M. Recent Advances in High Resolution Scanning Electrochemical Microscopy of Living Cells – a Review. *Anal. Chim. Acta.* **2013**, *775*, 1–13. DOI: 10.1016/j.aca.2012.12.042.

[23] Stratmann, L.; Clausmeyer, J.; Schuhmann, W. Non-Destructive Patterning of Carbon Electrodes by Using the Direct Mode of Scanning Electrochemical Microscopy. *Chemphyschem* **2015**, *16*, 3477–3482. DOI: 10.1002/cphc.201500585.

[24] Nebel, M.; Erichsen, T.; Schuhmann, W. Constant-Distance Mode SECM as a Tool to Visualize Local Electrocatalytic Activity of Oxygen Reduction Catalysts. *Beilstein J. Nanotechnol.* **2014**, *5*, 141–151. DOI: 10.3762/bjnano.5.14.

[25] Takahashi, Y.; Shevchuk, A. I.; Novak, P.; Babakinejad, B.; Macpherson, J.; Unwin, P. R.; Shiku, H.; Gorelik, J.; Klenerman, D.; Korchev, Y. E.; et al. Topographical and Electrochemical Nanoscale Imaging of Living Cells Using Voltage-Switching Mode Scanning Electrochemical Microscopy. *Proc. Natl. Acad. Sci. U S A* **2012**, *109*, 11540–11545. DOI: 10.1073/pnas.1203570109.

[26] Li, M. S. M.; Filice, F. P.; Ding, Z. Determining Live Cell Topography by Scanning Electrochemical Microscopy. *Electroanal. Chem.* **2016**, *779*, 176–186. DOI: 10.1016/j.jelechem.2016.02.042.

[27] Shi, X.; Qing, W.; Marhaba, T.; Zhang, W. Atomic Force microscopy - Scanning Electrochemical Microscopy [AFM-SECM] for Nanoscale Topographical and Electrochemical Characterization: Principles, Applications and Perspectives. *Electrochim. Acta* **2020**, *332*, 135472. DOI: 10.1016/j.electacta.2019.135472.

[28] Morkvenaite-Vilkonciene, I.; Valiūnienė, A.; Petroniene, J.; Ramanavicius, A. Hybrid System Based on Fast Fourier Transform Electrochemical Impedance Spectroscopy Combined with Scanning Electrochemical Microscopy. *Electrochem. Commun.* **2017**, *83*, 110–112. DOI: 10.1016/j.elecom.2017.08.020.

[29] Valiūnienė, A.; Petroniene, J.; Morkvenaite-Vilkonciene, I.; Popkirov, G.; Ramanaviciene, A.; Ramanavicius, A. Redox-Probe-Free Scanning Electrochemical Microscopy Combined with Fast Fourier Transform Electrochemical Impedance Spectroscopy. *Phys. Chem. Chem. Phys.* **2019**, *21*, 9831–9836. 101039/C9CP00187E. DOI: 10.1039/C9CP00187E.

[30] Hou, Z-z.; Yue, Q-x.; Lv, J.; Wang, Y-y.; Zhu, B-q.; Liang, X.; Ding, R.; Yu, H-b.; Wang, X.; Gui, T-j Research on the anti-Corrosion Performance of Organosilane Modified Basalt Scales Epoxy Coating by EIS and SECM. *Int. J. Electrochem. Sci.* **2022**, *17*, 220327. DOI: 10.20964/2022.03.12.

[31] Nagamine, K.; Takahashi, Y.; Ino, K.; Shiku, H.; Matsue, T. Influence of Tip Size on Single Yeast Cell Imaging Using Scanning Electrochemical Microscopy. *Electroanalysis* **2011**, *23*, 1168–1174. DOI: 10.1002/elan.201000595.

[32] Shi, M.; Wang, L.; Xie, Z.; Zhao, L.; Zhang, X.; Zhang, M. High-Content Label-Free Single-Cell Analysis with a Microfluidic Device Using Programmable Scanning Electrochemical Microscopy. *Anal. Chem.* **2021**, *93*, 12417–12425. DOI: 10.1021/acs.analchem.1c02507.

[33] McKelvey, K.; Martin, S.; Robinson, C.; Unwin, P. R. Quantitative Local Photosynthetic Flux Measurements at Isolated Chloroplasts and Thylakoid Membranes Using Scanning Electrochemical Microscopy (SECM). *J. Phys. Chem. B* **2013**, *117*, 7878–7888. DOI: https://doi.org/10.1021/jp403048f.

[34] Ma, Y.; Colin, C.; Descamps, J.; Arbault, S.; Sojic, N. Shadow Electrochemiluminescence Microscopy of Single Mitochondria. *Angew. Chem. Int. Ed. Engl.* **2021**, *60*, 18742–18749. DOI: https://doi.org/10.1002/anie.202105867.

[35] Thind, S.; Lima, D.; Booy, E.; Trinh, D.; McKenna, S. A.; Kuss, S. Cytochrome c Oxidase Deficiency Detection in Human Fibroblasts Using Scanning Electrochemical Microscopy. *Proc. Natl. Acad. Sci. U S A* **2024**, *121*, e2310288120. DOI: https://doi.org/10.1073/pnas.2310288120.

[36] Santos, C. S.; Kowaltowski, A. J.; Bertotti, M. Single Cell Oxygen Mapping (SCOM) by Scanning Electrochemical Microscopy Uncovers Heterogeneous Intracellular Oxygen Consumption. *Sci. Rep.* **2017**, *7*, 11428. DOI: https://doi.org/10.1038/s41598-017-11956-w.

[37] Nebel, M.; Grützke, S.; Diab, N.; Schulte, A.; Schuhmann, W. Microelectrochemical Visualization of Oxygen Consumption of Single Living Cells. *Faraday Discuss.* **2013**, *164*, 19–32. DOI: 10.1039/C3FD00011G.

[38] Kaya, T.; Torisawa, Y-s.; Oyamatsu, D.; Nishizawa, M.; Matsue, T. Monitoring the Cellular Activity of a Cultured Single Cell by Scanning Electrochemical Microscopy [SECM]. a Comparison with Fluorescence Viability Monitoring. *Biosens. Bioelectron.* **2003**, *18*, 1379–1383. DOI: 10.1016/S0956-5663[03]00083-6.

[39] Zhao, Y.; Li, Y.; Kuermanbayi, S.; Liu, Y.; Zhang, J.; Ye, Z.; Guo, H.; Qu, K.; Xu, F.; Li, F. In Situ and Quantitatively Monitoring the Dynamic Process of Ferroptosis in Single Cancer Cells by Scanning Electrochemical Microscopy. *Anal. Chem.* **2023**, *95 [3*, 1940–1948. DOI: 10.1021/acs.analchem.2c04179.

[40] Cremin, K.; Meloni, G. N.; Valavanis, D.; Soyer, O. S.; Unwin, P. R. Can Single Cell Respiration Be Measured by Scanning Electrochemical Microscopy [SECM]? *ACS Meas. Sci. Au.* **2023**, *3*, 361–370. DOI: 10.1021/acsmeasuresciau.3c00019.

[41] Zhan, D.; Fan, F.-R. F.; Bard, A. J. The K_v Channel Blocker 4-Aminopyridine Enhances Ag^+ Uptake: A Scanning Electrochemical Microscopy Study of Single Living Cells. *Proc. Natl. Acad. Sci. U S A* **2008**, *105*, 12118–12122. DOI: 10.1073/pnas.0805286105.

[42] Polcari, D.; Hernández-Castro, J. A.; Li, K.; Geissler, M.; Mauzeroll, J. Determination of the Relationship between Expression and Functional Activity of Multidrug Resistance-Associated Protein 1 Using Scanning Electrochemical Microscopy. *Anal. Chem.* **2017**, *89*, 8988–8994. DOI: 10.1021/acs.analchem.7b01601.

[43] Selva, J. S. G.; Voltarelli, V. A.; Brum, P. C.; Bertotti, M. SECM Investigation on pH Changes in Cellular Environment Induced by Caffeine. *Electrochim. Acta* **2023**, *444*, 142015. DOI: 10.1016/j.electacta.2023.142015.

[44] Zhang, J.; Zhu, T.; Lang, J.; Fu, W.; Li, F. Recent Advances of Scanning Electrochemical Microscopy and Scanning Ion Conductance Microscopy for Single-Cell Analysis. *Curr. Opin. Electrochem.* **2020**, *22*, 178–185. DOI: 10.1016/j.coelec.2020.06.001.

[45] Darch, S. E.; Koley, D. Quantifying Microbial Chatter: Scanning Electrochemical Microscopy as a Tool to Study Interactions in Biofilms. *Proc. Math. Phys. Eng. Sci.* **2018**, *474*, 20180405. DOI: 10.1098/rspa.2018.0405.

[46] Puri, S. R.; Almeida, E.; Elangovan, S.; Labossiere, A.; Collins, C.; Ramsey, M.; Kim, J. Mechanistic Assessment of Metabolic Interaction between Single Oral Commensal Cells by Scanning Electrochemical Microscopy. *Anal. Chem.* **2023**, *95*, 8711–8719. DOI: 10.1021/acs.analchem.3c01498.

[47] Page, A.; Kang, M.; Armitstead, A.; Perry, D.; Unwin, P. R. Quantitative Visualization of Molecular Delivery and Uptake at Living Cells with Self-Referencing Scanning Ion Conductance Microscopy-Scanning Electrochemical Microscopy. *Anal. Chem.* **2017**, *89*, 3021–3028. DOI: 10.1021/acs.analchem.6b04629.

[48] Takahashi, Y.; Ida, H.; Matsumae, Y.; Komaki, H.; Zhou, Y.; Kumatani, A.; Kanzaki, M.; Shiku, H.; Matsue, T. 3D Electrochemical and Ion Current Imaging Using Scanning Electrochemical–Scanning Ion Conductance Microscopy. *Phys. Chem. Chem. Phys.* **2017**, *19*, 26728–26733. 101039/C7CP05157C. DOI: 10.1039/C7CP05157C.

[49] Berger, C. E. M.; Rathod, H.; Gillespie, J. I.; Horrocks, B. R.; Datta, H. K. Scanning Electrochemical Microscopy at the Surface of Bone-Resorbing Osteoclasts: Evidence for Steady-State Disposal and Intracellular Functional Compartmentalization of Calcium. *J. Bone Miner. Res.* **2001**, *16*, 2092–2102. DOI: 10.1359/jbmr.2001.16.11.2092.

[50] Prabhakaran, V.; Kalsar, R.; Strange, L.; Marina, O. A.; Prabhakaran, R.; Joshi, V. V. Understanding Localized Corrosion on Metal Surfaces Using Scanning Electrochemical Cell Impedance Microscopy [SECCIM]. *J. Phys. Chem. C* **2022**, *126*, 12519–12526. DOI: 10.1021/acs.jpcc.2c03807.

[51] Cheng, L.; Jin, R.; Jiang, D.; Zhuang, J.; Liao, X.; Zheng, Q. Scanning Electrochemical Cell Microscopy Platform with Local Electrochemical Impedance Spectroscopy. *Anal. Chem.* **2021**, *93*, 16401–16408. DOI: 10.1021/acs.analchem.1c02972.

[52] Valiūnienė, A.; Petronienė, J.; Dulkys, M.; Ramanavičius, A. Investigation of Active and Inactivated Yeast Cells by Scanning Electrochemical Impedance Microscopy. *Electroanalysis* **2020**, *32*, 367–374. DOI: 10.1002/elan.201900414.

[53] Morkvenaite-Vilkonciene, I.; Genys, P.; Ramanaviciene, A.; Ramanavicius, A. Scanning Electrochemical Impedance Microscopy for Investigation of Glucose Oxidase Catalyzed Reaction. *Colloids Surf. B Biointerfaces* **2015**, *126*, 598–602. DOI: 10.1016/j.colsurfb.2015.01.007.

[54] Valiūnienė, A.; Sabirovas, T.; Petronienė, J.; Ramanavičius, A. Towards the Application of Fast Fourier Transform - Scanning Electrochemical Impedance Microscopy [FFT-SEIM]. *Electroanal. Chem.* **2020**, *864*, 114067. DOI: 10.1016/j.jelechem.2020.114067.

[55] Poderyte, M.; Valiūnienė, A.; Ramanavicius, A. Scanning Electrochemical Microscope as a Tool for the Electroporation

of Living Yeast Cells. *Biosens. Bioelectron.* **2022**, *205*, 114096. DOI: 10.1016/j.bios.2022.114096.

[56] Koley, D.; Bard, A. J. Triton X-100 Concentration Effects on Membrane Permeability of a Single HeLa Cell by Scanning Electrochemical Microscopy [SECM]. *Proc. Natl. Acad. Sci. U S A* **2010**, *107*, 16783–16787. DOI: 10.1073/pnas.1011614107.

[57] Valiūnienė, A.; Gabriunaite, I.; Poderyte, M.; Ramanavicius, A. Electroporation of a Hybrid Bilayer Membrane by Scanning Electrochemical Microscope. *Bioelectrochemistry* **2020**, *136*, 107617. DOI: 10.1016/j.bioelechem.2020.107617.

[58] Poderyte, M.; Ramanavicius, A.; Valiūnienė, A. Scanning Electrochemical Microscopy Based Irreversible Destruction of Living Cells. *Biosens. Bioelectron.* **2022**, *216*, 114621. DOI: 10.1016/j.bios.2022.114621.

[59] Li, Y.; Ye, Z.; Zhang, J.; Zhao, Y.; Zhu, T.; Song, J.; Xu, F.; Li, F. In Situ and Quantitative Monitoring of Cardiac Tissues Using Programmable Scanning Electrochemical Microscopy. *Anal. Chem.* **2022**, *94*, 10515–10523. DOI: 10.1021/acs.analchem.2c01919.

[60] Ye, Z.; Li, Y.; Zhao, Y.; Zhang, J.; Zhu, T.; Xu, F.; Li, F. Effect of Exogenous Electric Stimulation on the Cardiac Tissue Function in Situ Monitored by Scanning Electrochemical Microscopy. *Anal. Chem.* **2023**, *95*, 4634–4643. DOI: https://doi.org/10.1021/acs.analchem.2c04758.

[61] Xiong, Q.; Song, R.; Wu, T.; Zhang, F.; He, P. In Situ Potentiometric SECM Monitoring of the Extracellular pH Changes under Electrical Stimulation Using a Dual-Microelectrode Tip. *Electroanal. Chem.* **2021**, *887*, 115169. DOI: https://doi.org/10.1016/j.jelechem.2021.115169.

[62] Song, R.; Xiong, Q.; Wu, T.; Ning, X.; Zhang, F.; Wang, Q.; He, P. Real-Time Monitoring of Extracellular pH Using a pH-Potentiometric Sensing SECM Dual-Microelectrode. *Anal. Bioanal. Chem.* **2020**, *412*, 3737–3743. DOI: https://doi.org/10.1007/s00216-020-02625-5.

[63] Bironaite, D.; Petroniene, J.; Miksiunas, R.; Zinovicius, A.; Morkvenaite-Vilkonciene, I.; Ramanavicius, A. Scanning Electrochemical Microscopy for the Stimulation and Investigation of Human Skeletal Muscle-Derived Mesenchymal Stem/Stromal Cells. *Electrochim. Acta* **2023**, *455*, 142389. DOI: https://doi.org/10.1016/j.electacta.2023.142389.

[64] Soldà, A.; Valenti, G.; Marcaccio, M.; Giorgio, M.; Pelicci, P. G.; Paolucci, F.; Rapino, S. Glucose and Lactate Miniaturized Biosensors for SECM-Based High-Spatial Resolution Analysis: A Comparative Study. *ACS Sens.* **2017**, *2*, 1310–1318. DOI: 10.1021/acssensors.7b00324.

[65] Chen, B.; Hu, Q.; Xiong, Q.; Zhang, F.; He, P. An Ultrasensitive Scanning Electrochemical Microscopy [SECM]-Based DNA Biosensing Platform Amplified with the Long Self-Assembled DNA Concatemers. *Electrochim. Acta* **2016**, *192*, 127–132. DOI: 10.1016/j.electacta.2015.12.102.

[66] Stoica, L.; Neugebauer, S.; Schuhmann, W. Scanning Electrochemical Microscopy [SECM] as a Tool in Biosensor Research. In *Biosensing for the 21st Century*, Renneberg, R., Lisdat, F. Eds.; Springer Berlin Heidelberg, **2008**; pp 455–492

[67] Morkvenaite-Vilkonciene, I.; Ramanaviciene, A.; Kisieliute, A.; Bucinskas, V.; Ramanavicius, A. Scanning Electrochemical Microscopy in the Development of Enzymatic Sensors and Immunosensors. *Biosens. Bioelectron.* **2019**, *141*, 111411. DOI: 10.1016/j.bios.2019.111411.

[68] Wu, J.; Gao, Y.; Pan, N.; Lu, L.; Wang, X. An Isolated Single-Particle-Based SECM Tip Interface for Single-Cell NO Sensing. *Biosens. Bioelectron.* **2023**, *223*, 115048. DOI: 10.1016/j.bios.2022.115048.

[69] Zhao, X.; Zhu, R.; Anikovskiy, M.; Wu, Q.; Ding, Z. Profiling H2O2 from Single cos-7 Cells by Means of Scanning Electrochemical Microscopy. *Biosens. Bioelectron.* **2023**, *227*, 115123. DOI: 10.1016/j.bios.2023.115123.

[70] De Zio, S.; Becconi, M.; Soldà, A.; Malferrari, M.; Lesch, A.; Rapino, S. Glucose Micro-Biosensor for Scanning Electrochemical Microscopy Characterization of Cellular Metabolism in Hypoxic Microenvironments. *Bioelectrochemistry* **2023**, *150*, 108343. DOI: 10.1016/j.bioelechem.2022.108343.

[71] Lhenry, S.; Leroux, Y. R.; Hapiot, P. Chemically Irreversible Redox Mediator for SECM Kinetics Investigations: Determination of the Absolute Tip–Sample Distance. *Anal. Chem.* **2013**, *85*, 1840–1845. DOI: 10.1021/ac303226e.

[72] Sundaresan, V.; Marchuk, K.; Yu, Y.; Titus, E. J.; Wilson, A. J.; Armstrong, C. M.; Zhang, B.; Willets, K. A. Visualizing and Calculating Tip–Substrate Distance in Nanoscale Scanning Electrochemical Microscopy Using 3-Dimensional Super-Resolution Optical Imaging. *Anal. Chem.* **2017**, *89*, 922–928. DOI: 10.1021/acs.analchem.6b04073.

[73] Barforoush, J. M.; McDonald, T. D.; Desai, T. A.; Widrig, D.; Bayer, C.; Brown, M. K.; Cummings, L. C.; Leonard, K. C. Intelligent Scanning Electrochemical Microscopy Tip and Substrate Control Utilizing Fuzzy Logic. *Electrochim. Acta* **2016**, *190*, 713–719. DOI: 10.1016/j.electacta.2015.12.112.

UŽRAŠAMS

Vilniaus universiteto leidykla
Saulėtekio al. 9, III rūmai, LT-10222 Vilnius
El. p. info@leidykla.vu.lt, www.leidykla.vu.lt
bookshop.vu.lt, journals.vu.lt
Tiražas 10 egz.